

Studies on the control and function
of chromatin fragmentation during apoptosis

Dissertation
zur Erlangung des Doktorgrades
der Mathematisch-Naturwissenschaftlichen Fakultäten
der Georg-August-Universität zu Göttingen

vorgelegt von
Wiebke Goebel
aus Würselen

Göttingen 2005

D7	
Referent	Prof. Dr. D. Doenecke
Korreferent	Prof. Dr. R. Hardeland
Tag der mündlichen Prüfung	28.06.2005

Meinen Eltern
gewidmet

I. CONTENTS

I. Contents	I
II. Figure index	VIII
III. Table index	X
IV. Abbreviations	XI
1. Introduction.....	1
1.1. Evolutionary and phylogenetic aspects of programmed cell death.....	1
1.1.1. Programmed cell death in bacteria and unicellular eukaryotes.....	2
1.1.2. Programmed cell death in animals	3
1.1.3. Programmed cell death in plants	4
1.1.4. A central role for mitochondria	5
1.1.5. Summary: Evolution and phylogeny of PCD	5
1.2. Some milestones in apoptosis research	6
1.2.1. The early years	6
1.2.2. Recognizing apoptosis as a basic biological phenomenon.....	7
1.2.3. First markers indicating apoptosis.....	7
1.2.4. Important input from <i>C. elegans</i> and <i>Drosophila</i>	8
1.2.4.1. Apoptosis in nematodes.....	8
1.2.4.2. Apoptotic homologous proteins in nematodes and vertebrates	9
1.2.4.3. Evidence for homologous apoptotic proteins in insects	10
1.2.4.4. Bcl-2 family members in nematodes, insects, and mammals	11
1.2.4.5. Other inhibitors of apoptosis in mammals and insects	12
1.2.4.6. Homologous proteins in a core apoptotic pathway	12
1.3. Apoptosis in mammalian cells.....	13
1.3.1. Mammalian caspases.....	14
1.3.1.1. Mechanisms of caspase activation	14
1.3.1.2. Substrate specificities of caspases	15
1.3.1.3. Regulation of caspase activities	16
1.3.2. Mammalian bcl-2 family members and the mitochondria.....	18
1.3.3. Mammalian signalling pathways during apoptosis.....	21
1.3.3.1. The death receptor pathway (extrinsic).....	22
1.3.3.2. The stress-induced mitochondrial pathway (intrinsic)	23
1.3.3.3. Summary: Mammalian apoptosis	25
1.3.4. Apoptotic chromatin changes	27
1.3.4.1. Apoptotic chromatin condensation.....	27

1.3.4.2. Apoptotic DNA fragmentation.....	28
1.3.4.2.1. Discovery of DFF40 as an apoptotic endonuclease	29
1.3.4.2.2. DFF45, the inhibitor and chaperone of DFF40.....	31
1.3.4.2.3. Other apoptotic nucleases	31
1.3.4.2.4. Contribution of DNA fragmentation to apoptosis	32
1.4. Aims of this study	34
2. Materials and methods	36
2.1. Materials	36
2.1.1. Technical equipment	36
2.1.2. Chemicals.....	37
2.1.3. Dyes	39
2.1.4. Oligonucleotides	40
2.1.4.1. PCR primers	40
2.1.4.2. Sequencing primers	40
2.1.5. Standards.....	40
2.1.6. Antibodies	40
2.1.6.1. Primary antibodies	40
2.1.6.2. Secondary antibodies	41
2.1.7. Enzymes	41
2.1.8. Other biological agents.....	42
2.1.9. Other materials.....	42
2.1.10. Kits, sets, and ready-made mixes	43
2.1.11. Buffers and solutions.....	43
2.1.12. Media.....	49
2.1.13. Vectors.....	50
2.1.13.1. Vectors for transformation of bacteria.....	51
2.1.13.1.1. pGEM [®] T easy	51
2.1.13.1.2. pRSet B.....	52
2.1.13.2. Vector for transformation of yeast	54
2.1.13.3. Vector for transfection of mammalian cells.....	55
2.1.14. Microorganisms.....	56
2.1.15. Cell lines.....	57
2.2. Methods.....	58
2.2.1. Working with bacteria	58
2.2.1.1. E. coli standard culture.....	58
2.2.1.2. E. coli stock cultures	58
2.2.1.3. Preparing competent cells.....	58

2.2.1.4. Transformation of <i>E. coli</i>	59
2.2.1.5. Preparing bacteria for plasmid purification.....	59
2.2.1.5.1. Preparing bacteria for plasmid preparations (TELt-method)	59
2.2.1.5.2. Preparing bacteria for plasmid preparations (Qiagen).....	60
2.2.1.5.3. Bacteria and endotoxin-free plasmid preparation	60
2.2.1.6. Expression of recombinant DFF40/DFF45 complex in <i>E. coli</i>	60
2.2.1.7. Pilot expression experiments.....	61
2.2.2. Working with yeast	62
2.2.2.1. Yeast culturing.....	62
2.2.2.2. Transformation of yeast.....	62
2.2.2.2.1. Transformation of yeast by the Li-acetate-method	62
2.2.2.2.2. Transformation of yeast by electroporation	63
2.2.2.3. Expression of recombinant proteins in yeast.....	63
2.2.2.3.1. Expressing H1 histones or caspase-3 in <i>S. cerevisiae</i>	64
2.2.2.3.2. Plasmids for expression of H1 histones and caspase-3 in yeast	65
2.2.3. Protein biochemical methods.....	65
2.2.3.1. Protein purification by Ni-NTA affinity chromatography.....	65
2.2.3.1.1. Purification of recombinant DFF40/DFF45 complex from bacteria ..	66
2.2.3.1.2. Purification of recombinant caspase-3 from yeast	68
2.2.3.2. Purification of recombinant H1 histone subtypes from yeast	69
2.2.3.3. Purification of H1 histones by gel filtration on P60 columns	70
2.2.3.3.1. Preparing the column	70
2.2.3.3.2. H1 histone purification process.....	70
2.2.3.4. In vitro phosphorylation of H1 histones.....	71
2.2.3.5. Analyzing H1 histones by CZE	71
2.2.3.6. SDS-PAGE (according to Laemmli, 1970).....	72
2.2.3.6.1. Preparation of the gel.....	73
2.2.3.6.2. Running the gel	74
2.2.3.6.3. Staining the gel	74
2.2.3.7. Western blotting (Towbin et al., 1979).....	74
2.2.3.7.1. Preparing the blotting stack	74
2.2.3.7.2. Ponceau-staining	75
2.2.3.7.3. Immunostaining of the membrane.....	75
2.2.3.7.4. Detection by enhanced chemiluminescence (ECL).....	76
2.2.3.7.5. Detection by alkaline phosphatase reaction	77
2.2.3.7.6. Dilution of antibodies used for western blotting	77
2.2.3.8. Quantitation of protein contents (Bradford, 1976).....	78

2.2.3.8.1. Protein standard curve	78
2.2.3.8.2. Bradford assay	78
2.2.3.9. In vitro plasmid assay for DFF40	78
2.2.3.9.1. Dialysis of recombinant purified proteins.....	79
2.2.3.9.2. Assay conditions	79
2.2.3.10. Assay with nuclei	80
2.2.3.11. Caspase-3 activity assay	80
2.2.4. Molecular biological methods	81
2.2.4.1. Cloning strategy for over-expression in human cells.....	81
2.2.4.2. Isolation of RNA with the RNeasy kit	82
2.2.4.3. Quantitation of nucleic acids	82
2.2.4.3.1. Quantitation of DNA or RNA by UV spectrometry	82
2.2.4.3.2. Quantitation of DNA by gel titration.....	83
2.2.4.4. PCR	83
2.2.4.4.1. PCR conditions used in the experiments.....	83
2.2.4.5. RT-PCR.....	84
2.2.4.5.1. Reverse transcriptase reaction	84
2.2.4.5.2. DNase digestion of RNA.....	85
2.2.4.5.3. cDNA synthesis.....	85
2.2.4.6. Restriction digestion.....	86
2.2.4.7. Ligation of DNA fragments into a vector.....	86
2.2.4.7.1. Cloning into pGEM [®] -T easy vectors	86
2.2.4.7.2. Cloning into multiple cloning sites of other vectors.....	87
2.2.4.8. DNA gel electrophoresis.....	88
2.2.4.8.1. Determination of DNA fragment sizes	88
2.2.4.9. RNA gel electrophoresis.....	88
2.2.4.10. DNA purification methods	89
2.2.4.10.1. Phenol/chloroform extraction of DNA	89
2.2.4.10.2. DNA precipitation by ethanol.....	89
2.2.4.10.3. DNA precipitation by isopropanol.....	90
2.2.4.10.4. Plasmid DNA purification by the TELT method	90
2.2.4.10.5. Plasmid DNA purification using Qiagen maxi prep kits	90
2.2.4.10.6. DNA purification from human cells.....	91
2.2.4.10.7. Purification of DNA fragments from agarose gels	92
2.2.4.11. Sequencing (Sanger, 1977).....	93
2.2.4.11.1. Generation of fluorescence-tagged DNA strands	94
2.2.4.11.2. Preparing the fluorescence tagged DNA for sequence analysis	94

2.2.4.11.3. Sequence analysis using an ABI prism DNA sequencer	94
2.2.4.11.4. Comparison of sequences	95
2.2.5. Cell biological methods	95
2.2.5.1. Cell culture standard conditions.....	95
2.2.5.1.1. Inactivation of FCS.....	95
2.2.5.1.2. Cultivation and passaging of adherent cells	96
2.2.5.1.3. Cultivation and passaging of suspension cells	96
2.2.5.1.4. Cell counting	96
2.2.5.1.5. Freezing cells for storage.....	97
2.2.5.1.6. Thawing cells for cultivation.....	97
2.2.5.1.7. Harvesting procedure for cells.....	97
2.2.5.2. Preparing proteins from cells.....	97
2.2.5.2.1. Purification of H1 histones from human cells	97
2.2.5.2.2. Preparing nuclei from human cells.....	98
2.2.5.2.3. Preparing cytosol from human cells	99
2.2.5.2.4. Preparing whole-cell extracts for western blots	99
2.2.5.3. Stable transfection	99
2.2.5.3.1. Establishing a killing curve for an antibiotic	100
2.2.5.3.2. Transfection procedure.....	100
2.2.5.3.3. Selection for stably transfected cells	101
2.2.5.4. MACS	102
2.2.5.5. Induction of apoptosis.....	102
2.2.5.6. Microscopy	103
2.2.5.6.1. Mounting cells to object slides.....	103
2.2.5.6.2. Fluorescence labelling of cellular molecules	103
2.2.5.6.3. Annexin V-FITC-labelling of apoptotic cells.....	104
2.2.5.6.4. Immunofluorescence.....	105
2.2.5.6.5. Microscopic analysis	106
2.2.6. Statistical analysis	106
2.2.7. Densitometry	108
3. Results	109
3.1. Factors influencing the activity of DFF40	109
3.1.1. Purification of recombinant proteins.....	110
3.1.1.1. Purification of DFF40/DFF45 as a complex from E. coli	110
3.1.1.1.1. Optimizing the expression rates in pilot expression experiments..	110
3.1.1.1.2. Purification of the DFF40/DFF45 complex on Ni-NTA columns	114
3.1.1.2. Purification of caspase-3 from S. cerevisiae	116

3.1.1.3. Titration of enzyme activities in DFF plasmid assays.....	118
3.1.1.4. Purification of H1 histone subtypes from yeast	120
3.1.2. Experiments with different human H1 histone subtypes.....	121
3.1.2.1. Effects of H1 ^o	121
3.1.2.2. Effects of H1.3.....	123
3.1.2.3. Effects of H1.4.....	124
3.1.2.4. Effects of bulk H1 histones	125
3.1.2.5. Effect of core histone H3	126
3.1.3. Experiments with in vitro phosphorylated histone H1.2.....	127
3.1.4. Experiments with cellular H1 histones	130
3.1.5. Experiments with cellular proteins	134
3.1.5.1. Effect of H1 histones on DFF40 activity on a chromatin substrate.....	134
3.1.5.2. Effects of cytoplasm from different cell types on DFF40 activity	136
3.2. Summary: Factors influencing DFF40 activity.....	143
3.3. DFF40 as a putative factor promoting apoptosis	145
3.3.1. Characterization of apoptosis in different human cell lines	145
3.3.1.1. Expression and localization of DFF40 and DFF45.....	146
3.3.1.2. Different protein levels of proteins involved in apoptosis	147
3.3.1.3. Morphology of Jurkat and Raji cells during apoptosis	149
3.3.1.4. Summary: Apoptotic features of Jurkat and Raji cells	153
3.3.2. Stable transfection	155
3.3.2.1. Establishing a Blasticidin killing curve.....	155
3.3.2.2. Monitoring of cell growth during selection after stable transfection....	156
3.3.3. Experiments with transfected Raji cells	158
3.3.3.1. Detection of the tagged recombinant proteins	158
3.3.3.2. Morphological changes of transfected Raji cells	159
3.3.3.3. Changes in protein levels during apoptosis in Raji cells.....	161
3.3.3.4. Changes in the DNA fragmentation pattern in Raji cells.....	163
3.3.3.5. Single cell cloning	164
3.3.4. Comparison of caspase-3 activities in transfected Raji cells.....	167
3.3.4.1. Two-way ANOVA with Bonferroni post-tests	173
3.3.4.2. Analysis of interaction by two-way ANOVA on column pairs	175
3.3.5. Summary: Apoptosis in stably transfected Raji cells	177
3.3.6. Experiments with transfected Jurkat cells.....	178
3.3.6.1. Changes in protein levels during apoptosis in Jurkat cells	178
3.3.6.2. Changes in the DNA fragmentation pattern in Jurkat cells	179
3.3.7. Comparison of caspase-3 activities in transfected Jurkat cells	181

3.3.7.1. Two-way ANOVA with Bonferroni post-tests	182
3.3.7.2. Analysis of interaction by two-way ANOVA on column pairs	185
3.4. Summary: Apoptosis in stably transfected cells	185
4. Discussion	187
4.1. Characterizing the recombinantly expressed proteins	189
4.1.1. Purification of H1 histone subtypes from yeast	189
4.1.2. Purification of caspase-3 from yeast	191
4.1.3. Purification of DFF40/DFF45 complex from bacteria	191
4.2. Factors influencing the activity of DFF40 in vitro	192
4.2.1. Effect of different H1 histone subtypes	192
4.2.2. Effect of phosphorylated H1 histones on the activity of DFF40	194
4.2.3. Effect of H1 histones from apoptotic and control HL60 cells	196
4.2.4. Effect of other cellular proteins on the activity of DFF40	198
4.3. Factors affecting progression of apoptosis in vivo	201
4.3.1. Expression and cellular localization of DFF40 and DFF45	202
4.3.2. Topotecan as an inducer of apoptosis in lymphoma cells	204
4.3.3. Expression patterns of selected proteins during apoptosis.....	205
4.3.4. Stable transfection procedure.....	208
4.3.5. Morphology of apoptotic Jurkat and Raji cells	210
4.3.6. DNA fragmentation patterns in transfected lymphoma cells	211
4.3.7. Protein expression levels in transfected lymphoma cells	213
4.3.8. Comparison of caspase-3 activities in transfected lymphoma cells	217
4.3.9. Future experiments	219
4.3.10. Perspectives.....	220
5. Summary.....	221
6. References	I

II. FIGURE INDEX

Figure 1-1: The core molecular mechanism of PCD in <i>C. elegans</i>	9
Figure 1-2: Basic signalling and regulation of mammalian apoptosis (simplified presentation) ..	26
Figure 2-1: pGEM [®] T easy vector (figure adapted from www. Promega.com, modified)	52
Figure 2-2: pRSET vector A, B, C	54
Figure 2-3: yEP51 vector	55
Figure 2-4: pcDNA6 myc-his vector	56
Figure 3-1: Pilot expression experiments: Detection of DFF40/DFF45	112
Figure 3-2: Pilot expression experiments: Detection of the N-terminal 6xHis-tag	113
Figure 3-3: Purification of DFF40/DFF45 complex on Ni-NTA columns	114
Figure 3-4: Detection of DFF40 in the Ni-NTA-purified protein complex	115
Figure 3-5: Caspase-3 purification by Ni-NTA affinity chromatography	116
Figure 3-6: Detection of the active caspase-3 subunits by western blotting	117
Figure 3-7: Titration of DFF40 activity	118
Figure 3-8: Titration of caspase-3 activity	119
Figure 3-9: PCA-extracted human recombinant H1 histone subtypes expressed in yeast	120
Figure 3-10: Influence of H1 [°] on the DNase activity of DFF40 when digesting plasmid DNA ..	122
Figure 3-11: Influence of H1.3 on the DNase activity of DFF40 when digesting plasmid DNA ..	123
Figure 3-12: Influence of H1.4 on the DNase activity of DFF40 when digesting plasmid DNA ..	124
Figure 3-13: Influence of bulk H1 on the DNase activity of DFF40 digesting plasmid DNA	125
Figure 3-14: Influence of both core histone H3 and linker histone H1.4 on DFF40 activity	126
Figure 3-15: Different migration features of in vitro phosphorylated H1.2 in SDS-PAGE	127
Figure 3-16: No differences in the activating features of differently phosphorylated H1.2	128
Figure 3-17: SDS-PAGE of purified H1 histones from HL60 cells	131
Figure 3-18: CZE of H1 histones from control and apoptotic HL60 cells	132
Figure 3-19: Effect of H1 histones from control and apoptotic HL60 cells on DFF40 activity ...	133
Figure 3-20: Effect of H1 [°] on the DFF40 activity in purified nuclei	135
Figure 3-21: DNA fragmentation during apoptosis in HL60, Jurkat, and Raji cells	136
Figure 3-22: Effect of DFF40 and cytoplasm from HL60 and Raji cells on purified nuclei	137
Figure 3-23: Effect of caspase-3 and cytoplasm from HL60 and Raji cells on purified nuclei ...	139
Figure 3-24: DFF45 in native and heat-treated cytoplasmic extracts from HL60 and Raji cells	140
Figure 3-25: Plasmid assay with heat-treated cytoplasmic extracts from HL60 and Raji cells ..	141
Figure 3-26: Plasmid assay with native cytoplasm from HL60 and Raji cells	142
Figure 3-27: Expression levels of DFF45/DFF35 and caspase-3 in HL60 and Raji cells	143
Figure 3-28: Expression and localization of DFF40 and DFF45 in different cell types	146
Figure 3-29: DNA fragmentation and concomitant changes in protein levels during apoptosis	148
Figure 3-30: Localization of caspase-3, DFF45/DFF35, and HDAC-1 in Jurkat and Raji cells ...	149
Figure 3-31: LSM series demonstrating a mostly cytoplasmic localization of caspase-3	150
Figure 3-32: Morphologic features of Jurkat and Raji cells during apoptosis	151

Figure 3-33: Phase contrast microscopy and Hoechst 33342 staining of Jurkat cells.....	152
Figure 3-34: Phase contrast microscopy and Hoechst 33342 staining of Raji cells	153
Figure 3-35: Example for a killing kurve using Blasticidin on non-transfected Raji cells.....	156
Figure 3-36: Growth of Raji cells during selection using 10 µg/ml Blasticidin	157
Figure 3-37: Detection of recombinant myc-tagged proteins in stably transfected Raji cells...	158
Figure 3-38: Apoptotic morphology of mock-transfected Raji cells	159
Figure 3-39: Apoptotic morphology of DFF40-transfected Raji cells.....	160
Figure 3-40: Apoptotic morphology of DFF45-transfected Raji cells.....	161
Figure 3-41: Detection of PARP, DFF40, and DFF45 in the course of apoptosis in Raji cells ...	163
Figure 3-42: DNA fragmentation in stably transfected Raji cells	164
Figure 3-43: Expression levels of selected proteins in Raji single-cell clones	165
Figure 3-44: DNA fragmentation in the course of apoptosis in Raji cells	169
Figure 3-45: Changes in the protein levels in the course of apoptosis in Raji cells.....	170
Figure 3-46: Caspase-3 activities in Raji cells after induction of apoptosis by Topotecan	172
Figure 3-47: Caspase-3 activities in Raji cells: Two-way ANOVA with Bonferroni post-tests ...	174
Figure 3-48: Changes in the protein levels during the course of apoptosis in Jurkat cells.....	179
Figure 3-49: DNA fragmentation in the course of apoptosis in Jurkat cells.....	180
Figure 3-50: Caspase-3 activities in Jurkat cells after induction of apoptosis by Topotecan	182
Figure 3-51: Caspase-3 activities in Jurkat cells: Two-way ANOVA with Bonferroni post-tests	184
Figure 4-1: Structural formula of Topotecan-hydrochloride (trademark name: Hycamtin [®])...	204
Figure 4-2: Apoptotic events in Jurkat and Raji cell populations.....	208

III. TABLE INDEX

Table 1-1: Homologous apoptotic proteins in nematodes, mammals, and insects.....	13
Table 1-2: A comparison of events during apoptosis and necrosis.....	21
Table 2-1: Plasmids used for the expression of recombinant proteins in yeast	65
Table 2-2: Buffers for the purification of DFF40/DFF45 complex from E. coli.....	66
Table 2-3: Buffers for the purification of recombinant caspase-3 from yeast.....	68
Table 2-4: Separation conditions for CZE of H1 histones	72
Table 2-5: Composition of gels used for SDS-PAGE	73
Table 2-6: Composition of the western blotting stack.....	75
Table 2-7: Protocol used for immunostaining of proteins on NC-membranes.....	76
Table 2-8: Dilutions of the antibodies used for western blotting.....	77
Table 2-9: Titration of DFF40 activity	79
Table 2-10: Titration of caspase-3 activity	80
Table 2-11: Composition of PCR reactions	84
Table 2-12: PCR conditions.....	84
Table 2-13: Composition of the master-mixes used for cDNA synthesis	85
Table 2-14: Composition of ligase reactions using the vector pGEM [®] T easy.....	87
Table 2-15: Composition of ligase reaction mixtures using other vectors	87
Table 2-16: Buffers supplied with the Qiagen maxi prep kit	91
Table 2-17: Components of the MinElute gel extraction kit	92
Table 2-18: Conditions during sequencing reactions.....	94
Table 2-19: Apoptotic parameters tested in the course of this study	103
Table 2-20: Fluorescent dyes used in this study.....	104
Table 2-21: Working scheme for immunofluorescence labelling of cells	105
Table 3-1: Comparison of selected features in Raji single-cell clones.....	166
Table 3-2: Two-way ANOVA of caspase-3 activities in Raji cells (analysis of interaction).....	176
Table 3-3: Two-way ANOVA of Jurkat cells including analysis of interaction.....	185

IV. ABBREVIATIONS

Commonly used abbreviations are omitted.

A	
ADH1	Yeast alcohol dehydrogenase gene 1
AIF	Apoptosis inducing factor
ANOVA	Analysis of variance
AP	Alkaline phosphatase
Apaf	Apoptotic protease activating factor
APS	Ammonium persulfate
ATM	Ataxia telangiectasia mutated kinase
ATR	Ataxia telangiectasia related kinase
B	
Bad	Bcl X _L /Bcl-2 associated death promoter
Bak	Bcl-2 antagonist killer
Bax	Bcl-2-associated X protein
Bcl-2	A human proto-oncogene from a B cell lymphoma
BH	Bcl-2 homology domain
BCIP	5-Bromo-4-chloro-3-indolyl-phosphate
Bid	Bcl-2 interacting domain
Bik	Bcl-2 interacting killer
Bim	Bcl-2 interacting mediator of cell death
BIR	Baculoviral IAP repeat
BL21(DE3)pLysS	E. coli strain carrying the DE3 bacteriophage lambda lysogen
bp	Base pair
bsr	Blasticidin resistance gene from Bacillus cereus
BSD	Blasticidin resistance gene from Aspergillus terreus
C	
C.	Caenorhabditis
CAD	Caspase-activated DNase
CARD	Caspase recruitment domain
Caspase	Cystein-dependent aspartate-directed proteinase
CD	Cluster of differentiation
cDNA	Complementary DNA
Ced	C. elegans cell death abnormal gene

CED	C. elegans cell death abnormal gene product
CHAPS	(3-[(3-Cholamidopropyl)-dimethyl-ammonio]-1-propane sulfonate (a nondenaturing zwitterionic detergent)
CIP-1	See WAF1
CMV	Human cytomegalovirus
D	
$\Delta\Psi_m$	Mitochondrial inner transmembrane potential
Dapaf-1	Drosophila Apaf-1
DAPI	4',6-Diamidino-2-phenylindole
Dark	Drosophila Apaf-1 related killer
DCRM	Dead cell removal microbeads
DD	Death domain
Debcl	Death executioner Bcl-2 homologue (from Drosophila)
DED	Death effector domain
DEPC	Diethyl pyrocarbonate
DEVD-afc	(Aspartate-glutamate-valine-aspartate)-7-amino-4-trifluoromethylcoumarin (a fluorogenic tetrapeptide substrate for caspases 1, 3, 7, and 8)
DFF35	DNA fragmentation factor with a molecularweight of 35 kDa (inhibitor but no chaperone of DFF40)
DFF40	DNA fragmentation factor with a molecular weight of 40 kDa
DFF45	DNA fragmentation factor with a molecularweight of 45 kDa (inhibitor and chaperone of DFF40)
diablo	direct IAP binding protein with low pI
DMF	Dimethylformamide
DMSO	Dimethylsulfoxide
DNA-PK	DNA dependent protein kinase
DNase	Deoxyribonuclease
Dredd	Drosophila caspase with a long prodomain and a DED-motif
Dronc	Drosophila caspase with a long prodomain and a CARD-motif
ds	Double strand
DTT	D_L -Dithiothreitol
E	
E.	Escherichia
ECL	Enhanced chemiluminescence

Eco RI	Restriction enzyme from <i>E. coli</i> RY13 (5'...G/AATTC...3')
EDTA	Ethylenediaminetetraacetic acid
Egl-1	Egg-laying abnormal (phenotype of a <i>C. elegans</i> mutant)
EndoG	Endonuclease G (an evolutionary conserved mitochondrial protein)
EGTA	Ethylene glycol-bis-[β -amino-ethylether)-N,N,N',N'-tetraacetic acid
F	
FACS	Fluorescence activated cell sorter
Fas	Fibroblast associated
FADD	Fas associated protein with a death domain
FCS	Fetal calf serum
FLICE	FADD-like interleukin-1- β converting enzyme (caspase-8)
FLIP	FLICE-inhibitory protein
FITC	Fluorescein isothiocyanate
G	
Grim	Derived from the german term 'Sensenmann' (Grim reaper)
H	
H	Histone
HAC-1	<i>Drosophila</i> homolog of Apaf-1 and Ced-4
HEPES	N-2-Hydroxyethylpiperazine-N'-2-ethanesulfonic acid
HID	Head involution defective phenotype of a <i>Drosophila</i> mutant
Hind III	Restriction enzyme from <i>Haemophilus influenzae</i> (5'...A/AGCTT...3')
HMG	High mobility group
HMW	High molecular weight
HPMC	Hydroxypropylmethyl cellulose
HRP	Horseradish peroxidase
HSP	Heat shock protein
I	
IAP	Inhibitor of apoptosis protein
ICAD	Inhibitor of CAD
ICAD-L	Inhibitor of CAD large form
ICAD-S	Inhibitor of CAD short form
ICE	Interleukin-1- β -converting enzyme
insert	inserted DNA, DNA strand to be ligated into a vector
IPTG	Isopropyl- β -D-thiogalactopyranoside

K	
kb	Kilobase
kDa	Kilodalton
L	
LB	Luria Bertani
LSM	Laser scanning microscopy
M	
MACS	Magnetic activated cell sorting
mastermix	Pre-mixture of constant compounds in a reaction
MCS	Multiple cloning site
mM	mMole per liter
MOMP	Mitochondrial outer membrane permeabilization
MOPS	3-[N-Morpholino]propanesulfonic acid
N	
NBT	p-Nitro blue tetrazolium, also called 3,3'-(3,3'-Dimethoxy-4,4'-biphenylene)-bis-(2-p-nitrophenyl)-5-(phenyl)-2H-tetrazolium chloride
NF	Nuclear factor (usually a transcription factor)
NLS	Nuclear localization signal
NPC	Nuclear pore complex
NP-40	Nonidet P-40 (Igepal [®] CA-630) (a non-ionic detergent)
Nuc-1	Nuclease abnormal phenotype of a <i>C. elegans</i> mutant
NTA	Nitrilotriacetic acid
O	
OD ₆₀₀	Optical density measured at 600 nm
ORF	Open reading frame
P	
p _x	Protein with a molecular weight of <i>x</i> kDa
PAGE	Polyacrylamide gel electrophoresis
PARP	Poly (ADP-ribose) polymerase
PBS	Phosphate buffered saline
PCA	Perchloric acetic acid
PCD	Programmed cell death
PCR	Polymerase chain reaction
PFA	Paraformaldehyde
PIPES	Piperazine-N,N'-bis[2-ethanesulfonic acid]

PK	Proteinase K
PS	Phosphatidylserine
Puma	P53 upregulated modulator of apoptosis
R	
Reaper	Derived from the german term 'Sensenmann' (Grim reaper)
RNase A	Ribonuclease A, hydrolyses single-stranded RNA
RNase H	Ribonuclease H, hydrolyses RNA from a DNA:RNA hybrid
RPMI	Roswell Park Memorial Institute
RT	Reverse transcriptase
S	
S	Svedberg unit
S.	Saccharomyces
SCD ^{-Leu}	Synthetic complete medium except leucin with glucose
SCGL ^{-Leu}	Synthetic complete medium except leucin with glycerole and lactic acid
SDS	Sodium dodecyl sulfate (a denaturing anionic detergent)
SEM	Standard error of the mean
Smac	Second mitochondria derived activator of caspases, also called diablo
SOB	Complex cell growth medium for generating competent E. coli
ss	Single strand
SSP	Restriction enzyme from Sphaerotilus natans (5'-AAT/ATT-3')
T	
Taq	Thermophilus aquaticus
TBS	Tris buffered saline
TBST	Tris buffered saline containing Tween-20
TCA	Trichloroacetic acid
TE	Tris-EDTA-buffer
TELT	Tris-EDTA-lithium chloride-Triton X 100
TEMED	N,N,N',N'-Tetramethylethylenediamine
TNFR	Tumour necrosis factor receptor
TRADD	TNF-receptor associated protein with a death domain
Tween-20	Polyoxyethylenesorbitan monolaurate
V	
VDAC	Voltage-dependent anion channel

W	
WAF1	Wildtype p53-activated fragment 1, also called p21 or CIP-1
X	
x g	Multiplied by the acceleration of gravity (9.81 m/s ²)
Xba I	Restriction enzyme from <i>Xanthomonas badii</i> (5'...T/CTAGA...3')
Y	
YEPD	Yeast extract-peptone-glucose-medium
YPGLA	Yeast extract-peptone-glucose-lactic acid-medium

1. INTRODUCTION

Nowadays, it is a commonly accepted fact that life, at least that of multicellular organisms, is impossible without death. Programmed cell death (PCD) is a widespread biological phenomenon and its special form apoptosis is an exciting field of research, and currently one of the 'hottest spots' in cell biology. This is actually reflected in more than 98,000 publications, accessible via PubMed, containing the item 'apoptosis'. Though in the last two decades our understanding of this process has increased substantially, many of the underlying principles still remain obscure, especially those concerning the regulation of this process. The term PCD is often mixed up with apoptosis, but it should be mentioned in advance that apoptosis is a special form of PCD and that apoptosis is restricted to metazoan organisms.

Generally, apoptosis is an active mechanism for the silent removal of excess, unwanted or potentially dangerous cells, and it usually leaves no traces of the removed cell in vertebrates, thus avoiding an inflammatory reaction in immuno-competent organisms. Apoptosis is often contrasted with necrosis; however, presumably there is no clear borderline between both kinds of cell death as transitional forms are increasingly recognized. Moreover, recent findings suggest the existence of other forms of controlled death, which are subject to other regulation mechanisms.

'Classical' apoptosis may be defined as an active, energy-dependent process, characterized by morphologic changes which are caused as a consequence of a cascade of specific enzyme activities; these participating enzymes belong to the **caspase** family (cystein dependent **aspartate-directed proteinase**). Further hallmarks of apoptosis are: A central involvement of the mitochondria in the death process, a specific form of DNA degradation, and the final engulfment of the tightly packaged dying cell by surrounding cells. The executive and regulatory mechanisms of apoptosis are easier to see if they are considered in the evolutionary context, as detailed in the following.

1.1. EVOLUTIONARY AND PHYLOGENETIC ASPECTS OF PROGRAMMED CELL DEATH

The evolution of eukaryotes and the association of individual cells to a multicellular entity required an evolutionary process resulting in the invention of several apparently fundamental new functions and systems. Examples for such major eukaryotic innovations, apparently lacking direct prokaryotic precursors, are the eukaryotic chromatin remodelling machinery, the cell cycle regulation system, the nuclear envelope, the

cytoskeleton, and the process of programmed cell death (PCD) (*Maynard-Smith and Szathmary, 1997*).

Research on PCD has focused mainly on vertebrates, however, for an understanding of the basic mechanisms it is important to understand the reasons why and the way how PCD has been developed in the course of evolution. Therefore, this overview starts with a short introduction on evolutionary aspects of PCD in the different kingdoms.

1.1.1. PROGRAMMED CELL DEATH IN BACTERIA AND UNICELLULAR EUKARYOTES

The phenomenon of programmed cell death is not restricted to animals, not even to metazoan organisms because some unicellular eukaryotes and even bacteria are able to undergo PCD under certain environmental conditions, too. In these organisms PCD may occur in a state resembling a multicellular organism, e.g. during fruit body formation of myxobacteriae or building-up of the stalk of slime moulds (*Lewis, 2000*). Alternatively, it may have been developed in some species due to parasitic adaptation, as in the case of adaptation of unicellular eukaryotes to the host's organism. PCD in these organisms is presumably aiming at a downregulation of the host's immune response as described e.g. in *Leishmania major* (*Arnoult et al., 2002*). Interestingly, these ancient unicellular eukaryotes already display some key features of apoptosis, namely DNA fragmentation, caspase-like enzyme activities, and involvement of the mitochondria (*reviewed in Boyce et al., 2004*).

PCD is found in bacteria growing as individuals in suspension as well, so it was demonstrated during sporulation of *Bacillus subtilis* (*Smith and Foster, 1995; Levin and Grossman, 1998*), and PCD even allows an exchange of genetic material by transformation in *Streptococcus pneumoniae* (*Mortier-Barriere et al., 1998*). However, the mechanisms of PCD in prokaryotes seem to be unrelated to the mechanisms observed in eukaryotes (*Engelberg-Kulka and Glaser, 1999*), despite the fact that some of the enzymes involved in metazoan PCD obviously have phylogenetically ancient roots. These roots become evident in an increasing number of prokaryotic sequence homologues of these death enzymes which interestingly are found in a broad phyletic distribution including bacteria, but not in archaea (*reviewed in Koonin and Aravind, 2002*).

The fact that even single-celled organisms are able to undergo PCD suggests one more evolutionary reason for developing this altruistic mechanism. As, in addition to the parasitic threat, all living cells are prone to 'cell piracy' by viral infections, there is a considerable selective pressure to develop defence strategies preventing the infection of surrounding cells. And in turn, viruses are under the same selective pressure to defeat

the host-cell's defence system by cheating the death machineries of invaded cells by antagonizing mechanisms. Perhaps some of these antagonizing mechanisms were later overtaken by the hosts, subsequently again contributing to regulative mechanisms of the host-cells (*e.g. reviewed in Vaux et al., 1994*). In another, contrary scenario viruses may also promote excessive PCD to ensure their release from the infected cell (*Boya et al., 2001*). This is not necessarily a contradiction to the aforesaid since those mechanisms probably even exist in parallel in one type of virus or parasite and may be used differently in subsequent life phases of the respective virus or parasite. So, repression of PCD may occur during propagation, and induction of PCD may be necessary for dissemination.

1.1.2. PROGRAMMED CELL DEATH IN ANIMALS

Since PCD influences fundamental (patho-) physiological functions in animals, and a still growing number of human diseases, the overflowing literature concerning PCD and especially concerning apoptosis in the animal kingdom is immense and just a few examples can be cited here. Emerging evidence is found for a conserved core mechanism of apoptosis in the animal kingdom though there are also differences which are specific to the different phyla.

Important insights on apoptosis in development, especially concerning the nervous system, were obtained from research on the nematode *C. elegans*, as detailed later. Many neurons in the developing brain of vertebrates are condemned to die by apoptosis, thus allowing the formation of the complex structures in the nervous system (*e.g. reviewed in Yuan and Yankner, 2000*). But apoptosis also occurs during other steps of vertebrate embryogenesis *e.g.* in sculpturing the limbs by removing cells from the interdigital region or in the fusion of two epithelial sheets during neural tube closure. Furthermore, PCD deletes unneeded tissues during development *e.g.* the pronephric tubules in mammals (*reviewed in Mirkes, 2002*). But apoptosis is not restricted to the vertebrate's embryonal development. About 100,000 cells per second are generated by mitosis in a human, and this is balanced by a similar number of dying cells; most of them die by PCD (*Vaux and Korsmeyer, 1999*).

In the vertebrate immune system, apoptosis plays an important part in the elimination of auto-reactive B- and T-cell clones and during the killing of target cells by natural killing cells or cytotoxic T-lymphocytes. Furthermore, the number of reactive immune cells after an immune reaction is eventually downregulated by apoptosis to terminate the immune response (*e.g. reviewed in Janeway and Travers, 1999; Krammer, 2000*).

A lot of diseases are correlated with abnormalities in PCD; these may often be characterized as a consequence of excess apoptosis or by lacking apoptosis (*Nicholson,*

2000). Examples for diseases involving lack of PCD are autoimmune diseases, most cancers and many viral infections. Conversely, too much PCD occurs e.g. during neurodegenerative disorders (Alzheimer's Disease, Parkinson's Disease, Huntington's Disease), AIDS, stroke, myocardial infarction, and many traumatic injuries.

Nevertheless, some types of PCD in vertebrates obviously proceed without classical apoptosis. No enzymatic activity of caspases is observed in keratinocytes extruding their nuclei during terminal differentiation, and mammalian erythrocytes even survive for 120 days after they lost their nuclei; they are finally phagocytosed without the contribution of caspases (*reviewed in Vaux and Korsmeyer, 1999*).

In insects PCD involving caspase activities and DNA fragmentation is observed e.g. during embryogenesis and metamorphosis; so it is observed in *Drosophila* during ecdysone-dependent remodelling of larval organs such as the gut and salivary glands (*Quinn et al., 2000; Jiang et al., 1997*). PCD in *Drosophila* is often mediated by pro-apoptotic proteins as detailed later. These proteins principally act by counteracting the functions of apoptosis-inhibiting proteins which leads to the activation of caspases and finally results in cell death. This activation mechanism, using caspases and an additional indispensable protein which physically interacts with the caspase for activation, is homologous to the mechanism in vertebrates and nematodes (*e.g. Rodriguez et al., 1999; reviewed in Lee and Baehrecke, 2000*) and is described below.

Moreover, in the future the fly will turn out to be a valuable model organism to investigate regulation mechanisms for apoptosis because an increasing number of homologous apoptosis-relevant proteins is continued to be identified in *Drosophila* (*Rodriguez et al., 1999; Colussi et al., 2000; Zhang et al., 2000; reviewed in Vernooij et al., 2000, and Chen and Abrams, 2000; Sogame et al., 2003*).

1.1.3. PROGRAMMED CELL DEATH IN PLANTS

Increasing numbers of processes involving PCD are found in higher plants (*reviewed in Greenberg, 1996; Grudkowska and Zagdanska, 2004*). PCD contributes to the differentiation of the vascular system by generating xylem and phloem and influences senescence of leaves and petals (*Rubinstein, 2000; Thomas et al., 2000*). Furthermore, PCD is an integral part of the hypersensitivity-reaction in plants, aiming at a control of pathogens in plants (*e.g. Greenberg et al., 1994; Heath 2000; Lam et al., 2001*). Since PCD in plants is an active process, often accompanied by caspase-like enzyme activities, DNA degradation, and release of cytochrome c from mitochondria, it was occasionally compared with apoptosis in animals. However, PCD in plants often involves other signalling mechanisms and serves other aims than apoptosis in animals. An evident example for this difference is seen in trees, which mostly consist of dead cells. These

cells often died by PCD but their corpses still serve an architectural function. The existence of these dead cells is a first key feature separating plant PCD from apoptosis in animals, as the resulting corpse in plants is not necessarily removed from the organism, which, in contrast, is a paradigm of apoptosis in animals. In plants engulfment of a dying cell by surrounding cells is prevented by the plant cell wall. And, since the cell wall may be lysed in the course of subsequent degradation processes, the content of the dying cell is often spilled in the surrounding milieu; this is the second key feature separating plant PCD from apoptosis in animals (*reviewed in Beers, 1997; Lam, 2004*). Finally, in contrast to apoptotic animal cells, plant cells rather take part in their mode of decomposition by autophagy, using their vacuole as a storage vessel for the required special degrading enzymes. Vacuole collapse in the course of PCD is a controlled event and does not occur in necrotic plant cells (*Jones, 2001*). The composition of the vacuole content, actively determined in advance by the dying plant cell, often determines the resulting kind of tissue formed by PCD, so in the formation of aerenchyma or tracheary elements (*Jones, 2001; Kuriyama and Fukuda, 2002; Kozela and Regan, 2003*).

1.1.4. A CENTRAL ROLE FOR MITOCHONDRIA

Remarkably, the mitochondria have important regulatory and executive functions during PCD in all eukaryotes. Meanwhile, increasing evidence is found for multiple horizontal gene transfers from bacteria to eukaryotes and at least a part of the apoptosis-involved proteins most likely derive from the endosymbiont that gave rise to the mitochondrion. At least three theories, not necessarily excluding each other, exist concerning the acquisition of apoptosis-related proteins from the bacterial mitochondrion-precursor. Apoptosis-related proteins might have been imported pre-adaptations with a different function in early eukaryotes (*Koonin and Aravind, 2002*). Alternatively, these proteins might have been a parasite's tool for killing a host that became inhospitable, thus enabling the parasite to use the host's corpse until it moved to another host (*Frade and Michaelidis, 1997*). Another idea is that programmed cell death was necessary in metazoan organisms to get rid of infected cells before they infected neighbouring cells, and this host's defence reaction was compromised e.g. by anti-death proteins of the parasites (*James and Green, 2002*) which might have finally led to the symbiosis, generating the early eukaryote.

1.1.5. SUMMARY: EVOLUTION AND PHYLOGENY OF PCD

Considering the aforementioned facts, it may be concluded that at least altruistic PCD already has a role for survival of prokaryotes whereas a metazoan organism lacking the

ability to remove excess or potentially dangerous cells by PCD is hardly imaginable. This is also reflected by a broad phyletic distribution of this phenomenon in all eukaryotes, often involving the mitochondria as an organelle integrating regulative and executive steps in apoptosis. Though PCD may occur by differing mechanisms in the different kingdoms, it is obviously detectable in all multicellular eukaryotes, and it should even be regarded as one of the hallmarks of the multicellular state (*Skulachev, 2001*).

1.2. SOME MILESTONES IN APOPTOSIS RESEARCH

As indicated above, the often used term 'apoptosis' refers to a special case of PCD in metazoans and correctly should be restricted to members of the animal kingdom because it describes a process which differs from other types of PCD which may be observed in bacteria, plants, or fungi (*Koonin and Aravind, 2002; James and Green, 2002; Ameisen, 2002*). Moreover, it is often difficult to define a type of cell death as apoptosis since the existence of other forms of controlled death, which are subject to other regulation mechanisms, is increasingly recognized (*Wyllie and Golstein, 2001*). The term apoptosis refers to a mode of PCD which occurs as a consequence of a cascade-like activation of caspases. As a consequence of caspase activity, apoptosis may be associated with changes in cell morphology, cleavage of chromatin into large and nucleosomal fragments, and exposure of surface markers which target the dying cell for phagocytosis (*Samali et al., 1999*).

1.2.1. THE EARLY YEARS

The phenomenon of apoptosis was first recognized in vertebrates more than 150 years ago. In the year 1842 dying neuronal cells were recognized during normal amphibian development of the toad *Alytes obstetricians* (*Vogt, 1842*).

But the fact that cells die during normal development was forgotten and rediscovered several times; in these days many classical embryologists found it 'difficult to accept the idea of cells dying during embryogenesis and particularly in actively growing regions' (*Glucksmann, 1951*). So, it was not until 1951 when Glucksmann summarized the available data on cell death during vertebrate ontogenesis in an influential review, showing cell death to play an important part in the formation of virtually every tissue and organ (*Glucksmann, 1951*). However, it took until the 1970's when *Lockshin and Williams (1964)* discovered an underlying, obviously hormonally controlled mechanism for this kind of cell death in insects and created the term 'programmed cell death'. Two years later *Tata* found out that this mode of cell death is an active process and requires RNA- and protein synthesis during tail regression of tadpoles (*Tata, 1966*).

1.2.2. RECOGNIZING APOPTOSIS AS A BASIC BIOLOGICAL PHENOMENON

The term 'apoptosis' and the conceptual differentiation of apoptosis and necrosis was ultimately coined by Kerr and his colleagues (*Kerr et al., 1972*). By comparing the morphology of toxin-treated liver cells to that of hormone-treated lymphocytes, they found striking differences in the respective cell morphologies during cell death.

An electrifying recognition was that the hormone-treated lymphocytes showed a morphology already described for cells during developmental cell death by Glucksmann. Kerr, Wyllie, and Currie were the first who recognized that this form of cell death is ubiquitous in the animal kingdom and hypothesized that this type of death is a controlled process, complementary to mitosis, aiming at a regulation of cell populations and therefore completely different from uncontrolled 'accidental' necrotic cell death. To emphasize this difference, they proposed the greek term 'apoptosis', which describes the dropping off of petals from flowers or falling of leaves from trees (*Mirkes, 2001*).

But despite this fundamental finding, the interest in apoptosis remained low in the first instance. This was certainly caused by the circumstance that investigations on programmed cell death at that time were restricted mainly to a description of the correlated morphologic features. These were extensively characterized by light microscopy (*reviewed in Clarke and Clarke, 1996; Lockshin, 1997*) and electron microscopy (*e.g. Bellairs, 1961; O'Connor, 1974*).

1.2.3. FIRST MARKERS INDICATING APOPTOSIS

Apart from the microscopic characterization of morphologic features the first morphology-independent marker for apoptosis was the rapid activation of endonucleases during apoptosis (*Williams et al., 1974*) which results in a typical DNA ladder seen after electrophoresis (*Hewish and Burgoyne, 1973*). Subsequently, this DNA laddering was considered as one hallmark of apoptosis (*Wyllie, 1980*). However, it took another 17 years until the major responsible DNase - named DFF (DNA fragmentation factor) or CAD (caspase-activated DNase) - was identified (*Liu et al., 1997; Enari et al., 1998*).

Another apoptotic marker, which was established much later, was the exposure of phosphatidyl serine (PS) on the outer membrane of the cell surface. Additionally, this observation gave a first hint on the mechanisms of removal of apoptotic cells under physiological conditions (*Fadok et al., 1992*). PS-exposition is one of the 'eat-me' signals for surrounding cells or macrophages which subsequently leads to the engulfment of the apoptotic cell. This hypothesis was confirmed later by demonstration of a putative PS-receptor protein on phagocytes (*Fadok et al., 2000*).

1.2.4. IMPORTANT INPUT FROM C. ELEGANS AND DROSOPHILA

In the field of developmental genetics in invertebrates the nematode *Caenorhabditis elegans* proved as an ideal model organism for a further understanding of the underlying mechanisms. It was already known that nematodes are eutelic, possessing constant cell numbers after hatching. Additionally, the fate of any cell can be easily observed in this transparent organism. So, by selecting *C. elegans* for the study of developmental genetics, S. Brenner created the fundamentals for the genetic analysis of cell fates during development. Already in 1963 he proposed, '...to identify every cell in the worm and trace lineages. We shall also investigate the constancy of development and study its genetic control by looking for mutants.' (*Cited by Brenner in: Horvitz and Sulston, 1990*).

Finally, the studies from Brenner, Horvitz, and Sulston established a Nobel-Prize-winning model for an 'overall molecular genetic pathway for PCD in *C. elegans*' (*Horvitz, 2002*) Generally, PCD involves an interaction of a death signalling molecule with an inhibitor of PCD thus freeing an adaptor molecule which finally activates an executioner of PCD. These molecules are arranged in a cascade-like manner (*reviewed in Putcha and Johnson, 2004*).

Importantly, increasing evidence is found that the same basic principles apply to PCD in vertebrates and even in insects because these cell death mechanisms were already demonstrated in *Drosophila* (*e.g. reviewed in Chen and Abrams, 2000*).

1.2.4.1. Apoptosis in nematodes

Interest concerning PCD-research focused on *C. elegans* by the finding that exactly 131 of the 1090 somatic cells are genetically destined to die during the worm's development (*Ellis and Horvitz, 1986*), thus ensuring constant cell numbers in these organisms. Cell death in developing *C. elegans* was already recognized 10 years before (*Sulston, 1976*), and it was already supposed that cell death in *C. elegans* is an active process, solely aiming at the removal of unwanted cells (*Horvitz et al., 1982*).

Experiments with *C. elegans* provided the first evidences for the existence of genetic information specific for the control of cell death during neuronal development (*Hedgecock et al., 1983; Horvitz et al., 1983; Ellis et al., 1986*). The first identified gene affecting cell-death in *C. elegans* was *nuc-1* (**nuc**lease-abnormal), controlling an endonuclease activity, so the mutants were defective in DNA degradation during PCD (*Sulston, 1976*). The analysis of genetic mutants of *C. elegans* with abnormal patterns of PCD finally revealed that developmental PCD in neuronal cells of *C. elegans* is dependent on the gene products of only four genes (*Hengartner, 2000; Meier et al.,*

2000). Additionally, there are at least another six or seven proteins involved in the final engulfment of the dying cells by neighbouring cells (*Savill and Fadok, 2000; Horvitz, 2002*). One of the death-associated genes is **ced-3** (*C. elegans cell death abnormal gene*). It was identified by analyzing mutants lacking PCD and revealed that cells normally fated to die during development instead survived and differentiated into functional cells in *ced-3* mutants (*Ellis et al., 1986; Avery and Horvitz, 1987*).

Other key cell death genes of *C. elegans* were subsequently identified, among them were *ced-4*, *ced-9* and **egl-1** (*egl* refers to the **egg** laying mutant phenotype). **CED-4** (*CED*, written in capital letters, means the respective *ced* gene product) was shown to be essential for the activity of *CED-3* by direct interaction of both proteins (*Yuan and Horvitz 1990; Yuan and Horvitz, 1992*); it is an adaptor-molecule and enables auto-catalyzed cleavage of *CED-3* by oligomerizing *CED-3*, putting it in spatial proximity which is a prerequisite for its enzymatic self-activation (*Salvesen and Dixit, 1999*).

On the other hand, **CED-9** was demonstrated to protect cells which are determined to survive during *C. elegans* development from PCD (*Hengartner et al., 1992*). It acts by binding *CED-4*, thus preventing it from oligomerizing *CED-3*. *EGL-1* was later found to act upstream of *CED-3* in promoting apoptosis because it is an antagonist of *CED-9*: *EGL-1* prevents *CED-9* from binding to *CED-4*, allowing *CED-4* to oligomerize and activate *CED-3* (*Conradt and Horvitz, 1998*). The mode of action of these proteins occurs by a cascade-like activation mechanism which finally results in cell death.

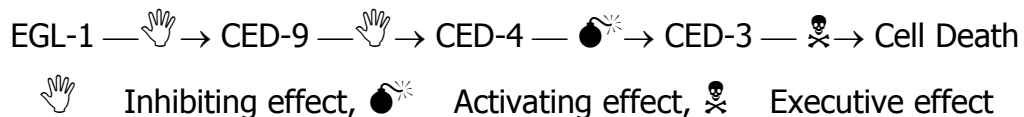


Figure 1-1: The core molecular mechanism of PCD in *C. elegans*

1.2.4.2. Apoptotic homologous proteins in nematodes and vertebrates

So far, these findings in *C. elegans* demonstrated an elegant activation mechanism for PCD, but interest in *C. elegans* increased only when the participating molecules were eventually shown to be the genuine homologues of vertebrate proteins acting during apoptosis. A first comparison of developmental cell death during early morphogenesis in vertebrates and invertebrates was made in 1969 (*Whitten, 1969*), but it was not until 1992 when a first link between apoptosis in vertebrates and PCD in invertebrates was demonstrated. Human **bcl-2** is a **B** cell lymphoma proto-oncogene, which was known to be transformed in follicular lymphoma cells (*Tsujimoto et al., 1985; Vaux et al., 1988*) resulting in its over-expression. By comparing the amino acid sequences of human *bcl-2* and the open reading frame of *ced-9* from *C. elegans*, Hengartner and

Horvitz found striking similarities and concluded that bcl-2 might function in human cancers by antagonizing PCD (*Hengartner and Horvitz, 1994; reviewed in Horvitz, 2002*). At about the same time, Vaux demonstrated in transfection-experiments that human bcl-2 was able to inhibit PCD in *C. elegans* (*Vaux et al., 1992*). Subsequently, Hengartner found that human bcl-2 restored ced-9 activity in ced-9 mutant *C. elegans* (*Hengartner and Horvitz, 1994*). These were important linking experiments in apoptosis research since they showed that apoptosis in vertebrates and PCD in invertebrates are likely to be the same, evolutionary conserved process. Furthermore, it put the basis for general conclusions from the nematode *C. elegans* concerning the genetic understanding of PCD and the molecular processes during PCD.

However, even homologous molecules may have distinct interaction modes in different species. So, in *C. elegans* CED-9 physically interacts with CED-4 to inhibit apoptosis whereas mammalian bcl-2 and apaf-1 presumably do not (*reviewed in Cecconi, 2001*). Nevertheless, bcl-2 is a molecule with an anti-apoptotic effect in mammals.

Later findings further confirmed the cell death homologies between nematodes and vertebrates, so CED-3 was e.g. later shown to be similar to a mammalian **ICE**-protein (**interleukin-1- β converting enzyme**) (*Yuan et al., 1993*) and to have cleavage preferences similar to that of human caspase-3 (*Xue, 1996*).

1.2.4.3. Evidence for homologous apoptotic proteins in insects

The results obtained later from *Drosophila* support the hypothesis of homologous cell death mechanisms: Both *C. elegans* CED-3 and human caspase-3 are similar to the *Drosophila*-caspase **drICE** (**Drosophila ICE**) (*Fraser and Evan, 1997*). CED-3 and ICE were the founding members of a new enzyme family, namely the caspases (**c**ystein dependent **a**spartate-directed protein**a**ses) in which inactive pro-enzymes are activated in a cascade-like manner by (auto-) catalytic cleavage (*e.g. reviewed in Cohen, 1997; Earnshaw et al., 1999; Kidd, 2000*). CED-4 has a human counterpart in the homologous protein **Apaf-1** (**a**poptotic **p**rotease **a**ctivating **f**actor), which participates in cytochrome c dependent activation of the executioner caspase-3 (*Zou et al., 1997*). While accessible CED-4 is sufficient for activation of CED-3 in nematodes, the human counterparts Apaf-1 and caspase-9 need cytochrome c and ATP to form a structure called apoptosome, which serves to generate active effector caspases (see chapters 1.3.1.3. and 1.3.3.2).

In homology to the molecule CED-4 in *C. elegans* or Apaf-1 in mammals, a molecule named **Dark** (**Drosophila Apaf-1 related killer**, also called Dapaf-1 or HAC-1) is necessary for the activation of the *Drosophila* caspase-9 homologues Dredd and Dronc during some apoptotic pathways in *Drosophila* cells. In contrast to its homologue CED-4 in *C. elegans*, but interestingly in parallel to its homologue Apaf-1 in mammals, Dark

presumably needs cytochrome c for the activation of the caspase Dronc. In contrast to mammals, cytochrome c is not released from the mitochondria in *Drosophila*. Instead, the *Drosophila* apoptosome is formed in the vicinity of the mitochondria (*Dorstyn et al., 2002*).

1.2.4.4. Bcl-2 family members in nematodes, insects, and mammals

While trying to investigate the mechanism of bcl-2 action, the search for binding partners for bcl-2 revealed other pro- and anti-apoptotic members of the bcl-2 superfamily in mammals. These family members share certain protein domains which were named **BH** domains (**bcl-2 homology**). They may interact with each other via their homologous domains, and the domains define their specific actions as pro- or anti-apoptotic proteins. The BH-3-only proteins generally promote apoptosis whereas bcl-2-like proteins containing additional BH-domains (BH1-4) act as pro- or anti-apoptotic proteins. The first, discovered pro-apoptotic bcl-2-family member was **bax** (**bcl-2-associated X** protein). Bax was demonstrated to homodimerize with itself and to heterodimerize with bcl-2, and overexpressed bax was found to accelerate apoptosis by countering bcl-2-mediated survival of the cells. This suggested a model in which the ratio of bax to bcl-2 determines the cell's fate after obtaining an apoptotic stimulus (*Oltvai et al., 1993; Oltvai and Korsmeyer, 1994*). The role of other bcl-2 family members during mammalian apoptosis and their interactions with mitochondria is described in chapter 1.3.2. Interestingly, domains similar to BH3 were found in the pro-apoptotic *C. elegans* protein EGL-1 as well, once again demonstrating a conserved mechanism of PCD (*Conradt and Horvitz, 1998*).

The bcl-2 family of proteins may be subdivided into three groups (*Adams and Cory, 1998*):

- Anti-apoptotic bcl-2 members are e.g. bcl-2, bcl-X_L (*Boise et al., 1993*), and CED-9.
- Pro-apoptotic bcl-2 members are e.g. bax, bak (*Chittenden et al., 1995*), bok (*Hsu et al., 1997*), and bcl-X_S (*Boise et al., 1993*).
- Members of the BH3-family are e.g. bid (*Wang et al., 1996*), bad (*Yang et al., 1995*), bim (*O'Connor et al., 1998*), and EGL-1.

Bcl-2 like proteins were also demonstrated in *Drosophila*, e.g. pro-apoptotic **Debcl** (**Death executioner bcl-2** homologue, *Colussi et al., 2000*) or pro-apoptotic **Drob-1** (first **Drosophila bcl-2** family member, *Igaki et al., 1999*). In contrast to the existence of BH3-only proteins in both mammals and nematodes, BH3-only proteins were not yet identified in *Drosophila*. Another *Drosophila* bcl-2 member, buffy, shows weak anti-apoptotic activities (*Quinn et al., 2003; reviewed in Igaki and Miura, 2004*).

1.2.4.5. Other inhibitors of apoptosis in mammals and insects

PCD in *Drosophila* is often mediated by the pro-apoptotic proteins **grim** (*Chen et al., 1996*), **reaper** (*White et al., 1996; Nordstrom et al., 1996*), and **hid** (**head involution defective**) (*Grether et al., 1995*). Interestingly, though neither mammalian nor *C. elegans* homologous counterparts for these pro-apoptotic proteins have been identified to date, these molecules are able to induce apoptosis in mammalian cultured cells as well (*McCarthy and Dixit, 1998; Claveria et al., 1998; Haining et al., 1999*), and thus they are not necessarily a contradiction to the idea of a general conserved core-mechanism for apoptosis in the animal kingdom. These proteins act by inhibiting the functions of **IAPs** (**I**nhibitor of **A**poptosis **P**rotein) which leads to the activation of caspases and finally results in apoptosis. A putative functional mammalian analogue to grim, hid, and reaper may be **smac** (**s**econd **m**itochondria derived **a**ctivator of **c**aspase, also termed Diablo) (see chapter 1.3.1.3) but mammalian smac/diablo has no sequence similarities to *Drosophila* reaper, grim, or hid (*reviewed in Tittel and Steller, 2000*)

1.2.4.6. Homologous proteins in a core apoptotic pathway

The experimental data obtained until now demonstrate the existence of a conserved core molecular pathway which is found in nematodes, insects, and vertebrates. However, though there are important core molecular parallels in the apoptotic pathways of these organisms, it should be noticed that there are additional specific molecules and pathways, which are active during apoptosis in the different organisms. Moreover, there is increasing evidence that caspases are not the only executioners of apoptosis since the existence of caspase-independent apoptotic pathways was clearly demonstrated in the last years. Interestingly, even these caspase-independent pathways are obviously evolutionary conserved. Concerning the caspase-dependent signalling pathways to apoptosis, there is an important mechanistic difference in the apoptotic signalling when nematodes are compared with vertebrates or insects: It seems that cytochrome c is not necessary for progression of apoptosis in *C. elegans*, suggesting less mitochondrial input on caspase-dependent apoptosis in nematodes.

The following table (1-1) gives an overview on homologous proteins which act during caspase-dependent apoptosis in organisms of the few different phyla investigated to date.

Feature	Protein	C. elegans	Mammals	Drosophila
Cell death signalling protein	BH3-only	EGL-1	e.g. Bid	Not yet identified
	Bcl-2 like		e.g. Bax	Debcl/Drob-1
Inhibitor of PCD	Bcl-2-like	CED-9	e.g. Bcl-2	Buffy
Adaptor	Apaf-1-like	CED-4	Apaf-1 (+cytochrome c +ATP)	Dark/Dapaf-1/HAC-1 (+cytochrome c)
Executioner	Caspases	CED-3	e.g. Caspase-9	Dronc/Dredd
Cell death				

Table 1-1: Homologous apoptotic proteins in nematodes, mammals, and insects

However, the signalling events, finally leading to the apoptotic cascade in *C. elegans*, mammals, and *Drosophila*, are far away from being completely understood to date. Especially the early events during apoptotic signalling, affecting the decision of a cell to die or not to die, rather seem to resemble a three-dimensional network, which serves to integrate a multitude of both pro- and anti- survival/death signals.

1.3. APOPTOSIS IN MAMMALIAN CELLS

To simplify the matters, the biochemistry of apoptosis is described for mammalian cells only in the following section. Apoptosis may be induced in mammalian cells via two basically different signalling mechanisms: The death receptor pathway and the mitochondrial pathway. This fact reflects the ability of the mammalian cell to respond to external apoptotic signals as well as to internal cell death signals. External death signals are mediated by receptors to the cell whereas internal signals aim in a first step on the mitochondria as an organelle able to integrate both pro- and anti-apoptotic signals. The exact characteristics of the internal signals, which often 'activate' the mitochondria as an executing organelle of apoptosis, are still controversially discussed and may be affected e.g. by p53-dependent pathways after DNA damage or 'mitotic catastrophes' (reviewed in *Evan and Littlewood, 1998; Green and Kroemer, 2004*). In general, it is obvious that stress and damage is sensed by the cell very carefully by different mechanisms and that mild injury may result in apoptosis rather than necrosis. A growing number of identified pro- and anti-apoptotic proteins suggests that susceptibility to apoptosis is, at least in part, determined by multiple dimerizing pro- and anti-apoptotic molecules (e.g. reviewed in *Oltvai and Korsmeyer, 1994*). These

proteins are competing for binding partners and thus act as a 'cellular rheostat' by determining the threshold for apoptotic signals in inducing a cell response. Members of the bcl-2-super family e.g. play an important part in this cellular rheostat. Moreover, there are different IAPs and viral proteins, e.g p35, which are able to keep apoptotic caspase activities under control (*reviewed in Deveraux and Reed, 1999; Clem, 2001*).

Though there are two major signalling pathways during apoptosis, there are cross-linking steps between both extrinsic and intrinsic signalling ways which may be activated in the course of already initiated apoptosis to ensure a fast progression of apoptotic events in those cells which are condemned to die. Since caspases and bcl-2 family members are important key molecules in mammalian apoptosis, these proteins are characterized first in the following chapters.

1.3.1. MAMMALIAN CASPASES

To date, 14 members of the caspase family have been identified in mammals, and out of these, seven may be activated during apoptosis in humans (*Kumar, 1999; Fuentes-Prior and Salvesen, 2004*). The caspase-family of cystein proteases may be divided into two basic subfamilies: One is involved in processing of cytokines, e.g. during inflammatory responses (caspase-1 subfamily, ICE proteases), and the other one plays an important role in apoptosis (CED-3-like subfamily). The latter group of caspases may be further subdivided into two groups: Caspases containing a short prodomain and caspases with a long prodomain.

Mammalian ICE proteases were the first characterized members of the caspase family, identified as a novel kind of aspartate-specific cystein-dependent proteases required to convert pro-interleukin-1 β into its mature form by proteolysis (*Cerretti et al., 1992; Thornberry et al., 1992*). Involvement of ICE-like proteases during apoptosis was first demonstrated in *C. elegans* with the cloning of the *C. elegans* caspase gene *ced-3* (*Yuan et al., 1992*). A striking link to mammalian apoptosis emerged when transient expression of CED-3 or ICE was demonstrated to induce apoptosis in mammalian fibroblasts as well (*Miura et al., 1993*). As detailed in the following, all members of the caspase-family share several unifying features.

1.3.1.1. Mechanisms of caspase activation

Caspases are ubiquitously and constitutively expressed as catalytically inactive proenzymes which require specific proteolysis to be converted into active enzymes. Generally, caspases consist of three domains: An amino-terminal prodomain which is variable in length, a large subunit, and a small subunit. Cleavage of the proenzyme at specific aspartate residues (caspase consensus sites) activates the caspase by removing

the prodomain and releasing both the small and the large subunit which subsequently form a heterodimer. Active caspase is composed of two such heterodimers forming a tetrameric structure (*Walker et al., 1994; Wilson et al., 1994; Rotonda et al., 1996*). As indicated by their name, all **caspases** cleave their substrates carboxyterminal to an **aspartate** residue (called P1 site). The fact that most caspases are themselves activated by cleavage at specific aspartate residues suggests that at least some caspases may be responsible for their own activation by autoproteolysis and/or may trans-activate other caspases in a cascade-like manner. This mode of activation resembles the activation process of the complement or the coagulation system: A cascade-like arrangement of (auto) proteolytic enzymes serves to transmit and amplify death signals during apoptosis.

Apoptotic caspases may be subdivided in two basic groups: Initiator caspases containing a long prodomain and effector caspases with a short prodomain. Initiator caspases presumably possess intrinsic proteolytic activity and are activated by an adaptor-mediated oligomerization which is mediated by certain domains in their long prodomain (see chapter 1.3.1.3). Putting several initiator procaspases of the same type into spatial proximity leads to trans-activation of the oligomerized caspases (induced proximity hypothesis by *Salvesen and Dixit, 1999*). These activated initiator caspases serve to cleave and activate effector procaspases which are characterized by a short prodomain and subsequently cleave a large number of cellular proteins as detailed below.

1.3.1.2. Substrate specificities of caspases

Despite their absolute requirement for an aspartate at the substrate's P1 site, the individual caspases have different substrate preferences especially concerning the four amino acids following directly amino-terminal to the P1 site. Moreover, the tertiary structure of the proteins seems to be important for the different caspases in recognizing their specific substrates since not all of the possible caspase consensus sites are cleaved in vivo. Hence, all caspases show a substrate specificity which is indispensable in their functioning during apoptosis or inflammation (*reviewed in Cryns and Yuan, 1998; Nicholson, 1999*). Since all caspases cleave their substrates after aspartate sites, they are among the most specific proteases characterized to date. Remarkably, inactivation of proteins by caspases is often achieved by just one single, specific cut in the substrate. This way caspases are able to disassemble a cell within 30 to 60 min during apoptosis by using three basic strategies (*reviewed in Thornberry and Lazebnik, 1998*):

- Caspase-induced cleavage of proteins during apoptosis may inactivate inhibitors of apoptosis or activate proteins which promote apoptosis and the engulfment of the dying cell by inducing the presentation of eat-me signals to surrounding cells.
- Destruction of proteins which are important for the maintenance of cell structures contributes to the disassembly of the cell.
- Caspases often deregulate important cellular proteins effectively by separating regulatory and catalytic subunits.

Consequently, possible victims of caspase activity are found in a wide variety of cellular functions: Cytoskeletal and structural proteins as well as proteins involved in cell cycle and replication, transcription and translation, DNA cleavage and repair, signal transduction (e.g. kinases, phosphatases), immune regulation, and, as detailed above, even other procaspases may be the targets (*e.g. reviewed in Stroh and Schulze-Osthoff, 1998; Utz and Anderson, 2000; Fischer et al., 2003*). Finally, despite their destructive role during apoptosis there is increasing evidence that activities of apoptotic caspases even seem to contribute to proliferation and differentiation in some cases (*Wang and Lenardo, 2000; Fischer et al., 2003*). So, caspase-8 activity seems to be essential for the differentiation of heart muscle cells and haematopoietic progenitor cells during embryogenesis (*Varfolomeev et al., 1998*), and caspases play important roles in synaptic plasticity and even neuroprotection in the brain (*reviewed in McLaughlin, 2004*).

1.3.1.3. Regulation of caspase activities

Though the prodomain is no longer present in an active apoptotic caspase, it has an important role during the activation process by determining the activating molecules for interaction with a specific caspase. Therefore, the amino-terminal prodomains vary considerably in length and amino acid sequence. Regarding the apoptotic caspases, effector caspases (caspase-3, -6, and -7) possess short prodomains whereas initiator caspases (caspase-8, -9, and -10) are characterized by long prodomains. (The position of a further apoptotic caspase, caspase-2, is not exactly clarified yet: Though it contains a long prodomain and is activated by oligomerization, it presumably has effector caspase functions as well [*Kumar and Vaux, 2002; Troy and Shelanski, 2003*]). Furthermore, the initiator caspases may be additionally subdivided into two subgroups since two distinct modules dictating the protein-protein interaction of the procaspases have been identified in the long prodomains.

The first identified interacting module has been called **DED** (**d**eath **e**ffector **d**omain), and two DEDs are present in both caspase-8 and -10 (*Boldin et al., 1996; Fernandes-Alnemri et al., 1996; Muzio et al., 1996; Vincenz and Dixit, 1997*). These DEDs target the

respective caspase to ligand-activated death receptors (e.g CD95/Fas/APO-1, TNFR1, or DR3) in the cell membrane when these receptors are crosslinked and oligomerized by binding their respective, extracellular ligand. DEDs are therefore responsible for initiating the extrinsic apoptotic pathway. However, DEDs do not bind directly to the receptor but require specific adaptor molecules containing a **death domain (DD)**: **FADD** (Fas associated protein with **DD**) for oligomerization near the CD95/Fas/APO-1 receptor or **TRADD** (TNF-receptor associated protein with **DD**) for oligomerization near TNF-receptors. This may in part explain the regulation of susceptibility or resistance of an individual cell towards certain extrinsic triggers for apoptosis: By regulating the number of receptors and/or the number of adaptor proteins, the cell may be fine-tuned in its caspase-mediated response to extrinsic apoptotic signals. Receptor, adaptor, and caspase form a membrane bound **death inducing signalling complex (DISC)** upon activation.

Another module which determines the interaction of procaspases with other molecules is called **CARD** (**caspase recruitment domain**). In contrast to DED, it acts in cellular intrinsic pathways of apoptosis and is found in the human apoptotic caspases -2 and -9 as well as in the human inflammatory caspases -1, -4, and -5. CARD domains were also found in adaptor proteins acting during apoptosis e.g. in *C. elegans* CED-4 and in its mammalian homologue apaf-1 as well as in other adaptor proteins acting during inflammation. In analogy to its extrinsic counterpart DED, the CARD domain mediates an oligomerization of their initiator procaspases on scaffold molecules in the cytoplasm. So, these caspases are subsequently activated in a special structure called apoptosome in the case of apoptotic caspases or inflammasome for inflammatory caspases (*Srinivasula et al., 2002; Martinon et al., 2002; Fuentes-Prior and Salvesen, 2004; Philchenkov, 2004*). In the mammalian apoptosome, the adaptor protein apaf-1 serves as a molecular scaffold for the activation of caspase-9. However, a functional mammalian apoptosome requires additional ATP and cytochrome c, linking this intrinsic pathway to the mitochondria as an apoptosis-signalling organelle. This also allows an interaction of another family of apoptotic regulators: The bcl-2-family members (see chapter 1.2.4.4. and 1.3.2).

Considering the potential autocatalytic properties of caspases, it is evident that caspase activities have to be tightly regulated in the cell since unwanted activation of the enzymatic activation cascade would be fatal for the cell. Furthermore, viruses and intracellular parasites are under a constant selective pressure to refine their strategies for controlling their host cells' apoptotic defense mechanisms. Therefore, several inhibiting mechanisms have been described in mammalian cells, and expression levels of those caspase-inhibitors might affect a cell's sensitivity towards apoptotic signals.

An important group of caspase-inhibitors are the inhibitors of apoptosis proteins (**IAPs**). They were first identified in baculoviruses (*Crook, 1993*) and are characterized by carrying one or more **BIR**-domains (**b**aculoviral **I**AP **r**epeat) (*Deveraux and Reed, 1999*). They are able to inhibit both initiator and effector caspases, but they target distinct caspases (*reviewed in Fesik and Shi, 2001; Bortner and Cidlowski, 2002*). So, several IAPs directly bind to and inhibit caspases -3, -7, and -9, whereas other caspases (-1, -6, -8, and -10) are not affected by these inhibitors (*Roy et al., 1997; Deveraux et al., 1998*). Interestingly, there are other inhibitors which in turn inhibit these inhibitors and thus contribute to the induction of apoptosis: Human **smac** (**s**econd **m**itochondria-derived **a**ctivator of **c**aspase) or its mouse homologue **diablo** (**d**irect **I**AP **b**inding protein with **l**ow pI) (*Du et al., 2000; Verhagen et al., 2000*).

Another group of inhibitors, e.g. **FLIPs** (**F**LICE-inhibitory **p**roteins), acts at the level of the DISC-formation during receptor-mediated apoptotic signalling (FLICE is another name for caspase-8), and both mammalian and viral members of this group have been described (*Thome et al., 1997; Irmeler et al., 1997*).

1.3.2. MAMMALIAN BCL-2 FAMILY MEMBERS AND THE MITOCHONDRIA

The mitochondria play a critical role in mammalian apoptosis, and loss of mitochondrial membrane potential or depolarization occurs in numerous apoptotic systems though altered mitochondrial functions have also been identified in other kinds of cell death, e.g. necrosis. Apart from their role as cellular power stations, mitochondria are an important reservoir for a number of caspase-dependent and caspase-independent death proteins which may be released under tightly controlled conditions during apoptosis (or accidentally during necrosis). In non-apoptotic cells those proteins are stored in the intermembrane space of the mitochondria. Interestingly, some of these death proteins have dual-functions: They fulfil important, vital tasks in a normal cell and are converted to deathly weapons after induction of apoptosis. Prominent examples for such dual-function proteins in mitochondria are cytochrome c and **AIF** (**a**poptosis **i**nducing **f**actor). The in-vivo functions of AIF in the mitochondria are still elusive: AIF seems to be an oxidoreductase which is at least in vitro able to catalyze a reduction of cytochrome c; furthermore, it might act as a general mitochondrial antioxidant (*reviewed in Cande et al., 2002*). As soon as it is released from the mitochondria, AIF causes chromatin condensation and high molecular weight (HMW) DNA fragmentation in the nucleus (*Susin et al., 1999*), whereas cytosolic cytochrome c is essential for the formation of the apoptosome in vertebrates (*Liu et al., 1996; Yang et al., 1997; Kluck et al., 1997; Zou et al., 1997*). Anti-apoptotic Bcl-2 was able to inhibit cytochrome c release whereas the pro-apoptotic bcl-2-family member bax was shown to promote

cytochrome c release from the mitochondria (Yang *et al.*, 1997; Kluck *et al.*, 1997; Zamzani *et al.*, 1996; Reed, 1997). This indicated that mitochondrial events during apoptosis are affected by bcl-2 family members, and there is increasing evidence that mammalian pro- and anti-apoptotic bcl-2 family members integrate apoptotic signals by using the mitochondria as a molecular scaffold and even as a launching basis for death proteins. However, a direct interaction of pro- and anti-apoptotic bcl-2 family members is just one mode of action for the control of apoptosis in mammals.

Members of the bcl-2 family carry at least one out of four BH-domains (see chapter 1.2.4.4), and more than 20 family members have been found to date. Many bcl-2 family members, both pro- and anti-apoptotic, contain a C-terminal membrane anchoring sequence which localizes them to the outer membranes of the nucleus or the mitochondria as well as to membranes of the endoplasmic reticulum (Krajewski *et al.*, 1993; Akao *et al.*, 1994; Nguyen *et al.*, 1994; Lithgow *et al.*, 1994).

A pivotal prerequisite for the participation of mitochondria in apoptosis is a controlled **mitochondrial outer membrane permeabilization (MOMP)** which allows the release of pro-apoptotic proteins from the intermembrane space. The mechanisms of MOMP are not well understood to date and remain controversial. At least two classes of mechanisms have been described, and those are not necessarily excluding each other since they might be activated under differing cellular circumstances. The first mechanism affects the inner mitochondrial membrane: Apoptotic stimuli may open a putative **permeability transition (PT)** pore in the inner membrane, thus allowing an exchange of water and molecules up to ~1.5 kDa in size. Opening of this putative PT pore results in a loss of the mitochondrial inner transmembrane potential ($\Delta\Psi_m$) due to an equilibrating migration of ions. Furthermore, entering water causes swelling of the matrix. Matrix swelling may be sufficient to rupture the outer mitochondrial membrane while the inner membrane is still intact (Green and Reed, 1998; Green and Kroemer, 2004).

A second mechanism does not involve PT pore formation on the inner mitochondrial membrane but action of bcl-2 family members on the outer mitochondrial membrane. The multi-BH domain proteins bax and **bak (bcl-2 antagonist killer)** seem to be essential for MOMP at least in mice (Wei *et al.*, 2001), and some studies indicate an interaction of the **voltage-dependent anion channel (VDAC)** with these proteins (Shimizu *et al.*, 2001). Members of the pro-apoptotic bcl-2 subfamily of bh3-only proteins act by either inhibiting anti-apoptotic bcl-2 members or by activating multi-BH domain proteins which contribute to MOMP (Letai *et al.*, 2002).

There are several basic mechanisms of bcl-2 family members which contribute to protecting cells from apoptosis via mitochondria:

- Strengthening the outer mitochondrial membrane may prevent mitochondria from excessive swelling and subsequent rupturing and is e.g. one of the modes of protective action of bcl-X_L and bcl-2 (*Harris and Thompson, 2000*).
- Maintaining the normal physiology of mitochondria prevents loss of $\Delta\Psi_m$ and an overproduction of reactive oxygen species (ROS); this was e.g. demonstrated for bcl-X_L (*Gottlieb et al., 2000*).
- Some proteins may regulate apoptotic permeabilization of mitochondrial membranes by controlling the activity or formation of channels.
- Other bcl-2 family members support physiologically active channels: Inhibiting closure of VDAC e.g. occasionally promotes survival by maintaining metabolite exchange across the outer mitochondrial membrane (*van der Heiden et al., 2001*).

On the other hand, bcl-2 family members may promote apoptosis via mitochondria by the following basic mechanisms:

- **Dimerization** may promote or inhibit cell death depending on the respective binding partners: Bax-bax homodimers localize to the mitochondria and promote apoptosis (*Wolter et al., 1997, Gross et al., 1998*), and this pro-apoptotic signal can be inactivated by bcl-2, which preferably resides in the mitochondrial membrane. Bcl-2 in turn may be inactivated e.g. by bim (*Gross et al., 1999*) or bad.
- **Translocation** of pro-apoptotic bcl-2 family members to the mitochondria upon an apoptotic stimulus has an important part in signalling apoptosis: Bim e.g. is localized to microtubules in viable cells and translocates to the mitochondria during apoptotic signalling (*Puthalakath et al., 1999*). In contrast, anti-apoptotic family members are often already an integral membrane protein, e.g. bcl-2.
- **Phosphorylation** of BH3-only proteins may increase or decrease their pro-apoptotic potential. Phosphorylated Bad is sequestered to the cytosol by binding to 1344-scaffold proteins. Upon dephosphorylation, e.g. after growth factor withdrawal, it translocates to the mitochondria and inactivates anti-apoptotic bcl-2 molecules (*Zha et al., 1996*). In contrast, phosphorylation of Bik increases its pro-apoptotic activities (*Verma et al., 2001*).
- **Cleavage** of molecules may affect their apoptogenic features. So, cleavage of Bid by caspase-8 generates an active fragment (truncated Bid, tBid) which translocates to the mitochondria and promotes apoptosis by activating pro-apoptotic bax which results in cytochrome c release (*Desagher et al., 1999*). This may be even enhanced by cleaving the anti-apoptotic bcl-2-family member bcl-X_L which otherwise is able to inhibit tBid-mediated cytochrome c release (*Gross et al., 1999b*).
- An **ability to generate pores** in membranes, e.g. selective for distinct ions, has been described for both pro- and anti-apoptotic bcl-2 family members by using

synthetic membranes (Minn *et al.*, 1997; Schlesinger *et al.*, 1997). Thus, bcl-2 family members may affect formation of channels in mitochondria by creating either autonomous pores or by interacting with other mitochondrial proteins, e.g. interaction of bax or bak with the VDAC (Shimizu *et al.*, 2001).

1.3.3. MAMMALIAN SIGNALLING PATHWAYS DURING APOPTOSIS

The activation of effector caspases finally leads to a fast, safe, and traceless removal of the apoptotic cell from a metazoan organism by cleaving a selected set of cellular proteins. Therefore, apoptosis is a unique cell death process and clearly distinct from other cell death procedures, e.g. necrosis. Though transitional forms of these death processes are quite common, full-blown apoptosis and necrosis differ in various features as summarized in the table below (table 1-2):

Feature	Apoptosis	Necrosis
Stimulus	Physiological or mild injury	Pathological or heavy injury
Occurrence	Active response in single cells	Passive response in cell groups
Cellular contacts	Lost early	Lost late
Lysosomal enzymes	Not released	Released
Organelle swelling	In late stages, if any	Early
Energy depletion	In late stages, if any	Early
Caspase activation	Ordered	Random, if any
Eat-me signals	Presented early	No
Chromatin condensation	Yes	No
DNA fragmentation	HMW and oligonucleosomal	Random
Inflammation induced	No	Yes
Cell fate	Phagocytosis	Disintegration
Membrane integrity	Conserved (tight)	Lost (leaky)
Early morphology	Shrinking	Swelling
Late morphology	Apoptotic bodies	Ruptured cells

Table 1-2: A comparison of events during apoptosis and necrosis

(compiled from different sources, e.g.: Gerschenson and Rotella, 1992 (modified); Yen and Savill, 1998; Hug, 2000; Watanabe *et al.*, 2002).

Nevertheless, it should be emphasized once more that both apoptosis and necrosis represent the extreme ends in a wide range of different cell death procedures with gradual similarities in morphological and biochemical features (*Nicotera et al., 1999; Formigli et al., 2000; Watanabe et al., 2002*). As already mentioned before, there are two major pathways during mammalian apoptosis. Both pathways converge in the activation of effector caspases. It should be mentioned in advance that some of the proteins acting during these two pathways are not ultimately restricted to the respective pathways but may be rather cross-activated in the course of apoptosis depending on the cellular signalling context.

1.3.3.1. The death receptor pathway (extrinsic)

As already indicated in chapter 1.3.1.3, cross-linking of death receptors, e.g. CD95 or TNFR, by their respective ligands leads to receptor clustering in the plasma membrane (*reviewed in: Ashkenazi and Dixit, 1998; Peter and Kramer, 2003*). These clusters allow the formation of a DISC by recruiting adaptor proteins like FADD or TRADD, and these adaptor proteins, via their DDs, in turn bind multiple initiator procaspase molecules: Procaspase-8 and -10. According to the induced proximity model, these procaspases are subsequently trans-activated by cleavage. The activated initiator caspases subsequently activate effector caspases, e.g. caspase-3 and -7 which cleave a multitude of apoptotic substrates. This finally leads to a fast and irreversible shut-down of the apoptotic cell. However, two different pathways have been described downstream of CD95 oligomerization during T- and B-lymphocyte maturation and during down-regulation of the immune response after a clonal expansion (*Dhein et al., 1995; Alderson et al., 1995; Brunner et al., 1995; Ju et al., 1995; Kramer, 1999*): Type-I cells form sufficient DISCs for an effective activation of procaspase-8. Subsequently, effector caspases are activated and induce rapid cell death. In contrast, Type-II cells form only few DISCs (*Scaffidi et al., 1998; Kramer, 2000*). Therefore, the weak apoptotic signal, transduced by only weak caspase-8 activity, has to be amplified by the mitochondrial pathway. The link to mitochondria is supported by the bcl-2 member bid: Bid is cleaved by caspase-8 and truncated bid activates mitochondria (*Luo et al., 1998; Li et al., 1998*), allowing an accelerated progression of apoptosis by using the intrinsic pathway to apoptosis in an amplifying manner.

However, signalling by death receptors is certainly more complex than described above. It is increasingly recognized that signalling by death receptors may induce proliferation rather than apoptosis in some cases by inducing signalling cascades which e.g. involve **NF κ B** (nuclear factor) as a survival factor (*Wajant, 2002*). So, induction of apoptosis by TNFR-1 occurs only if NF κ B signalling fails to transmit its survival signal (*Micheau and*

Tschopp, 2003) which involves induction of FLIP by this transcription factor. FLIP subsequently suppresses activation of caspase-8 (see chapter 1.3.1.3).

1.3.3.2. The stress-induced mitochondrial pathway (intrinsic)

To date, the signalling cascade which leads to initiation of the stress-induced pathway to apoptosis is still poorly understood because a multitude of factors seems to affect the induction of this pathway. Growth factor withdrawal, DNA damage by chemicals or irradiation, recognized defects during mitotic or meiotic cell cycle checkpoints, or mild cell insults may initiate arresting of the cell in a distinct phase of the cell cycle and/or induction of apoptosis. Generally, the stress-induced pathways initiate apoptosis via the mitochondria.

Concerning the cellular response to DNA damage, some details have been obtained in the last years. The basic strategy in the response of eukaryotic cells to DNA damage consists of three components: Recognizing the DNA damage, rating its extent, and induction of the appropriate cellular reaction, either cell cycle arrest allowing DNA repair or cell death (*Rich et al., 2000*). Importantly, these components are not activated in a linear manner, but rather parallel: Therefore, the recognition of DNA damage in a cell may trigger both DNA repair processes and preparations for apoptosis. Playing a double-game on the one hand ensures a safe elimination of the cell in the cases of unsuccessful DNA repair, but on the other hand it may result in cell death even if the DNA repair machines had been successfully engaged (*van Sloun et al., 1999*).

According to our current understanding, all kinds of DNA damage in eukaryotic cells are finally converted to either **single strand (ss)** or **double strand (ds)** DNA breaks which are eventually detected by a sensor system (*Stergiou and Hengartner, 2004*). Prominent examples for DNA damage signal transducers and checkpoint activators are proteins from the **ATM** family (**ataxia telangiectasia mutated kinase**) and the **ATR** family (**ataxia telangiectasia related kinase**) as well as **DNA-PK** (**DNA dependent protein kinase**). DNA-PK, ATM, and ATR proteins are phosphatidylinositol-3-kinase-related protein kinases which contain a DNA-binding domain (*Falck et al., 2005*). ATM is e.g. activated downstream from DNA-binding factors which are able to act as sensor molecules for damaged DNA (*reviewed in Khanna et al., 2001*). Presumably, ATM/ATR and DNA-PK are even able to detect ds DNA breaks on their own by binding directly to free DNA ends, thus acting as DNA damage sensors themselves (*Smith et al., 1999; Gatley et al., 1998; Lakin et al., 1999; Hall-Jackson et al., 1999; Fukushima et al., 2001*). Subsequently, ATM/ATRs catalyze phosphorylation cascades which transmit the DNA damage signal to checkpoint and repair proteins. Therefore, those cascades may act as sensitive molecular switches for intercellular signalling cascades (*Goldbeter and*

Koshland, 1981). Remarkably, the sensitivity of such a detection system is theoretically sufficient to arrest the cell cycle due to a single DNA ds-break (*Huang et al., 1996*).

The amplification of the signal occurs by phosphorylating a small subset of effector kinases, e.g. the serine threonine kinases Chk1 and Chk2 as well as the tyrosine kinase c-Abl. These effector kinases phosphorylate, and thus trans-activate, a number of downstream target proteins, which finally promotes either cell cycle arrest and DNA repair or apoptosis (*reviewed in Taylor and Stark, 2001; Waxman and Schwartz, 2003*).

An important target protein which is phosphorylated during ATM/ATR signalling is p53, a central molecule for the surveillance of genomic integrity. Phosphorylation of p53 at distinct residues increases its stability - and thus elongates its cellular half-life - by blocking the binding of p53 to Mdm-2, a protein which otherwise targets p53 for proteasome degradation by catalyzing ubiquitylation of p53 (*Banin et al., 1998; Shieh et al., 1997; Haupt et al., 1997; Kubbutat et al., 1997*). Therefore, p53 levels in the cell increase within minutes after DNA damage. Furthermore, MDM-2 is associated with intracellular trafficking of p53, and DNA damage-induced phosphorylation of p53 localizes p53 to the nucleus (*reviewed in Liang and Clarke, 2001*), allowing its action as a transcription factor. This finally initiates various cellular processes by increasing the expression from p53 target genes, e.g.:

- p21 which induces cell cycle arrest by inhibiting cyclin dependent kinases (*Rich et al., 2000; Gartel and Tyner, 2002*)
- Pro-apoptotic bcl-2 members bax, noxa (*Oda et al., 2000*), and **puma** (**p53 upregulated modulator of apoptosis**, *Yu et al., 2003*).
- Death receptors Fas and DR5 (*Rich et al., 2000*)

Since many cancer cell types which lack a functional p53 protein are still able to arrest in cell cycle and undergo apoptosis in response to DNA-damaging agents, it is important to know that p53-independent DNA damage-signalling pathways exist. These pathways are redundant pathways because they are activated in parallel to p53-dependent pathways by ATM (*reviewed in Rich et al., 2000*). They may be activated either by the tyrosin kinase c-Abl which activates e.g. stress-activated protein kinase pathways and pathways induced by the transcription factor p73, which may substitute some of the p53 functions (*reviewed in Waxman and Schwartz, 2003; Levrero et al., 2000*) or by the transcription factor E2F-1, an important factor for DNA damage-induced initiation of apoptosis in p53 deficient tumour cells. E2F-1 actions in p53-independent apoptosis include:

- Enhancing the expression of apaf-1, thus improving the activation of caspase-9 (*Moroni et al., 2001; Furukawa et al., 2002*)

- Sensitizing tumor cells to apoptotic signals by enhancing the expression of pro-caspases (*Nahle et al., 2002*)
- Transcriptional down-regulation of the anti-apoptotic Bcl-2 member Mcl-1 (*Croxtton et al., 2002*)
- Transcriptional up-regulation of p73 (*Pediconi et al., 2003*)

Both p53-dependent and p53-independent pathways finally converge on the mitochondria, which upon activation release their reservoir of previously tightly packaged pro-apoptotic proteins, especially cytochrome c, AIF, and smac/diablo. Cytosolic cytochrome c subsequently triggers the energy-dependent association of the apoptosome. By binding to the C-terminus of apaf-1, cytochrome c allows binding of (d)ATP to apaf-1 which induces conformational changes thus allowing oligomerization of apaf-1. Oligomerization of apaf-1 allows recruitment of multiple procaspase-9 molecules by their CARD domains which, according to the induced proximity model, generates active caspase-9 by trans-activating cleavage (*Zou et al., 1999; Benedict et al., 2000; Hu et al., 1998; Adrain et al., 1999; Srinivasula, 1998; Salvesen and Dixit, 1999*). The apoptosome, once activated, is a stable structure which persists during apoptosis and serves to cleave and activate multiple effector caspase molecules, above all caspase-3 (*Jiang and Wang, 2000; Rodriguez and Lazebnik, 1999*).

1.3.3.3. Summary: Mammalian apoptosis

There are a variety of signals which may lead to apoptosis in mammalian cells, but increasing evidence has been found in the last years which support the hypothesis for a mammalian network of pro- and anti-apoptotic signalling molecules. Therefore, the final response - necrosis, apoptosis, or survival - of a cell to any insult depends on the cellular context and on the strength of the signal. A still increasing number of cellular or viral IAPs, FLIPs, anti-apoptotic bcl-2 members, and pro-survival signalling by receptors are important 'veto-molecules' and may save cells which in another context system would have been condemned to die. The opposite scenario is imaginable as well.

Once initiated, the apoptotic cascade ultimately leads to cell death if all of the 'veto-molecules' are successfully removed or inactivated. The mitochondria contain an important, tightly controlled reservoir of pro-apoptotic molecules which, once released, may define a point of no return for the cell since they amplify the apoptotic signal by allowing cytochrome c-mediated formation of the apoptosome. Remarkably, in contrast to its vital functions in the respiratory chain in intact mitochondria, cytochrome c is a decisive molecule on the way to apoptosis, as soon as it is released from the mitochondria. On the other hand, mitochondria integrate the signalling of important

anti-apoptotic bcl-2 members and may promote survival as well. Therefore, mitochondria may be regarded as a scaffold integrating both pro- and anti-apoptotic signalling. The following figure (figure 1-2) may illustrate some features of the complex network signalling during apoptosis. As any diagram depicting apoptosis in the literature, it is far away from being complete, and the processes mentioned in this introduction are depicted in a simplified fashion only.

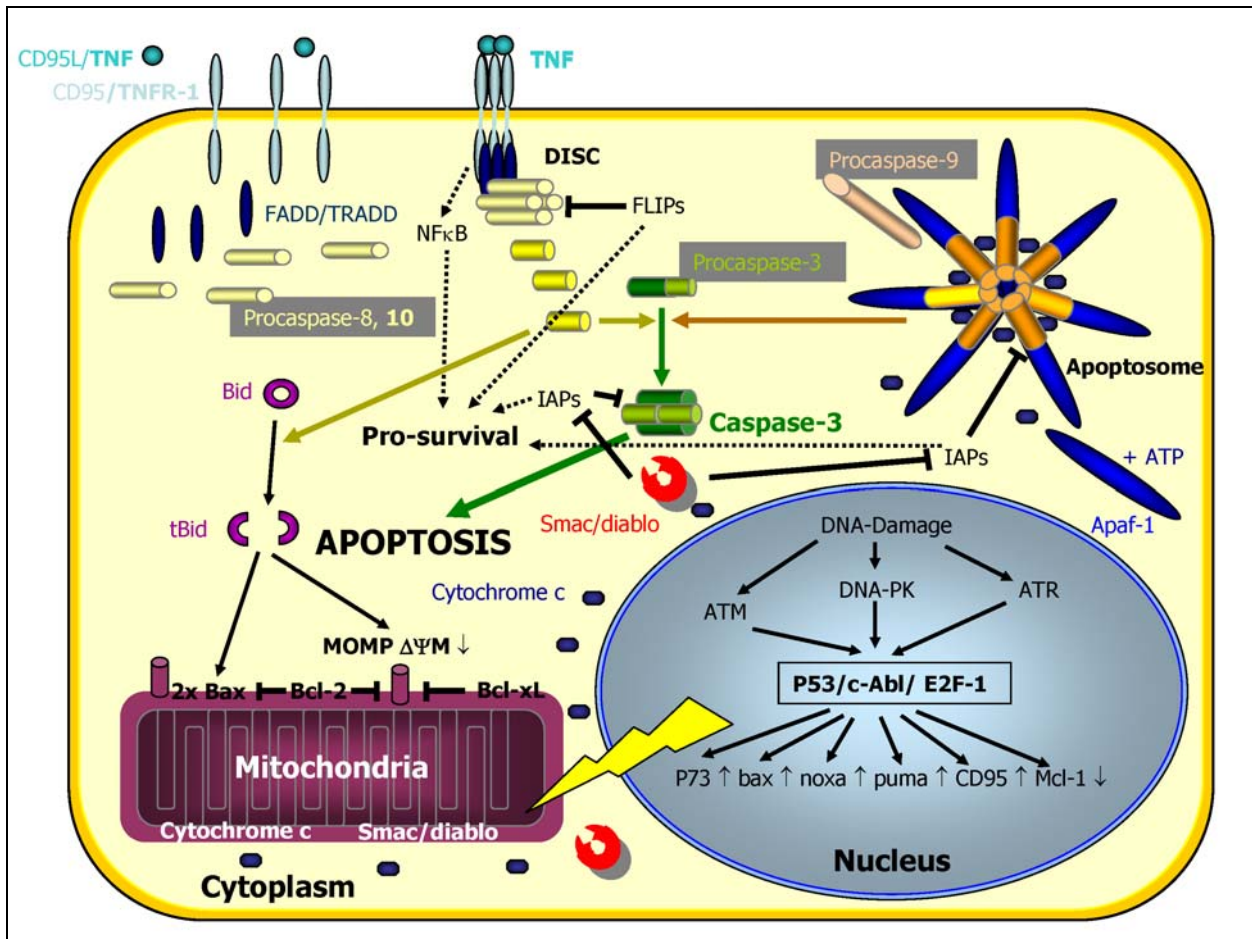


Figure 1-2: Basic signalling and regulation of mammalian apoptosis (simplified presentation)

This figure depicts some of the apoptotic processes described in this introduction (for details see chapter 1.3.3.1 and 1.3.3.2). The death receptor pathway and intrinsic pathways, e.g. induced by DNA damage, converge in activation of effector caspases, e.g. caspase-3 (green), which finally induces apoptosis by cleaving a multitude of substrates. Mitochondria serve as a molecular scaffold for pro- and anti-apoptotic molecules. They may be activated for release of pro-apoptotic molecules both during the intrinsic pathway to apoptosis, e.g. in response to DNA damage (yellow thunderbolt), or by truncated bid (tBid) during receptor-mediated apoptosis. Cytoplasmic cytochrome c mediates energy-dependent formation of the apoptosome, a heptameric structure containing both caspase 9 and apaf-1 in a 1:1 ratio. Smac/diablo, once released from mitochondria, inactivates IAPs and thus contributes to pro-apoptotic signalling.

1.3.4. APOPTOTIC CHROMATIN CHANGES

Apoptotic chromatin changes were among the first features which were noticed in some kinds of cell death and subsequently led to the discovery of apoptosis itself. Since that time oligonucleosomal DNA cleavage has been used as a common marker indicating apoptosis. In contrast to caspases, the activity of DNases is commonly regarded as a 'downstream event', which usually occurs beyond the point of no return for a cell which received an apoptotic signal (*Ferri and Kroemer, 2000*). DNA degradation is not a necessary event for cell death because enucleated cells may be induced to undergo apoptosis, and inhibition of DNA degradation does not prevent apoptosis (*Mc Ilroy et al., 2000*). However, DNases allow a complete degradation and recycling of the chromatin from a dying cell, and lacking DNA degradation may result in persisting potentially auto-antigenic materials and plays e.g. a role in the pathogenesis of systemic lupus erythematosus (*Herrmann et al., 1998; van Nieuwenhuijze et al., 2003*) or other auto-immune diseases. Moreover, according to an early hypothesis, an efficient destruction of the genomic DNA may prevent transfer of mutant genes or viral DNA to the surrounding healthy cells (*Howell and Martz, 1988; de la Taille et al., 1999*).

1.3.4.1. Apoptotic chromatin condensation

One of the characteristics of apoptosis is a condensation of chromatin which results in the formation of apoptotic bodies of various forms. These apoptotic bodies result from collapsing chromatin which may adopt a typical half-moon shape near the nuclear periphery, shrink to a single ball in the centre of the nucleus, or may be even budding to generate smaller vesicles, resulting in a shape resembling a cluster of grapes (*Earnshaw, 1995*). Both proteolysis of key nuclear matrix proteins and high molecular weight (HMW) DNA fragmentation may contribute to early apoptotic chromatin condensation. Nevertheless, DNA cleavage is not essential for chromatin condensation which may occur prior to DNA fragmentation in some apoptotic cell types. Importantly, apoptotic chromatin condensation is completely different from mitotic chromatin condensation because phosphorylation of histones is not required for apoptotic chromatin condensation. Moreover, it is not an active process, but it rather results from the consequence of changes in chromatin, matrix, and in the nuclear lamina. Nevertheless, chromatin condensation is energy-dependent because it requires ATP, a feature typical for early apoptotic events since early energy depletion may result in necrosis rather than apoptosis (*Nicotera and Leist, 1997; Tsujimoto, 1997*). Nuclear events during apoptosis obviously require continued energy supply since many proteins which are essential for apoptosis are actively transported into the nucleus during the

onset of apoptosis (*Robertson et al., 2001*), and inhibition of active nuclear transport may prevent nuclear apoptotic changes (*Yasuhara et al., 1997*).

Chromatin condensation may occur as a consequence of caspase activity or caspase-independent. Caspase-6 e.g. contributes considerably to a fast nuclear breakdown during apoptosis by cleaving lamin A and lamin C (*Rao et al., 1996; Orth et al., 1996; Takahashi et al., 1996*). However, the other effector caspases, caspase-3 and -7, cleave nuclear substrates too and thus contribute to chromatin condensation, despite a differential cleavage pattern, as demonstrated in caspase-6 knockout mice (*Hirada et al., 1998; Zheng et al., 1999*). Another caspase-dependent mode of chromatin condensation involves a molecule called acinus. Upon cleavage by caspase-3, acinus is actively transported into the nucleus and induces chromatin condensation (*Sahara et al., 1999*). Another caspase-independent mode of chromatin condensation is provided by the mitochondria: AIF is an important and conserved pro-apoptotic molecule. When released from the mitochondrial inner membrane space during MOMP, AIF induces peripheral chromatin condensation and HMW DNA fragmentation in the nucleus (*Susin et al., 1999; Earnshaw, 1999; Daugas et al., 2000; Cande et al., 2002*).

1.3.4.2. Apoptotic DNA fragmentation

Early work demonstrated that a substantial amount of complexed chromatin - containing double-stranded DNA arranged in multimers of 180bp - was released from the nucleus of apoptotic mouse thymocytes. From these results it was concluded that specific DNase(s) must be activated during apoptosis (*Wyllie, 1980*). These DNases were thought to be double-strand specific and specifically activated during apoptosis. Apoptotic DNases have cleavage preferences which favour the generation of a typical DNA ladder, i.e. they digest preferably the linker DNA connecting adjacent nucleosomes in natural chromatin substrates. Moreover, it was demonstrated that chromatin of apoptotic cells is initially cleaved into large fragments of 50 to 300 kb (*Filipski et al., 1990; Beere et al., 1995*). As the favoured sequences for apoptotic HMW DNA cleavage was shown to be A/T rich, it was concluded that the responsible DNase cleaves chromatin preferably at the nuclear scaffold attachment sites (*Khodarev et al., 2000*). Generation of large fragments generally preceded nucleosomal DNA fragmentation but was obviously independent from it since it was detectable even in several cell types which lack nucleosomal DNA fragmentation (*Lagarkova et al., 1995; Oberhammer et al., 1993; Cohen, 1994*). The purification and subsequent identification of the responsible DNases was hampered by the fact that it was quite a labile protein which was available only in low amounts.

None of the known DNases seemed to fit the 'wanted' circular: Among the proposed candidates were e.g. DNase I, DNase II, cyclophilins, and DNase γ , but none of them covered all of the features of the putative apoptotic DNase (reviewed in Khodarev *et al.*, 1998; Nagata *et al.*, 2003).

1.3.4.2.1. Discovery of DFF40 as an apoptotic endonuclease

With the discovery of caspases as important effectors during apoptosis, it was found that both chromatin condensation and DNA fragmentation appear 'downstream' of caspase activity (Enari *et al.*, 1995; Enari *et al.*, 1996; Janicke *et al.*, 1998). Furthermore, it was shown that a DNase activity could be induced in cytosolic cell extracts by adding caspase-3, and these caspase-treated extracts were subsequently able to induce DNA fragmentation in isolated nuclei. The protein responsible for this DNA fragmentation was subsequently purified by different groups from both HeLa cells and mouse lymphoma cells (Liu *et al.*, 1997; Enari *et al.*, 1998), and it was named **DFF** (DNA Fragmentation Factor) or **CAD** (caspase-activated DNase), respectively. The protein is a heterodimer, which consists of two subunits, 40 kDa and 45 kDa in size. Trying to find the exact cellular localization of the complex led to contradictory results. Initially, a cytosolic localization was reported since the complex was purified from cytosolic fractions (Liu *et al.*, 1997; Enari *et al.*, 1998), but GFP-ICAD fusion proteins were reported to be nuclear in various species (Samejima and Earnshaw, 1998), and immunostaining experiments detected DFF45 both in the nucleus of epithelial cells (Liu *et al.*, 1998; Lechardeur *et al.*, 2000) and in the cytoplasm of lymphocytes (Xerri *et al.*, 2000; Nagata *et al.*, 2002). Both DFF40 (Nagata *et al.*, 2003) and DFF45 (Lechardeur, 2000; Samejima and Earnshaw, 2000) possess a nuclear localization signal (NLS) in most species. However, it might be dispensable for the proteins cellular functions in the nucleus since a similar NLS is obviously lacking in Drosophila CAD and ICAD (Yokoyama *et al.*, 2000; Mukae *et al.*, 2000). Caspase-3 cleaves the 45-kDa subunit (called DFF45) at two sites to release the active 40 kDa factor (termed DFF40) which subsequently induces DNA fragmentation in nuclei. However, Liu *et al.* (1997) initially supposed that this factor rather activates a DNase in nuclei than being the DNase itself because they could not demonstrate a DNase activity of the purified factor itself. Presumably, they could not demonstrate DFF40's DNase activity since this labile enzyme rapidly degrades in vitro (Nagata *et al.*, 2003). The DNase activity of DFF40 itself (and its instability) was demonstrated later (Enari *et al.*, 1998; Halenbeck *et al.*, 1998; Liu *et al.*, 1998). The caspase-activated DNase activity of DFF40/CAD was inhibitable by DFF45/ICAD (Inhibitor of CAD), and it was found during in vitro expression experiments that

DFF45/ICAD additionally acts as an indispensable chaperone on DFF40 (*Mitamura et al., 1998; Enari et al., 1998*).

To date, besides its presence in humans and mice, CAD/DFF40 has been identified in four more species (rat, chicken, zebrafish, and *Drosophila*) and hence represents an evolutionary conserved protein (*reviewed in Nagata et al., 2003*). Generally, vertebrate CAD/DFF40 is a basic protein which is about 40 kDa in size. Its enzymatic properties were characterized for mouse and human CAD/DFF40: The endonuclease activity of CAD/DFF40 requires oligomerization and has its enzymatic optimum at pH 7.5, but still works well at a broad pH range (7.0 to 8.5); however, DFF40/CAD is thermally unstable and rapidly degrades at 42°C. In the presence of Mg²⁺, DFF40/CAD cleaves double-stranded DNA; it is not co-stimulated by Ca²⁺, may be inhibited by Zn²⁺ or Cu²⁺, and is markedly affected by ionic strength, e.g. by the concentration of K⁺. Cleavage occurs preferably in A/T-rich regions, and single-stranded DNA or RNA is not cleaved by CAD/DFF40 (*Widlak et al., 2000; Widlak and Garrard, 2001*). Furthermore, it cuts DNA in the internucleosomal linker DNA, thus generating the typical oligonucleosomal DNA ladder. The DNA fragments generated by CAD/DFF40 possess blunt ends carrying a 5'-phosphate and a 3'-hydroxyl group, and these DNA ends may be substrates of the terminal transferase. They are detected in some apoptosis assay systems using the **TUNEL** method (**T**dT mediated **d**UTP-biotin **n**ick **e**nd **l**abelling) (*Sakahira et al., 2001*). Several conserved histidine, lysine, and tyrosin residues are essential for the DNase activity of CAD/DFF40, and thus CAD/DFF40 is classified as a member of the histidine nuclease family (*Sakahira et al., 2001; Meiss et al., 2001; Korn et al., 2002*). Histone H1, HMG-1, HMG-2, heat shock protein (HSP) -70, and DNA topoisomerase II α enhance CAD/DFF40's DNase activity in vitro by directly binding to it (*Liu et al., 1998; Liu et al., 1999; Durrieu et al., 2000*). However, to date it is not clear if these molecules regulate CAD/DFF40 activity in vivo since these proteins may exert their activating function by just stabilizing DFF40 in the in vitro assays. Alternatively, they may promote the removal of cleaved DFF45 from the nuclease (*Nagata et al., 2003*). Cleavage of DFF45 releases DFF40 from the complex and allows subsequent oligomerization of DFF40 to form a catalytically active DNase (*Liu et al., 1999; Widlak et al., 2003*). The active DNase may be formed by a large complex of oligomerizing DFF40 molecules, presumably forming tetramers as the smallest active unit (*Widlak et al., 2003*). Analysis of the crystal structure of active DFF40 revealed that it presumably forms a 'pair of molecular scissors' with a deep cleft in which the active site is located. The deep cleft was recently suggested to contribute to the recognition of nucleosomally organized genomic DNA (*Woo et al., 2004*).

1.3.4.2.2. DFF45, the inhibitor and chaperone of DFF40

ICAD/DFF45, the inhibitor and chaperone of CAD/DFF40, has been identified in several mammals and in *Drosophila*. Furthermore, there are two variants of the inhibitor generated by alternative splicing in mouse, human, and rat: ICAD-L (DFF45) and ICAD-S (DFF35) (*Enari et al., 1998; Sakahira et al., 1998; Gu et al., 1999; Chen et al., 2000*). DFF35/ICAD-S is localized in the cytoplasm since it lacks a NLS due to alternative splicing. Both DFF45/ICAD-L and DFF35/ICAD-S are acidic proteins with a molecular weight of 45 and ~30 kDa, respectively. Both proteins inhibit DFF40 activity to the same extent by preventing its binding to DNA, but only DFF45/ICAD-L acts as a chaperone for proper folding of DFF40 during translation (*Sakahira et al., 1999; Sakahira et al., 2001; Gu et al., 1999*). Furthermore, the DFF40/DFF45 or CAD/ICAD complex in proliferating cells contains only DFF45/ICAD-L but no DFF35/ICAD-S (*Liu et al., 1999; Enari et al., 1998*). This was explained by elucidating the translation process of DFF40: Only DFF45/ICAD-L, perhaps assisted by HSP-70 and HSP-40, but not DFF35/ICAD-S binds to the nascent DFF40 polypeptide chain generated by the ribosomes and mediates correct co-translational folding of DFF40 (*Sakahira and Nagata, 2002*).

Both human and mouse ICAD/DFF45 carry two caspase consensus cleavage sites and must be cleaved at both sites to release active DFF40. Though both caspase-7 and caspase-3 cleave DFF45/ICAD, only cleavage by caspase-3 generates active DFF40 since caspase-7 recognizes and cleaves only one of the cleavage-sites. Another protease which is able to cleave DFF45/ICAD twice, and this way may activate DFF40 in a caspase-independent manner, is granzyme B, a key molecule in the induction of apoptosis by cytotoxic T-lymphocytes (*McIlroy et al., 1999; Wolf et al., 1999; Tang and Kidd, 1998; Thomas et al., 2000; Sharif-Askari et al., 2001; Heusel et al., 1994; Shresta et al., 1995*).

1.3.4.2.3. Other apoptotic nucleases

Most DFF45/ICAD-deficient (knockout) cells lack apoptotic nucleosomal DNA fragmentation and HMW DNA fragmentation because no functional DFF40/CAD is produced in the absence of DFF45/ICAD. Moreover, experiments with cells expressing an uncleavable caspase-resistant DFF45 protein, thus unable to release the active nuclease from the complex, behave like DFF40 knockout cells, indicating that DFF40/CAD is the main apoptotic endonuclease, responsible for both HMW and nucleosomal DNA cleavage (*Zhang et al., 1998; Zhang et al., 1999; Zhang et al., 2000b; Sakahira et al., 1999b; McIlroy et al., 2000; Kawane et al., 2003*). However, despite the absence of functional DFF40, some tissues still show DNA laddering and/or

HMW DNA degradation after induction of apoptosis (*Zhang et al., 1998; Samejima et al., 2001*) suggesting that there may be additional, perhaps redundant, nucleases involved in DNA cleavage during apoptosis. One of the most promising candidates is **endonuclease G (EndoG)**, an evolutionary conserved endonuclease which is released from the mitochondria during apoptosis in some cell types and subsequently induces caspase-independent internucleosomal DNA cleavage. (*Parrish et al., 2001; Li et al., 2001; van Loo et al., 2001; Hengartner, 2001*). However, the nuclease activity of EndoG is different from DFF40/CAD: In contrast to DFF40/CAD which generates ds-DNA breaks, EndoG preferentially generates ss-DNA nicks in G-C rich regions and cleaves some of the nucleosomal DNA too. Moreover, its activity is enhanced by damaged DNA (*Ruiz-Carrillo and Renaud, 1987; Ikeda and Ozaki, 1997; Widlak et al., 2001b*). Similar to other mitochondrial 'Jekyll and Hide' proteins released during apoptosis, EndoG fulfills opposite vital tasks inside the mitochondria: The physiological role of mitochondrial EndoG is presumably the generation of RNA primers during initiation of mitochondrial DNA replication (*Cote and Ruiz-Carrillo, 1993*).

Another important DNase which is involved in DNA degradation of apoptotic cells is DNase II. DFF45- or DFF40-deficient mice are generally viable and fertile (*Nagata, 2003*) since another DNase finally digests DNA from apoptotic cells independently from DFF40 during physiological cell death. In contrast, DNase II-knockout mice accumulate undigested nuclei in their macrophages e.g. in liver and thymus and finally die as fetuses as a consequence of defects in thymus development and failing erythropoiesis. Since exclusively engulfed apoptotic cells in macrophages become TUNEL-positive even in mice which lack a functional DFF40 protein, the DNA from apoptotic cells is obviously degraded by lysosomal enzymes from the engulfing cell and not from the apoptotic cell itself (*McIlroy et al., 2000; Odaka and Mizuochi, 2002; Kawane et al., 2001; Kawane et al., 2003*).

The precise functioning of AIF during apoptotic DNA degradation is still unknown. As indicated above, AIF induces HMW DNA fragmentation and chromatin condensation when released from the mitochondria. However, since no nuclease activity could yet be demonstrated for AIF, it may just activate another nuclease (*Nagata, 2003*).

1.3.4.2.4. Contribution of DNA fragmentation to apoptosis

DNA fragmentation is commonly regarded as a pure down stream event in apoptosis which is dispensable for cell death since it does not occur in several cell types without affecting cell death.

Cells from DFF45 mutant mice, which possess no functional DFF40 too, were reported to be more resistant to apoptosis indicating that lacking internucleosomal DNA cleavage

could contribute to enhanced survival in some experimental systems. (*Zhang et al., 1999; Zhang et al., 2001; Boulares et al., 2001*). However, using other apoptotic systems there were no differences in the progression of apoptosis detectable when comparing DFF40 deficient mouse cells to wild type mouse cells (*Nagata, 2003*). However, because DNA fragmentation results in considerable DNA damage in apoptotic cells, it could be supposed that this DNA damage may contribute to an amplification loop to enhance progression of apoptosis. This could be an important positive feedback mechanism in conditions with a low cellular response to triggers of apoptosis. Thus, DFF40-mediated DNA cleavage may play a role in progression of apoptosis induced by weak apoptotic stimuli. If the weak pro-apoptotic signal itself is not sufficient to kill the cell, it might be assisted by the apoptotic pathways induced by DFF40-catalyzed DNA damages.

1.4. AIMS OF THIS STUDY

Chromatin changes are among the most obvious modifications seen in cells undergoing apoptosis, and cleavage of DNA into nucleosomal fragments is one hallmark of apoptosis, often used to distinguish apoptosis from necrosis. Though internucleosomal DNA cleavage is dispensable for cell death itself, as it is lacking in some apoptosis systems, this type of DNA degradation ensures a fast and efficient inactivation of DNA during apoptosis which functions independently from the DNA-degrading actions of engulfing cells. Internucleosomal DNA cleavage rapidly inactivates DNA and this is not a minor matter in apoptosis, keeping in mind that DNA of dying cells might contain virus DNA or otherwise mutated DNA. Therefore, DNA from apoptotic cells represents a serious danger for the neighbouring healthy cells in cases of massive cell death which may overcharge phagocytes, thus impairing the clearance of apoptotic cells and their DNA. Finally, as DNA damage itself causes cell cycle arrest and apoptosis, this DNA damage may even support progression of apoptosis in cells with increased resistance to apoptosis (or a delay in progression of apoptosis) by enhancing the triggering signals for apoptosis. A delay in progression of apoptosis or resistance to apoptosis can be a major problem in various pathological conditions, e.g. during cancer therapy. Therefore, the investigation of factors which influence the extent of nucleosomal DNA degradation might be of increasing interest in apoptosis research and maybe later in developing clinical therapies aiming at a controlled process of apoptosis in some diseases.

The first part of this study attempts to further characterize the influence of H1 histone proteins on DFF40 activity *in vitro*. As detailed in the introduction, H1 histones and other proteins were reported to enhance DFF40 activity. Until now it was not known if there is a differential specificity of the different H1 histone subtypes or of differentially modified H1 histones in activating or inhibiting DFF40 activity. The proteins required for this study were purified as recombinant proteins from transformed *E. coli* and yeast and were subsequently used in *in vitro* assays which allowed an estimation of their effects on DFF40 nuclease activity.

Furthermore, other components which may affect DFF40 activity were investigated in cell lines with differential susceptibility towards induction of apoptosis. The differences detected by comparing HL60, Jurkat, and Raji cells finally led to the experiments conducted in the second part of this study. Raji cells are generally characterized by lacking DNA fragmentation and increased resistance to apoptosis induced by various stimuli. In contrast, Jurkat cells readily undergo internucleosomal DNA cleavage, and subsequent cell death occurs earlier than in Raji cells. The results obtained in the first part of the study finally suggested a role of the different ratio between DFF40 and

DFF45 during progression of apoptosis. Therefore, a cell culture system was established which allowed an altered expression ratio of DFF40 and DFF45 in both Raji and Jurkat cells. This system was used to check for putative consequences of DFF40 activity during apoptosis and to analyze consequences of inhibitory effects of DFF45 on DNA fragmentation during apoptosis. This further required a comparative characterization of selected apoptotic features of Raji and Jurkat cells by analyzing the expression patterns and cellular distribution of selected key proteins. Finally, it allowed to check for a correlation between DNA damage and enzymatic activity of caspase-3. Subsequently, stably transfected Jurkat and Raji cell lines, expressing either additional recombinant DFF40 or DFF45, were generated and analyzed for differences in the DNA fragmentation patterns and the correlated caspase-3 activities. Since the enzymatic activity of caspase-3 may be correlated with cell viability and is a quantifiable parameter, the inducible caspase-3 activities in the course of apoptosis in the differentially transfected cells were subsequently subjected to a statistical analysis of variances. This should reveal whether restoring of DFF40-catalyzed DNA fragmentation in Raji cells is sufficient to increase caspase-3 activities and progression of apoptosis in Raji cells. Furthermore, this system allowed testing for consequences of increased DFF45 levels on DNA fragmentation and caspase-3 activity *in vivo*. In case excess DFF45 suppresses DFF40 activity *in vivo*, thus interfering with a putative apoptotic amplification loop, this may result in lower caspase-3 activities and in increased resistance to apoptosis.

2. MATERIALS AND METHODS

2.1. MATERIALS

2.1.1. TECHNICAL EQUIPMENT

Agarose gel electrophoresis chambers	Precision workshop (Göttingen)
Capillary zone electrophoresis unit 270 A-HT	Perkin Elmer (Weiterstadt)
Cell counting unit CASY 1 TT	Schärfe System (Reutlingen)
Centrifuge 5415	Eppendorf (Hamburg)
Centrifuge Biofuge pico	Heraeus (Hanau)
Centrifuge Megafuge 1.0	Heraeus (Hanau)
Centrifuge Sorvall RC2B (refrigerated)	Kendro (Hanau)
Centrifuge Varifuge 3.0R	Heraeus (Hanau)
Cooling trap RVT 100	Savant (Holbrook NY, USA)
Cytospin system	Heraeus Sepatech (Osterode)
Digital sonifier	Branson (Schwäbisch Gmünd)
DNA Sequencer ABI prism model 3100	Perkin Elmer (Weiterstadt)
Duomax 1030 rocking mixer	Heidolph (Schwabach)
Fluorimeter Fluoroskan Ascent FL	Thermo Electron Corporation
Fraction collector FRAC 10	Pharmacia (Freiburg)
Freeze-drying apparatus	Christ (Osterode)
Incubator Cytoperm 2	Heraeus (Hanau)
Incubator Model CO24	New Brunswick Scientific Co. Inc. (Edson, New Jersey, USA)
Incubator type B 5050	Heraeus (Hanau)
MACS Midi cell separation system	Miltenyi Biotec (Bergisch- Gladbach)
Micro scales	E. Mettler (Zürich)
Micropulser™	BioRad (München)
Microscope LK40	Olympus (Planegg)
pH-Meter CG820	Schott (Mainz)
Photometer Ultrospec 4050	Amersham (Freiburg)
Photometric RNA/DNA calculator Genequant II	Amersham Pharmacia (Freiburg)
Power supply Power Pack 1000	BioRad (München)

Quartz glass distilling apparatus Destamat	Heraeus (Hanau)
Scales	Sartorius (Göttingen)
SDS-PAGE gel electrophoresis chambers	Precision workshop (Göttingen)
Semidry blotting apparatus	Precision workshop (Göttingen)
Speed vac SC 100	Savant (Holbrook NY, USA)
Standard power supply P25	Biometra (Göttingen)
Sterile bench Herasafe type 18/2	Heraeus (Hanau)
Thermocycler TC 2	Perkin Elmer (Weiterstadt)
Ultracentrifuge LZ	Beckman (München)
UV Transilluminator model TM40	UVP (San Gabriel, California)
Vacuum pump	Millipore (Schwalbach)

2.1.2. CHEMICALS

All chemicals were of analytical grade unless stated otherwise.

Acetone	Roth (Karlsruhe)
Acrylamide/Bisacrylamide 30/08	Roth (Karlsruhe)
Activated carbon	Roth (Karlsruhe)
Adenine	Sigma (Steinheim)
Ammonium persulfate	Serva (Heidelberg)
Ammonium sulfate	Serva (Heidelberg)
Arginin	Fluka (Taufkirchen)
Benzamide	Sigma (Steinheim)
Boric acid	Roth (Karlsruhe)
CHAPS	Sigma (Steinheim)
Chloroform	Roth (Karlsruhe)
D(+)-Glucose	Sigma (Steinheim)
dATP	Roche (Mannheim)
dCTP	Roche (Mannheim)
DEPC	Roth (Karlsruhe)
D-Galactose research grade	Serva (Heidelberg)
dGTP	Roche (Mannheim)
Dipotassium hydrogen phosphat	Roth (Karlsruhe)
Disodium hydrogen phosphate	Roth (Karlsruhe)
DL-Lactic acid	Serva (Heidelberg)
D-Maltose	Serva (Heidelberg)
DMSO	Sigma (Steinheim)
D-Sorbitol	Roth (Karlsruhe)

DTT	Applichem (Darmstadt)
dTTP	Roche (Mannheim)
EDTA disodium salt	Serva (Heidelberg)
EGTA	Serva (Heidelberg)
Ethanol	Roth (Karlsruhe)
Glacial acetic acid	Roth (Karlsruhe)
Glycerol	Roth (Karlsruhe)
Glycine	Roth (Karlsruhe)
HEPES	Roth (Karlsruhe)
Histidine	Fluka (Taufkirchen)
Hydrochloric acid 32%	Roth (Karlsruhe)
Igepal (corresponds to Nonidet P 40)	Sigma (Steinheim)
Imidazole	Sigma (Steinheim)
IPTG	BioMol (Hamburg)
Isoamyl alcohol	Roth (Karlsruhe)
Isopropanol	Roth (Karlsruhe)
L-Isoleucine	Fluka (Taufkirchen)
Lithium acetate	Merck (Darmstadt)
Lithium chloride	Serva (Heidelberg)
L-Lysine-Monohydrochloride	Fluka (Taufkirchen)
L-Methionine	Fluka (Taufkirchen)
L-Phenylalanine	Fluka (Taufkirchen)
L-Serine	Serva (Heidelberg)
L-Threonine	Serva (Heidelberg)
L-Tryptophane	Fluka (Taufkirchen)
L-Tyrosine	Serva (Heidelberg)
L-Uracil	Fluka (Taufkirchen)
L-Valine	Fluka (Taufkirchen)
Magnesium chloride hexahydrate	Merck (Darmstadt)
Methanol	Roth (Karlsruhe)
N,N-Dimethyl formamide	Roth (Karlsruhe)
o-Phosphoric acid 85%	Roth (Karlsruhe)
Perchloric acid 70%	Fluka (Taufkirchen)
Phenol equilibrated	BioRad (München)
PIPES	Sigma (Steinheim)
Polyethylene glycol 4000	Serva (Heidelberg)
Polyoxyethylene sorbitane monolaurate (Tween 20)	Sigma (Steinheim)

Potassium chloride	Merck (Darmstadt)
Potassium dihydrogen phosphate	Roth (Karlsruhe)
Potassium hydroxide	Merck (Darmstadt)
SDS	Serva (Heidelberg)
Sodium acide	Merck (Darmstadt)
Sodium chloride	Roth (Karlsruhe)
Sodium dihydrogenphosphate monohydrate	Merck (Darmstadt)
Sodium hydrogen carbonate	Roth (Karlsruhe)
Spermidine-3-HCl	Serva (Heidelberg)
Spermine-4-HCl	Serva (Heidelberg)
Sucrose	Serva (Heidelberg)
Sulphuric acid	Roth (Karlsruhe)
TEMED	Serva (Heidelberg)
Topotecan (a topoisomerase I inhibitor)	SmithKline Beecham (München)
Trichloroacetic acid	Applichem (Darmstadt)
Tris-base	Roth (Karlsruhe)
Triton X 100	Sigma (Steinheim)
Urea	Sigma (Steinheim)
β -Mercaptoethanol	Boehringer (Ingelheim)

2.1.3. DYES

BCIP	BioMol (Hamburg)
Bromophenol blue	Merck (Darmstadt)
Coomassie brilliant blue G250 (Serva-Blue)	Serva (Heidelberg)
Coomassie brilliant blue R250	Fluka (Taufkirchen)
DAPI	Sigma (Steinheim)
DEVD-afc	BioSource (Camarillo, USA)
Ethidium bromide	Sigma (Steinheim)
Hoechst 33342	Molecular Probes (Eugene, USA)
NBT	BioMol (Hamburg)
Ponceau S concentrate	Sigma (Steinheim)
Propidium iodide	Molecular Probes (Eugene, USA)

2.1.4. OLIGONUCLEOTIDES

All oligonucleotides were purchased from MWG Biotech AG (Ebersberg).

2.1.4.1. PCR primers

OWG 1c DFF40 Kozak	5'-TGA AGC TTG CCA CCA TGC TCC AGA AGC CCA AGA GC-3'
OWG 3c DFF45 Kozak	5'-TGA AGC TTG CCA CCA TGG AGG TGA CCG GGG ACG CC-3'
OWG1 DFF40	5'-TGA AGC TTA TGC TCC AGA AGC CCA AGA GC 3'
OWG2 DFF40 rev	5'-AGT CTA GAC TGG CGT TTC CGC ACA GGC TG-3'
OWG3 DFF45	5'-TGA AGC TTA TGG AGG TGA CCG GGG ACG CC-3'
OWG4 DFF45 rev	5'-AGT CTA GAT GTG GGA TCC TGT CTG GCT CG-3'

2.1.4.2. Sequencing primers

DFF40-367-fw	5'-CTG CAC AAC GTC AGC CAG AAC-3'
DFF40-601-fw	5'-CAG TAC AAT GGC AGC TAC TTC-3'
DFF40-60-rev	5'-GAA GTA ATC TTC CGT CAG CTC-3'
DFF45-400-fw	5'-GAT CTG TCC AGC ATC ATC CTC-3'
DFF45-754-fw	5'-GAG CTG AGC TTA TCT AGT CAG-3'
pcDNA3 rev primer	5'-TAG AAG GCA CAG TCG AGG-3'
pcDNA6 myc his a	5'-CTG GCT AAC TAG AGA ACC CAC TGC-3'
T7 primer	5'-GCT AGT TAT TGC TCA GCG G-3'

2.1.5. STANDARDS

Broad range protein molecular weight standard	BioRad (München)
Prestained protein standard Seeblue plus 2	Invitrogen (Karlsruhe)
DNA Standard λ -DNA cut by Eco RI and Hind III (fragment sizes: 21700, 5150, 5050, 4300, 1980, 1900, 1570, 1340, 930, 870, 570 bp)	MBI Fermentas (Vilnius, Litauen)

2.1.6. ANTIBODIES

2.1.6.1. Primary antibodies

Antibody specific for:

Bax	BD Biosciences (Heidelberg)
Bcl-2	BD Biosciences (Heidelberg)
CD95	BD Pharmingen (Heidelberg)
DFF40	Pro Sci Inc. (Poway, USA)

HDAC-1	ABR Affinity Reagents (Golden, USA)
HSP-70	Stressgen (Victoria, Canada)
Penta-his tag	Qiagen (Hilden)
Myc tag	Invitrogen (Karlsruhe)
p21	BD Biosciences (Heidelberg)
p53	BD Biosciences (Heidelberg)
Phospho-H2A.X (Serine 139)	Upstate (New York, USA)
PARP	Cellsignal (Beverly, USA)
Caspase-3	BD Pharmingen (Heidelberg)
DFF45/35	Alexis (Grünberg)

2.1.6.2. Secondary antibodies

Anti mouse IgG coupled to alkaline phosphatase	Sigma (Steinheim)
Anti mouse IgG coupled to HRP	Sigma (Steinheim)
Anti rabbit coupled to CY3	DAKO (Glostrup, Denmark)
Anti rabbit coupled to FITC	DAKO (Glostrup, Denmark)
Anti rabbit IgG coupled to alkaline phosphatase	Dianova (Hamburg)

2.1.7. ENZYMES

Alkaline phosphatase	Boehringer (Mannheim)
Cdc2 kinase (recombinant)	New England Biolabs (Frankfurt)
Creatine phosphokinase	Sigma (Steinheim)
Hind III	MBI Fermentas (Vilnius, Litauen)
Lysozyme (from chicken white of egg)	Sigma (Steinheim)
Proteinase K	Boehringer (Mannheim)
Red Taq TM polymerase	Sigma (Steinheim)
RNase A	Roche (Mannheim)
SSP I	New England Biolabs (Frankfurt)
Xba I	MBI Fermentas (Vilnius, Litauen)
Zymolyase	Seikagaku corp. (Japan)

2.1.8. OTHER BIOLOGICAL AGENTS

Ampicillin solution for injection	Ratiopharm (Ulm)
Bacto agar	DIFCO (Detroit, USA)
Bacto peptone	DIFCO (Detroit USA)
Blasticidin S HCl	Invitrogen (Karlsruhe)
Chloramphenicol	Sigma (Steinheim)
Fetal calf serum	Biochrom (Berlin)
Gentamycin	Biochrom (Berlin)
LMP agarose ultra pure	Gibco BRL (Maryland, USA)
peq Gold universal agarose	peqLab (Erlangen)
Ribonuclease inhibitor	MBI Fermentas (Vilnius, Litauen)
Trypsin-EDTA	Biochrom (Berlin)
Tryptone	Applichem (Darmstadt)
Yeast extract	Applichem (Darmstadt)
Yeast nitrogen base without amino acids	DIFCO (Detroit, USA)

2.1.9. OTHER MATERIALS

2-mm-Electroporation cuvette	BioRad (München)
96 well micro plates	Sarstedt Inc. (Newton, USA)
Blotting paper type 2668	Schleicher & Schuell (Dassel)
Cell culture dishes	Sarstedt Inc. (Newton, USA)
Cell culture flasks	Sarstedt Inc. (Newton, USA)
Developer Kodak LX24	Kodak (Paris, France)
Dialysis tube	Roth (Karlsruhe)
Exposure cassette	AGS GmbH (Heidelberg)
Glass beads 0.45 – 0.5 mm	B. Braun (Melsungen)
Hyperfilm ECL	Amersham-Pharmacia (Frankfurt)
Nitrocellulose membrane Optitran	Schleicher & Schuell (Dassel)
Parafilm	American Chicago National Can
Petri dishes	Sarstedt Inc. (Newton, USA)
Sterile filter (cell culture)	Sarstedt Inc. (Newton, USA)
Sterile filter 0.22 µm	Sartorius (Göttingen)

2.1.10. KITS, SETS, AND READY-MADE MIXES

ABI Prism Big Dye sequencing kit	Perkin Elmer (Weiterstadt)
Apo-Alert-Annexin V-Assay	Clontech (Heidelberg)
Complete protease inhibitor mix (EDTA-free)	Roche (Mannheim)
ECL detection kit	Pierce (Rockford, USA)
Effectene [®] transfection kit	Qiagen (Hilden)
Endofree [™] plasmid maxi kit	Qiagen (Hilden)
Isoton [™] solution for cell culture	Schärfe System (Reutlingen)
MACS Dead Cell Removal Kit	Miltenyi Biotec (Bergisch Gladbach)
MEM	Biochrom (Berlin)
MinElute [™] gel extraction kit	Qiagen (Hilden)
N-acetyl-L-alanyl-L-glutamine 200 mM	Biochrom (Berlin)
PBS for cell culture	Biochrom (Berlin)
Permafluor	Dianova (Hamburg)
pGEM [®] T Easy Vector Kit I	Promega (Madison, USA)
Plasmid Maxi Prep Kit	Qiagen (Hilden)
RNeasy Mini Kit	Qiagen (Hilden)
RPMI	Biochrom (Berlin)

2.1.11. BUFFERS AND SOLUTIONS

All buffers and solutions were prepared with aq. bidest and stored at room temperature unless stated otherwise.

Alkaline phosphatase developing solution

100 mM Tris-HCl, 100 mM NaCl, 5 mM MgCl₂, 0.0175% (w/v) BCIP, 0.02625% (w/v) NBT, 0.67% (v/v) DMF, always freshly prepared

Amino acid/base mix^{-Leu}

200 mg adenine; 400 mg of each arginine, histidine, lysine, methionine, tryptophan, uracil, 600 mg of each isoleucine, serine, threonine, tyrosine, valine; 1000 mg phenylalanine per liter, stored at -20°C (supersaturated suspension must be mixed thoroughly before use)

Annexin-V-labelling-buffer

10 mM HEPES/NaOH, 140 mM NaCl, 5 mM CaCl₂, pH 7.6, stored at 4°C

Anode buffer I (for semidry blotting)

0.3 M Tris/HCl, 20% (v/v) methanol, pH 10.4

Anode buffer II (for semidry blotting)

25 mM Tris/HCl, 20% (v/v) methanol, pH 10.4

AP-buffer

100 mM Tris-HCl, 100 mM NaCl, 5 mM MgCl₂, pH 9.5, stored at 4°C

ATP-regenerating system

20 mM ATP, 100 mM phosphocreatine, 400 U/ml creatine kinase, mixed from stock solutions just before use, stock solutions were stored at -20°C

BCIP stock solution

5% (w/v BCIP) in 100% DMF, stored at -20°C

Blasticidin stock solution

5 mg/ml Blasticidin in aq. bidest, sterilized by filtration, aliquots were stored at -20°C

Blocking buffer

TBST with 5% (w/v) skim milk powder

Bradford dye solution

0.007% (w/v) Serva-Blue (Coomassie G250), 5% (v/v) ethanol, 8.5% (w/v) ortho-phosphoric acid, stored in the dark

Buffer RLN (for use with the RNeasy-Kit)

50 mM Tris/HCl, 140 mM NaCl, 1.5 mM MgCl₂, 0.5% (v/v) Igepal, sterilized by filtration

CaCl₂ solution

50 mM CaCl₂, sterilized by filtration

Caspase-3 reaction buffer

50 mM HEPES/KOH, 1% (w/v) sucrose, 0.1% (w/v) CHAPS, pH 7.5, sterilized by filtration

Cathode buffer (for semidry blotting)

25 mM Tris/HCl, 20% (v/v) methanol, pH 9.4

Coomassie decolourant I

50% (v/v) methanol, 10% (v/v) acetic acid

Coomassie decolourant II

10% (v/v) methanol, 5% (v/v) acetic acid

Coomassie dye solution

0.15% (w/v) Coomassie R250, 30% (v/v) methanol, 10% acetic acid

DB solution (for histone preparation from yeast)

1 M sorbitole, 1 mM EDTA, adjusted to pH 7.7 with 1 N HCl, autoclaved

DEPC-treated water

0.1% DEPC, in RNase free glass bottles, autoclaved

DFF in vitro assay buffer

20 mM Hepes/KOH, 10 mM KCl, 1 mM EDTA, 1 mM EGTA, pH 7.5, autoclaved; 1 mM DTT was added just before use

DFF nucleus buffer

10 mM Hepes/KOH, 50 mM NaCl, 20% (w/v) glycerol, pH 7.0, autoclaved; 2 mM MgCl₂ and 5 mM DTT were added just before use

DNA loading buffer 4x

40% (w/v) sucrose, 0.1 M EDTA, 0.1% (w/v) bromophenol blue, stored at 4°C

DNA lysis buffer

10 mM Tris-HCl, 1 mM EDTA, adjusted to pH 8.0 with NaOH, 0.2% Triton X 100

DTT stock solution

1M DTT, sterilized by filtration, stored at -20°C

EDTA stock solution

0.5 M EDTA, pH 8.0, autoclaved

Ethidium bromide stock solution

10 mg/ml ethidium bromide, stored in the dark at 4°C

Imidazole stock solution

1 M, adjusted to pH 8.0 with HCl, autoclaved

IPTG stock solution

100 mM IPTG, sterilized by filtration, stored at -20°C

Laemmli gel buffer A

1.5 M Tris/HCl, pH 8.8, autoclaved

Laemmli gel buffer B

0.5 M Tris/HCl, pH 6.8, autoclaved

Laemmli gel loading buffer 5x

250 mM Tris/HCl, 50% (v/v) Glycerine, pH 6.8, 1% SDS; 5% (v/v) β -mercaptoethanol was added just before use

Laemmli gel running buffer 4x

0.77 M glycine, 100 mM Tris, pH 8.7, 0.4% (w/v) SDS

Lithium acetate stock solution

0.2 M in TE-buffer, autoclaved

Lysis buffer I (for preparation of recombinant DFF40/DFF45) 2x

100 mM sodium phosphate buffer, 600 mM NaCl, pH 8.0, autoclaved

Lysis buffer II (for preparation of recombinant caspase-3) 2x

100 mM Tris-HCl, 800 mM NaCl, pH 7.9, autoclaved

Lysis buffer III (for caspase-3 activity assays)

5 mM Hepes/KOH, 0.1 mM EDTA, 1 mM DTT, 0.1 mM CHAPS, pH 7.5

MOPS buffer (10x)

200 mM MOPS, 30 mM sodium acetate, 10 mM EDTA, adjusted to pH 7.0 with NaOH

1M NaH₂PO₄ stock solution**NBT stock solution**

7.5% (w/v) NBT in 70% (v/v) DMF, stored at -20°C

Nucleus buffer I

50 mM Tris/HCl, 250 mM sucrose, 25 mM KCl, pH 7.5, autoclaved; 10 mM MgCl₂ was added just before use

Nucleus buffer II

50 mM Tris/HCl, 2.2 M sucrose, 25 mM KCl, pH 7.5; 10 mM MgCl₂ was added just before use

Nucleus buffer III

60 mM KCl, 15 mM NaCl, 340 mM sucrose, pH 7.4, autoclaved, 0.15 mM spermine; 0.5 mM spermidine and 15 mM β-mercaptoethanol were added just before use

Paraformaldehyde solution

3% (w/v) paraformaldehyde in PBS, warmed to 80°C, and alkalized with NaOH for solubilization, stored at 4°C

PARP sample buffer 2x

0.0625 Tris/HCl, 6 M urea, 10% (v/v) glycerol, pH 6.8, 2% (w/v) SDS, 0.00125% (w/v) bromophenol blue, 5% (v/v) β-mercaptoethanol

PCR lysis buffer

67 mM Tris/HCl, 16.6 mM ammonium sulphate, 6.7 μM EDTA, pH 8.8, autoclaved, 5 mM β-mercaptoethanol, 6.7 mM MgCl₂; 1.7 μM SDS, and 50 μg/ml proteinase K were added just before use

PEG solution

50% (v/v) polyethylene glycol 4000, autoclaved

Perchloric acid (5% v/v)

prepared by dilution from a 70% stock solution

PIPES buffer (for cytoplasm extraction)

50 mM Pipes/KOH, 50 mM KCl, 5 mM EGTA, pH 7.4, autoclaved; 2 mM MgCl₂ and 1 mM DTT were added just before use

PK buffer 2x

200 mM Tris/HCl, 10 mM EDTA, 0.4 M NaCl, pH 8.5, 0.4% (w/v) SDS; 200 μg/ml proteinase K was added just before use

PTB buffer (for histone preparation from yeast)

1 M sorbitol, 4.25 mM KH_2PO_4 , 45.75 mM K_2HPO_4 pH 7.7, autoclaved; 20 mM DTT was added just before use

RNA-sample buffer

1 mM EDTA, 0.1% bromophenol blue, 50% (v/v) glycerol, pH 7.0

RNase, DNase-free

10 mg/ml RNase A in 0.01 M sodium acetate was heated to 97°C for 15 min, cooled down to room temperature slowly, and neutralized by adding 0.1 volumes of 1 M Tris solution pH 7.4, 100- μl -aliquots were stored at -20°C

Sodium acetate stock solution

3 M sodium acetate/acetic acid, pH 4.8

Sodium azide stock solution

20% (w/v) sodium azide

Sodium phosphate buffer (0.1 M)

93.2 mM Na_2HPO_4 , adjusted to pH 8.0 with NaH_2PO_4 , autoclaved

TBE buffer 10x

0.9 M Tris, 0.89 M boric acid, 25 mM EDTA, pH 8.3, autoclaved

TBS

20 mM Tris/HCl, 137 mM NaCl, pH 7.6, autoclaved

TBST

TBS with 0.5% (v/v) Tween-20

TE buffer 10x

100 mM Tris/HCl, 10 mM EDTA, pH 8.0

TELT buffer

50 mM Tris/HCl, 62 mM EDTA, 2.5 M LiCl, 4% (w/v) Triton X 100, pH 7.5, sterilized by filtration

Topotecan stock solution

1 mg/ml in aq. bidest, aliquots were stored at -20°C

Tris/SO₄ buffer 10x (for preparation of histones from yeast)

1M Tris adjusted to pH 9.2 with H₂SO₄, autoclaved

2.1.12. MEDIA**LB medium**

1% (w/v) tryptone, 0.5% (w/v) yeast extract, 1% (w/v) NaCl, 0.2% (w/v) maltose were dissolved in demineralized water. The pH was adjusted to 7.0 with NaOH and the solution was autoclaved. For solid media 1.5% (w/v) agar was added and mixed gently after autoclaving. After cooling down to 50°C in a water bath, the solution was completed with antibiotics (50 µg/ml ampicillin, 35 µg/ml chloramphenicol) if desired for selective cultivation and poured into petri dishes. Plates were stored at 4°C.

RPMI medium(for cultivation of HL60, Raji, and Jurkat cells)

The instant powder was completed with 10 g NaHCO₃ (24 mM) and 17.88 g Hepes (15 mM), pH was adjusted to 7.3 and the solution was sterilized by filtration (0.2 µm pore size). Shortly before use 10% (v/v) FCS and 50 µg/ml Gentamycin were added. Medium was stored at 4°C.

RPMI-freezing medium

RPMI medium was completed with 20% FCS and 10% DMSO.

SCD-Leu (synthetic medium for transformed yeast)

0,67% (w/v) yeast nitrogen base, 4% (w/v) glucose, 10 mg/l adenine; 20 mg/l of each arginine, histidine, lysine, methionine, tryptophan, uracil, 30 mg/l of each isoleucine, serine, threonine, tyrosine, valine; 50 mg/l phenylalanine. For solid media pH was adjusted to 6.5 with solid NaOH, and 1.5% agar was added and mixed gently after autoclaving. After cooling down to 50°C in a water bath, the solution was poured into petri dishes. Plates were stored at 4°C.

SCGL-Leu (synthetic medium for transformed yeast)

0,67% (w/v) yeast nitrogen base, 3% (w/v) glycerol, 2% (w/v) lactic acid, 10 mg/l adenine; 20 mg/l of each arginine, histidine, lysine, methionine, tryptophan, uracil, 30 mg/l of each isoleucine, serine, threonine, tyrosine, valine; 50 mg/l phenylalanine, adjusted to pH 5 to 6 with solid NaOH.

SOB (for expression of recombinant protein in bacteria)

2% (w/v) tryptone, 0.5% (w/v) yeast extract, 0.5 g/l NaCl, 0.186 g/l KCl, pH was adjusted to 7.0 with NaOH; 10 mM MgCl₂ was added after autoclaving.

YEPD (complete medium for yeast)

1% (w/v) yeast extract, 2% (w/v) bactopectone, 4% (w/v) glucose were dissolved in demineralized water and autoclaved. For solid media 1.5% (w/v) agar was added, mixed gently after autoclaving and, after cooling down to 50°C in a water bath, the solution was poured into petri dishes. Plates were stored at 4°C.

YPGLA (complete medium for expression in transformed yeast)

1% (w/v) yeast extract, 2% (w/v) bactopectone, 0.2% (w/v) glucose, 2% (w/v) lactic acid, 0.002% (w/v) adenine hemisulfate salt. The pH was adjusted to pH 5-6 with solid NaOH followed by autoclaving.

2.1.13. VECTORS

All the vectors used in this work confer resistance to ampicillin to the bacteria used for propagation of the respective vector. **Ampicillin** belongs to the penicillin family of antibiotics and is a semi synthetic acid-stable antibiotic containing a β -lactam ring. Like all β -lactam antibiotics, it potently inhibits cell wall synthesis in bacteria by binding tightly and specifically to the transpeptidases which catalyze the cross-linking of two glycan-linked peptide chains. These enzymes, when bound to the antibiotic, can no longer catalyze the transpeptidase reaction; yet, the cell wall is still continued to be formed but is no longer cross-linked. This results in a progressive weakening of the bacterial cell wall because the peptidoglycan backbone is compromised by lack of cross-linking. Additionally, the complex formed by antibiotic and enzyme induces the release of autolysins which digest the still existing cell wall; this finally leads to cell lysis by osmotic pressure differences.

β -lactamases are enzymes that destroy β -lactam rings and this way inactivate the antibiotic. The expression of β -lactamases confers resistance to all β -lactam antibiotics (*reviewed in Madigan et al., 1997*). Plasmids which allow expression of a β -lactamase enzyme are commonly used for transformation of bacteria because they permit an antibiotic selection of the successfully transformed and therefore resistant bacteria cells.

Chloramphenicol was used in this study for co-selection of the pLysS vector (see chapter 2.1.13.1.2) together with the pRSetB vector. It is a broad-range antibiotic and

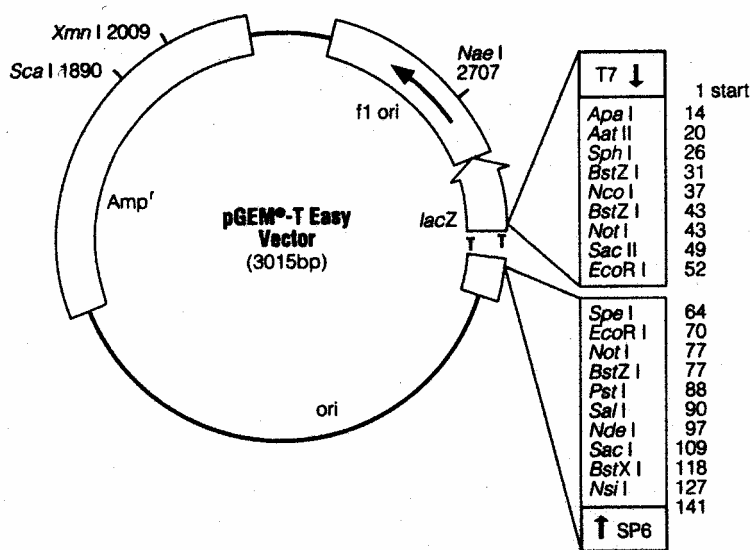
inhibits 'prokaryotic' 70S ribosomes from both bacteria and chloroplasts or mitochondria. Chloramphenicol inhibits elongation of peptide chains during translation by blocking the formation of the peptide bond. By binding to the 50S ribosome subunit, chloramphenicol inhibits the activity of the peptidyltransferase since the 3'-CCA part of t-RNAs can no longer interact with the loop region of the 23S rRNA. Chloramphenicol may be inactivated by acetylation. Enzymes that are able to acetylate and inactivate chloramphenicol are e.g. encoded on R-plasmids from enteric bacteria (*reviewed in Madigan et al., 1997; Stryer, 1995*).

Blasticidin S was used in this study for the selection of stably transfected mammalian cells. It is a peptidyl nucleoside antibiotic isolated from *Streptomyces griseochromogenes* and inhibits protein synthesis in both prokaryotic and eukaryotic cells by inhibiting the formation of peptide bonds in both 70S and 80S ribosomes (*Takeuchi et al., 1958; Yamaguchi et al., 1965; Perez-Gonzalez et al., 1991*). Highly toxic Blasticidin S can be converted to a non-toxic derivative by a deaminase-reaction. To date, two deaminase genes, which confer resistance to Blasticidin S, have been identified, respectively: 'bsr' from *Bacillus cereus* (*Itaya et al., 1990; Izumi et al., 1991*) and 'BSD' from *Aspergillus terreus* (*Kimura et al., 1994a, b*). One of these resistance genes, bsr or BSD, may be used as an efficient, dominant selection marker in transfected mammalian (or plant) cells.

2.1.13.1. Vectors for transformation of bacteria

2.1.13.1.1. pGEM[®]T easy

This vector (purchased from Promega, Madison, USA) was used for 'conservation' and subsequent sequencing of PCR products. PCR-products generated by DNA polymerases which add a template-independent single A to the 3'-end of its product can be cloned directly into this vector. A restriction digest is omitted because the already linearized vector possesses free 3'-T-overhangs. Selection of transformed bacteria can be carried out with Ampicillin, and sequencing is possible with primers specific for a sequence from the T7 promotor since this sequence is present in the vector upstream of the insert DNA. The insert can be excised from the vector for further subcloning into other vectors by using restriction enzymes which cut in the multiple cloning site provided by the pGEM[®]T easy vector.



T7	T7 promoter (followed by a MCS)
SP6	SP6 promoter (followd by a second MCS)
lacZ	lac operon
ori	origin of replication
Amp ^r	β-lactamase-gen
F1 ori	phage f1 region

Figure 2-1: pGEM[®] T easy vector (figure adapted from www. Promega.com, modified)

2.1.13.1.2. pRSet B

pRSet B (purchased from Qiagen, Hilden) is a pUC-derived vector for high level expression of recombinant proteins with a N-terminal 6xHis-tag in the E. coli strain BL21 (DE3) pLysS. pRSet vectors are available with three different ORFs marked as pRSet A, B, or C. Choice of the vector type A, B, or C depends on the restriction enzymes used for cloning and simplifies in-frame cloning of the insert referring to the 6xHis-tag. pRSet vectors confer resistance to Ampicillin. Expression from pRSet B is under control of the strong T7 promoter and is enhanced additionally because transcripts from this plasmid carry a transcript-stabilizing sequence from gene 10 of phage T7. For the expression of proteins under control of this promoter, the presence of T7 RNA-polymerase is necessary, an enzyme which specifically recognizes this promoter. T7 RNA polymerase may be expressed from the plasmid **pLysS** present in the E. coli strain BL21 (DE3) pLysS. Expression of T7 RNA-polymerase from plasmid pLysS may be induced in this strain by adding IPTG (Isopropyl-β-D-thiogalactopyranoside) to an exponentially growing cell population. Induction with IPTG is possible as the plasmid pLysS contains a part of the *lacZ* gene carrying the T7 RNA polymerase coding sequence under control of the promoter *LacUV5*. Therefore, plasmid pLysS must be present for any expression of recombinant proteins in the E. coli strain transformed with the plasmid pRSet B. pLysS

confers an additional resistance to Chloramphenicol; hence, transformed bacteria may be selected by culturing them in medium containing both Chloramphenicol and Ampicillin. Co-selection using both antibiotics is generally recommended since bacteria containing the pLysS plasmid are more sensitive to lysis than bacteria that (by chance) lost this plasmid. Therefore, bacteria containing pLysS have a selective disadvantage in the absence of Chloramphenicol and may be displaced from a bacteria population in the course of culturing.

Unless expression of the recombinant protein is induced by adding IPTG, the expression of T7 RNA polymerase is suppressed because the promoter is inactivated not only by the *lac* repressor but also by T7-lysozyme produced from the plasmid pLysS. Nevertheless, the promoter is slightly 'leaky' (allows expression of the recombinant protein at a low level in the absence of inductor) as there is always some basal expression of T7 RNA-polymerase. Addition of IPTG activates the *LacUV5* promoter and this way induces strong expression of T7 RNA polymerase from plasmid pLysS. T7 RNA polymerase in turn activates the T7 promoter and allows expression of the recombinant protein from plasmid pRSet B.

In this work the pRSet B vector system was used for the expression of the recombinant DFF40/DFF45 complex. This vector is shown in figure 2-2 on the following page.

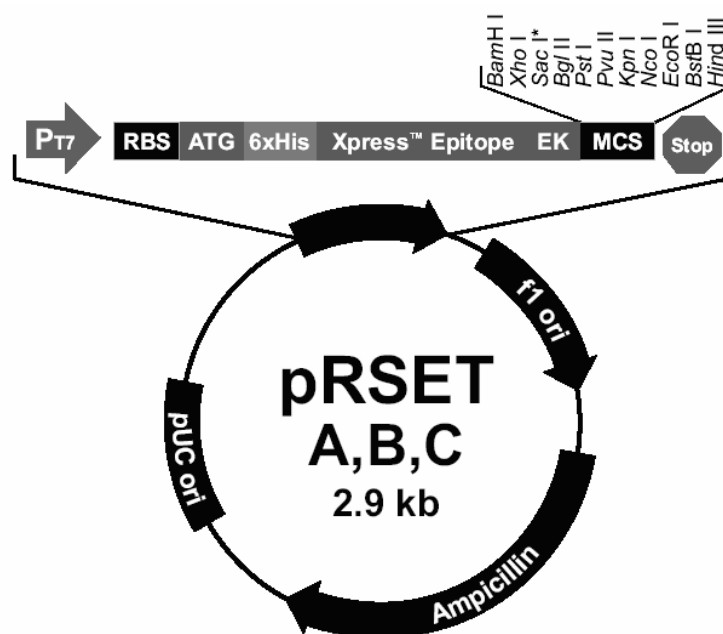


Figure 2-2: pRSET vector A, B, C

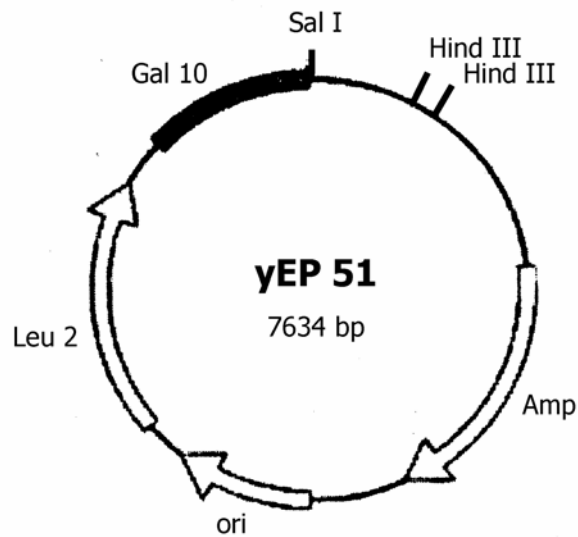
P _{T7}	T7 promotor
RBS	ribosome binding site
ATG	translational initiation site
6XHis	N-terminal 6xHis-tag
Xpress™ Epitope	contains the T7 gene 10 leader followed by the xpress™ epitope for the detection of the recombinant protein
EK	enterokinase cleavage site (for removal of the tag)
MCS	multiple cloning site
Stop	T7 terminator of transcription
pUC ori	origin of replication
f1 ori	origin of replication for the generation of single-stranded DNA
Ampicillin	Ampicillin resistance gene (β -lactamase) for the selection of bacteria carrying the plasmid
pUC ori	origin for high copy replication in <i>E. coli</i>

(Figure adapted from www.qiagen.com, modified)

2.1.13.2. Vector for transformation of yeast

Plasmid yEP51 is a yeast shuttle vector, 7.9 kb in size, for the expression of recombinant protein in yeast. Expression of the recombinant protein is induced by galactose since the vector contains the GAL10 promotor. Cloning into the vector by using the SalI restriction site puts the protein to be expressed under control of the GAL10 promotor. Yeast transformed by this vector can be selected by culturing the cells in leucine deficient medium; the vector restores the ability of leucine-synthesis in leucine deficient yeast strains. Propagation of this vector is possible in *E. coli* as well because the plasmid carries a suitable origin of replication for *E. coli* and includes the β -lactamase-gene. Transformed bacteria may be selected by growing the cells in medium containing

Ampicillin. YEP51 was used in this study for the expression of human H1 histone subtypes and caspase-3 in yeast.



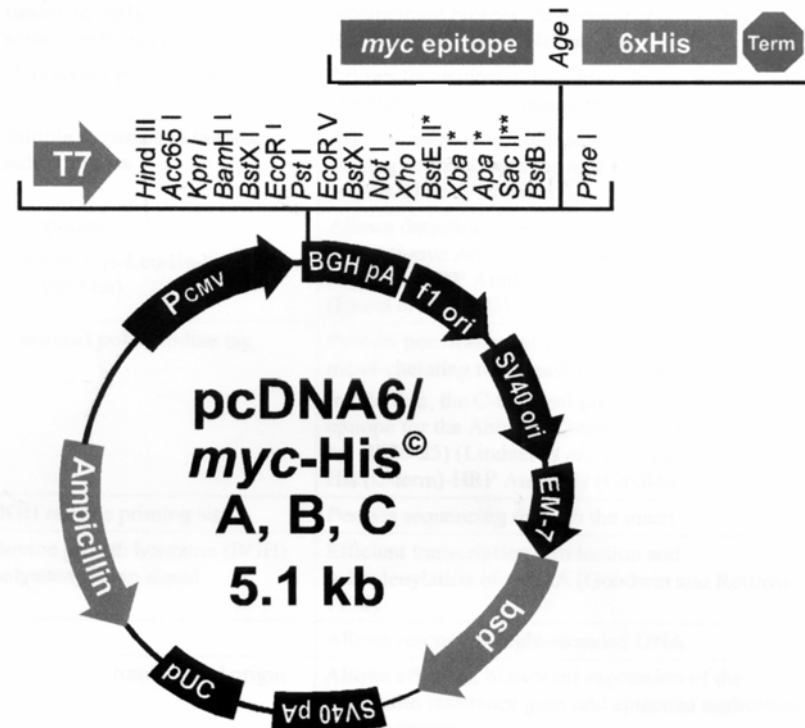
Amp	Ampicillin resistance gene (β -lactamase) for the selection in bacteria
ori	origin of replication in <i>E. coli</i>
Leu 2	yeast Leu 2 gene, allows leucine synthesis in transformed yeast cells
Gal 10	galactose inducible promoter
Sal I	cloning site for proteins to be induced by galactose

Figure 2-3: yEP51 vector

2.1.13.3. Vector for transfection of mammalian cells

pcDNA6 myc-his A (purchased from Invitrogen, Karlsruhe) is a vector used for the overexpression of a recombinant protein in mammalian cells. In-frame-cloning is simplified because the vector is available in 3 ORFs (compare chapter 2.1.13.1.2). Expression of the desired protein is under control of the CMV-promotor, one of the strongest promoters known for mammalian cells to date. Mammalian cells can be stably transfected with this vector by selecting positive transfectants with Blasticidin. The vector is designed in a way that allows expression of the desired recombinant protein with a C-terminally attached 6xHis-tag (for purification on Ni-NTA-column) and a myc epitope (for immuno-detection using an anti-myc antibody). Additionally, the resulting recombinant protein can be easily distinguished from the corresponding endogenous protein in western blots due to its higher molecular weight resulting from these two tags. The plasmid can also be propagated in *E. coli* by selecting for Ampicillin resistance. This vector was used in this study for the additional expression of tagged

DFF40 or DFF45 in human cell lines, which already express the corresponding untagged proteins endogenously.



PCMV	CMV promotor
T7	T7 promotor/priming site
BGH pA	reverse priming site and polyadenylation signal
f1 ori	f1 origin
SV40 ori	SV 40 promotor and origin
EM-7	promotor for blasticidin resistance
bsd	Blasticidin resistance gene from aspergillus terreus
SV40 pA	SV40 polyadenylation signal
pUC ori	pUC origin for amplification of the plasmid in E. coli
Ampicillin	Ampicillin resistance gene

(Figure adapted from www.invitrogen.com, modified)

Figure 2-4: pcDNA6 myc-his vector

2.1.14. MICROORGANISMS

E coli strain **BI21 (DE3) pLysS** was used for the expression of recombinant protein (see chapter 2.1.13.1.2). E. coli strain **DH5 α** and E. coli strain **JM109** were used for the propagation of plasmid-DNA.

Yeast strain **ENY.WA-4D**, deficient for the synthesis of leucine, was used for the expression of H1 histone subtypes and caspase-3.

2.1.15. CELL LINES

HL60 cells are an acute promyelocytic leukemia cell line which originally derived from the peripheral blood of a 36 year old caucasian female. They were first described in 1977 by *Collins et al.* and further characterized by *Gallagher et al. (1979)*. These cells grow as round, relatively small single cells in suspension culture. In the presence of certain reagents, e.g. DMSO, HL60 cells may differentiate to monocytes.

HeLa cells are an adherently fast-growing cell line deriving from an epitheloid cervix carcinoma of a 31 year old female, **Henrietta Lacks**, in 1951; diagnosis of the patient was later changed to adenocarcinoma. This commonly used cell line was first described by *Gey et al. (1952)*.

Jurkat cells were established in 1976 from the peripheral blood of a 14 year old boy with acute lymphoblastic leukaemia. They were identified as immature T-precursor-cells. The related cell line JM is derived from a sister clone of the same patient, but have slightly different features. Jurkat cells grow in suspension culture and tend to form clusters. Viable cultures can be easily identified by the cell's 'spiky' look. These cells were first described by *Schneider et al. (1977)*.

The **Raji cell line** was established in 1963 from the left maxilla of a 12 year old african boy suffering from Burkitt lymphoma, so they represent immature B-cells. Raji cells are the first continuous hematopoietic cell line. They grow in suspension as round cells and tend to form cell clusters. *Pulvertaft* first described this cell line in 1964.

2.2. METHODS

A detailed specification of the applied materials is omitted in the following if the material (e.g. composition of the buffers used in the described experiment) was already explained in the chapter 'materials' (2.1).

Molecular biological work was always carried out in appropriate laboratories, applying S1-conditions as described in the German 'Gentechnik-Sicherheitsverordnung' (GenTSV, 1994).

2.2.1. WORKING WITH BACTERIA

2.2.1.1. E. coli standard culture

E. coli strains were usually cultured in LB medium at 37°C, continuously shaking at 150 to 200 rpm. For overnight cultures 3 ml LB medium were inoculated with either 50 µl of a stock culture or a picked clone from a selective media plate. Usually 100 µl of an overnight culture were used to inoculate 100 ml medium on the following day. Selective media contained either 50 µg/ml Ampicillin or a combination of 50 µg/ml Ampicillin and 35 µg/ml Chloramphenicol. For expression of recombinant proteins E. coli was usually cultured in SOB-medium.

2.2.1.2. E. coli stock cultures

Stock cultures were prepared by mixing an exponentially growing culture at a cell density corresponding to an OD₆₀₀ of 0.6 to 0.9 with sterile glycerol to a final glycerol concentration of 50% (v/v). These stocks were stored at -20°C and were usually stable for at least one year.

2.2.1.3. Preparing competent cells

Bacteria are called 'competent' at a physiological state which enables them to take up DNA, preferably double stranded DNA, from the environment. This feature is called transformation and can only be found in certain bacteria strains in the middle phase of an exponentially growing cell culture. The capability of transformation decreases quickly at inappropriate culture conditions (*Schlegel, 1985*). E. coli cells can be rendered to competent cells for the uptake of plasmid DNA by treatment with a cold solution containing CaCl₂ followed by cold storage. The exact mechanisms of this treatment are still unknown but may depend on changes in the cell surface, presumably due to changes in the charge of certain molecules (*Madigan et al., 1997*). Probably, positively charged

calcium ions neutralize negative charges of the plasmid DNA and lipopolysaccharides in the bacteria cell wall, which in combination facilitates the uptake of plasmid DNA.

An *E. coli* overnight culture was used to inoculate a starter culture of 2 to 5 ml LB medium and was grown to a cell density corresponding to an OD₆₀₀ of 0.6. Cells were kept on ice for at least 30 min to stop growth and were then harvested by centrifugation at 4,000x g at 4°C for 10 min. The resulting pellet was gently resuspended in 25 ml chilled 50 mM CaCl₂ solution and was incubated on ice for another 30 min before carrying out a second centrifugation step as mentioned above. The pellet was gently resuspended in 4.5 ml cold CaCl₂ solution and mixed with 1 ml sterile glycerol. 120 µl aliquots were frozen in liquid nitrogen and stored up to 6 months at -80°C until use.

2.2.1.4. Transformation of *E. coli*

A quantity of 100 to 200 ng plasmid DNA were added to the freshly thawed competent cells and kept on ice for 30 min, followed by an incubation step at 42°C for 2 min and a second incubation on ice for another 5 min. After having added 1 ml LB medium the cells were incubated constantly shaking at 200 rpm for 1 h at 37°C and centrifuged at 4,000x g for 5 min. One ml of the supernatant was removed, and the pellet was gently resuspended in the remaining medium before streaking on selective media plates.

2.2.1.5. Preparing bacteria for plasmid purification

Two methods for the purification of plasmids from bacteria were used. TELT-preparation proved most suitable for screening large numbers of clones for successful integration of an insert into a plasmid, but the resulting plasmid DNA was not clean enough for procedures like sequencing or transformation. If large quantities of pure plasmid DNA were required, the Qiagen Maxi Prep Kit provided reliable and reproducible results.

2.2.1.5.1. Preparing bacteria for plasmid preparations (TELT-method)

Bacterial clones grown under selective conditions were picked from a plate and incubated by shaking overnight at 37°C in 5 ml LB medium under selective conditions. A 1.5-ml-volume of the overnight culture was centrifuged for 5 min at 8,000 rpm in a microcentrifuge. The remaining culture was used to prepare glycerol stocks (see chapter 2.2.1.2), and the pellets were processed as described in chapter 2.2.4.10.4.

2.2.1.5.2. Preparing bacteria for plasmid preparations (Qiagen)

Bacterial stock cultures from clones containing an insert, as analyzed by the TELT-method or by sequencing, were used to inoculate a starter culture of 2 to 5 ml LB medium under selective conditions. For plasmid preparation according to the Qiagen maxi prep kit, 100 ml LB medium were inoculated with 200 µl of the starter culture and incubated shaking overnight at 37°C. (For plasmid preparations using the endofree™ maxi kit: 150 to 200 ml LB medium were inoculated with 300 to 400 µl of the starter culture). Bacterial cells were harvested by centrifugation using a Sorvall GSA rotor (6,000x g, 15 min, 4°C). The supernatant was removed completely, and the pellets were stored at -20° C until further processing as described in chapter 2.2.4.10.5.

2.2.1.5.3. Bacteria and endotoxin-free plasmid preparation

Endotoxins are components from the outer cell membranes of gram negative bacteria and consist of a lipid unit, a complex array of sugar residues, and negatively charged phosphate groups. They are also called lipopolysaccharides (LPS) and due to their chemical properties define the interactions of bacteria with other molecules or cells. LPS cause fever and shock syndromes in animals and humans by activating the complement cascade which leads to a non-specific immune response. In plasmid preparations from bacteria, endotoxins are co-purified with plasmid DNA, mainly because they tend to form micellar structures which behave like DNA.

For transfection of eukaryotic cells, plasmid DNA should be endotoxin-free since endotoxins decrease the transfection efficiency due to their DNA-like behaviour. Moreover, endotoxins may activate cultured immune cells in a non-specific manner.

LPS are very stable and cannot be removed by autoclaving. Plastic ware should be certified endotoxin-free, and heating to 180°C overnight is necessary to destroy these molecules on glassware.

The protocol used for endotoxin-free plasmid preparations is described in detail in chapter 2.2.4.10.5.

2.2.1.6. Expression of recombinant DFF40/DFF45 complex in E. coli

DFF40/DFF45 complex was expressed as a soluble protein from the plasmid pWA 379¹. This plasmid contained the ORF of DFF40 and DFF45 cloned into the vector pRset B and was used to transform the strain E. coli BL21 pLys, which is optimized for expression and easy purification of recombinant proteins. The co-expression of DFF40 and DFF45 is necessary to obtain DFF40 in a correctly folded manner because DFF45 is required as

¹ kindly provided by PD Dr. Werner Albig

a chaperone even during expression in bacteria. It stays bound to DFF40 until it is cleaved by certain proteases in vivo and in vitro. DFF45 used in this study contained the N-terminal 6xHis-tag. Though DFF40 itself had no tag, it was co-purified with DFF45 on Ni-NTA columns due to its binding to DFF45. A suitable IPTG concentration and incubation-time for the expression of the recombinant protein complex as a soluble protein were determined in pilot expression experiments (see chapter 2.2.1.7).

A single colony from a freshly streaked selective plate containing Chloramphenicol and Ampicillin was used to inoculate a starter culture of 2 ml selective LB medium at the day prior to the experiment. The starter culture was used to inoculate an overnight culture of 200 ml SOB medium under selective conditions. On the day of the experiment 1.8 liters SOB medium without antibiotics were inoculated with the overnight culture to a cell density corresponding to an OD_{600} of 0.5 in a 300 ml volume, respectively. Bacteria were incubated at 37°C while constantly shaking at 200 rpm until OD_{600} was 1.0. At this density the cells were induced for the expression of recombinant protein by adding IPTG to a final concentration of 2 mmol/l. Cells were incubated for 3h at 37°C and harvested by centrifugation at 5,000 rpm in a Sorvall GSA rotor at 4°C. The resulting pellets were pooled and washed once with 100 ml 50 mM Na-phosphate-buffer prior to freezing in liquid nitrogen. The pellets were stored at -80°C until processing.

2.2.1.7. Pilot expression experiments

The *E. coli* strain BL21 (De3) pLys S, transformed with the expression plasmid pWA 379, was induced with IPTG, using varying concentrations, for the expression of recombinant protein at differing times. Bacteria from 1 ml cell suspension per sample were harvested by centrifugation (13,000 g, 10 min, 4°C), supernatants were removed, and pellets were stored at -20°C until all samples were collected. Bacteria were extracted by adding 100 µl 20 mM phosphate buffer, pH 7.0 and applying 4 freeze-thaw-cycles (freezing in liquid nitrogen, thawing in a 42°C waterbath). Samples were centrifuged as described above, and the supernatants were removed completely. Pellets and 100 µl of each supernatant were kept for analytical gels. 200 µl SDS-sample buffer were added to each sample; 20 µl of each sample were analyzed by electrophoresis on a 12% gel (see chapter 2.2.3.6) and by western blotting (see chapter 2.2.3.7).

2.2.2. WORKING WITH YEAST

2.2.2.1. Yeast culturing

The leucine deficient yeast strain *S. cerevisiae* ENY.WA-4D was routinely cultured on YEPD plates. Plates were stored tightly sealed with parafilm at 4°C for up to half a year before streaking the yeast culture onto fresh plates again. Prior to transformation experiments, a single clone from a storage plate was picked and used to inoculate an overnight culture in 5 ml liquid YEPD medium.

2.2.2.2. Transformation of yeast

In contrast to bacteria, competent yeast cells cannot be stored at -80°C, so competent yeast cells always have to be prepared freshly for transformation. Competence can be induced in yeast cells by treating the cells with lithium acetate and polyethylene glycol 4000. This leads to changes in the yeast cell wall and membranes, which enables the cells to take up DNA during a subsequent heat shock (*Ito et al., 1983; Rothstein, 1985*). Alternatively, yeast cells can be transformed by electroporation (*Ausubel et al., 1987; Becker and Guarente, 1991*). For electroporation it is essential to remove all traces of salts by washing the cells carefully with aq. bidest. This is decisive for the success of the transformation process because too many ions in the cell suspension increase the current during electroporation which in turn decreases the chance of survival for the electroporated yeast cells.

2.2.2.2.1. Transformation of yeast by the Li-acetate-method

The strain *S. cerevisiae* ENY.WA-4D was grown in YEPD to an OD₆₀₀ of 1.0 (corresponding to 1 x 10⁸ cells per ml). 50 ml cell suspension were harvested by centrifugation at 3,000 rpm at 4°C in a Heraeus centrifuge. Cells were washed subsequently with 50 ml TE-buffer, pH 8.0 and 20 ml 0.2 M Li-acetate. The pellet was suspended in 2 ml Li-acetate and incubated at 30°C while shaking continuously at 150 rpm. The plasmid DNA to be transformed into the cells was diluted to 500 ng/μl with sterile aq. bidest, and 130 μl yeast suspension were added to 20 μl DNA followed by an incubation step at 30°C with slight agitation at 50 rpm. 350 μl of a 50% (v/v) polyethylene glycol solution were added and mixed immediately followed by an incubation step at 30°C with very gentle agitation at 25 rpm for another hour. Cells were exposed to a heat shock at 42°C for 5 min in a water bath; immediately after this 700 μl sterile aq. bidest were added, followed by washing the cells twice with sterile aq. bidest. Cells were pelleted at 3,000 rpm in a microcentrifuge, resuspended in 80 μl sterile aq. bidest and

streaked out on SCD^{-Leu} plates. Colonies were detected following a 2-3 days lasting incubation at 30°C. There were no colonies in negative control transformations which had been performed without DNA.

2.2.2.2. Transformation of yeast by electroporation

All reagents were sterile and cooled on ice before use.

Yeast cells were grown in YEPD to an OD₆₀₀ of 1.0, and 100 ml cell suspension were harvested by centrifugation at 3,000 rpm in a Heraeus centrifuge at 4°C. Cells were washed twice with 10 ml aq. bidest, twice with 50 ml aq. bidest, and once with 4 ml 1M sorbitol. Finally, the pellets were resuspended in 100 µl 1 M sorbitol. Plasmid DNA was diluted in aq. bidest to a concentration of 40 – 100 ng/µl, and 5 µl of the diluted DNA were used for the transformation reaction. A 40-µl-volume of competent yeast cells was incubated with the plasmid DNA in a 2 mm electroporation cuvette on ice for 5 min followed by electroporation using program Sc-2 in a BioRad micropulser. Program Sc-2 delivers a voltage of 1.5 kV and a time constant of 5 ms. Immediately after electroporation, one ml 1 M sorbitole solution was added to the cells. Subsequently, the cells were transferred to a microtube and then centrifuged at 2,000 rpm for 2 min in a microcentrifuge. The supernatant was removed partially, leaving a residue of 100 µl in the micro tube. Cells were gently resuspended in the remaining supernatant and streaked on selective media plates. Colonies became visible after an incubation step at 30°C for 2-3 days. There were no colonies in negative transformation controls which had been electroporated with aq. bidest.

2.2.2.3. Expression of recombinant proteins in yeast

YEp51 is a yeast vector which can be amplified in bacteria as well when selecting for Ampicillin resistance. In yeast this vector restores the ability of yeast with an auxotrophy for leucine to grow in leucine-deficient media. Therefore, transformed yeast cells can be selected in media lacking leucine. Expression of recombinant protein from this vector is under control of the GAL-10-promotor, which is one of the strongest promoters known in yeast. Administration of galactose to a carbohydrate-deprived medium induces the expression of the recombinant protein from this vector.

S. cerevisiae is a suitable system for the expression of human H1 histones (*Albig et al., 1998*) since it does not possess acid-extractable H1 histones. Thus, recombinant H1 histones can be isolated with high purity since no endogenous H1 histones are co-purified from *S. cerevisiae* when using 5% PCA for the extraction. A further advantage is that H1 histones are not degraded by yeast; this often happens if eukaryotic H1 histones are expressed in bacteria.

Expression of caspase-3 in *S. cerevisiae* leads to purification of the active form of this enzyme. Obviously, yeast is able to cleave this protein in the required way or, more likely, cleavage occurs during the lysis process. Although yeast expressing caspase-3 was growing slower than non-transformed yeast, no strong toxicity was seen in *S. cerevisiae* expressing this potent proteinase with a lot of substrates in higher eukaryotes. Human caspase-3 was expressed as a fusion protein with an N-terminal 6xHis-tag and purified by Ni-NTA-affinity chromatography. The coding region of this fusion protein was amplified from a plasmid DNA² by PCR and cloned into the SalI/BamHI sites of the yeast vector YEp51.

Generally, purification of recombinant proteins from yeast is hampered by the very stable cell wall of yeast. Especially when cells are harvested at a high density and in the late log phase, many cells are resistant to a digestion step with zymolyase. So, enzymatic digestion alone was not sufficient to release the recombinant proteins. Therefore, a mechanical treatment was included in the lysis protocols. Vigorous and long-lasting vortexing with glass beads proved suitable for the extraction of H1 histones and caspase-3 from *S. cerevisiae*.

Caspase-3 was purified from the resulting protein mix by Ni-NTA affinity-chromatography according to the principles described below for recombinant DFF40/DFFF45.

H1 histones can be purified without a tag due to their high acid solubility. The extraction of H1 histones from the cell lysate with 5% PCA selectively enriches H1 histone proteins. The recombinant H1 histones extracted from yeast are quite pure since, in contrast to cells of higher eukaryotes, there are no other acid soluble proteins in yeast which could be co-precipitated.

2.2.2.3.1. Expressing H1 histones or caspase-3 in *S. cerevisiae*

A single colony from a plate containing the desired transformed yeast strain was picked and incubated shaking at 160 rpm overnight in 5 ml SCD^{-Leu} at 30°C. This starter culture was diluted 1:10 in SCD-Leu and incubated with shaking at 30°C for ~ 9 h. The resulting culture was used to inoculate 6 x 200 ml SCGL-Leu to an OD₆₀₀ corresponding to 1.0 to 1.3 to be reached in the next morning (generation time was assumed to be 3 h for the transformed yeast strain ENY.WA-4D). At an OD₆₀₀ of 1.0 to 1.3 200 ml YPGLA were added to each culture, and the cultures were incubated shaking at 30°C for another 3 h before the expression of recombinant protein was induced by adding 2% (w/v) galactose. After an incubation step for 6 h at 30°C, cells were harvested by centrifugation for 30 min at 4°C at 4,000 rpm in a Heraeus centrifuge. The supernatant

² kindly provided by Thomas Meergans, Konstanz, Germany

was incubated overnight shaking at 30°C for a second harvest in the following morning. Pellets were washed twice with 40 ml cold 0.1 M Tris/SO₄ pH 9.2, frozen in liquid nitrogen, and stored at -80°C until further processing.

2.2.2.3.2. Plasmids for expression of H1 histones and caspase-3 in yeast

The following plasmids³ were used for transformation:

Plasmid	Recombinant protein
pWA 310	Histone H1°
pWA 311	Histone H1.2
pWA 317	Histone H1.4
pWA 320	Histone H1.1
pWA 326	Histone H1t
pCZ 2	Histone H1.3
pCZ 6	Histone H1.5
pWA 337	Caspase-3

Table 2-1: Plasmids used for the expression of recombinant proteins in yeast

The expression plasmids had already been constructed as described by *Albig et al. (1998)*. Briefly, the corresponding gene fragment of an H1 histone was isolated by restriction digestion from plasmids containing the respective entire H1 coding sequence. For blunt end ligation into the vector yEp51, the sticky ends were filled in by Klenow-polymerase and ligated to the SalI-sites of the vector, which were also blunt-ended by a filling in reaction. Enhanced expression of histones H1.1, H1.2, H1.4, and H1° was achieved by cloning the 3' termination sequence of the yeast ADH1 gene downstream of the histone gene into the respective yEp51 derivative.

2.2.3. PROTEIN BIOCHEMICAL METHODS

2.2.3.1. Protein purification by Ni-NTA affinity chromatography

To facilitate purification of recombinant protein, tags like 6xHis-tags are widely used to generate fusion proteins which can be separated from undesirable proteins by affinity chromatography. These recombinant proteins can be readily detected using anti-His-tag-antibodies. The 6xHis-tag easily binds to Ni-NTA resins, is poorly immunogenic, and at pH 8.0 it is small and uncharged and should not interfere with the correct folding or functioning of the respective protein. It had already been used successfully for the purification of enzymes, transcription factors, and vaccines. However, a suitable tag for

³ kindly provided by PD Dr. Werner Albig

a specific protein, or even a suitable N- or C-terminal position for the tag, has to be found empirically because consequences for the biological activity and proper folding of a protein cannot be excluded generally.

Qiagen provides Ni-NTA as a matrix for purification of 6xHis-tagged proteins under native or under denaturing conditions. NTA is a tetradentate chelating adsorbent, which occupies four out of six ligand binding sites in the coordination sphere of a nickel ion. Two ligand binding sites are free and able to interact with the 6xHis-tag of the recombinant protein. The binding capacity for 6xHis-tagged proteins on Ni-NTA Superflow™ resin is 5-10 mg/ml. The bound protein is eluted with increasing concentrations of imidazole. Due to its similar chemical structure, imidazole competes for the binding sites of the 6xHis-tags on Ni-NTA resins. Low affinity binding of other proteins containing dispersed His residues can be prevented by adding 5 to 20 mM imidazole to the lysis buffers and wash buffers. Detergents or high salt concentrations (up to 2 M NaCl) also reduce nonspecific binding to the matrix as they suppress hydrophobic or ionic interactions.

2.2.3.1.1. Purification of recombinant DFF40/DFF45 complex from bacteria

Purification of DFF40/DFF45 complex from bacteria was carried out using the following buffers:

	NaH₂PO₄/Na₂HPO₄ buffer pH 8.0 [mM]	NaCl [mM]	Imidazole [mM]
Lysis buffer I	50	300	-
Wash buffer	50	300	5
Elution buffer I	50	1600	5
Elution buffer II	50	300	50
Elution buffer III	50	300	100

Table 2-2: Buffers for the purification of DFF40/DFF45 complex from E. coli

Purification of recombinant proteins always requires an individually optimized protocol for efficient cell lysis without degrading the desired protein. The following protocol involves an incubation step with lysozyme which specifically cleaves peptidoglycans and digests only bacterial cell walls this way (*Madigan et al., 1997*). However, incubation at 4°C is always recommended to avoid degradation of recombinant proteins. The sonification steps are necessary to shear the genomic DNA, which makes handling of the

suspension easier. The DNA fragments are removed during the following purification process. The use of the detergent Igepal (Nonidet P-40) facilitates the release of the recombinant protein from cell debris.

Pellets were thawed on ice for 15 min and resuspended in lysisbuffer I, containing complete EDTA-free protease inhibitor mix at a ratio of 3 ml buffer per gram of bacteria wet-weight. Lysozyme was added to a final concentration of 1 mg per ml suspension followed by an incubation step on ice for 30 min and a sonification step (5 times for 10 sec in a digital Branson sonifier at 46% of the maximum amplitude power). Subsequently, Igepal was added to a final concentration of 1% (v/v) followed by a second sonification step as described above and an incubation step at permanent mixing in an end-over-end rotator at 4°C for 1 h. Finally, the suspension was centrifuged at 9500rpm using a Sorvall SS-34 rotor at 4°C and immediately processed for purification of recombinant proteins using Ni-NTA-chromatography.

Purification of a functional DFF40/DFF45 complex is only possible if native conditions are applied. DFF45 is required as a chaperone and to prevent DFF40 from oligomerization which results in precipitation of the protein under in vitro conditions. However, applying native conditions means that some protein is lost during preparation because it stays enclosed in bacterial inclusion bodies. A further disadvantage is the fact that applying native conditions involves a higher risk of background contaminants binding to the Ni-NTA resin.

The following steps were all carried out at 4°C.

The Ni-NTA matrix was equilibrated by washing it three times with four volumes of lysis buffer I, all centrifugation steps were carried out at 4°C at 1,000 rpm in a Heraeus centrifuge. Subsequently, the matrix was incubated in six volumes of lysis buffer I at 4°C while permanently mixing in an end-over-end rotator for at least 15 min, followed by a final centrifugation step. The bacterial protein suspension was added to the equilibrated Ni-NTA matrix at a ratio corresponding to 2 ml Ni-NTA bed volume per 15 g initial bacterial pellet wet weight. The mixture was poured into a 5 ml column, and the first eluted fraction was applied to the column for a second time prior to washing the column with 20 ml washing buffer. During the following elution, aliquots of 500 µl were collected while successively adding 1.5 ml elution buffer I, 2 ml elution buffer II, and 2 ml elution buffer III. Subsequently, 200 µl sterile glycerol were added to each fraction, and the solution was mixed thoroughly. 50-µl-samples for western blotting were taken prior to freezing the fractions in liquid nitrogen. The fractions were stored at -20°C.

2.2.3.1.2. Purification of recombinant caspase-3 from yeast

Purification of recombinant caspase-3 from yeast was carried out involving native conditions as no inclusion bodies of this protein could be detected in yeast. Purification methods using denaturing conditions may have yielded purer preparations. However, active caspase consists of four subunits; therefore, denaturing conditions lead to inactivation of the disintegrating enzyme.

The following buffers were used during the purification process:

	Tris/HCl [mM] pH 7.9	NaCl [mM]	Imidazole
Lysis buffer II	50	400	-
Equilibration buffer	50	400	10
Washing buffer	50	400	20
Elution buffer I	50	400	150
Elution buffer II	50	400	200
Elution buffer III	50	400	500

Table 2-3: Buffers for the purification of recombinant caspase-3 from yeast

All steps were carried out at 4°C or on ice.

Pellets were thawed on ice for 15 min and resuspended in lysis buffer II, containing Complete EDTA-free protease inhibitor mix, at a ratio of 1 ml buffer per 3 grams pellet wet weight. 10 ml of the suspension were mixed with the same volume of glass beads, which had been previously equilibrated in lysis buffer II, in a 30 ml Corex glass tube. After having sealed the tube tightly with Parafilm, cells were lysed by vigorous vortexing for 4 min. Vortexing was interrupted by cooling the sample on ice every minute. Following a centrifugation step at 5,000 rpm for 5 min in a Sorvall SS-34 rotor, the supernatant was kept on ice in a fresh corex tube while the pellet was re-extracted once with 1 ml of lysis buffer II per 3.5 gram pellet wet weight as described above. The supernatants were pooled and centrifuged in an SW-41 rotor in a Beckman ultracentrifuge. The Ni-NTA matrix was equilibrated by washing it three times with equilibration buffer and incubating it in this buffer for at least 5 min. After this, supernatant was added to 3 ml equilibrated Ni-NTA-Superflow matrix (corresponding to 1.5 ml bed volume) and incubated constantly mixing in an end-over-end rotator at 4°C for 2.5 h. Subsequently, the matrix containing the bound recombinant protein was poured into a 5 ml column. The first eluted fraction was applied to the column for a second time (this allowed binding of previously 'escaped' His-tagged protein) prior to washing the column with 20 ml washing buffer. The matrix-bound proteins were eluted

by adding buffers with increasing concentrations of imidazole. Fractions of 500 μ l were collected while 3 ml elution buffer I, 3 ml elution buffer II, and 4 ml elution buffer III were added subsequently. Finally, 200 μ l sterile glycerol were added to each fraction and mixed well. 50- μ l-samples for western blots were taken prior to freezing the fractions in liquid nitrogen. The samples were stored at -20°C until use.

2.2.3.2. Purification of recombinant H1 histone subtypes from yeast

Purification of recombinant H1 histones from yeast is possible without using a tag since an extraction step with 5% PCA precipitates all proteins except the desired H1 histones. This procedure is only hampered by the yeast cell wall; therefore, an incubation step with zymolyase, an enzyme which specifically digests yeast cell walls, and intensive vortexing with glass beads is included in the purification protocol to facilitate the release of intracellular proteins. H1 histones were precipitated from the resulting supernatant by adjusting it to a final concentration of 20% TCA.

Pellets were thawed on ice for 15 min. Each pellet (4 pellets per preparation) was suspended in 20 ml ice-cold PTB-buffer and incubated for 30 min in a water bath at 37°C. After a centrifugation step for 10 min at 4,000 rpm and 4°C in a Heraeus centrifuge. Each pellet was resuspended in 10 ml DB-solution (containing 1 mg/ml Zymolyase) and incubated for 45 min in a water bath at 37°C. Following centrifugation as described above, each pellet was re-suspended in 20 ml ice-cold DB-solution and transferred into 30 ml Corex glass tubes. After a further centrifugation step for 10 min at 8,000 rpm, using a Sorvall SS-34 rotor at 4°C, PCA-equilibrated glass beads (incubated in 5% PCA overnight) were added at a ratio of 1:1 (volume pellet /volume glass beads). The tube was sealed tightly with Parafilm™, and the pellet was suspended by vigorous shaking and vortexing, interrupted by cooling on ice every minute. Once the pellet was suspended completely, 1 ml 5% PCA was added, and the suspension was vortexed for 30 sec. After this, the suspension was incubated in watery ice for 30 min, followed by vortexing for another 30 sec and a centrifugation step at 10,000 rpm in a Sorvall SS-34 rotor at 4°C for 10 min. The supernatant was transferred to a fresh Corex tube and kept on ice while the pellets were re-extracted once with 2 ml 5% PCA. The supernatants were pooled and centrifuged at 8500 rpm in a HB-4 rotor at 4°C for 20 min.

H1 histones in the resulting supernatant were precipitated by adding 100% TCA to a final concentration of 20% (w/v) and incubating the samples at -20°C overnight.

The precipitated H1 histones were collected by centrifugation at 10,000 rpm at 4°C in an HB-4 rotor for 30 min and subsequently washed in 10 ml of 70% (v/v) ethanol (-20°C) to remove traces of TCA; centrifugation was carried out as described above.

Pellets were suspended in 1 ml 70% (v/v) ethanol (-20°C) and transferred to microtubes for another centrifugation step at 14,000 rpm for 30 min at 4°C in a microcentrifuge.

The supernatant was removed completely, and pellets were vacuum-dried before they were suspended in 100 µl DFF-in-vitro-assay buffer. The suspension was kept on ice overnight to solubilize the H1 histones. This was followed by a last centrifugation step at 14,000 rpm for 30 min at 4°C to remove insoluble proteins. The supernatants were transferred to fresh microtubes and stored at -20°C until use. 12-µl-samples were taken to analyze the H1 histones for purity by SDS-PAGE.

2.2.3.3. Purification of H1 histones by gel filtration on P60 columns

Gel filtration or size exclusion chromatography is a method for separating soluble molecules according to their molecular size. It is based on the differential permeation of molecules into a porous matrix with a defined pore size. Molecules larger than the pores cannot enter the matrix and are eluted in the exclusion volume of the column. Migration of particles smaller than the pore size is delayed because they enter the matrix. Thus, smaller molecules are retained for longer times than large molecules, and large molecules are eluted faster. P60 Biogel columns are suitable for the purification of proteins smaller than 60 kDa. Proteins should be applied to the column in a small volume for a better resolution of the separated molecular sizes.

2.2.3.3.1. Preparing the column

5 g Biogel P60 matrix were soaked in 30 mM HCl overnight, degassed by applying a vacuum for 30 min, and poured into a column, 30 cm in length, without trapping air-bubbles. The column was rinsed with 3 volumes of 30 mM HCl before it was used for the separation of H1 histones.

2.2.3.3.2. H1 histone purification process

The column was adjusted to an elution volume of 0.28 to 0.33 ml per min. The sample was first centrifuged at 13,000 rpm for 5 min to remove last traces of solid particles and then applied to the column in a volume of 1 ml. After the protein solution had entered the column bed almost completely, the elution of the column was started with 3 column volumes of 30 mM HCl. 50 fractions, 1 ml in size, were collected with an automatic fraction collector, and 16 µl of each fraction were removed for an analytical SDS-gel prior to freezing all fractions at -20°C until further processing. The column was rinsed with at least 3 column volumes of 30 mM HCl and stored, tightly sealed to avoid dehydration, at room temperature until further use.

Fractions containing H1 histones, as analyzed by SDS-PAGE (see chapter 2.2.3.6), were pooled, freeze-dried for 24 h, and dissolved in 10 mM HCl for CZE or in another desired buffer for further applications or functional assays.

2.2.3.4. In vitro phosphorylation of H1 histones

5 µg recombinant H1.2 were incubated with 10 units of recombinant cdc2 kinase in a 30 µl volume at 30°C for 30 min in reaction buffer supplied by the manufacturer (containing 50 mM Tris HCl, 10 mM MgCl₂, 2 mM DTT, 1 mM EGTA, 0.01% Brij 35, pH 7.5 at 25°C, 200 µM ATP were added just before use). Controls were included: One of the controls was incubated without cdc2 kinase, and the other control was incubated in the absence of ATP. The phosphorylation reaction was stopped by heating to 65°C for 20 min, aliquots of the samples were analyzed for effective phosphorylation by SDS-PAGE, and the remaining solutions were subsequently used in plasmid assays.

2.2.3.5. Analyzing H1 histones by CZE

Generally, electrophoresis is defined as a migration of charged particles in an electric field. Most methods involve the use of a carrier matrix like gel or paper to avoid convection of the separated molecules. However, this is always a time-consuming process, and there is always a risk of interactions between matrix and the molecules to be analyzed. CZE is a high-resolution system and allows the separation of molecules without a carrier matrix in aqueous buffer systems by using a very thin capillary. An advantage of this system is that high voltages are applicable to accelerate separation. Furthermore, the current stays low due to the small inner diameter of the capillary, and the capillary can be easily cooled down to avoid convection. A CZE unit principally consists of a high voltage power supply connected to two platinum electrodes which are immersed in two different buffer reservoirs. The buffer reservoirs are connected by a thin fused-silica-capillary filled with buffer which crosses an on-column-detector. The detector usually detects proteins by UV-spectroscopy at a wavelength of 230 nm and generates a constantly recordable signal.

CZE was performed on a Perkin Elmer/Applied Biosystems 270A-HT system. The separation conditions were optimized according to a method of *Lindner et al. (1995)*. The capillary consisted of fused silica, 122 cm in length, with an inner diameter of 50 µm.

CZE-separations were performed applying the following conditions (table 2-4):

Temperature	30°C
Voltage	20 kV
Current	approx. 35 μ A
Separation time	50 min
Sample injection	by pressure
Injection time	2 sec
Sample protein concentration	approx. 0.5 mg/ml
Absorbance detection	at 200 nm
Separation buffer	30 mM H ₃ PO ₄ , 60 mM HClO ₄ , 0.02% (w/v) HPMC, pH 2.00, adjusted with triethylamine

Table 2-4: Separation conditions for CZE of H1 histones

Absorbance data were recorded and analyzed by a PC-based integration system (Kontron).

2.2.3.6. SDS-PAGE (according to Laemmli, 1970)

Denaturing electrophoresis is a common method for the analytic separation of proteins according to their molecular weight. By adding the anionic detergent SDS all charged groups of proteins are compensated, and the proteins are unfolded. This is facilitated by adding β -mercaptoethanol as a reducing agent to break disulfide bonds. The SDS-protein complex is negatively charged, and the motility of the complex in a gel matrix only depends on the molecular size of the extended ellipsoid protein. During separation on a polyacrylamide matrix gel system with a defined pore size, the proteins treated with an excess of SDS migrate according to their molecular weight. An even better resolution of the separated proteins is achieved in a discontinuous gel system by using a Tris-HCl/Tris-glycine buffering system. This discontinuous system uses differently composed stacking and separation gels. The proteins first cross the wide-meshed stacking gel. Due to the composition of the gel, all ions migrate at the same speed in this part of the gel. The proteins migrate as a 'stack' located between the leading chloride ions and the following glycine ions. As soon as the stack arrives at the border of the close-meshed separating gel, containing another buffer-system, the proteins are decelerated. This change in velocity leads to a jam which results in even more sharpening of the protein bands. Glycine is not decelerated at this border because it is too small and passes the proteins in this part of the gel. In concert with the increase in pH of the separating gel, this leads to a change of the charges in the surrounding

buffer, so the proteins migrate solely according to their molecular size in the separating gel.

2.2.3.6.1. Preparation of the gel

Two glass plates with already fixed spacers were cleaned with 70% (v/v) ethanol and assembled to a tight gel casting unit by using a gasket. The polyacrylamide gel solution was mixed just before use according to the scheme shown in the table below and poured between the glass-plates, leaving 2 cm of the upper space for a stacking gel. Before polymerization at room temperature for 30 min, the gel was carefully layered with aq. bidest to avoid dehydration. This layer was removed as soon as the separating-gel was polymerized, and the glass-plates were dried with blotting paper before casting the stacking-gel. Sample pockets were made by putting a teflon comb into the polymerizing gel.

The gel could be stored in a humidified atmosphere at 4°C for up to a month without affecting the separating features.

Different concentrations of acrylamide/bisacrylamide lead to different mesh-sizes in the gel, suitable for differently sized proteins. For the detection of large proteins (90 to 130 kDa) 10 % separating gels were used, proteins of middle size (40 to 80 kDa) were analyzed on 12% gels, and for smaller proteins (20 to 40 kDa) 15% separating gels were used. The compositions of the gels are shown in the following table:

	10% separating gel	12% separating gel	15% separating gel	stacking gel
Gel buffer A [ml]	2.5	2.5	2.5	-
Gel buffer B [ml]	-	-	-	2
Acrylamide/bisacrylamide 30/08 solution [ml]	3.3	4.3	5	1
Aq. bidest [ml]	4	3.0	3.3	1
10% (w/v) SDS [μl]	100	100	100	40
10% (w/v) APS [μl]	100	100	100	24
TEMED [μl]	5	5	5	4

Table 2-5: Composition of gels used for SDS-PAGE

2.2.3.6.2. Running the gel

The gel, still positioned between the glass plates, was fixed in a vertical electrophoresis unit, and both the upper and the lower buffer tanks were filled with 1x Laemmli gel running buffer. Samples were mixed with sample buffer and heated to 95°C for 5 min. Depending on the protein concentration, 2 - 20 µl were pipetted into the sample pockets of the gel. The gel was connected to a power supply by linking the upper buffer tank (stacking gel) to the cathode and the lower buffer tank (separating gel) to the anode. Subsequently, the gel was run at a constant current of 15 mA until the bromophenol blue front had crossed the stacking gel. As soon as the front had reached the separating gel, the current was increased to 20 mA. The voltage during the run varied between 45 V - 140 V under these conditions. The electrophoretic separation was stopped when the bromophenol blue front reached the end of the gel; usually, this was achieved after 2 to 2.5 h. Subsequently, the gel was stained with Coomassie dye solution or blotted as described below.

2.2.3.6.3. Staining the gel

The gel was carefully detached from the glass plates and put into Coomassie dye solution at room temperature for at least 2 h. Subsequently, the gel was destained by shaking it in decolourant I, followed by shaking in decolourant II. When the background was destained completely, the gel was documented by scanning the wet gel.

2.2.3.7. Western blotting (Towbin et al., 1979)

Western blotting permits the analysis of proteins which previously have been separated by SDS-PAGE. First, the separated proteins are transferred from the gel to a protein-binding membrane in an electric field. Subsequently, the proteins can be analyzed by immunochemical methods. Alternatively, a certain protein band can be isolated from the membrane to determine the protein by sequencing. In this work the semi-dry blotting method was used. Two different membrane types are commonly used: Either nitrocellulose membranes for immunochemical detection or PVDF-membranes; the latter are suitable for immunochemical detection as well as for sequencing from the membrane.

2.2.3.7.1. Preparing the blotting stack

Filter papers were equilibrated in the respective blotting buffers prior to assembling the blotting sandwich on the graphite anode of a semidry blotting apparatus. The blotting

sandwich was stacked, carefully avoiding air-bubbles, according to the following scheme (table 2-6).

Cathode
Three sheets of filter paper soaked in cathode buffer
Gel
Nitrocellulose-membrane
One sheet of filter paper soaked in anode buffer II
Two sheets of filter paper soaked in anode buffer I
Anode

Table 2-6: Composition of the western blotting stack

After weighting the apparatus with a 1-kg-load, the proteins were blotted at a constant current of 0.5 mA per cm² of the gel for 90 min.

2.2.3.7.2. Ponceau-staining

To confirm equal transfer of the proteins to the nitrocellulose membrane, it was reversibly stained with Ponceau S dye solution. The membrane was immersed into the staining solution for 1 min and subsequently incubated in demineralized water until the background was destained. After having scanned the membrane for documentation, it was completely destained by constantly shaking it in TBST for 30 min.

2.2.3.7.3. Immunostaining of the membrane

Detection of a protein can be carried out by using a primary antibody recognizing an epitope specific for the protein to be analyzed. This antibody binds to the immobilized protein on the membrane and is usually detected by a secondary antibody coupled to an enzyme. The secondary antibody binds to the primary antibody and can be detected by a specific reaction catalyzed by the coupled enzyme. This reaction may lead to the deposition of an insoluble dye at the sites of the respective protein bands on the membrane or, alternatively, to a chemiluminescent reaction. Blocking of unspecific protein binding sites on the membrane with an indifferent protein (skim milk powder or BSA) is necessary to prevent antibodies from being bound to the membrane in an unspecific manner. Immunostaining with different antibodies was carried out with the blocked membranes according to the following scheme (table 2-7).

Blocking	Incubate shaking in blocking buffer overnight at 4°C
Membrane washing I	Rinse three times with TBS Incubate for 15 min shaking in 3 changes of TBS Rinse three times with TBS
Primary antibody , diluted in TBS containing 5% (w/v) BSA, 0.02% (w/v) NaN ₃	Incubate in 10 ml antibody solution, shaking at room temperature for 2 h
Membrane washing II	Rinse three times with TBST Incubate for 15 min shaking in 3 changes of TBST Rinse three times with TBST
Secondary antibody , diluted in blocking buffer	Incubate in 10 ml antibody solution shaking at room temperature for 2 h
Membrane washing III	Rinse three times with TBST Incubate for 25 min shaking in 5 changes of TBST Rinse three times with TBST
Detection	By chemiluminescence or colorimetric (see below)

Table 2-7: Protocol used for immunostaining of proteins on NC-membranes

2.2.3.7.4. Detection by enhanced chemiluminescence (ECL)

Detection by ECL systems using a peroxidase-coupled secondary antibody, is a very sensitive method for the detection of proteins in western blots. The chemiluminescence reaction, which involves the oxidation of luminol by horseradish peroxidase, can be enhanced by adding certain types of phenol, naphthol or amines.

The detection solution was mixed from the stock solutions supplied with a commercially available kit, according to the manufacturer's instructions just before use. The membrane was incubated in the solution for 5 min in the dark, wrapped in transparent cling film (carefully avoiding air-bubbles), and put into an exposure cassette. In the dark room, a film was applied to the tightly wrapped membrane and exposed to chemiluminescence for 30 sec to 15 min. The exposure time was chosen depending on the expected signal intensity. Subsequently the film was developed by gently swiveling it in developer until bands were visible. After a short rinse in water, the film was cleared by immersing it for 2 min in a fixing bath. Finally, the film was rinsed thoroughly with water and dried before scanning it for documentation.

2.2.3.7.5. Detection by alkaline phosphatase reaction

Proteins on nitrocellulose membranes can be readily detected by enzymatically produced, precipitating dyes. In systems using antibodies coupled to alkaline phosphatase, the enzyme catalyzes a dephosphorylation reaction of BCIP, followed by a coupled redox reaction with NBT. In this reaction NBT is reduced and BCIP is oxidized, leading to the formation of a blue-violet dye. This dye precipitates at the site of the enzyme-coupled antibody which in turn is specifically attached to the protein to be detected.

2.2.3.7.6. Dilution of antibodies used for western blotting

Dilutions of the primary and secondary antibodies used in this study are summarized in the following table. Usually, 5% (w/v) BSA buffered with TBS (pH 7.4) was used for dilutions of all antibodies. To avoid microbial contamination, 0.02% NaN₃ were added as a preservative to solutions containing primary antibodies. These solutions were stable for up to three months and allowed multiple re-use of the primary antibody solution.

Antibody recognizing	Dilution
DFF40 (from rabbit)	1:500
PARP (from rabbit)	1:1,000
DFF45/DFF35 (from rabbit)	1:1,000
Caspase-3 (from rabbit)	1:1,000
HDAC-1 (from mouse)	1:2,000
Rabbit IgG coupled to AP	1:2,000
Mouse IgG coupled to AP	1:2,000
Mouse IgG coupled to HRP	1:10,000
Penta-His tag	1:1,000
bcl-2	1:250
bax	1:125
p53	1:250
p21 (CIP)	1 µg/ml
H2A.X	1:1,000
HSP-70	1:1,000
Myc-tag	1:2,000

Table 2-8: Dilutions of the antibodies used for western blotting

2.2.3.8. Quantitation of protein contents (Bradford, 1976)

The dye Coomassie brilliant blue G250 may be used for photometrical quantitation of proteins (Bradford assay). This acid dye changes its absorption maximum from 465 nm to 595 nm in the presence of proteins in an acidic environment. This shift is caused by the formation of a dye-protein-complex, stabilizing the dye in its deprotonized, anionic sulfonate form. Binding occurs on cationic and unpolar hydrophobic side chains of the amino acids, i.e. it mainly binds to arginine.

The Bradford assay is a sensitive and fast protein quantitation method. A great advantage, compared with other protein assays, is that it does not interfere with too many substances. So it is possible to determine protein concentrations in solutions containing relatively high amounts of reducing agents and SDS. However, a disadvantage may be seen in its differential sensitivity concerning different proteins, which may contain different amounts of arginine. Accordingly, protein contents determined by Bradford assay should only be compared with each other when using the same protein as a standard.

2.2.3.8.1. Protein standard curve

In this work BSA was used as a standard protein to determine the protein contents of solutions containing a mixture of cellular proteins, so all stated protein concentrations refer to BSA as a standard protein.

A standard curve was calculated by linear regression (using the program Excel) from values of different duplicate dilutions of the standard protein, ranging from 0.01 µg/ml to 250 µg/ml. The resulting equation was used to calculate a factor for fresh preparations of Bradford dye solution. This factor was used to calculate protein contents in different sample preparations which contained mixtures of proteins.

2.2.3.8.2. Bradford assay

For each assay 50 µl of the protein solution were mixed with 1 ml of Bradford dye solution in a micro-cuvette and incubated at room temperature for 10 min. Absorption was measured using a photometer at an absorption wavelength of 595 nm, and the protein content was calculated by using a factor which was previously determined using BSA as a standard protein (see above).

2.2.3.9. In vitro plasmid assay for DFF40

Cleavage characteristics of a DNase similar to DFF40 can be tested in an in vitro assay using plasmid DNA as a substrate. The in vitro assay described in the following sections

allowed the examination of effects caused by histone proteins on the enzyme's activity. This assay is a commonly used system to test for DNase activity.

2.2.3.9.1. Dialysis of recombinant purified proteins

Prior to the experiment, the recombinant DFF40/DFF45 complex as well as recombinant caspase-3 were dialyzed two times for 2 h at 4°C against a 200-fold volume of DFF-in-vitro-assay buffer. The 3K-membrane used for dialysis was previously boiled two times for 30 s in sterile aq. bidest without adding EDTA because this chelating reagent might have interfered with the following assay.

2.2.3.9.2. Assay conditions

In general, plasmid DNA was incubated in a 110 µl reaction volume containing 1 µg of circular plasmid DNA, 4.5 mM MgCl₂, 4 mM DTT, and different amounts of the respective recombinant proteins. The activity of caspase-3 and DFF40 varied with each preparation and had to be titrated in another plasmid assay before conducting the main experiment. The titration protocol is summarized in the table below. The reactions were incubated at 37°C for 1 h, subsequently stopped by adding 7.5 µl stopping buffer, and finally 20 µl of each sample were analyzed by agarose gel electrophoresis.

In experiments involving histone proteins it was necessary to digest the H1 histones with 1 mg/ml proteinase K at 55°C for 1 h before adding stopping buffer since the presence of proteins impaired subsequent electrophoretic separation of the DNA.

Enzymatic activities of DFF40 and caspase-3 were titrated according to the following schemes (table 2-9 and 2-10):

DFF in vitro assay buffer	50	90	85	80	65	40	100
100 mM MgCl₂	5	5	5	5	5	5	5
100 mM DTT	4.4	4.4	4.4	4.4	4.4	4.4	4.4
Plasmid DNA	1	1	1	1	1	1	1
DFF40/DFF45^{*2}	50	-	5	10	25	50	-
Caspase-3	-	10	10	10	10	10	-

Specifications are given in µl ^{*2} Diluted 1:20 in DFF in vitro assay buffer

Table 2-9: Titration of DFF40 activity

DFF in vitro assay buffer	70	40	60	50	40	30	20	10	100
100 mM MgCl₂	5	5	5	5	5	5	5	5	5
100 mM DTT	4.4	4.4	4.4	4.4	4.4	4.4	4.4	4.4	4.4
Plasmid DNA	1	1	1	1	1	1	1	1	1
DFF40/DFF45^{*2}	30	-	30	30	30	30	30	30	30
Caspase-3	-	50	10	20	30	40	50	60	-

Specifications are given in μl ^{*2} Diluted 1:20 in DFF in vitro assay buffer

Table 2-10: Titration of caspase-3 activity

2.2.3.10. Assay with nuclei

The assay with nuclei utilizes human nuclei instead of plasmid-DNA to test the effects of a protein on the activity of a DNase. Due to the organization of DNA in chromatin it represents a more 'natural' substrate for DFF40. Nuclei were prepared as described in chapter 2.2.5.2.2 and incubated for up to 2 h at 37°C with DFF40, caspase-3, and the respective proteins to be tested. Reactions were stopped by adding 5 μl 0.5 M EDTA and subjected to digestion by proteinase K (final concentration 1 mg/ml) for 30 min at 55°C. DNA was purified from the samples as described in chapter 2.2.4.10.6 and analyzed by electrophoresis on 1% TBE agarose gels.

2.2.3.11. Caspase-3 activity assay

In this assay the activity of caspase-3 is quantitated by using the fluorescent dye DEVD-afc. By coupling an amino-fluormethyl-coumarin derivative (afc) to a protein tag containing the cleavage site of caspase-3 (DEVD), this assay is specific for the detection of caspase activities which are able to specifically cleave the substrate DEVD, namely caspase-3-like enzyme activities.

For the detection of caspase-3 activity in human cells, lysates were prepared using a neutral lysis buffer. Aliquots of the lysates were incubated in a microtiter plate with the substrate at defined conditions. Fluorescence of the samples was measured in a fluorimeter (Fluoroskan Ascent FL) before and after the incubation step, and enzyme activities were calculated using the program Excel (Microsoft).

5×10^6 cells per assay sample were harvested by centrifugation at 300x g and washed once with PBS. After resuspending the cells in 50 μl of lysis buffer III, the cells were lysed during an incubation step on ice for 10 min. Supernatants were collected after a centrifugation step at 500x g at 4°C for 5 min. 10 μl of each sample were pipetted in duplicates into wells of a microtiter plate. The caspase-3 reaction buffer was completed with 10 mM DTT and 50 μM DEVD-afc just before use, and 90 μl of the buffer were

added to each sample in the wells. Basal fluorescence values were determined in the fluorimeter using the setting pair 390 nm for excitation, 510 nm for emission, and a corresponding fluorescent filter. After having incubated the plates at 37°C in the dark for 20 min, the final fluorescence values were determined as described above. Enzyme activities were calculated in pmol afc per min and were finally referred to 1 mg protein per sample (corresponding to the unit $\mu\text{U}/\text{mg}$) by using a substrate specific factor which was determined in advance. This factor was 1.23 for the fluorimeter used in all the experiments. The basal fluorescence values were subtracted from the final fluorescence values. The resulting values were divided by the incubation time and the protein content, and the obtained values were multiplied by the factor.

2.2.4. MOLECULAR BIOLOGICAL METHODS

2.2.4.1. Cloning strategy for over-expression in human cells

The aim of this work was a stable over-expression of a recombinant protein in addition to the already present endogenous, respective protein. For that purpose a vector, carrying the strong CMV-promotor promotor, was chosen. Furthermore, the vector used in the experiments allowed for adding a specific tag to the protein to distinguish it from the endogenous protein during subsequent analysis of the expression patterns.

mRNA was isolated from Jurkat cells, transcribed into cDNA, and PCR was conducted using specific primers for the amplification of the coding region of DFF40 and DFF45, respectively. The primers were constructed in a way allowing the amplification of the respective protein without the terminal stop-codon. In addition, these primers had an overhang coding for different restriction sites, allowing in-frame-ligation of the resulting fragment into a vector which contains the respective restriction sites. The stop-codon was omitted since the vector used in this work already contained a stop-codon. The use of this stop-codon permitted expression of a recombinant protein with specific tags. This tag can be finally detected in western blots, allowing the discrimination between endogenous protein and additionally expressed recombinant protein.

Since cDNA is not stable for a long time, the PCR-product was first ligated into the vector pGEM[®] T easy. Before the insert was ligated into the vector used for stable transfection, it was sequenced using different sequencing primers to check for mutations. The fidelity of Taq-polymerase is comparatively low, which in average results to base exchanges every 1000 bp (indeed, in this study a non-silent mutation was seen in every second construct).

Inserts carrying no mutations were selected for cloning into pcDNA6 myc-his A; the vector was later used for stable transfection into human lymphoma cells.

2.2.4.2. Isolation of RNA with the RNeasy kit

Pure cytosolic mRNA was isolated from the cytoplasm of human cells according to the protocol provided by Qiagen. 1×10^7 cells were harvested by centrifugation and, after having removed all media, were resuspended in 175 μ l buffer RLN, completed with 30 U RNase-inhibitor and 1 mM DTT. After a centrifugation step (300 rpm, 4°C) for 2 min, 600 μ l of buffer RLT (completed with 10 μ l β -mercaptoethanol per ml) were added to the supernatant, and the suspension was vortexed vigorously. After this, 430 μ l 100% ethanol were added and mixed before applying 700 μ l of the sample to an RNeasy mini spin column, which was fixed in a 2-ml-collection tube. The samples were centrifuged at 8,000 g for 15 sec, and the process was repeated with the remaining sample.

Subsequently, samples were washed once with 700 μ l buffer RW1, twice with the same volume of buffer RPE, and the column was dried completely by centrifugation at maximum speed for 2 min. Finally, mRNA was eluted by washing the column twice with 30 μ l DEPC treated water.

2.2.4.3. Quantitation of nucleic acids

DNA contents were quantitated by UV spectrometry in most applications. An estimation of DNA contents by Gel-titration was applied in cases when only small amounts of DNA were available. Thus gel titrations were usually carried out with the gels used for the purification of the DNA fragments for ligation reactions to determine the correct vector/insert ratios.

2.2.4.3.1. Quantitation of DNA or RNA by UV spectrometry

RNA- or DNA contents were measured by UV spectrometry at 260 nm, which is the absorption maximum of TMP and UMP. These measurements were conducted in a photometer (Genequant II) using an UV-light-compatible quartz micro-cuvette. Quantitative values were calculated by using a factor. This factor was 50 in the case of DNA and 40 in the case of RNA and is based on the observation that a solution of double-stranded DNA has an OD_{260} of 1.0 at a concentration of 50 μ g/ml, whereas a solution containing single stranded DNA or RNA has an O_{260} of 1.0 at a concentration of 40 μ g/ml.

In addition, absorbance at 280 nm (absorption maximum of tryptophane) was measured to estimate the purity of the DNA or RNA. The content of contaminating proteins can be estimated by determining the 260/280 ratio. Pure RNA-solutions possess a quotient of 2.0, whereas the quotient should be 1.8 in case of pure DNA.

2.2.4.3.2. Quantitation of DNA by gel titration

DNA contents of DNA fragments can be estimated after DNA gel electrophoresis (see chapter 2.2.4.8) when a mixture of standard DNA fragments of known contents (usually 1 µg per fragment) is used for the calibration of a gel. For quantitation, sample DNA and standard DNA are run on the same gel. After staining with ethidium bromide, the DNA contents are estimated by comparing the intensity of the respective bands.

2.2.4.4. PCR

Polymerase chain reaction, invented by K.B. Mullis in 1983, is a fast in-vitro-method for the amplification of a DNA fragment flanked by a known, short DNA sequence.

The reaction needs double stranded DNA as a template, two single-stranded specific primers (sense and anti-sense, binding to the flanking region of the DNA fragment to be amplified), dNTPs, and a thermo-stable DNA polymerase. The PCR reaction consists of three successive steps: *Denaturing* the template DNA, *annealing* of the primers, and *elongation* of the bound primers. Repeating this reaction series for up to 30 times in a cycling reaction allows the exponential amplification of the desired DNA fragment. The reactions are performed in a thermocycler because this unit permits quick and exact changes of the incubation temperature at exactly defined times.

First, the template DNA is denatured by an initial incubation step at 94°C to 96°C, followed by a decrease of the temperature to a template-specific value between 55°C and 65°C. This second step enables annealing of the primers to the respective complementary single-stranded DNA. During the subsequent increase of the temperature to 72°C in a third step, the thermo-stable DNA polymerase elongates the DNA strands, starting from the primers. The resulting double stranded DNA is denatured in the following reaction cycle and serves as an additional template for the DNA polymerase.

An often used enzyme in this reaction is a DNA polymerase initially purified from the microorganism *Thermophilus aquaticus* (Taq-polymerase). The microorganism was first found in hot springs of the Yellowstone National Park. Due to its living conditions in hot environment - it is able to resist temperatures higher than 100°C - it has a very heat-stable DNA polymerase. Nowadays, recombinant Taq-polymerase and polymerases from other microorganisms with even better features for in-vitro-use are available. In this study a recombinant Taq-polymerase was generally used.

2.2.4.4.1. PCR conditions used in the experiments

PCR was conducted in 100 µl volumes in a specific buffer (10 mM Tris/HCl pH 8.3, 50 mM KCl, 1.5 mM MgCl₂, 0.01% gelatine) using thin walled PCR-microtubes according to the following scheme (a master-mix was commonly used):

10x Red Taq™ PCR buffer	10 µl	1x
10 mM dNTP-mix	2 µl	200 µM
25 mM sense primer 1	1 µl	0.25 nM
25 mM antisense primer 2	1 µl	0.25 nM
cDNA or plasmid-DNA	x µl	10 to 100 ng DNA/reaction
Red Taq™ DNA polymerase	3 µl	3 U
Aq. bidest	y µl	Added to 100 µl

Table 2-11: Composition of PCR reactions

PCR was carried out using a Perkin-Elmer thermocycler at the following conditions:

Initial denaturing	94°C	2 min	30 repeats
Denaturing	94°C	30 sec	
Annealing	55°C	45 sec	
Elongation	72°C	1 min 30 sec	
Final elongation	72°C	7 min	

Table 2-12: PCR conditions

Subsequently, samples were cooled down to 4°C until the program was finished manually and processed for analysis by agarose gel electrophoresis.

2.2.4.5. RT-PCR

PCR may be carried out using mRNA as a source for the sequence to be amplified but this requires an initial reverse transcription step to generate a suitable double-stranded DNA substrate for the Taq-polymerase.

2.2.4.5.1. Reverse transcriptase reaction

Since amplification of DNA from RNA-samples is hampered by the fact that RNA cannot be used as a template by Taq-polymerase, the RNA samples have to be transcribed to DNA by using reverse transcriptases (RT), available from different viral sources, to generate complementary DNA (cDNA). In a second step the remaining RNA is digested by RNase H to increase the performance of the following PCR.

All reverse transcriptases need a primer to catalyze the transcription process. Generally, three types of primers can be used:

Sequence specific primers bind to an already known sequence in the RNA. They are only recommended if large amounts of the sequence are supposed to be in the sample RNA (e.g. suitable for the detection of viral DNA in diagnostic tests).

Oligo-dT primers consist of a series of 12 to 18 deoxy-thymidines and bind to the poly-A-tail of eukaryotic RNA. They only lead to the transcription of RNA bearing a poly-A-tail, which is the case for many eukaryotic proteins.

Random primers are mixtures of different hexanucleotides, binding to the RNA in a random process. They are necessary for the transcription of mRNA without a poly-A-tail, e.g. histone proteins.

In this work oligo-dT primers were used for the reverse transcriptase reaction using RNA previously isolated with the RNeasy mini kit.

2.2.4.5.2. DNase digestion of RNA

RNA for use in RT-PCR was initially digested with DNase to eliminate traces of contaminating genomic DNA. 40 µg RNA were digested with 4 µl DNase (RNase-free) in a 40 µl volume by incubation at 37°C. After this, the RNA was denatured by heating the sample to 70°C for 5 min, which simultaneously stopped the DNase digestion.

2.2.4.5.3. cDNA synthesis

Each DNase-digested RNA sample was divided into four 10 µl-aliquots; 1 µl oligo-dT primer was added to each sample before they were heated to 65°C for 5 min to anneal the primers. After cooling down on ice for two minutes, 9 µl master-mix (see below) were added to each sample, followed by an incubation step at 55°C for 1 hour, which allowed cDNA synthesis. The reaction was stopped by an incubation step at 85°C for 5 min, 1 µl RNase H (10 U) was added to each sample, and finally the samples were incubated at 37°C for 20 min to digest remaining RNA strands. Controls, containing RNase-free water instead of reverse transcriptase, were always included to check for contaminating genomic DNA in the RNA-sample. Samples were stored at -20°C until they were used for PCR. Master-mixes were used for the preparation of the reactions, as described in the following table:

	Positive reaction mix	Negative control mix
5x cDNA synthesis buffer	16	8
0.1 M DTT	4	2
RNase out	4	2
dNTP	8	4
Reverse transcriptase	4	-
RNase-free water	-	4

Specifications are given in µl

Table 2-13: Composition of the master-mixes used for cDNA synthesis

2.2.4.6. Restriction digestion

Cutting DNA at defined positions *in vitro* is possible by using restriction enzymes from several prokaryotes. The original function of these enzymes is the specific destruction of foreign DNA, e.g. from viruses; this is particularly important in unicellular organisms lacking a complex host defense system. Therefore, restriction enzymes interact with DNA only at sites with specific recognition sequences. The recognition site usually consists of a short palindromic DNA sequence, 4 to 8 bp in length. Restriction *endonucleases* cut their respective DNA substrate by introducing double-stranded breaks *within* the recognition sequence. This may generate blunt-ended DNA or DNA with sticky ends: DNA termini with overhanging single-stranded DNA. Due to these features, restriction endonucleases are ideal tools in DNA research. They represent molecular scissors which are able to generate DNA fragments with defined termini.

Activity and specificity of restriction enzymes depend on the reaction conditions, in particular on the reaction temperature and buffer components. Therefore, restriction enzymes for *in-vitro*-use are commonly supplied by the manufacturer with a specially optimized buffer.

Reactions were performed in 1.5-ml microtubes according to the respective manufacturer's manual. Usually 5 units of restriction enzyme were used per μg of DNA to be digested in a 10- μl -volume containing the respective recommended buffer. If required, reactions were scaled up to a 100- μl -volume for a preparative digest. Restriction digests were conducted at the enzyme's recommended optimum temperature for 1 hour, stopped by adding $\frac{1}{4}$ volume of 4x-DNA loading buffer, and finally subjected to agarose gel electrophoresis.

2.2.4.7. Ligation of DNA fragments into a vector

DNA may be ligated into a vector by using the enzyme T4 ligase which is able to connect two DNA strands by creating phosphodiester bonds between the 3'-OH end of the one DNA strand and the 5'-phosphate end of the other DNA strand. This step is energy-dependent and needs hydrolysis of ATP.

The DNA strands may possess sticky ends or blunt ends. However, the ligation reaction is enhanced by sticky ends.

2.2.4.7.1. Cloning into pGEM[®]-T easy vectors

pGEM[®]-T vectors are linearized vectors carrying a free 3-terminal thymidine at each end of the DNA strand. Cloning into pGEM[®]-T-vectors is possible with PCR-products created by DNA polymerases, as these add a single additional 3' deoxyadenosine to each PCR-product in a template-independent manner. Enzymes similar to Taq-poly-

merase without a proof-reading activity and without a 3'→5'-exonuclease activity are suitable polymerases for the production of inserts containing an overhanging adenine. Reactions were prepared as summarized in the following table:

	Insert:Vector ratio 3:1	Insert:Vector ratio 1:1	Negative control
2x rapid ligation buffer	5 µl	5 µl	5 µl
T4 ligase	1 µl	1 µl	1 µl
pGEM[®] T easy (~3 kb)	1 µl (50 ng)	1 µl (50 ng)	1 µl (50 ng)
Insert-DNA (~1 kb)	50 ng	17 ng	-
Sterile aq. bidest	Added to 10 µl	Added to 10 µl	Added to 10 µl

Table 2-14: Composition of ligase reactions using the vector pGEM[®] T easy

Reactions were kept at 4°C overnight and were subsequently used for transformation in *E. coli* to propagate the modified vector.

2.2.4.7.2. Cloning into multiple cloning sites of other vectors

In this work cloning into the multiple cloning site of the vector pcDNA6 myc his A was done using two different restriction sites in the vector: XbaI and HindIII. By using this cloning-strategy a dephosphorylation step could be omitted, and the insert's direction of ligation was determined in advance. Prior to the experiment, the vector was linearized by a restriction digest with the respective restriction enzymes applying the appropriate reaction conditions (see chapter 2.2.4.6.). Usually, the reaction volume was 20 µl. Negative controls, containing no insert, were performed to test for a self-ligation reaction of the vector. Ligase reactions were prepared according to the following scheme:

	Positive reaction	Negative control
10x T4 ligase buffer	2 µl	2 µl
T4 ligase	6 U	6 U
Vector DNA	50 to 100 ng	50 to 100 ng
Insert DNA	50 to 150 ng*	-
Sterile aq. bidest	Added to a 20 µl volume	Added to a 20 µl volume

* corresponds to a 3- to 5-fold molar excess of the insert-DNA (1 kb) compared with the vector-DNA

Table 2-15: Composition of ligase reaction mixtures using other vectors

The reaction mixtures were kept at 12°C overnight and were subsequently used for transformation into *E. coli* (see chapter 2.2.1.4).

2.2.4.8. DNA gel electrophoresis

A common method for the analysis of DNA from different sources is electrophoresis using agarose as a matrix for the separation of DNA fragments which differ in their sizes.

Due to the phosphate groups in their backbones, DNA molecules are negatively charged and migrate to the anode when exposed to an electric field. During electrophoresis at a low voltage, DNA fragments migrate at different rates, where the electrophoretic mobilities are proportional to the fragment sizes in a reciprocal manner.

The DNA bands can be visualized under UV-light after staining with ethidium bromide. Ethidium bromide, once used for the treatment of certain parasites in cattle, is now, despite its highly mutagenic features, a widely used fluorescent dye for the detection of DNA. Due to its planar structure it combines tightly within the DNA molecule by interacting preferably with double-stranded DNA. Intercalating within DNA enhances the dye's fluorescence at 254 to 366 nm, leading to the emission of an orange-red light of 590 nm in wavelength.

Usually, agarose gels containing 1% w/v agarose as a separating matrix were prepared by boiling the respective amount of agarose in TBE-buffer. After cooling down to 50°C, the solution was poured into a gel casting tray, containing a comb to generate wells of defined sizes, and the gel was then allowed to solidify at room temperature for 30 min. After immersing the gel in TBE-buffer in the horizontal electrophoresis chamber, the samples were pipetted into the wells and electrophoresis was started by applying a constant voltage of 70 V. Electrophoresis was stopped after the bromophenol blue front had crossed two thirds of the gel length, and subsequently the gel was stained for 20 min in a dye solution containing 2.5 µg/ml ethidium bromide. Finally, the bands were analyzed under UV-light and digitally photographed for documentation.

2.2.4.8.1. Determination of DNA fragment sizes

The fragment sizes of the electrophoretically separated DNA can be determined by running a mixture containing DNA fragments of known sizes as a standard on the same gel. In this work λ -DNA digested by the restriction enzymes Eco RI and Hind III was used as a standard. The respective standard fragment sizes, resulting from digestion with these enzymes, range between values from 570 bp to 21,700 bp (see chapter 2.1.5.).

2.2.4.9. RNA gel electrophoresis

The gel casting chamber was cleaned with 70% ethanol prior to use. 200 mg agarose were added to 16 ml aq. bidest and boiled for 3 min in a microwave oven. After cooling

down to 55 - 60°C, 2 ml 10x MOPS buffer and 2 ml 37% formaldehyde were added to the solution prior to casting the gel.

The RNA samples were prepared for electrophoresis by mixing 10 µg RNA with 2 µl 37% formaldehyde, 1 µl 10x MOPS buffer, and DEPC-water to a final volume of 10 µl. The samples were heated to 65°C for 15 min, 3 µl RNA-sample buffer were added, and finally the samples were applied to the gel. Electrophoresis was carried out at a constant current of 20 mA using 1x MOPS buffer as a running buffer. Usually, electrophoresis was stopped when the bromophenol blue front had crossed two thirds of the gel. After staining in ethidium bromide, the gel was analyzed under UV-light.

2.2.4.10. DNA purification methods

2.2.4.10.1. Phenol/chloroform extraction of DNA

During phenol/chloroform extraction contaminating proteins are denatured by adding phenol and chloroform, the latter additionally leads to a stabilization of the two phases after a centrifugation step. The aqueous phase contains DNA, and the phenol-phase contains contaminating denatured proteins, which can be separated from the DNA this way. Phenol used for the extraction of DNA should be saturated with TE-buffer to avoid a dissolving of DNA in the phenol-phase. Small amounts of Isoamyl alcohol are added during the extraction process to avoid foaming of the sample.

The solution containing the desired DNA was completed with one volume TE-saturated phenol (BioRad) and one volume chloroform:isoamyl alcohol (24:1) and vortexed thoroughly. After a centrifugation step (1 min, 13,000 rpm), the upper phase containing DNA was transferred to a fresh microtube, and the procedure was repeated as described above but without adding phenol. DNA from the upper aqueous phase was subsequently precipitated by ethanol as described in the following chapter.

2.2.4.10.2. DNA precipitation by ethanol

DNA from aqueous solutions can be precipitated by adding ethanol in the presence of sodium-acetate as a supplier of monovalent cations; these molecules neutralize the negative charges of the DNA's phospho-diester backbones. This method of precipitation was used after a phenol/chloroform extraction or during sequencing.

Prior to ethanol-precipitation, the DNA solution was acidified by adding 1/10 volume 3 M Na-acetate, pH 4.8. Subsequently, DNA was precipitated by mixing this solution with 3 volumes ice-cold 100% ethanol. After an incubation step on ice for 1 h, the sample was centrifuged (15 min, 13,000 rpm, 4°C), the supernatant was removed, and the pellet was washed with 500 µl 70% ethanol to remove traces of salt. After a

centrifugation step as described above, the DNA was dried for 3 min in a Speedvac and dissolved in a suitable amount of Tris/HCl buffer pH 8.5.

2.2.4.10.3. DNA precipitation by isopropanol

This method was used for the precipitation of large amounts of DNA in a small volume. In contrast to ethanol-precipitation, usually 0.7 to 1 volume of isopropanol is sufficient for the efficient precipitation of DNA. A second advantage of this method is that it can be conducted at room temperature. This feature was useful for samples containing SDS to avoid co-precipitation of SDS. The principles of this method correspond to those described for ethanol-precipitation: Monovalent cations were usually supplied by using NaCl in the buffers used prior to the isopropanol precipitation step.

2.2.4.10.4. Plasmid DNA purification by the TELT method

The bacterial pellet was suspended in 150 µl TELT-buffer (a buffer containing Tris, EDTA, lithiumchloride, and Triton X 100). To lyse the walls of the bacterial cells, 25 µl of a lysozyme stock solution were added, and the suspension was heated to 95°C for 2 min, followed by vortexing and an incubation step on ice for 5 min. After a centrifugation step at 13,000x g for 10 min at 4°C, the pellet was removed, and the remaining plasmid DNA in the supernatant was precipitated by mixing it with 200 µl isopropanol, followed by a centrifugation step at 13,000x g for 25 min at 4°C. The pellet, containing the plasmid DNA, was washed with 200 µl 70% (v/v) ethanol and, after a final centrifugation for 5 min at 13,000 g at 4°C, the pellet was dried for 6 min in a Speedvac. The dried pellet was suspended in 30 µl aq. bidest and stored at -20°C before further analysis. To test for an insert by analytical gel electrophoresis, 10 µl of the solubilized DNA were subjected to a restriction digestion with 5 units of the respective restriction enzymes at the appropriate conditions for 1 h, as described by the manufacturer.

2.2.4.10.5. Plasmid DNA purification using Qiagen maxi prep kits

The following reagents were supplied with the kit:

Buffer P1 (resuspension)	50 mM Tris/HCl, 10 mM EDTA, 100 µg/ml RNase A (added immediately before use), pH 8.0
Buffer P2 (lysis)	200 mM NaOH, 1% (w/v) SDS
Buffer P3 (neutralization)	3.0 M potassium acetate, pH 5.5

Buffer QBT (equilibration)	750 mM NaCl, 50 mM MOPS, 15% (v/v) isopropanol, 0.15% (w/v) Triton X 100, pH 7.0
Buffer QC (washing)	1.0 M NaCl, 50 mM MOPS, 15% (v/v) isopropanol, pH 7.0
Buffer QF (elution)	1.25 M NaCl, 50 mM Tris/HCl, 15% (v/v) isopropanol, pH 8.5
Buffer QN (Endofree™ elution)	1.6 M NaCl, 50 mM MOPS, 15% (v/v) isopropanol, pH 7.0
Buffer TE (dissolving)	10 mM Tris/HCl, 1 mM EDTA, pH 8.0
Buffer ER (removing)	Endotoxin removal buffer

Table 2-16: Buffers supplied with the Qiagen maxi prep kit

Plasmid preparations were carried out according to the standard protocols provided by Qiagen. After having added buffer ER during the Endofree™ protocol, only endotoxin-free labware was used.

Both protocols use alkaline lysis and RNase treatment of the pelleted bacteria. The pellet was resuspended in 10 ml buffer P1, 10 ml buffer P2 were added, and the suspension was mixed by inverting the tube for several times. This was followed by an incubation step for 5 min at room temperature to release the DNA from the cells. The suspension was neutralized and SDS was precipitated from it by adding 10 ml chilled buffer P3. After an incubation step on ice for 20 min, the lysate was cleared from SDS, most genomic DNA, and debris by a centrifugation step at 20,000x g. Plasmid DNA from the supernatant was bound to an anion exchange resin, by applying it to a column which previously had been equilibrated with 10 ml buffer QBT.

Alternatively, during Endofree™ preparations the lysate was cleared by filtration through a QIAfilter cartridge, as described by Qiagen to avoid contamination with traces of genomic bacterial DNA. The filtered lysate was subsequently incubated with buffer ER for 30 min on ice to prevent endotoxins from later binding to the anion exchange resin.

Subsequently, RNA, proteins, and other impurities were removed by a medium-salt wash with 2 x 30 ml buffer QC before plasmid DNA was eluted in a high-salt elution step with 15 ml buffer QF or 15 ml buffer QN (in the endofree protocol), respectively. The plasmid DNA was concentrated and desalted by isopropanol precipitation and a final wash step with the more volatile 70% ethanol (see chapter 2.2.4.10.3).

2.2.4.10.6. DNA purification from human cells

Using the following protocol, samples were lysed, and RNA as well as proteins were removed by digestion during two successive incubation steps. The resulting DNA was

precipitated with an excess of isopropanol (2.5 volumes were necessary to precipitate the entire genomic DNA) and washed with the more volatile 70% ethanol to remove traces of salt.

5×10^6 cells per preparation were harvested (see chapter 2.2.5.1.7), resuspended in 200 μ l DNA lysis buffer and, after having frozen the samples in liquid nitrogen, were stored at -20°C until further processing. A volume of 2 μ l DNase-free RNase A (final concentration 100 $\mu\text{g}/\text{ml}$) was added to the thawing samples and those were incubated at 37°C for 30 min. 200 μ l 2x PK buffer (containing 200 $\mu\text{g}/\text{ml}$ proteinase K) were added to each sample, and the samples were incubated at 55°C for another 60 min. Subsequently 1 ml isopropanol was added, and the samples were shaken thoroughly to precipitate the entire genomic DNA. After an incubation step for 1 h at room-temperature, DNA was pelleted by centrifugation (15 min, 13,000 rpm) and washed with 500 μ l 70% (v/v) ethanol. The samples were centrifuged once again as described above and dried in a Speedvac for 6 to 8 min. A volume of 100 μ l TE-buffer was added per sample, and the samples were kept at 4°C overnight. This step was necessary to allow a partial dissolving of the genomic DNA in the solvent.

Prior to conducting electrophoresis, insoluble genomic DNA was removed to avoid an overloading of the gel, and 25 μ l DNA loading buffer were mixed with the samples. A volume of 25 μ l of each sample was used for analysis by electrophoresis on a 1% agarose gel (see chapter 2.2.4.8).

2.2.4.10.7. Purification of DNA fragments from agarose gels

DNA fragments were purified from an agarose gel using the MinElute gel extraction kit from Qiagen. Its working principle is based on melting the agarose at a defined pH in the presence of chaotropic salts. This allows a complete release of DNA from the agarose matrix. Subsequently, the released DNA is bound to silica spin columns, washed, dried, and finally eluted in a small buffer volume.

Reagents and materials supplied with the kit are summarized in the following table:

MinElute spin columns	Contain a silica membrane as a DNA binding matrix
Buffer QG (solubilization and binding)	Contains chaotropic salts and a pH indicator
Buffer PE (washing)	Completed with ethanol prior to use
Buffer EB (elution)	10 mM Tris-HCl, pH 8.5
2-ml collection tubes	

Table 2-17: Components of the MinElute gel extraction kit

Up to 400 mg agarose containing 5 µg DNA (70 bp to 4 kb) can be processed per MinElute spin column. Usually, 80% of the DNA is recovered.

The band containing the desired DNA fragment was visualized on a 366 nm-UV-illuminator and excised from the agarose gel using a clean scalpel. The gel slice was weighed in a 2-ml-microtube, and three volumes of buffer QG were added per volume of gel, assuming that 100 mg agarose correspond to a volume of 100 µl. The reactions were incubated for 10 min (or until all the agarose had dissolved) at 50°C, vortexing the sample every 3 min during this incubation step. One ml isopropanol was added to the yellow solution and mixed by inverting the microtube several times. The required number of MinElute columns was placed into the corresponding collection tubes, and DNA was bound to the silica membrane by applying the mixture to the columns, followed by a centrifugation step (10,000 g, 1 min). The flow-through was discarded, and another 500 µl buffer QG were applied to each column and centrifuged as described above. The flow-through was discarded, and the bound DNA was washed by applying 750 µl buffer PE to each column followed by a further centrifugation step as above. To remove residual ethanol, the columns were centrifuged once again (after having discarded the flow-through to enable complete removal of ethanol) and placed into clean 1.5-ml-micro tubes. The bound DNA was eluted by pipetting 10 µl buffer EB onto the centre of the silica membrane in each column, incubation at room temperature for 1 min, and a final centrifugation step as described above.

2.2.4.11. Sequencing (Sanger, 1977)

Sequencing was done using the Big Dye[®] deoxy terminator cycle sequencing kit provided by the manufacturer of the DNA sequencer (Applied Biosystems, ABI prism). In this system the DNA strands to be analyzed by sequencing are generated by T7-DNA polymerase in the presence of the four normal deoxynucleotides and a small amount of the respective dideoxy nucleotides (ddATP, ddCTP, ddGTP, ddTTP). Each of the four dideoxy nucleotides is coupled to a different fluorescence dye. Furthermore, in addition to a template-DNA, the reaction needs one sequence specific primer as a starting point for the DNA polymerase, leading to the generation of fluorescence-tagged DNA strands starting at a defined position. Similar to a PCR reaction, the reaction is processed in a thermo cycler. There are different temperature steps, which are passed through in a cycling process; however, the reaction is not a real chain reaction since a second reverse primer is not added to the reaction. During elongation of the DNA strands, the dye-coupled dideoxy nucleotides are incorporated in a random manner. This leads to the formation of truncated strands, all different in length, because the dideoxy nucleotides cannot form a phosphodiester bond with the next incoming dNTP. The type

of dye at the end clearly defines the nucleotide at the respective position. The position is determined by polyacrylamide gel electrophoresis or capillary electrophoresis: The mobility of a DNA strand is inversely proportional to the logarithm of its length. By using polyacrylamide gel electrophoresis, it is possible to separate DNA molecules differing in length by only one single nucleotide. Compared with this, the resolution of a capillary electrophoresis unit provides an even better resolution. Electrophoresis and subsequent fluorescence detection is carried out in an automatic sequencing machine (see chapter 2.2.4.11.3).

2.2.4.11.1. Generation of fluorescence-tagged DNA strands

450 ng DNA were mixed with 3 μ l sequencing premix (supplied as a ready mix by ABI) and 10 pmol primer in a 10 μ l volume and processed in a thermocycler according to the following conditions:

Initial denaturing	96°C	1 min	
Denaturing	96°C	10 sec	25 repeats
Annealing	50°C	5 sec	
Elongation	60°C	4 min	
Final elongation	60°C	7 min	

Table 2-18: Conditions during sequencing reactions

Subsequently samples were cooled down to 4°C until the program was finished manually, and DNA strands were purified (see chapter 2.2.4.11.2.) prior to sequencing in the automatic sequencer.

2.2.4.11.2. Preparing the fluorescence tagged DNA for sequence analysis

The reactions were mixed with 1 μ l Na-acetate, 50 μ l 95% (v/v) ethanol were added, and the reactions were centrifuged at room temperature (10,000x g, 20 min). The supernatant was removed, and the pellet was washed with 250 μ l 70% ethanol. After a second centrifugation step (10,000x g, 10 min), the supernatant was removed and the pellet was dried for 3 min in a speedvac. Finally, the pellet was dissolved in 25 μ l HPLC-water and stored at -20°C until sequencing.

2.2.4.11.3. Sequence analysis using an ABI prism DNA sequencer

The samples were analyzed in an ABI prism DNA sequencer model 3100. This sequencer uses 16 capillaries instead of a polyacrylamide gel; however, the detection system is based on the same principles as with gel-based sequencers. The different

dyes were detected using an argon laser (exciting at 488 nm and 514 nm) for the excitation of fluorescence and a laser scanning unit for the automatic recording of the four different emitted fluorescence signals. These signals were evaluated by translating them into the corresponding DNA sequence using the program basecaller-3100 version 3.7. Capillary electrophoresis and evaluation took place in the ABI prism sequencer model 3100 and were carried out by Andreas Nolte at the central service laboratory of the institute.

2.2.4.11.4. Comparison of sequences

Analysis for mutations and comparison of sequences were done by using the software MegAlign and EditSeq provided by DNASTar.

2.2.5. CELL BIOLOGICAL METHODS

2.2.5.1. Cell culture standard conditions

Cultured cells were generally handled in a clean bench (Herasafe) to avoid microbial contamination from the air. The materials and solutions used were kept exclusively for the use with cultured cells. Materials which had contact with cells were decontaminated by autoclaving (121°C, 2 bar, 20 min). Cells were routinely cultured in cell culture flasks of differing sizes in incubators at 37°C at conditions providing 5% CO₂, 21% O₂, and a relative humidity of 96 - 100%.

FCS was used as a supplier for growth factors and inactivated before use (see chapter 2.2.5.1.1). Though the tumour cell lines used for the experiments are generally immortal, they were cultured only for a limited time. To avoid alterations of the genotype, the cells were split up to 18 times, which corresponded to ~ 50 cell generations. After cells had reached this age, a fresh aliquot of cells was used.

2.2.5.1.1. Inactivation of FCS

Frozen FCS in a 500 ml glass bottle, as supplied by the manufacturer, was incubated at room temperature for 2h, rotating gently on an orbital mixer, to allow the formation of a liquid layer. This was followed by an incubation step in a water bath at 37°C, gently swirling the bottle until all FCS was thawed. Subsequently, the liquid FCS was heated to 56°C for 45 min to inactivate complement and coagulation factors. Finally the 500-ml volume of FCS was splitted up into 50 ml aliquots under sterile conditions. After pre-cooling at 4°C overnight, the aliquots were stored at -20°C until use.

2.2.5.1.2. Cultivation and passaging of adherent cells

Adherent cell lines attach tightly to the culture vessel and usually grow as a monolayer of cells. Attachment is necessary for the proliferation of these cells, which mostly derive from tissues. The adherently growing cell line HeLa was cultured in MEM-medium, completed with 10% (v/v) FCS and gentamycin as an antibiotic. Cells were seeded to a density of 2 to 3 x 10⁶ cells per 650 ml bottle (this corresponds to an area of 175 cm²). Usually, the cells were grown to 80 - 90% confluency (12 to 15 x 10⁶ cells per bottle) in a maximum of three days and were subsequently splitted to avoid detachment of cells due to a high density. For cell splitting, the medium was removed and the cells were washed two to three times with PBS to remove FCS. Subsequently, 2.5 ml trypsin-EDTA were added to the cells, and the cultures were kept at 37°C for 2-3 min to detach the cells from the vessel's bottom. Detachment was facilitated by gently swirling and tapping the flask until all cells were loosened. Trypsin digestion was stopped by adding 7.5 ml medium containing FCS. Finally, the cells were counted (see chapter 2.2.5.1.4), and 2 to 3 x 10⁶ cells were seeded in a 50 ml volume of fresh medium into a 650-ml flask.

2.2.5.1.3. Cultivation and passaging of suspension cells

Jurkat, Raji, and HL60 cells are derived from blood cells and therefore do not attach to the vessel's bottom but grow in suspension. These cells can be grown to a higher cell density per volume of medium because they do not form a monolayer as adherent cells do. Cells were seeded initially to a density of 5 x 10⁴ to 1.5 x 10⁵ cells per ml in RPMI-medium containing 10% (v/v) FCS and gentamycin (additional glutamine was added for the cultivation of Jurkat and Raji cells). Suspension cells were generally cultured to a maximum density of 8 x 10⁵ cells per ml. Cells were counted (see chapter 2.2.5.1.4) and diluted with fresh medium to the required concentration.

2.2.5.1.4. Cell counting

Cell densities were determined by counting the cells with a CASY TT electronic cell counter. This device not only records the number of cells exceeding a previously determined size, but also specifies the distribution of sizes in the examined cell population, allowing an estimation of the population's viability.

A 100 µl volume of the cell suspension was diluted in 10 ml Isoton solution (provided by the manufacturer), and cells were counted excluding particles with a diameter less than

7.5 μm . Particles less than 7.5 μm in diameter were assumed to be debris or dead cells.

2.2.5.1.5. Freezing cells for storage

Cells were adjusted to a density of 3.5×10^6 cells per ml in RPMI freezing medium, and aliquots of 5 to 6×10^6 cells were transferred into 1.8-ml cryo-tubes. The tubes were first stored in a Styrofoam-box at -70°C for two days to allow slow freezing of the cell suspension. Finally, the tubes were transferred to liquid nitrogen for long-time storage.

2.2.5.1.6. Thawing cells for cultivation

The required medium was pre-warmed to 37°C . Cryotubes were immersed in 100% methanol to inactivate mycoplasmas, possibly present in liquid nitrogen, prior to thawing the tube by gently rotating in running warm water. Immediately after thawing, the tubes were dried and disinfected by wiping off with ethanol. The content of the tube was transferred into a cell culture flask containing 50 ml of the fresh, pre-warmed medium, and cells were cultivated under standard conditions as described before (see chapter 2.2.5.1).

2.2.5.1.7. Harvesting procedure for cells

Cells were routinely harvested at room temperature in sterile 50 ml falcon tubes by centrifugation at $300\times g$ for 5 min. Subsequently, the pelleted cells were washed twice with 10 ml PBS; centrifugation steps were as described above. Subsequently, the cells were processed according to the protocols of the following experiments.

2.2.5.2. Preparing proteins from cells

2.2.5.2.1. Purification of H1 histones from human cells

H1 histones were purified by precipitating a large portion of contaminating proteins with 5% PCA. In contrast to yeast, human cells do contain acid soluble proteins, e.g. HMG proteins, which are not separable from H1 histones by using 5% PCA for differential precipitation. For that reason histones from human cells were further purified by gel filtration. By using a Biogel P60 column for gel-filtration it was possible to separate H1 histones from other PCA-soluble proteins.

1.2 to 1.5×10^8 cells were harvested and frozen at -20°C for 1 h in 2-ml-microtubes (this step was necessary to damage cell membranes for a better release of the H1 histones during the following extraction procedure). Pellets were thawed on ice, re-suspended in 1.8 ml 5% PCA, and incubated at room temperature for 1 h with occa-

sional vortexing. The acid-precipitable contaminating proteins were separated by centrifugation at 14,000 rpm for 30 min at 4°C in a micro centrifuge. The supernatant, containing H1 histones and HMG proteins, was kept on ice while the pellet was re-extracted once again for 10 min with 1 ml 5% PCA. The PCA-soluble proteins from the pooled supernatants were precipitated by adding a 7-fold volume of 100% acetone (-20°C) and an incubation step at -20°C for two days. Alternatively, the PCA-soluble proteins were precipitated with 20% TCA as described in chapter 2.2.3.2. The precipitated histones were collected by centrifugation at 10,000 rpm for 30 min at 4°C in a HB-4 rotor. The resulting pellets were freeze-dried for 30 min and air-dried for another 40 min before they were suspended in 30 mM HCl for gel filtration (see chapter 2.2.3.3). H1 histones were generally stored at -20°C for short time storage. Longer storage times required storage at -80°C to avoid a degradation of the proteins.

2.2.5.2.2. Preparing nuclei from human cells

This preparation procedure described in the following involves lysis of the cells by Triton X 100 which leaves the nuclear membrane essentially intact but solubilizes distinct components of the nuclear pore complexes (*Benditt et al., 1989*). Most cytosol is removed in the following centrifugation step. However, a further purification step using a sucrose cushion is included to remove last traces of cytosolic components by density gradient centrifugation. The sucrose cushion consisted of 2.2 M sucrose, which is a highly dense medium, allowing only the comparably heavy nuclei to migrate through it. Therefore, the resulting pellet contains only purified nuclei (*Chauveau et al., 1956*).

For the preparation 2×10^8 cells were harvested, resuspended in 40 ml nucleus buffer I containing 0.02 % (v/v) Triton X 100, and homogenized by 10 strokes in a small-sized Dounce glass homogenizer. Reactions were kept on ice for 10 min for complete lysis of the cells and subsequently centrifuged in a sorvall SS-34 rotor (2500 rpm, 5 min). The cytosolic components in the supernatant were discarded, and the nuclei from the pellets were pooled and resuspended in 20 ml nucleus buffer II by applying 10 strokes with a large-sized Dounce glass homogenizer. For further purification, the resulting suspension was layered on a 10 ml-sucrose-cushion (nucleus buffer II) in an ultracentrifuge tube and subjected to an ultracentrifugation step in a Beckman SW-28-rotor (90 min, 25,000 rpm). The supernatant was removed, and the nuclei from the pellet were washed in 10 ml nucleus buffer III. Nuclei were sedimented once again by a centrifugation step in a Sorvall HB-4 rotor (2,500 rpm, 5 min) and finally suspended in 1.5 ml nuclei-buffer III. This suspension was always prepared freshly for subsequent experiments.

2.2.5.2.3. Preparing cytosol from human cells

3×10^8 cells were harvested (see chapter 2.2.5.1.7) and washed in a 25-ml-volume of PIPES-buffer. The cells were resuspended in 1 ml PIPES-buffer and drawn up quickly 10 times using a syringe with a 21-gauge. The suspension was frozen in liquid nitrogen and thawed again. This procedure was repeated once again. Finally, the suspension was centrifuged in a HB-4 rotor (8,000 rpm, 15 min, 4°C), the supernatant was transferred to fresh microtubes and used as 'cytosol' for subsequent experiments.

2.2.5.2.4. Preparing whole-cell extracts for western blots

This extraction method uses a strongly denaturing sample buffer and a sonification step to shear genomic DNA. The process ensures that all proteins are dissolved in the sample buffer prior to electrophoresis. Even the nuclear enzyme PARP, normally tightly attached to DNA by its smaller DNA binding-unit, is detached from its substrate and can be detected in subsequent western blots.

100 μ l PARP-sample buffer were added per 10^7 cells, and the suspension was sonicated for 15 sec at 25% amplitude using a digital sonifier supplied by Branson. By using this type of sample buffer, protein contents of the cell-extracts could be determined by the method according to Bradford. For determination of protein contents, aliquots of the samples had to be diluted at least 20-fold due to the high protein contents in the samples. Dilution also decreased the amounts of interfering reagents like urea and SDS in the samples.

2.2.5.3. Stable transfection

During the transfection process macromolecules like DNA are transferred into higher eukaryotic cells. The use of plasmid DNA for transfection allows the expression of any desired protein from the plasmid, provided that a suitable promoter is included in the plasmid. This kind of expression is called transient because the plasmid is not replicated in the following cell division cycles and thus is lost during passaging of the cells. This leads to a continuous decrease of protein-expression from the plasmid in the cell culture.

Stable transfection requires the same experimental procedure as transient transfection does. The only difference is the subsequent selection for stably transfected cells; therefore, the plasmid should contain a sequence which codes for a selectable antibiotic resistance.

Stable expression of a protein encoded on the plasmid DNA is possible because in some cases the plasmid DNA is integrated randomly into the genomic DNA. This way the following generations, deriving from such a cell, are able to stably express the protein.

However, successful expression of the recombinant protein is a very rare event because the plasmid DNA, encoding the desired protein, should not only integrate into the genomic DNA for stable expression, but also stay under control of an active promoter in an active area of chromatin. Those randomly occurring cells can be effectively selected if the plasmid DNA additionally confers resistance to an antibiotic like Blasticidin. Only stably transfected cells, which have integrated plasmid DNA into active chromatin areas of their genomes, are able to survive for a long time under selective conditions. Non-transfected cells are eliminated from the cell population in a comparably quick manner if Blasticidin is used for selection.

2.2.5.3.1. Establishing a killing curve for an antibiotic

As different cell lines may show differing sensitivity to the distinct commonly used antibiotics, the dose which is sufficient to kill non-transfected cells has to be determined in advance before conducting transfection experiments.

20 ml suspension cells were seeded to a concentration of 2×10^5 cells per ml and cultured at different concentrations of Blasticidin ranking from 0 to 10 μg Blasticidin per ml medium. Cells were splitted when necessary, always keeping the cell concentration below 8×10^5 cells per ml to avoid cell death due to inappropriate culture conditions. The Blasticidin concentration which was sufficient to inhibit proliferation of the cells within 5 to 10 days was used in subsequent transfection experiments for the selection of Blasticidin-resistant transfectants.

2.2.5.3.2. Transfection procedure

Stable transfection was carried out using the Effectene[®] transfection kit. This is a lipid-based transfection reagent with only low cytotoxic effects. The plasmid DNA to be transfected should be very pure because especially contaminating endotoxins strongly decrease transfection efficiencies. Therefore, plasmid-DNA was purified from bacteria using the Endofree[™] plasmid preparation kit (see chapter 2.2.4.10.5).

Transfected DNA may be either maintained as an episome or it is integrated into the chromosomal DNA. Generally, a linearization of the plasmid ensures an optimal integration of the desired DNA into the host genome. The plasmid DNA was linearized by a digest with a restriction enzyme which cuts the plasmid DNA once without affecting the insert DNA, coding for the desired protein. SSPI was chosen to linearize the DNA because it cuts the plasmid used for transfection (pcDNA6 myc his A) once without cutting the insert-DNA.

Per transfection reaction 5 µg plasmid DNA were digested with 40 units SSP I for 1 h at 37°C. Subsequently the DNA was purified by phenol/chloroform extraction (see chapter 2.2.4.10.1) and finally dissolved in 10 µl endotoxin-free, sterile TE-buffer.

The cells were splitted the day prior to the transfection experiment resulting in a cell density of 5×10^5 cells per ml to be reached at the day of transfection. 2.5×10^5 cells were collected by centrifugation (300x g, 3min) and suspended in 40 ml fresh, complete RPMI medium. 2.5 to 3×10^6 cells were then seeded in a 4 ml volume into eight 60mm dishes, respectively, and kept in the incubator until use.

For each transfection reaction 1 µg plasmid DNA was diluted with the DNA condensing buffer EC (supplied with the Effectene[®] transfection kit) to a final volume of 150 µl. A quantity of 8 µl Enhancer (supplied with the Effectene[®] transfection kit) was added, and the mixture was vortexed for a short time. After an incubation step at room temperature for 2 min, 25 µl Effectene[®] transfection reagent were added, vortexed for 10 sec and kept at room temperature for 5 min to allow formation of the transfection-complex. Subsequently, 1 ml complete RPMI medium was added, and the solution was pipetted drop-wise to the cells in the 60 mm-dish. To ensure an equal distribution of the transfection complexes, dishes were gently swirled while adding the complex. Generally, transfection reactions were carried out in duplicates. A negative control without plasmid DNA was performed to test for effective selection conditions. Positive controls contained a plasmid without a DNA insert, this way Blasticidin-resistant cells without expressing the respective proteins (mock-transfected cells) were generated as a control for subsequent experiments.

2.2.5.3.3. Selection for stably transfected cells

Cells were incubated for 24 h to 48 h at normal, non-selective growth conditions to allow the expression of the transfected genes. Finally, the cell suspensions were transferred from the dishes to a 15-ml-volume of fresh medium in 50-ml culture flasks, containing Blasticidin at the appropriate concentration. The appropriate Blasticidin concentrations were 10 µg/ml for Raji cells and 7 µg/ml for Jurkat or HL60 cells, respectively.

Cells were kept at 37°C and splitted if necessary. Stable transfectants were usually detectable 3 to 4 weeks later. Dead cells were removed by MACS once during this time, usually after having cultured the cells for 5 to 6 days following transfection, as described in the following chapter.

2.2.5.4. MACS

Magnetic activated cell sorting was used to separate dead cells from the suspension cultures during selection for stably transfected cells. The dead cell removal kit purchased from Miltenyi Biotec contains a solution with antibodies coupled to colloidal super-paramagnetic beads (Dead cell removal microbeads: DCRM). Dead or dying cells, even early apoptotic cells, are tagged with these antibodies directed against an epitope (phosphatidylserine) only accessible on the plasma membranes of these cells (see chapter 2.2.5.6.3). During affinity chromatography, using paramagnetic selection columns in a strong magnetic field, only the living cells pass through the column while the antibody-tagged dead cells are retained in the column. The eluted living cell fraction can be kept in culture again for further propagation.

Cells were cultured under selective conditions using Blasticidin for 5 to 6 days following transfection before MACS was performed. After counting the cells (see chapter 2.2.5.1.4), they were collected by centrifugation at 300 g for 3 min and the supernatant was removed completely. 100 µl DCRM-suspension were added per 10^7 cells (because almost all cells were assumed to be dead), and the gently resuspended cells were incubated with the DCRM at room temperature for 15 min. Meanwhile, a MACS separation column type LS was mounted in the magnetic field of a strong magnet supplied by Miltenyi Biotec (type midi-MACS) and equilibrated by rinsing it with 3 ml of 1x binding buffer (supplied with the kit). A volume of 5 ml 1x-binding buffer was added to the DCRM-cell-suspension, and the mixture was applied to the prepared column. The eluate was collected and applied to the column once again before washing the column with 4 ml 1x-binding buffer. The cells from the eluate were collected by a centrifugation step (3 min at 300x g) and cultured again in fresh medium under selective conditions.

2.2.5.5. Induction of apoptosis

Apoptosis was induced by Topotecan, a topoisomerase-I-inhibitor (*Eng et al., 1988*). Topotecan induces single strand DNA breaks by selectively inhibiting this type of topoisomerase during replication (see chapter 4.3.2). Suspension cells were induced for apoptosis at a cell density of 2.5 to 3.5 x 10^5 cells per ml by administering 150 ng/ml Topotecan per ml of the suspension culture. Progression of apoptosis was monitored by harvesting aliquots of the cells at defined times and testing the samples for apoptotic parameters, as summarized in the following table (2-19).

Changes expected in:	Applied methods	Parameter tested
Morphology	Phase contrast microscopy Casy TT cell counting	Formation of apoptotic bodies
DNA	Agarose gel electrophoresis	Internucleosomal DNA fragmentation
	DAPI-staining	Structural chromatin changes
Cell membrane	Annexin-FITC labelling	Phosphatidylserine flip
Caspase-3 activity	Fluorimetric enzyme activity assay	Cleavage of DEVD-afc
Kinetic changes of protein levels	Western blotting	Bax, bcl-2, caspase-3, DFF40, DFF45/35, p21, p53

Table 2-19: Apoptotic parameters tested in the course of this study

2.2.5.6. Microscopy

2.2.5.6.1. Mounting cells to object slides

Cytospin centrifugation was carried out by the filter paper method. The Cytospin unit was assembled with a filter paper to collect the liquid which is flowing out during the centrifugation step. Centrifugation allows the cells to attach tightly to the slide. 50 μ l to 150 μ l cell suspension (2.5 to 7.5×10^4 cells) were pipetted into the well, and the unit was centrifuged for 2 min at 500 rpm in a Heraeus Megafuge 1.0. Subsequently, cells were treated according to the protocol of the respective experiment.

When large numbers of samples had to be evaluated simultaneously, the cells were attached onto coated glass slides by sedimentation. 5×10^6 cells grown in suspension were harvested as described in chapter 2.2.5.1.7 and finally resuspended in 500 μ l PBS. 50 μ l of the cell suspension were pipetted onto a glass slide and incubated at room temperature for 5 min to allow attaching of the sedimenting cells to the surface of the glass slide.

2.2.5.6.2. Fluorescence labelling of cellular molecules

Fluorescent dyes emit light of a specific wavelength as soon as they are excited by light of another specific wavelength. Different dyes with specific excitation and emission maxima are available, allowing multiple staining procedures in cells by coupling these dyes to molecules specifically binding to the molecule to be determined. Fluorescence labelling of cells does not only allow the detection of a specific molecule but also the analysis of a molecule's spatial distribution in the cell. Fluorescent labelling can be

carried out in a direct or indirect way. In direct fluorescence detection experiments the interacting molecule can be labelled directly with a fluorescent dye or it is a fluorescent dye in itself. Indirect staining means that the detection of a molecule is mediated by fluorescent molecules detecting another nonfluorescent adapter molecule which in turn specifically binds to the molecule to be detected. In immunofluorescence experiments antibodies are used as molecular probes for the protein to be detected in a direct or indirect way. The following table gives an overview on the fluorescent dyes used in the experiments:

Dye	λ_{Exc} [nm]	λ_{Em} [nm]	Detection modus
CY-3	546	570 (orange-red)	Indirect (coupled to a secondary antibody)
DAPI	358 (UV)	450 (blue)	Direct (DNA-binding dye)
Ethidium bromide	254 (when bound to nucleic acids)	605 (red)	Direct (DNA-binding dye)
FITC	450-490	526 (green)	Direct (coupled to Annexin) or indirect (coupled to a secondary antibody)
Hoechst 33342	350 (UV)	461 (blue)	Direct (DNA-binding dye)
Propidium iodide	535 (when bound to nucleic acids)	617 (red)	Direct (DNA-binding dye)

Table 2-20: Fluorescent dyes used in this study

2.2.5.6.3. Annexin V-FITC-labelling of apoptotic cells

Annexin V is a 36 kDa protein, which in the presence of Ca^{2+} ions specifically binds to phosphatidylserine (PS) in the cell membrane. In non-apoptotic cells PS is located only in the inner layer of the plasma membrane because its distribution in the membrane is tightly controlled by a specific transporter enzyme. Only early during apoptosis it is exposed at the outer intact cell membrane. Coupling FITC to Annexin V allows direct fluorescence detection of PS in the cellular membrane. Intact, viable cells are not stained because their PS is located inside the cell, out of reach of the externally applied Annexin V. Apoptotic cells are labelled by PS due to their deposition of PS in the outer cell membrane. Necrotic cells and artificially damaged cells may also get stained by using Annexin V because they are leaky. Leaky cells allow binding of Annexin to PS

which in fact is still located in the inner layer of the cell membrane. To discriminate between apoptosis and necrosis, the cells are counterstained with propidium iodide. This dye does not cross intact cell membranes and therefore labels nucleic acids only in cells with a leaky membrane, i.e. necrotic cells and artificially damaged cells.

The assay was conducted according to a modified protocol with the reagents supplied with the Apo-Alert-Annexin V-Assay (Clontech). 2.5 to 5×10^5 cells (1 ml cell suspension) were centrifuged in a 1.5-ml-microtube (2 min at $300 \times g$). The supernatant was removed completely, and cells were resuspended in $250 \mu\text{l}$ Annexin V-binding buffer for washing. Cells were again collected by centrifugation as described above. The supernatant was removed, and the cells were resuspended in $100 \mu\text{l}$ Annexin V-binding buffer. Subsequently, cells were stained in an incubation step at room temperature in the dark for 10 min after having added $2 \mu\text{l}$ propidium iodide ($5 \mu\text{g/ml}$), $2 \mu\text{l}$ Hoechst 33342 (1 mg/ml), and $2 \mu\text{l}$ Annexin-V-FITC ($20 \mu\text{g/ml}$). After a final centrifugation step as described above, $95 \mu\text{l}$ of the supernatant were removed, the cells were gently suspended in the remaining liquid, pipetted onto a glass slide, and covered with a $24 \times 24 \text{ mm}$ coverslip. Subsequently, the cells were analyzed by fluorescence microscopy.

2.2.5.6.4. Immunofluorescence

Cells were attached to glass slides as described in chapter 2.2.5.6.1 and treated according to the following scheme. All steps were performed at room temperature.

Fixation	20 min in PBS containing 3% PFA wash by rinsing 3 times with 1 ml PBS
Permeabilization	10 min in PBS containing 0.2% (v/v) Triton X 100 wash by rinsing 3 times with 1 ml PBS
Blocking	10 min in PBS containing 3% (w/v) BSA wash as described above
Primary antibody	1 hour in antibody solution diluted 1:100 in 3% (w/v) BSA in PBS, wash as above
Blocking	10 min in PBS containing 3% (w/v) BSA wash as described above
Secondary antibody	Diluted 1:60 (FITC-coupled) or 1:1,000 (CY3-coupled) in 3% (w/v) BSA in PBS, wash as described above
Counterstain	2 min in Hoechst 33342 ($2 \mu\text{g/ml}$ in PBS)

Table 2-21: Working scheme for immunofluorescence labelling of cells

Finally, the cells were embedded in a small drop of Permafluor, covered with a coverslip, and analyzed by fluorescence microscopy.

2.2.5.6.5. Microscopic analysis

Generally, microscopy was carried out using a Zeiss microscope type Axioskop 20. Samples may be analyzed with this microscope by phase contrast or by exciting fluorescence at differing wavelengths by using suitable filters.

Evaluation of some immuno-labelled cells was done by using a confocal Laser scanning microscope Zeiss LSM 510 with a 63x magnifying objective using an argon laser (488 nm) for excitation of fluorescence.

2.2.6. STATISTICAL ANALYSIS

Statistical analysis was required for an interpretation of the changes in the increase of caspase-3 activity of differently transfected cell culture cells after induction of apoptosis. This turned out to be quite a complex statistical problem, and finally two-way ANOVA was chosen as a statistical method despite ensuing problems with this statistical method as detailed later.

Computations were carried out using the software Graphpad Prism 4.00 for Windows, GraphPad Software, San Diego California, USA (www.graphpad.com). Row means and standard error of the means (SEM) were calculated for the presentation on graphs, and analysis of variance (ANOVA) was carried out by two different types of two-way ANOVA.

Two-way ANOVA determines whether the variances of experimental results (here: The differences in the increase of caspase-3 activity) is affected by two different independent factors (here: The parameter '*time after induction of apoptosis*' and the parameter '*transfection for expression of different recombinant proteins*'). Two-way ANOVA allows a statement concerning three basic questions:

1. Does the **first parameter** (here: 'time') systematically affect the response (here: The increase in caspase-3 activity)?
2. Does the **second parameter** (here: 'transfection') systematically affect the response (increasing caspase-3 activity)?
3. Is there an **interaction** between the two parameters (here: 'time' and 'transfection')? Which means here: Does the parameter 'transfection' affect the response (increase in caspase-3 activity) due to the parameter 'time' to the same extent? Or equivalently, is the increase of caspase-3 activity the same in the differently transfected cells?

The null hypothesis during two-way ANOVA concerning the interaction is that there is no interaction between columns ('transfection') and rows ('time'). If the p-value for interaction is high, the null hypothesis is true. Thus, the true meaning of a high p-value for interaction in two-way ANOVA is that any systematic differences between the rows (here: Increasing caspase-3 activity in the course of apoptosis) are the same for each column (here: Differentially transfected cells) and reversely. On the other hand, if the p-value for the interaction is low, the null hypothesis has to be rejected which means that there is an interaction between the two tested parameters. If there is a significant interaction, the column and row effects are difficult to interpret, which was the case in this study as detailed in chapters 3.3.4 and 3.3.6.

The null hypothesis concerning the columns ('transfection') and the rows ('time') is that the respective mean of each column or row is the same for the overall population and that any differences (variances) in the respective columns or rows are due to random effects (here: There is no difference in the increase of the caspase-3 activities in the course of the experiment in the differentially transfected cells). If the p-value is high, the null hypothesis is true and the differences may be explained by random effects. If the p-value is low, the null hypothesis has to be rejected which exactly means that it is unlikely that the observed difference (here: In the caspase-3 activities) is due to random effects, and the hypothesis that these populations (here: Differentially transfected cells) have identical means has to be rejected. However, a low p-value is commonly said to indicate that the differences between two or more compared populations is significant. Though this is actually statistically incorrect, this style of writing is used in the following, to preserve the readability in the following text.

Two-way ANOVA with Bonferroni tests was carried out with statistical raw data of all experimental groups entered in columns (parameter 'transfection') and rows (parameter 'time' after induction of apoptosis). Since this test indicated a significant interaction between both parameters without showing the exact source of interaction, a second type of two-way ANOVA was carried out which allowed a pairwise comparison of all 6 combinable column pairs. This allowed discrimination between column pairs with significant or not significant interaction. The calculated p-values differed slightly from those obtained when analyzing all four groups simultaneously but did not interfere with the final interpretation of statistical significancies.

GraphPad Prism calculates post tests during two-way ANOVA according to the Bonferroni method (*Neter et al., 1990*) using a 95% confidence interval. If some values are missing (as it was the case in the study in hand due to different numbers of conducted experiments), Prism uses a method which in principle converts the ANOVA problem to a multiple regression problem, according to *Glantz and Slinker (1990)*.

It is generally possible to perform Two-way ANOVA analysis by GraphPad prism with even unreplicated values because the mean values of columns and rows are used for calculations. However, in those cases GraphPad Prism assumes that there is no interaction between the parameters, and if this assumption is not valid, the obtained p-values are less powerful. Two-way ANOVA in this study was generally carried out with replicated values and thus allowed an analysis of interaction.

In this study the results of statistical analysis are presented as either 'significant' or 'not significant'; additional graduations are omitted, and the respective p-value interval is stated in the context.

2.2.7. DENSITOMETRY

Quantitations of selected western blots were carried out by densitometry. Gaussian integrated densities in the lanes were calculated using the software 1 D ScanEx 3.00. The number of bands to be detected for quantitation was adjusted, and the automatically detected lanes were corrected manually if necessary to assure correct recording of the bands to be detected. Concentrations or relative contents in the protein bands could be calculated by defining a standard lane and a respective unit (e.g. μg or %).

3. RESULTS

The first part of this section (chapter 3.1), summarizes experiments in which both the effects of different H1 histone subtypes and the effects of differently modified H1 histones on the activity of the apoptotic DNase DFF40 were investigated in an in vitro system. The obtained results finally led to the experiments which are described in chapter 3.2.: The establishing of a cell culture system and its investigation to check for a putative correlation between the extent of DNA fragmentation and progression of apoptosis in vivo.

3.1. FACTORS INFLUENCING THE ACTIVITY OF DFF40

Previous studies demonstrated a role for certain chromatin-associated proteins in enhancing the enzymatic activity of DFF40 on its DNA substrate. Results from in vitro experiments have led to the widely accepted statement that the linker histone H1 and the nuclear high mobility group proteins, HMG-1 (*Widlak et al., 2000; Liu et al., 1998*) and HMG-2 (*Toh et al., 1998*), as well as topoisomerase II (*Earnshaw et al., 2000*) have an activating effect on DFF40 when digesting DNA. This activating effect was more distinct when naked DNA substrates, i.e. plasmid DNA, were used rather than in vitro reconstituted chromatin. In some cases additional H1 histones even led to an inhibition of the nuclease activity on in vitro reconstituted chromatin substrates (*Widlak et al., 2000*).

Furthermore, from previous studies it is a commonly accepted fact that patterns of both H1 histones and core histones often vary during apoptosis. This change, concerning the respective proteins, was suspected to be rather due to changes in the posttranslational modifications than due to altered protein expression patterns of the different H1 histone subtypes (*Kratzmeier et al., 1999*). Later experiments showed an increase of dephosphorylated H1 histones subtypes during induction of apoptosis in HL60 cells; concomitantly, the content of phosphorylated H1 histone subtypes decreased (*Kratzmeier et al., 2000*).

Since H1 histones are located at the outside of the nucleosomal core histone octamer, they are the most likely candidates for possible interactions with other proteins during chromatin changes in apoptosis. Thus, the first part of chapter 3.1 summarizes experiments which were designed to characterize putative differential effects of the individual H1 histone subtypes on DFF40 activity. A possible effect of the state of phosphorylation of H1 histones on DFF40 activity is investigated in the second part of chapter 3.1.

The following experiments were conducted with purified recombinant proteins or with partially purified protein preparations from control or apoptotic cell cultures.

3.1.1. PURIFICATION OF RECOMBINANT PROTEINS

The effect of any substance on the activity of a DNase can be tested *in vitro* by using plasmid DNA (*Enari et al., 1998*) or nuclei (*Liu et al., 1997; Enari et al., 1995*) as a substrate for the DNase-catalyzed digestion under defined conditions. The enzymes and H1 histones used in the *in vitro* assays were purified as heterologously expressed, recombinant, human proteins from *S. cerevisiae* or from *E. coli*. Recombinant H1 histone subtypes and recombinant caspase-3 were purified from transformed *S. cerevisiae*, and the DNase DFF40 was purified from transformed *E. coli* as a recombinant enzyme complex together with its chaperone and inhibitor DFF45 as detailed in the following.

3.1.1.1. Purification of DFF40/DFF45 as a complex from E. coli

The DFF40/DFF45 complex was co-expressed as a recombinant protein complex, expressed upon induction with IPTG in *E. coli* and purified by Ni-NTA affinity chromatography prior to use. Co-expression of both proteins in the cell is indispensable to yield a biologically active DFF40 protein because DFF45 is not only the inhibitor of DFF40 but also acts as a chaperone for the correct folding of DFF40 during translation. During expression in the absence of its chaperone DFF45, DFF40 becomes insoluble and forms incorrectly folded, inactive aggregates which, when expressed in bacteria, are deposited in inclusion bodies (*Liu et al., 1998, and observations in our lab*). Co-expression of DFF40 and DFF45 from a single plasmid generates a DFF40/DFF45 complex which is inactive in the first instance. DFF40 can be activated from this complex as an apoptotic DNase in a specific manner by caspases that are activated during apoptosis. These caspases cleave a lot of different substrates, and among those substrates is DFF45. Cleavage is e.g. mediated by caspase-3 (*Sakahira et al., 1998; Liu et al., 1998*) and caspase-mediated disintegration of DFF45 releases activated DFF40 from the complex. DFF40 finally oligomerizes to form an active DNase.

3.1.1.1.1. Optimizing the expression rates in pilot expression experiments

Pilot expression experiments were carried out to optimize the expression rate of recombinant DFF40/DFF45 protein as a soluble complex. These experiments were carried out to establish expression conditions which provide a high yield of soluble protein since the DFF40/DFF45 complex cannot be purified from bacterial inclusion bodies at denaturing conditions. If the culturing time for protein expression is chosen

too long in bacteria, most recombinant proteins, which are of no use for the bacterium, are increasingly deposited in inclusion bodies within the bacterium. Recombinant proteins from bacterial inclusion bodies may be purified by using denaturing protocols for the release of the recombinant protein complex from the bodies. However, this was not possible with the DFF40/DFF45 protein complex since the complex would have been destroyed during the denaturing process. As soon as DFF40 is not complexed with DFF45 any longer, it forms precipitating oligomers which cannot be used in the subsequent *in vitro* assay. To find the optimal expression conditions for a high yield of soluble DFF40/DFF45 complex, bacteria were induced in small culture volumes with two different concentrations of IPTG. Samples were collected at different times, and expression rates were determined by comparing the respective protein bands in SDS gels and western blots. An extraction protocol applying freeze-thaw-cycles was used to determine the localization of the expressed protein in inclusion bodies or as a soluble protein in the bacterial cytoplasm. Figure 3-1, following on the next page, shows the respective extracts from *E. coli*. These samples were not yet purified by Ni-NTA chromatography and therefore still had a high background of contaminating endogenous bacterial proteins. The Coomassie-stained SDS-gel of the supernatants (fig. 3-1-A) contains bands resulting from soluble endogenous proteins from bacteria and additional bands increasing in size with progressing time of the experiment. The main increasing band was seen at a height in the gel corresponding to a molecular weight of 45 kDa as had been expected for DFF45. A weaker band occurred just below, corresponding to a molecular weight expectable for DFF40. The Coomassie-stained SDS gel of the pellets (fig. 3-1-B) depicts insoluble endogenous bacterial proteins and insoluble recombinant proteins from inclusion bodies. Generally, some of the recombinant proteins were trapped in inclusion bodies. Induction of protein expression for 4 hours gave rise to storing large amounts of the recombinant protein in insoluble bacterial inclusion bodies. A western blot of the supernatants (fig. 3-1-C) confirmed the presence of DFF45 in the main bands seen in SDS gels; the best yield of soluble recombinant protein was obtained after induction for 3 h. A western blot of the pellets (fig. 3-1-D) confirmed the presence of recombinant proteins in inclusion bodies as well. At up to 3h induction time, the deposition of recombinant protein in inclusion bodies was relatively constant at a low level, but deposition increased substantially after 4 hours. All figures show a low expression level of recombinant complex protein even without induction by IPTG, mainly as a soluble complex; this is due to the slightly leaky T7-promotor system used in this expression system (see chapter 2.1.13.1.2).

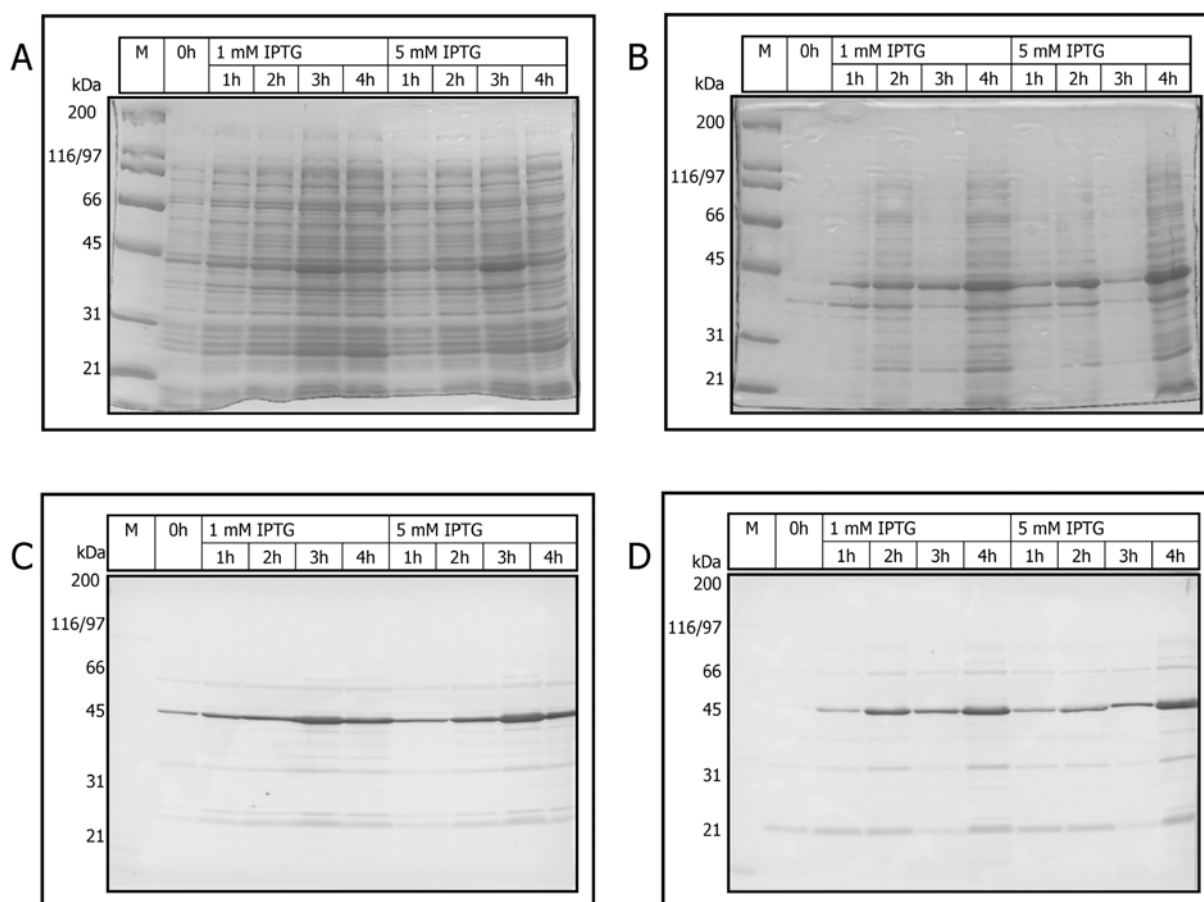


Figure 3-1: Pilot expression experiments: Detection of DFF40/DFF45

E. coli strain BL21 (De3) pLys S was transformed with the expression plasmid pWA 379. Expression of the recombinant DFF40/DFF45 complex was induced with IPTG, using the concentrations indicated in the figures above, for differing times as shown in the figures. The experimental procedure is described in chapter 2.2.1.7. Western blots were assayed by alkaline phosphatase reaction and BCIP/NBT as colouring substrates. **A:** Coomassie-stained SDS-gel of the supernatants, showing soluble proteins from the bacterial cell lysates. **B:** Coomassie-stained SDS-gel of the pellets, depicting insoluble proteins from the bacterial cell lysates. **C:** Western blot of the supernatants assayed for **DFF45**, confirming the presence of recombinant proteins in the soluble protein fraction. **D:** Western blot of the pellets assayed for **DFF45** confirming the presence of recombinant proteins in inclusion bodies as well. **M:** BioRad broad-range protein standard. Most efficient induction of soluble DFF40/DFF45 complex was obtained after induction with IPTG for 3h.

As detailed in figure 3-1, the highest yields of soluble proteins were obtained after 3h of induction with IPTG; most of the recombinant protein complex existed in soluble form at this time (details are specified in the figure legend of figure 3-1). There was no increase in the yields of recombinant proteins when 5 mM IPTG instead of 1 mM IPTG were used for induction. Therefore, 1 mM IPTG was subsequently used for the induction of the recombinant protein complex in large scale expression experiments, and bacteria were harvested 3 h after induction with IPTG.

Similar results were obtained in experiments in which DFF45 was detected by its His-tag. Additionally, this procedure further allows an estimation of the purity and quality of the recombinant protein since recombinant DFF45 expressed from plasmid pWA379 possesses an N-terminal His-tag which is translated first during translation. Therefore, incomplete protein chains may be co-purified by Ni-NTA chromatography. Western blots using a His-antibody are suitable tools to estimate the portion of incomplete protein chains as depicted in the following figure (3-2).

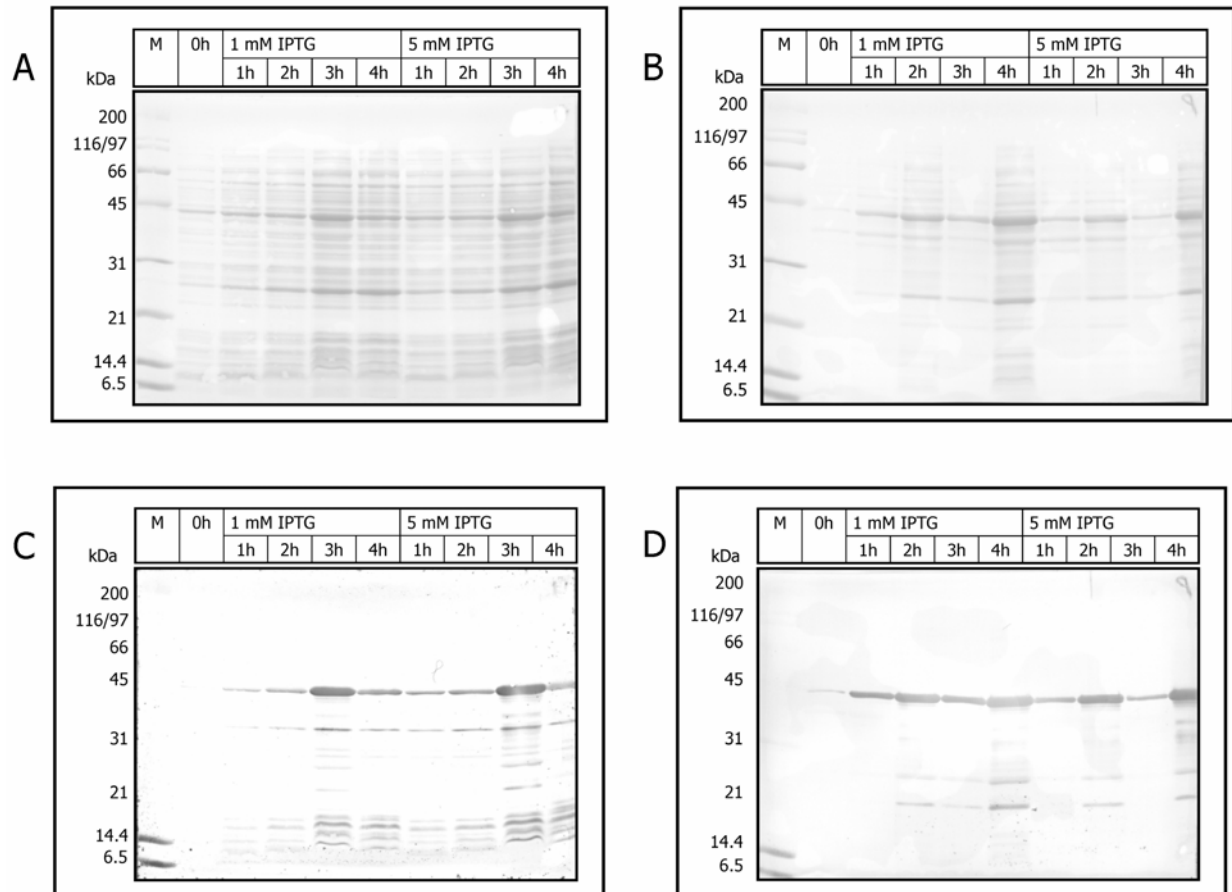


Figure 3-2: Pilot expression experiments: Detection of the N-terminal 6xHis-tag

Experimental procedure was carried out as already described in the legend of figure 3-1. In contrast to figure 3-1, this figure shows Ponceau-stained NC-membranes instead of SDS-gels in the upper row and an antibody directed against the 6xHis-tag was used instead of a DFF45-antibody for immuno-detection of the His-tagged DFF45 protein (fig. C and D in the lower row). All figures show an expression pattern for the recombinant protein which is comparable to fig. 3-1. Figures from the upper row and figures from the lower row show the respective membranes before and after immuno-detection. **A:** *Ponceau-stained blotted proteins from the supernatants.* **B:** *Ponceau-stained blotted proteins from the pellets.* **C:** *Western blots of the proteins from the supernatant assayed for the expression of His-tagged proteins, a large amount of bands was detectable in the low MW-range of the blot* **D:** *Western blots of the proteins from the pellets, containing the bacterial inclusions bodies, assayed for His-tagged proteins.* **M:** BioRad broad-range protein standard. Immuno-detection was carried out by using a secondary antibody coupled to alkaline phosphatase. BCIP/NBT was used as a colouring substrate.

Immunodetection with the 6xHis-tag-antibody (fig. 3.2) revealed that a small amount of the expressed soluble DFF45 protein was incomplete, but translation of a prevailing portion of DFF45 had been finished properly. Inclusion bodies, containing the recombinant protein, seemed to be formed mainly after complete translation of the protein since unfinished protein chains were hardly detectable in the pellets. However, purification of the DFF40/DFF45 complex from the pellets was not possible, as already detailed above. The observable differences in band intensities of the Ponceau-stained proteins (fig. 3-2) compared with the respective Coomassie-stained proteins (fig. 3-1) may have resulted from different staining properties of these dyes.

3.1.1.1.2. Purification of the DFF40/DFF45 complex on Ni-NTA columns

Before the recombinant proteins could be used in the plasmid assays, they had to be further purified from bacterial proteins. This was achieved by Ni-NTA affinity chromatography which allows a comparatively easy purification of 6xHis-tagged recombinant proteins from contaminating bacterial proteins (for details see chapter 2.2.3.1). Figure 3-3 demonstrates the presence of the 6x-His-tagged recombinant DFF45 protein in the eluted fractions obtained after Ni-NTA affinity chromatography.

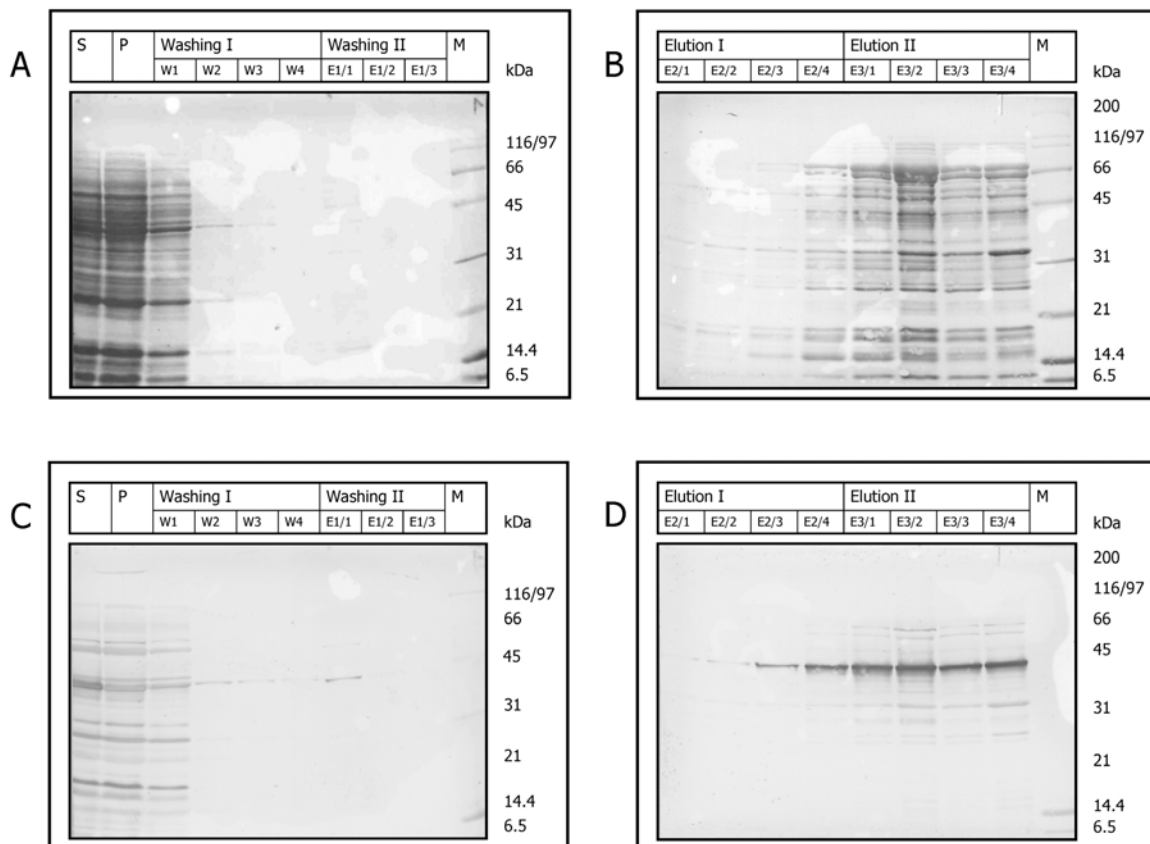


Figure 3-3: Purification of DFF40/DFF45 complex on Ni-NTA columns

Figure 3-3: Purification of recombinant DFF40/DFF45 complex from bacteria was carried out as described in chapter 2.2.3.1.1. 20 μ l of each sample were subjected to SDS-PAGE using a 12% gel and blotted onto NC-membranes; subsequent immunodetection was carried out as described in chapter 2.2.3.7.5. **A:** Ponceau-stained blotted proteins from the washing fractions. **B:** Ponceau-stained blotted proteins from the elution fractions. **C:** Blotted proteins from the washing fractions assayed with a **DFF45** antibody. **D:** Proteins from the elution fractions assayed with a **DFF45** antibody. **M:** BioRad broad-range protein standard. **S:** Supernatant, containing all proteins from the lysates, **P:** Suspension after passing the column, containing unbound proteins. Immunodetection was carried out by using BCIP/NBT as a substrate for alkaline phosphatase coupled to a secondary antibody. DFF45 was detected in distinct fractions obtained after Ni-NTA chromatography.

Though a large portion of bacterial protein was removed by passing the Ni-NTA column, not all contaminating proteins could be eliminated by Ni-NTA chromatography. Major problems were firstly a bad binding of the His-tagged DFF45 to the column (compare lane S and lane P in Figure 3-3-C) and secondly an early elution of matrix-bound protein at low imidazole concentrations. This way, contaminating proteins were co-eluted with the complex from the column. DFF40 itself had no 6xHis-tag. However, as it should be bound to DFF45 in a stable complex, it was supposed to be co-purified with DFF45 on Ni-NTA columns. Indeed, DFF40 was co-purified, indicating an intact DFF40/DFF45 complex during elution from the column, as demonstrated in figure 3-4.

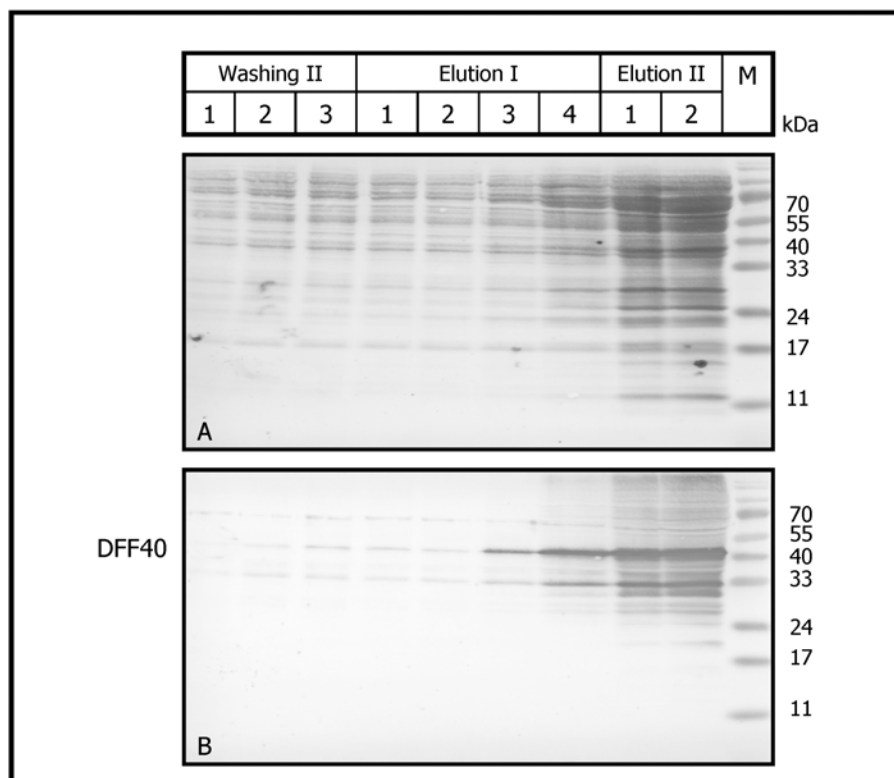


Figure 3-4: Detection of DFF40 in the Ni-NTA-purified protein complex

Samples from the fractions, after having passed a Ni-NTA column, were separated by SDS-PAGE on a 15% gel and transferred to NC-membranes by western blotting. **A:** Ponceau-stained transferred proteins on the NC-membrane. **B:** NC-membrane assayed for **DFF40**. Immunodetection was carried out by using BCIP/NBT as a substrate for alkaline phosphatase coupled to a secondary antibody. Recombinant DFF40 was co-purified in fractions containing recombinant DFF45 (see fig. 3-3).

The recombinant DFF40 protein was found at comparable amounts in exactly the same fractions containing recombinant DFF45 protein. Elution of both DFF40 and DFF45 started at fraction 'elution I/3' (as demonstrated in fig. 3-4), and the band intensities of both DFF40 and DFF45 increase at the same rate in the subsequent fractions (compare fig. 3-3 and 3-4). Since the recombinant DFF40, due to a lacking 6xhis-tag, was not bound by the Ni-NTA matrix, this co-localization in the same fractions demonstrates an intact DFF40/DFF45 complex.

3.1.1.2. Purification of caspase-3 from *S. cerevisiae*

Caspase-3 was expressed in the yeast strain *S. cerevisiae* ENY.WA-4D (*Albig, 1989*) and purified by Ni-NTA affinity chromatography prior to use. In contrast to bacterial proteins, most contaminating yeast proteins could be efficiently removed by Ni-NTA chromatography. Coomassie-staining of proteins after SDS-PAGE detected only one unknown contaminating protein with a MW of ~ 40 kDa. Procaspase-3 was found at a position in the gel corresponding to ~ 30 kDa (fraction E1/5 in fig. 3-5). This 30 kDa molecule was the inactive caspase-3-precursor, which has to be cleaved to generate a catalytically active caspase-3 enzyme.

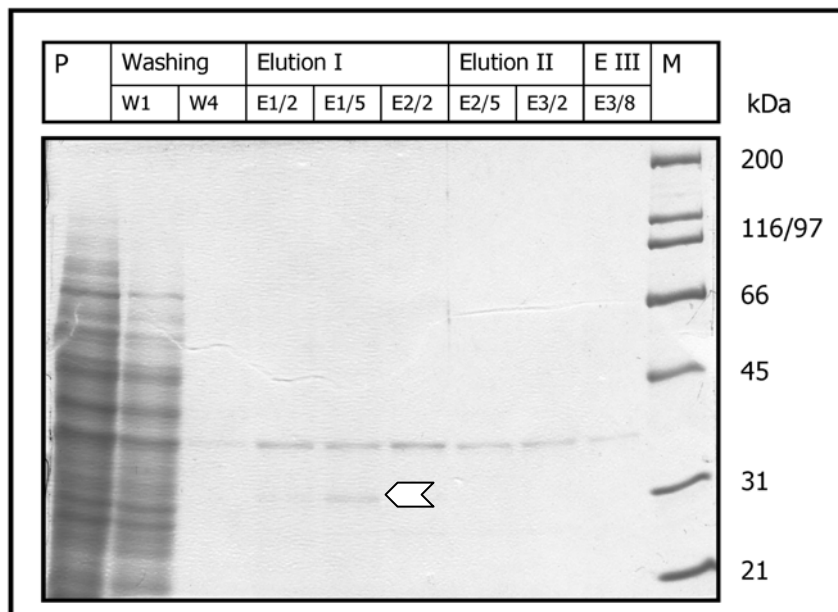


Figure 3-5: Caspase-3 purification by Ni-NTA affinity chromatography

Caspase-3 preparations from yeast were purified by Ni-NTA chromatography as described in chapter 2.2.3.1.2. Samples from selected fractions were subjected to SDS gel electrophoresis (12%-gel) and proteins in the gel were stained with Coomassie brilliant blue. Most of the yeast proteins could be removed efficiently by Ni-NTA chromatography. Caspase-3 precursor was detected as a ~ 30 kDa-protein (white arrow). In this figure the protein is seen mainly in fraction E1/5 (elution I). **P**: Unbound proteins (after having passed the column). **M**: BioRad broad-range protein standard.

The catalytically active fragments of caspase-3 were not visible in Coomassie-stained SDS gels (fig 3-5), but the presence of cleaved caspase-3 in fractions obtained after Ni-NTA chromatography could be demonstrated by western blotting. Active caspase-3-subunits, occurring in addition to the inactive precursor protein, were detectable in subsequent western blots in fractions from both elution step I and II. The two subunits, able to form the active enzyme tetramer, were detected with an antibody which recognizes both the uncleaved form of caspase-3 and its two subunits as shown in figure 3-6.

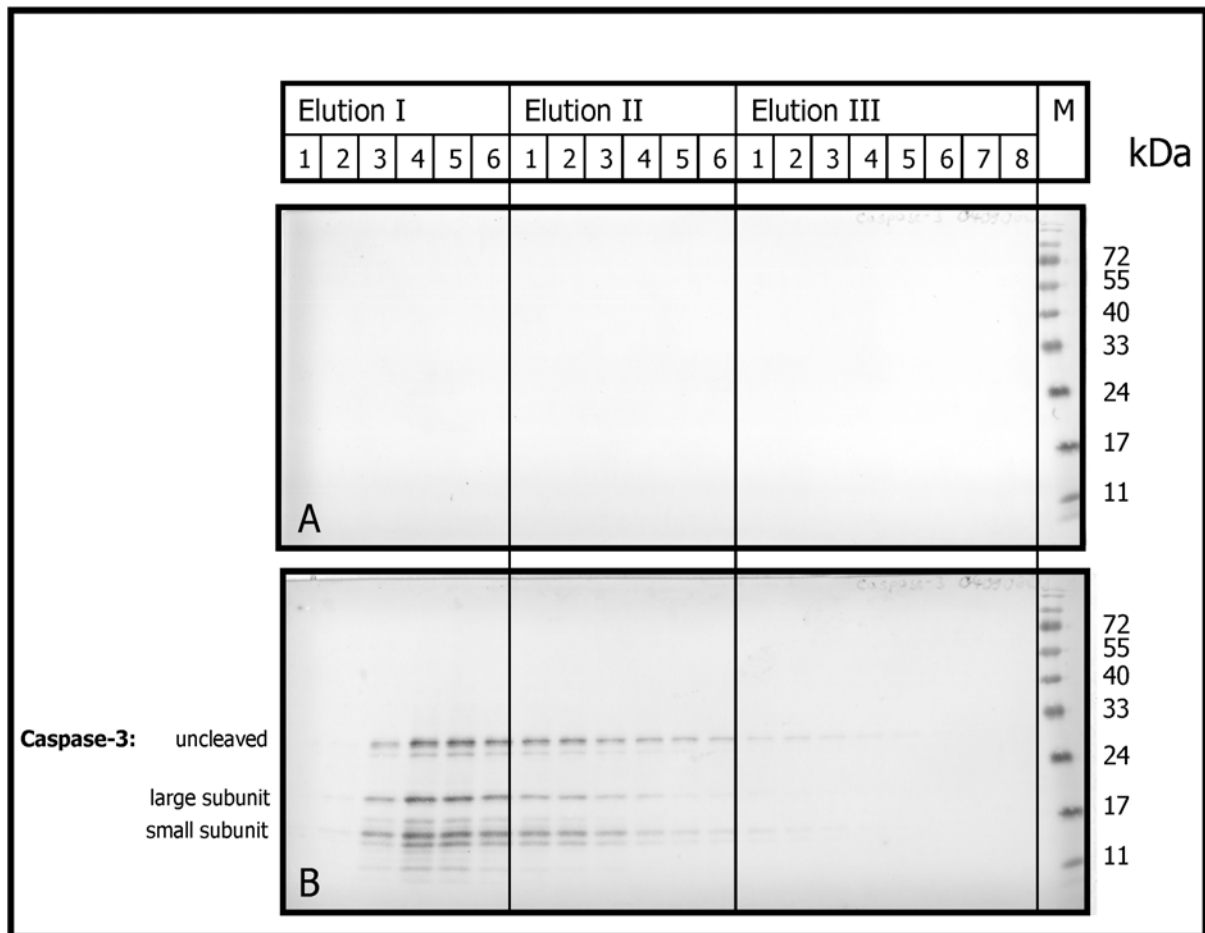


Figure 3-6: Detection of the active caspase-3 subunits by western blotting

Caspase-3 preparations from yeast were purified by Ni-NTA chromatography as described in chapter 2.2.3.1.2. Samples from the elution fractions were subjected to western blotting after SDS-PAGE using 15 % gels. **A:** Transfer was confirmed by reversible staining of the NC-membrane with Ponceau dye (protein contents in the caspase preparations were below the detection limit of Ponceau staining, so only the marker proteins were stained here, confirming successful transfer of proteins from the gel to the NC-membrane). **B:** NC-membranes were detected using a primary antibody recognizing both cleaved and uncleaved caspase-3 and a secondary AP-coupled antibody. Detection of the membrane was carried out using BCIP/NBT as substrates for AP and confirmed both the presence of uncleaved inactive caspase-3 and of the large/small subunits, able to form the active enzyme-tetramer. **M:** Prestained protein standard PageRuler™ (Fermentas).

Figure 3-6 further demonstrates that expression of caspase-3 precursor in yeast leads to purification of active caspase-3 since both the small 11-kDa-subunits and the large 17-kDa-subunits, which are able to form the active tetrameric enzyme, were detected in the preparations.

3.1.1.3. Titration of enzyme activities in DFF plasmid assays

The specific activation and the required amounts of the recombinant enzymes DFF40 and caspase-3 were determined in vitro by using plasmid DNA as a substrate for DFF40. Activity of DFF40 was determined by using equal amounts of caspase-3 and varying amounts of DFF40/DFF45 complex in the reactions. During co-incubation in the samples, caspase-3 cleaves DFF45 and thereby activates DFF40. The catalytic DNase activity of DFF40 was determined by visualizing the extent of plasmid DNA degradation after agarose gel electrophoresis. Specific activation was demonstrated by negative controls containing plasmid DNA incubated with DFF40/DFF45 complex or caspase-3 alone, respectively; plasmid DNA should not be digested in these control reactions if DFF40 is activated by caspase-3 in a specific manner. Furthermore, a dose-dependent increase in plasmid DNA degradation should be seen under activating conditions. This procedure of titrating the enzyme activities had to be repeated for each fresh preparation of enzymes before carrying out the main experiments. Examples for DFF40 and caspase-3 are shown in the following figures (3-7 and 3-8).

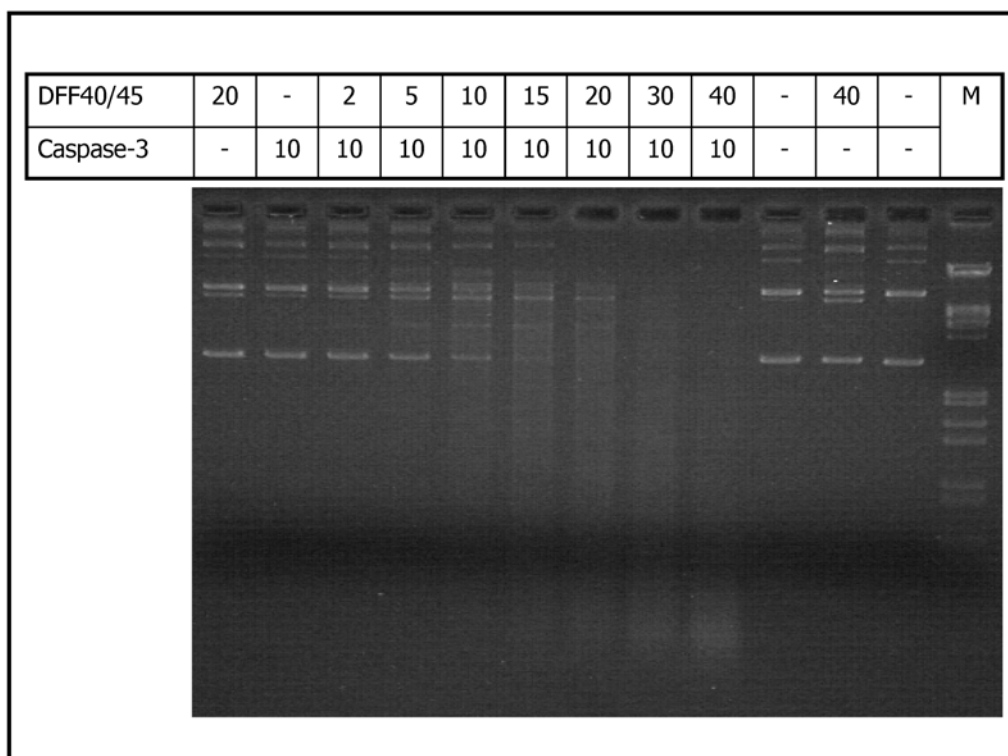


Figure 3-7: Titration of DFF40 activity

Figure 3-7: Plasmid DNA was incubated with purified, recombinant caspase-3 and DFF40 as indicated in the figure; specifications are given in μl (for details of the experiment see chapter 2.2.3.9). Samples were subjected to electrophoresis at 70 V on a 1% agarose gel and visualized by staining with ethidium bromide. Activity of DFF40 and of caspase-3 was specific because no degradation was seen in lanes containing only DFF40/DFF45 complex or caspase-3, respectively. Lanes containing both enzymes showed a dose dependent increase of DFF40 activity with increasing amount of DFF40.

Figure 3-7 demonstrates both dose-dependent and specific activation of the recombinant DNase DFF40 used for the subsequent assays.

The specific activity of caspase-3 was determined in a corresponding complementary experiment in which DFF40/DFF45 contents were kept constant and caspase-3 amounts varied (fig. 3-8).

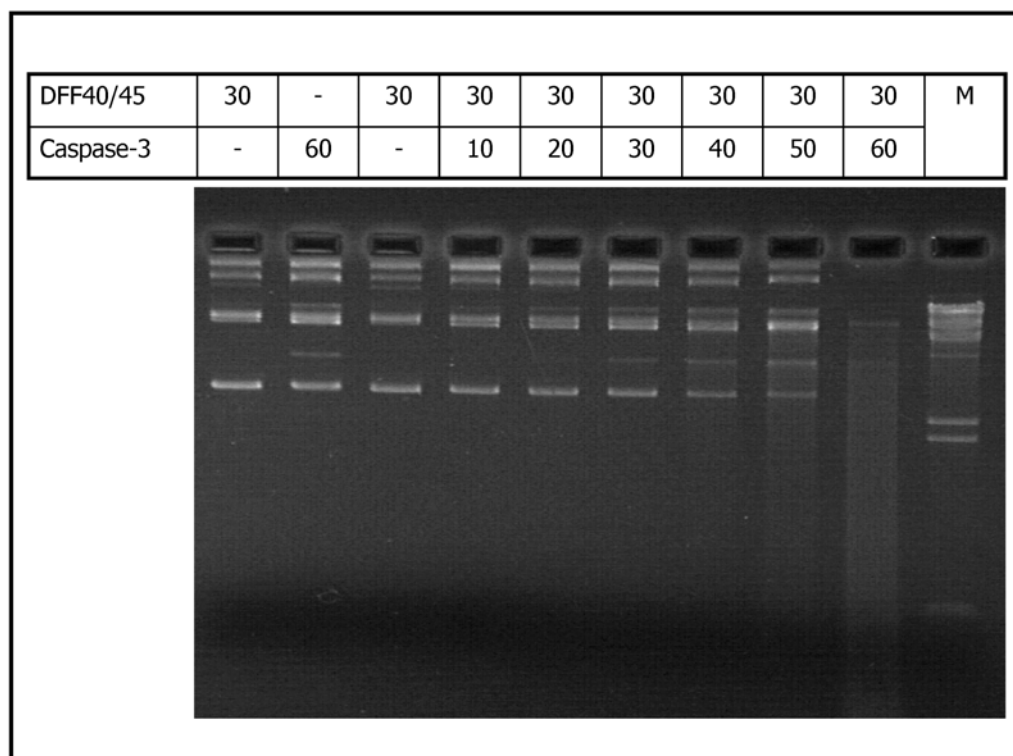


Figure 3-8: Titration of caspase-3 activity

Plasmid DNA was incubated with purified, recombinant caspase-3 and DFF40 as indicated in the figure; specifications are given in μl . Samples were subjected to electrophoresis at 70 V on a 1% agarose gel and visualized by staining with ethidium bromide. Activity of DFF40 and of caspase-3 was specific since no degradation was seen in lanes containing only DFF40/DFF45 complex or caspase-3, respectively. Lanes containing both recombinant enzymes showed a dose dependent increase of DFF40 activity with increasing amount of caspase-3.

This evidence of caspase-3-specific activation of DFF40 was particularly necessary since the results obtained after purification of the DFF40 complex by Ni-NTA affinity chromatography from bacterial proteins were unsatisfactory. However, the contaminating proteins did not interfere with the parameters tested in the plasmid assay, as demonstrated in the titration experiments. Particularly important was the proof for the

absence of contaminating DNases. If another DNase than DFF40 would have been present in the reactions, it would have catalyzed DNA degradation in a constitutive manner without being specifically activated by caspase-3. Since there was no DNase activity in samples containing DFF40/DF45 complex without added caspase-3 (and vice versa), the titration experiments proved a specific activity of DFF40 and caspase-3. As had to be expected for an enzymatic reaction, the experiment demonstrated a dose-dependent increase of enzyme activities, which was reflected by enhanced plasmid DNA degradation with increasing amounts of the respective enzyme.

3.1.1.4. Purification of H1 histone subtypes from yeast

Recombinant H1 histones were expressed in freshly transformed yeast (*according to Albig et al., 1998*) and enriched selectively by PCA extraction and TCA precipitation. Purity of the extracted H1 histones was assessed by SDS-Gel electrophoresis as shown in figure 3-9.

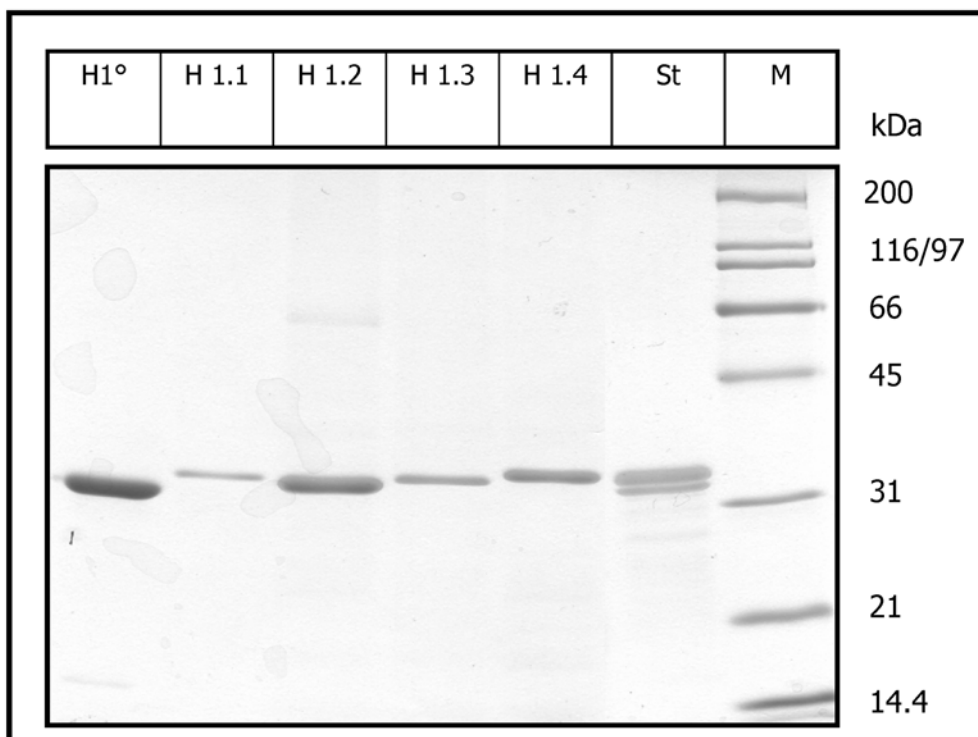


Figure 3-9: PCA-extracted human recombinant H1 histone subtypes expressed in yeast

H1 histones H1°, H1.1, H1.2, H1.3, and H1.4 were prepared from yeast as described in chapter 2.2.3.2. Aliquots of the respective preparations were subjected to SDS-PAGE using 12% gels and stained with coomassie brilliant blue. This gel was used for an estimation of H1 histones by densitometry using the software 1 D ScanEx. Estimated histone contents on the gel were 3 µg H1°, 0.5 µg H1.1, 1.9 µg H1.2, 0.8 µg H1.3, and 1.3 µg H1.4. **St**: H1 histone standard used for densitometric estimation (1 µg commercially available bovine bulk H1 histone, Alexis) **M**: BioRad broad-range protein standard.

Expression and purification of recombinant H1 histones from yeast yielded very pure histone preparations since all contaminating yeast proteins are precipitated by 5% PCA whereas the recombinant H1 histones are still soluble and thus extractable under these acid conditions. The purity of the H1 histone preparation was verified by SDS-PAGE, and no contaminating proteins were detectable in the Coomassie-stained gels as depicted in fig. 3-9.

The subsequent experiments required a quantitation of H1 histones contents. Since H1 histones are not reliably quantitated by using photometric protein assays, H1 histone contents were estimated by densitometric analysis of SDS-gels using the software 1 D ScanEx. One μg of commercially available bovine bulk H1 histone (Alexis) was used as a standard for this densitometric estimation (see figure legend of fig. 3-9).

3.1.2. EXPERIMENTS WITH DIFFERENT HUMAN H1 HISTONE SUBTYPES

To evaluate the effect of the different, purified, recombinant H1 histone subtypes on the enzymatic activity of DFF40, plasmid DNA was incubated with caspase-3-activated DFF40/DFF45 complex in the presence of varied concentrations of the H1 histone subtype to be analyzed.

3.1.2.1. Effects of H1^o

H1^o is a linker histone subtype restricted to differentiated tissues (*Doenecke et al., 1997*). In contrast to histone H1^o, the other linker-histone subtypes are detectable in proliferating cells at different ratios.

Highest DFF40 activity was seen with 1.3 to 3.1 μg of H1^o (lane 13 to 15 in fig. 3-10), higher amounts of H1^o resulted in an inhibition of DFF40 activity whereas DNase activity decreased with diminishing H1^o contents. In this assay DNA from the lower part of the gel represented residual plasmid DNA which was not yet completely digested by DFF40. Thus, in all plasmid assays total DNA content per lane had to be taken into consideration to determine the extent of DNA degradation. High activity of DFF40 generated a high amount of small fragments which migrate to the lower part of the gel (for a comparison see also fig. 3-12, lane 10).

In accordance to previous data, DFF40 activity in lanes containing moderate concentrations of H1^o was higher than DFF40 activity on naked plasmid DNA (lane 6 in fig 3-10), demonstrating an activating effect of H1^o on DFF40 activity. However, the inhibiting effect at higher concentrations of linker histones on DFF40 activity digesting a plasmid substrate was not reported before.

H1^o seemed to have an activating affect on DFF40 activity in a considerably larger concentration range than the other H1 histone subtypes (compare the plasmid assays

described in the following chapters). Importantly, since the quantitations of the histone contents in the assays were based on the results from a supplementary densitometric estimation, slight differences in the concentrations and the activating effect on DFF40 should not be over-interpreted using these assays. However, the markedly broader concentration range of H1^o in activating DFF40 activity in figure 3-10 was distinctly different from the activating range of the other tested H1 histone subtypes (described in the following chapters).

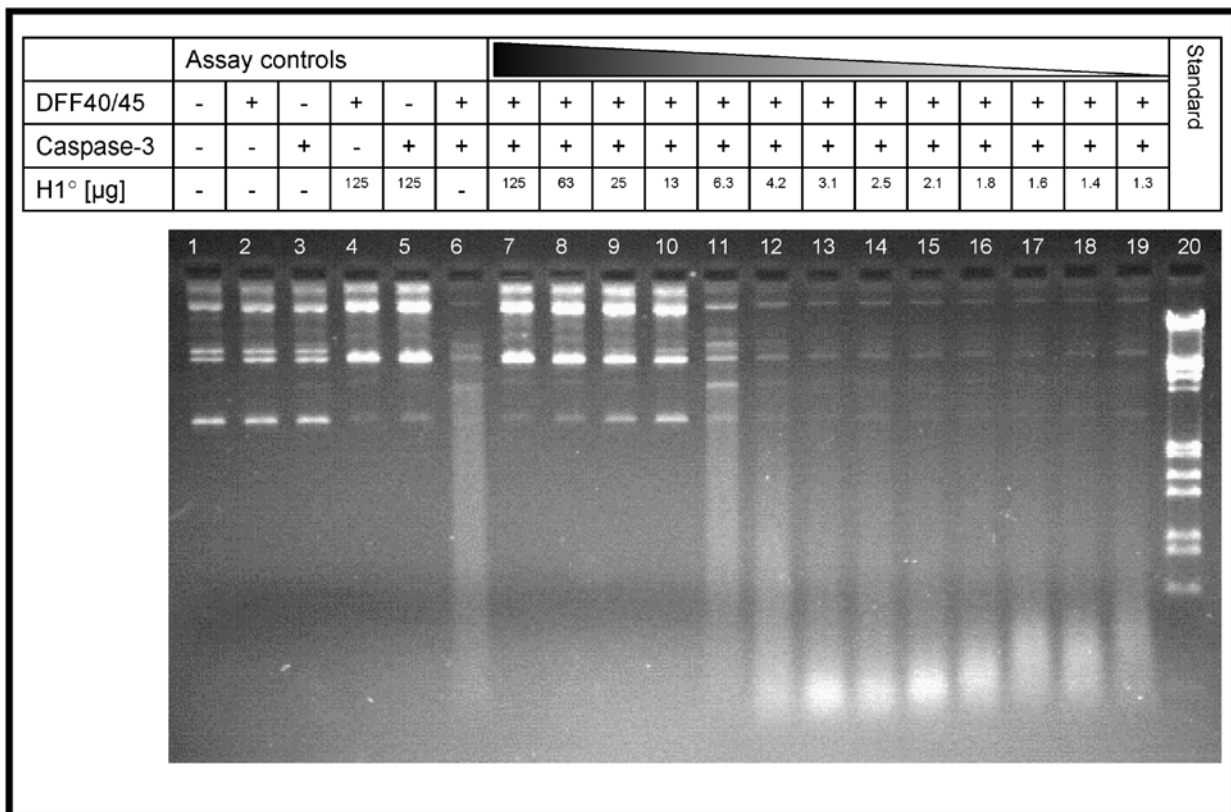


Figure 3-10: Influence of H1^o on the DNase activity of DFF40 when digesting plasmid DNA

One µg plasmid DNA was incubated for 2 hours at 37°C with purified, recombinant DFF40/DFF45 complex, caspase-3, and different amounts of recombinant H1^o-histone as indicated in the figure. Reactions were stopped by adding stop-buffer, samples were subjected to electrophoresis on a 1% agarose gel at a constant voltage of 70 V, stained with ethidium bromide, and visualized on an UV-transilluminator. Assay negative controls were performed to assess lacking effects of possibly contaminating DNases (lanes 1-5). DFF40 activity was dependent on the presence of caspase-3 since it did not occur in samples lacking caspase-3 (lanes 2 and 4). Caspase-3 specifically activated DFF40 which subsequently digested plasmid DNA (lane 6). DNA degradation occurred only in lanes containing active DFF 40 (lanes 6-19) except in those lanes, where high concentrations of H1 histones led to an inhibition of DNA degradation (lanes 7-11). In contrast to the other H1 histone subtypes, H1^o activates DFF40 activity on plasmid DNA in a considerably high concentration range (1.3 to 3.1 µg H1^o per µg plasmid DNA).

3.1.2.2. Effects of H1.3

In contrast to other human tumor cell lines, only traces of the linker histone H1.3 are expressed in HL60 cells (*Kratzmeier et al., 1999*). These cells are reported to be very sensitive to apoptosis induced by a multitude of different inducers, and DNA fragmentation is detected in these cells soon after induction of apoptosis (*Shimizu and Pommier, 1997; Schliephacke et al., 2004*). However, no significant differences in activating or inhibiting DFF40 could be detected in the experiment shown in fig. 3-11. Activation of DFF0 was most efficient at a concentration range of 0.5 to 1 μg histone H1.3 per μg plasmid DNA. This concentration is comparable with the values obtained for the other H1 histone subtypes. Therefore, lacking H1.3 presumably does not contribute to the rapid induction of DNA fragmentation during apoptosis in HL60 cells.

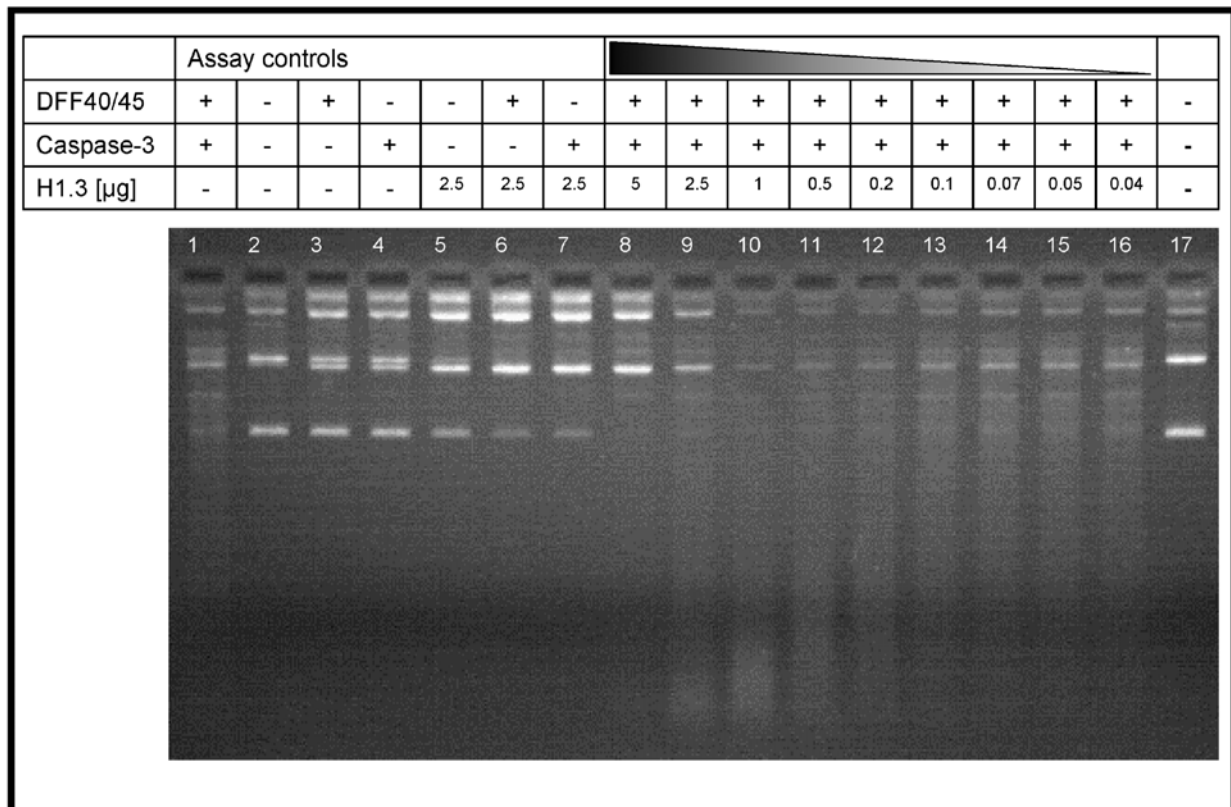


Figure 3-11: Influence of H1.3 on the DNase activity of DFF40 when digesting plasmid DNA

Samples were treated as already described in figure 3-10. Controls (lane 1-7) demonstrate specific activation of DFF40 in this assay. DFF40 activity was highest in the presence of 1 μg histone H1.3 (lane 10), increasing concentrations led to an inhibition of DFF40 (lanes 9 and 10). The activating effect decreased with decreasing histone contents in the samples.

3.1.2.3. Effects of H1.4

H1.4, as well as H1.2, is a very common linker histone. In most mammalian cells, H1.4 represents the largest part of cellular linker histones, followed by H1.2 (see standard lane in fig. 3-9). As already seen with the other tested H1 histones, there was firstly an inhibiting effect at high concentrations and secondly an activating effect which can be observed in the middle concentration range. The effect was dose-dependent since a further decrease of histone H1.4 content in the assays led to decreased activation of DFF40 in the assay as seen with the other subtypes before. The activating concentration range of H 1.4 was located between 0.75 and 1.5 μg .

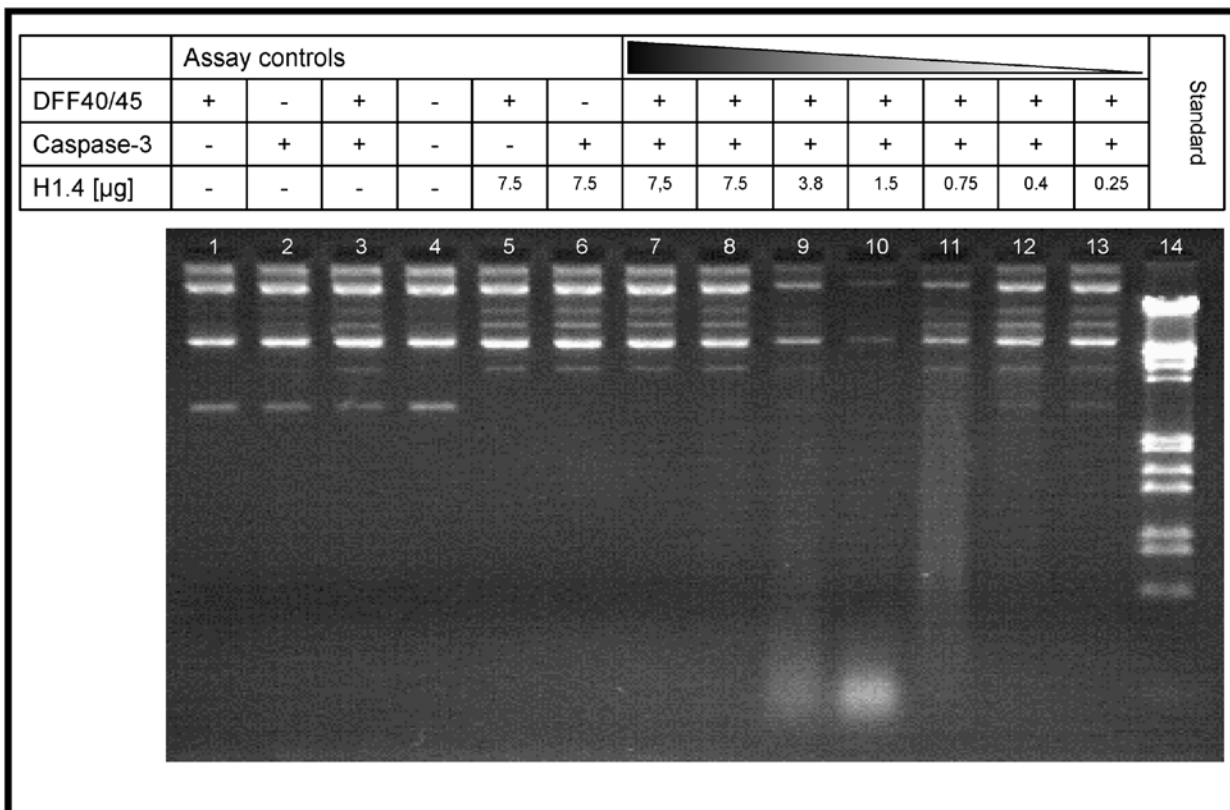


Figure 3-12: Influence of H1.4 on the DNase activity of DFF40 when digesting plasmid DNA

Samples were treated as already described in figure 3-10. Controls (lane 1-7) demonstrate specific activation of DFF40 in this assay. DFF40 activity was highest in the presence of 0.75 to 1.5 μg histone H1.4 (lane 10) and generated a high amount of small fragments which are visible in the lower part of the gel. Increasing histone concentrations led to an inhibition of DFF40 (lanes 7 -9). The activating effect decreased with decreasing histone contents in the samples.

3.1.2.4. Effects of bulk H1 histones

This assay was performed with commercially available H1 histones to exclude effects of preparation artefacts possibly generated during the purification of recombinant H1 histones from yeast. The H1 histone mixture used in the plasmid assay was also used as a standard for SDS-PAGE (see fig. 3-9). The prevailing H1 histone subtypes in this H1 histone mixture, which was prepared from bovine thymus, are H1.4 and H1.2 (compare fig 3-9). Highest DFF40 activity was seen at a histone content of 0.5 μg per assay (lane 11 in fig. 3-13). As already observed in the experiments with the other H1 histone subtypes, the effects were dose dependent: Increasing H1 histone contents inhibited DFF40 activity more and more (lanes 8-10), while the activating effect was reduced with decreasing H1 histone contents (lanes 12-16).

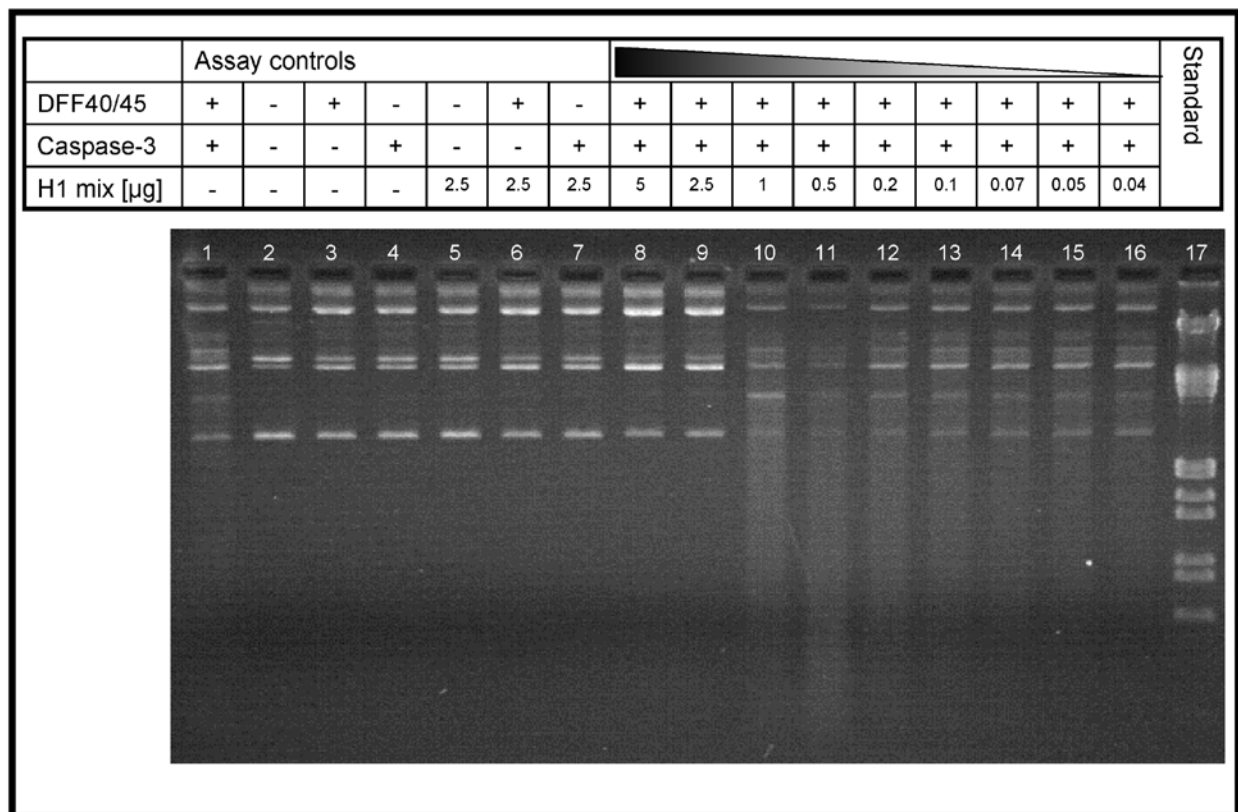


Figure 3-13: Influence of bulk H1 on the DNase activity of DFF40 digesting plasmid DNA

Samples were treated as already described in figure 3-10. Controls (lane 1-7) demonstrate specific activation of DFF40 in this assay. DFF40 activity was highest in the presence of 0.5 μg bulk histone (lane 11), increasing concentrations led to an inhibition of DFF40 (lanes 7-9). The activating effect decreased with decreasing histone contents in the samples.

3.1.2.5. Effect of core histone H3

Since an inhibiting effect as well as an enhancing effect on DFF40 activity of all the linker histone subtypes tested so far was seen, the question arose whether this is a feature which is specifically restricted to linker histones or may be seen with related proteins, i.e. core histones, as well. Commercially available core histone H3 from bovine thymus was used to test for effects on DFF40 activity in another plasmid assay.

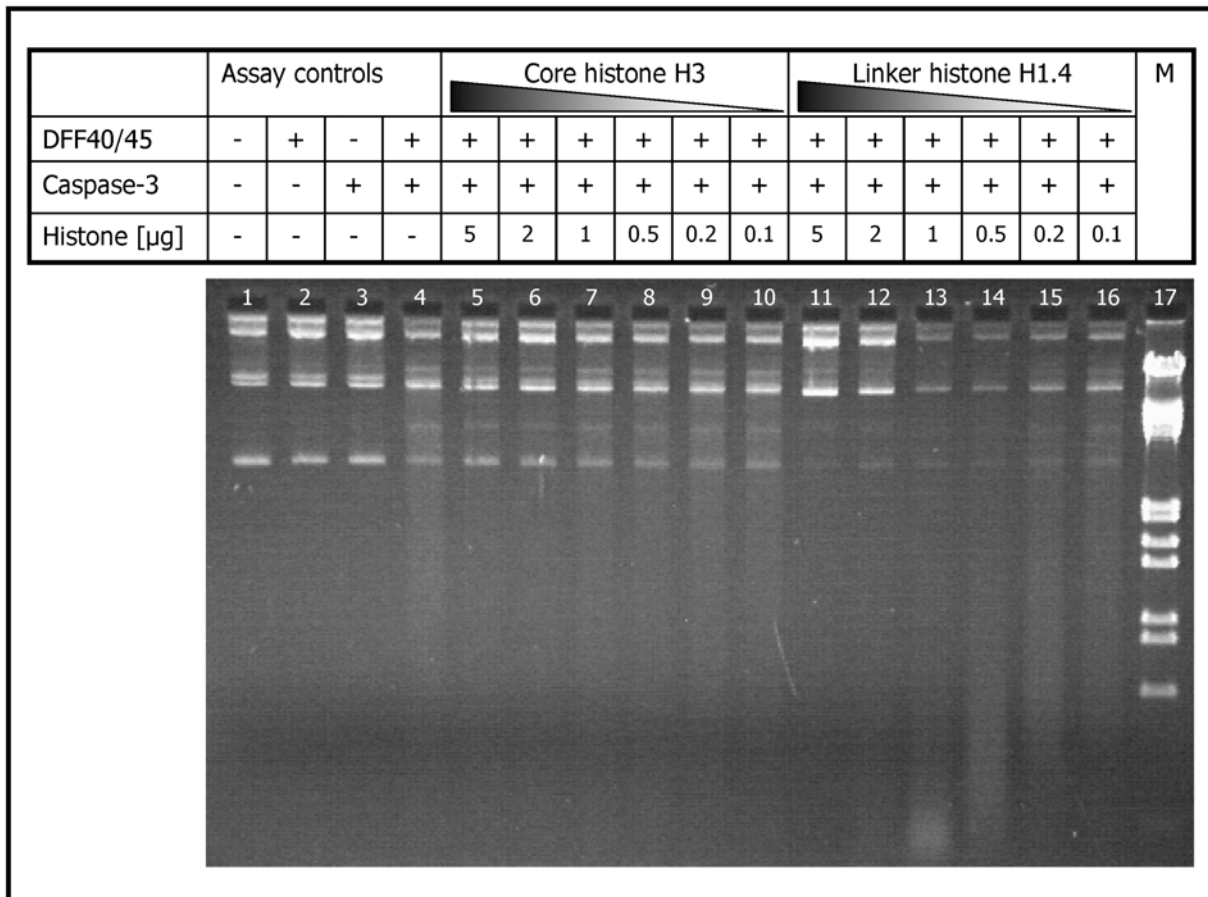


Figure 3-14: Influence of both core histone H3 and linker histone H1.4 on DFF40 activity

Samples were treated as already described in figure 3-10. Controls (lane 1-4) demonstrate specific activation of DFF40 in this assay. Only an inhibiting but no enhancing effect on DFF40 was seen with core histone H3. In contrast to core histone H3, the linker histone H 1.4 enhanced DFF40 activity at a concentration of about 1.0 μg per μg plasmid DNA, as had been expected (see figure 3-12).

The enhancing effect on DFF40 activity seemed to be a specific feature of linker histones since core histone H3 only had an inhibitory but no activating effect on DFF40 activity. This inhibitory effect of core histones may be an unspecific effect due to the high amount of a DNA binding protein in the assays. It may further indicate that inhibition of DFF40 activity by high amounts of linker histone subtypes may be an in vitro artefact due to unphysiologically high concentrations (see also chapter 3.1.5.1)

3.1.3. EXPERIMENTS WITH IN VITRO PHOSPHORYLATED HISTONE H1.2

Phosphorylation as well as dephosphorylation of both core histones and linker histones was described for various human cell lines in the course of apoptosis (see chapter 4.2.2). Thus, it could be assumed that the phosphorylation state of H1 histones might be an important feature during apoptotic DNA fragmentation. To test this hypothesis, recombinant purified H1.2 was phosphorylated *in vitro* by incubating it with cdc2 kinase under *in vitro* conditions. Cdc2 kinase catalyzes a hyperphosphorylation of H1 histones *in vitro*; this can be easily detected in stained SDS gels. The increase in the molecular weight of the hyperphosphorylated histone protein alters its electrophoretic mobility during SDS-gel electrophoresis as demonstrated in figure 3-15.

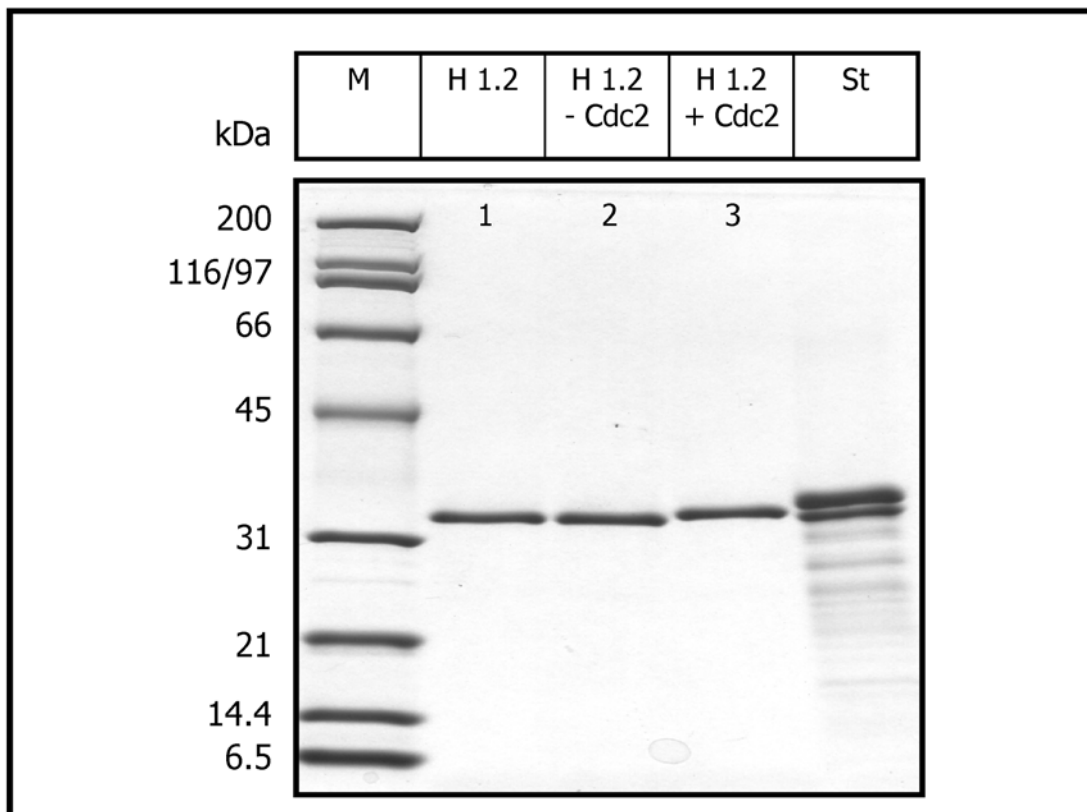


Figure 3-15: Different migration features of *in vitro* phosphorylated H1.2 in SDS-PAGE

Recombinant purified histone H1.2 was phosphorylated *in vitro* as described in chapter 2.2.3.4. Proteins were subjected to SDS-PAGE on a 12 % gel and visualized by staining with Coomassie brilliant blue. Lane **1**: Untreated H1.2. Lane **2**: H1.2 kept under the applied phosphorylation conditions except addition of cdc2-kinase. Lane **3**: Hyperphosphorylated H1.2 was generated by treating recombinant H1.2 with cdc2-kinase. Electrophoretic mobility of phosphorylated H1.2 (lane 3) is slightly changed compared with non-phosphorylated recombinant H1.2 in lane 1.2. **M**: BioRad broad-range protein standard, **St**: 1 μ g standard bulk H1 histone protein (Alexis). The lower band of the standard lane corresponds to H1.2, the upper band corresponds to H1.4.

The electrophoretic mobility of untreated H1.2 (lane 1 in fig. 3-15) did not differ from that of H1.2 which was incubated in the absence of cdc2 kinase (lane 2) under the conditions used for phosphorylation with cdc2 (lane 3). In contrast, migration of phosphorylated H1.2 (lane 3) was slightly retarded compared with migration of unphosphorylated H1.2, which is seen in lane 1, lane 2, and in the lower band of lane St (the upper band of the standard lane consists of histone H1.4, compare fig. 3-9).

These differently treated, recombinant H1.2 histones were subsequently used for plasmid assays to assess possible differences in the effects on the activity of DFF40 when comparing phosphorylated and unmodified histones. A representative gel is shown below.

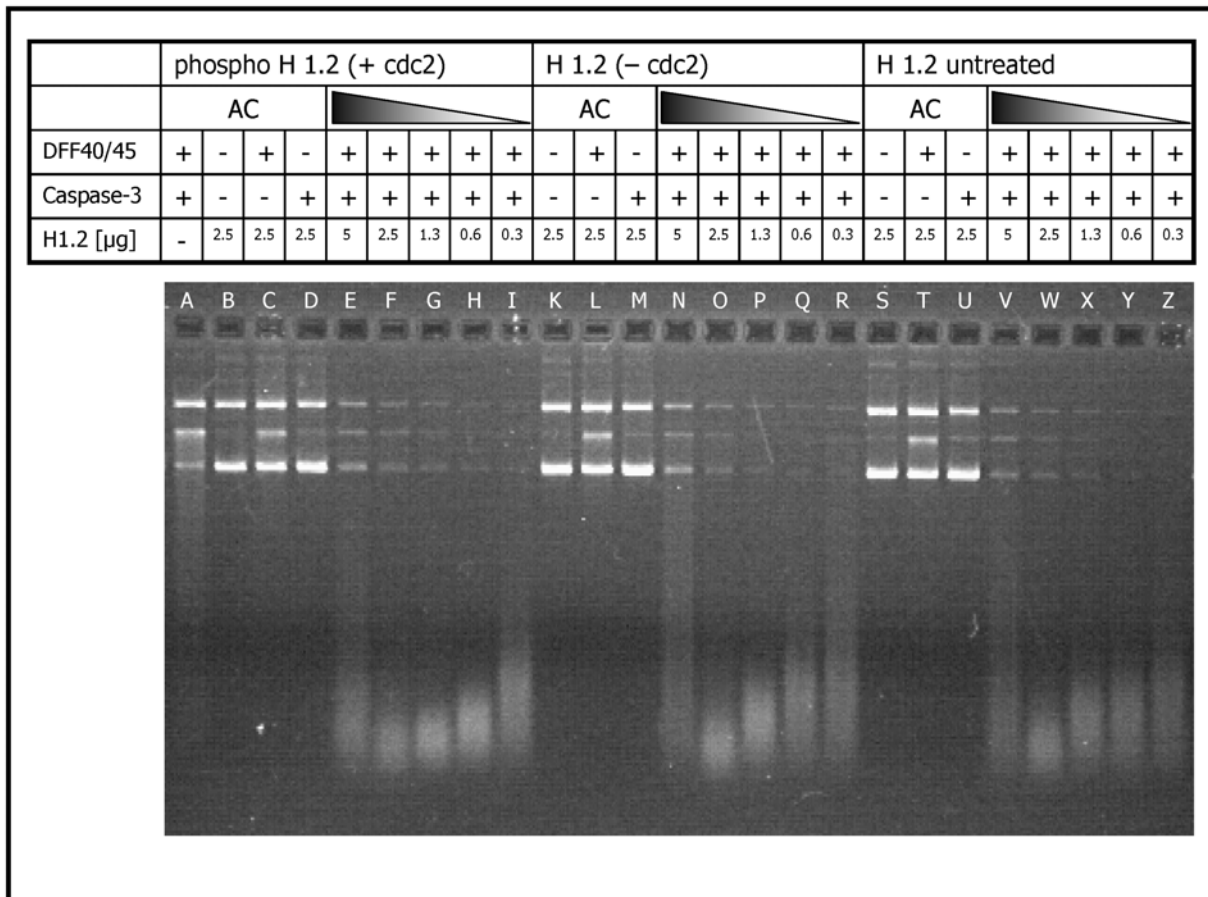


Figure 3-16: No differences in the activating features of differently phosphorylated H1.2

In vitro phosphorylated recombinant H1.2 (lanes A-I), unphosphorylated H1.2 (lanes K-R), and untreated H1.2 (lanes S-Z) were used in this plasmid assay. There were no differences in the inhibiting and activating features due to phosphorylation of the H1 histone. AC: Assay controls.

No differences in the activating or inhibiting effect of in vitro phosphorylated H1.2 were detected in the plasmid assays. However, the point in question now was whether the in vitro conditions correctly reflected the in vivo conditions. Firstly, linker histones are not a natural substrate of cdc2 kinase, and secondly in vitro phosphorylation leads to a hyperphosphorylation of H1 histone. In vitro phosphorylation of H1.2 probably results at phosphorylation at different sites than those phosphorylated in vivo. Thus, the effect of naturally modified linker histones on DFF40 activity still remained to be determined. Therefore, the experiments in the following section were carried out with cellular proteins instead of recombinant, in vitro modified proteins.

3.1.4. EXPERIMENTS WITH CELLULAR H1 HISTONES

To exclude artefacts by *in vitro* phosphorylation of recombinant H1 histones, the experimental conditions were approximated to the *in vivo* conditions by using H1 histones purified from human cells undergoing apoptosis and H1 histones from non-treated control cells. If there was an effect due to differently modified linker histones, this should be detectable in a plasmid assay using these naturally modified histones instead of recombinant histones. A second advantage of this system is that the effect of all naturally occurring modifications during apoptosis are included in the experimental design. Because a dephosphorylation of H1 histones was already shown in Topotecan-treated apoptotic HL60 cells, these cells were considered as the ideal apoptosis system to test the hypothesis. HL60 cells were treated for 6 hours with the topoisomerase inhibitor Topotecan to induce apoptosis, control cells were left untreated, and H1 histones were extracted from both control and apoptotic cells by PCA extraction. The H1 histones were further purified from other acid-soluble proteins by gel filtration using P60 columns and subjected to SDS-PAGE for an estimation of the H1 histone contents. Capillary zone electrophoresis was performed to check for histone modifications, and finally the purified H1 histones were used in the plasmid assays to determine the effect of *in vivo* modified, cellular H1 histones on the activity of DFF40.

There were no obvious differences visible when comparing the Coomassie-stained purified H1 histone proteins separated by SDS-PAGE. This was an expected result since only hyperphosphorylated H1 histones change their migration features in an extent which can be detected by SDS-PAGE. Similar to bovine H1 histones, H1.4 and H1.2 represented the prevailing H1 histone subtype in HL60 cells, as could be expected for cells deriving from the haematopoietic stem line. Furthermore, SDS-PAGE of a serial dilution from the H1 histone preparations allowed an estimation of the protein contents in the H1 histone preparations. A serial dilution of 1:8 resulted in a protein content of one μg per lane in H1 histone preparations of both control and apoptotic HL60 cells as shown in figure 3-17.

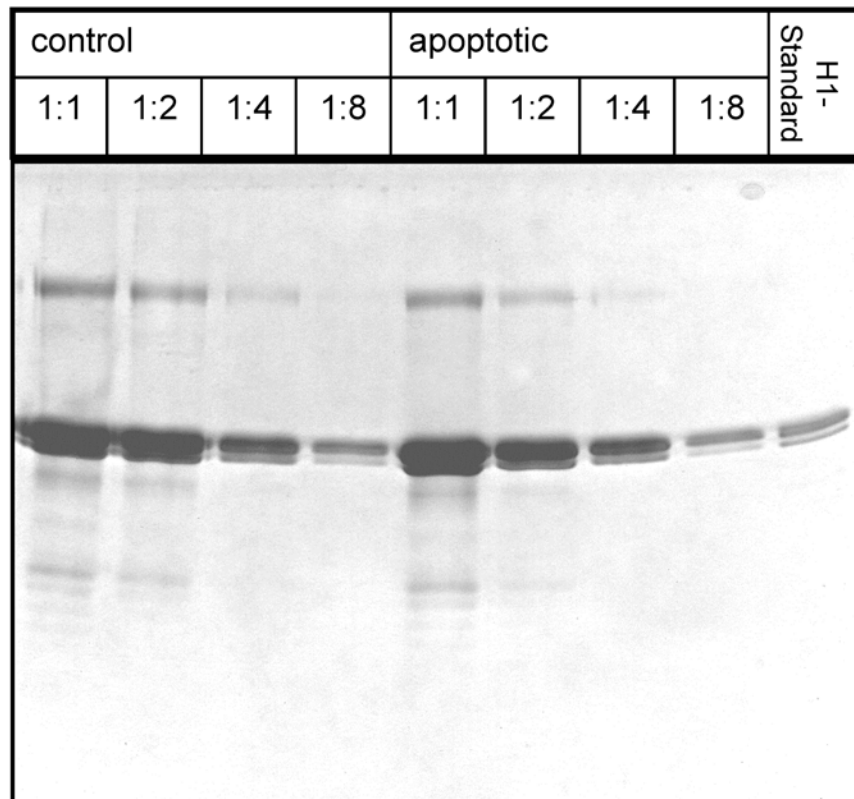


Figure 3-17: SDS-PAGE of purified H1 histones from HL60 cells

H1 histones were extracted from control and apoptotic HL60 cells, respectively, (see chapter 2.2.5.2.1) and purified by gel filtration on a P60 column. The figure shows two dilution series analyzed by quantitative SDS-PAGE on a 12% gel and subsequent Coomassie-staining. Histone contents were estimated to be identical in the corresponding dilution steps from control cells and from apoptotic cells. 1 μ g H1-standard histone preparation (Alexis) was used as a standard for the estimation of protein contents.

Analysis of the phosphorylation state of H1 histones required the molecular resolution of an analytical capillary zone electrophoresis unit. CZE was performed as described in chapter 2.2.3.5 and allowed both a separation of different H1 histone subtypes and the analysis of their phosphorylation state.

CZE confirmed that H1.4 is the prevailing subtype in HL60 cells followed by H1.2. Additionally, a small portion of H1.5 was detected; other subtypes (H1.1 and H1.3) were not detected in HL60 cells as described before (*Kratzmeier et al., 1999*). As had been expected, the content of phosphorylated H1 histones decreased during apoptosis of HL60 cells, concomitantly the portion of dephosphorylated H1 histones increased. This had already been explained to be the result of posttranslational modifications rather than being the consequence of an altered protein expression pattern (*Kratzmeier et al., 1999; Kratzmeier et al., 2000*). A representative CZE-electropherogram is shown in figure 3-18.

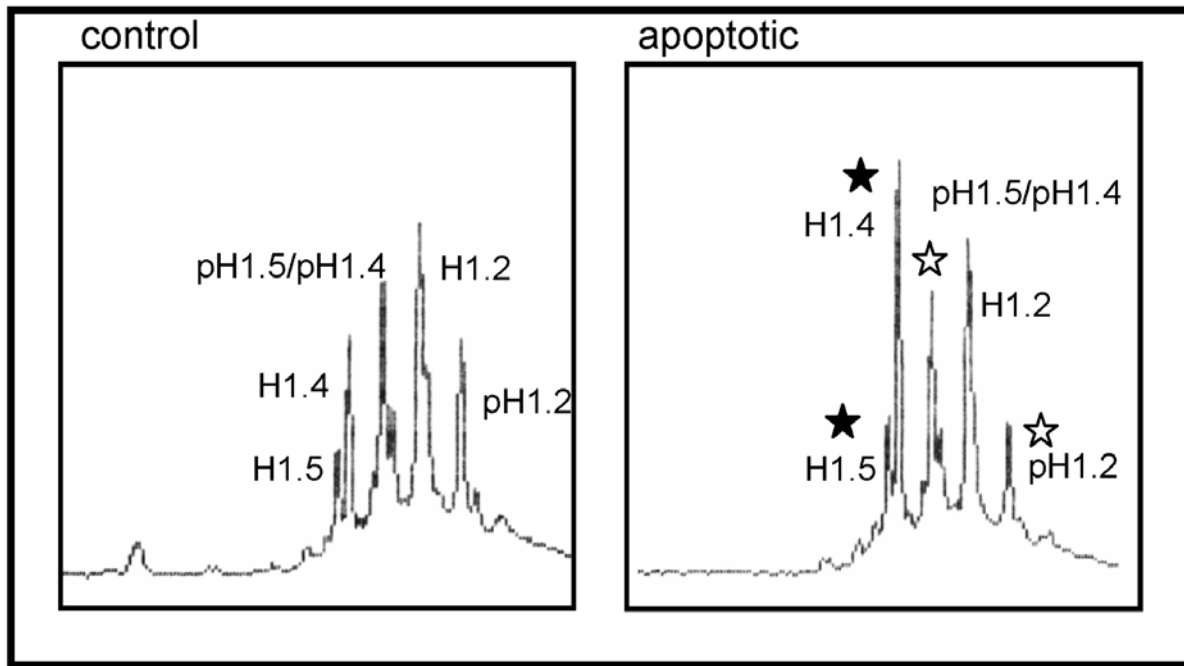


Figure 3-18: CZE of H1 histones from control and apoptotic HL60 cells

Histones were extracted from HL60 cells by PCA extraction and TCA precipitation and CZE was performed as described in chapter 2.2.3.5. Analysis of the respective relative peak heights for the depicted subtypes allowed the determination of the phosphorylation state of the individual H1 histone subtypes. The content of phosphorylated subtypes decreased during apoptosis (compare the peak height of pH1.5 and pH1.4 in control cells and apoptotic cells), and the peaks for the respective unphosphorylated subtypes increased concomitantly. p: Phosphorylated histone subtype. Filled stars indicate peaks resulting from increasing H1 histone fractions, and empty stars indicate peaks of decreasing H1 histone fractions.

Other posttranslational modifications than the observed dephosphorylation might have occurred on H1 histones during apoptosis, but these were not detectable under the CZE conditions used for these separations. However, in addition to phosphorylation only poly(ADP) ribosylation has been described for H1 histones (*Okayama et al., 1978*). Since the H1 histones used for subsequent experiments in the present study were modified under cellular conditions, they reflected the *in vivo* conditions in control cells and in cells undergoing apoptosis much better than the *in vitro* phosphorylated recombinant H1 histones. Therefore, they were used to test them for effects on the DFF40 activity on plasmid DNA.

As shown in figure 3-19, there were no differences detectable when comparing the effect of H1 histones from control and apoptotic HL60 cells. Therefore, it may be concluded that any posttranslational modifications of H1 histones during apoptosis in these cells do not alter their influence on DFF40 activity.

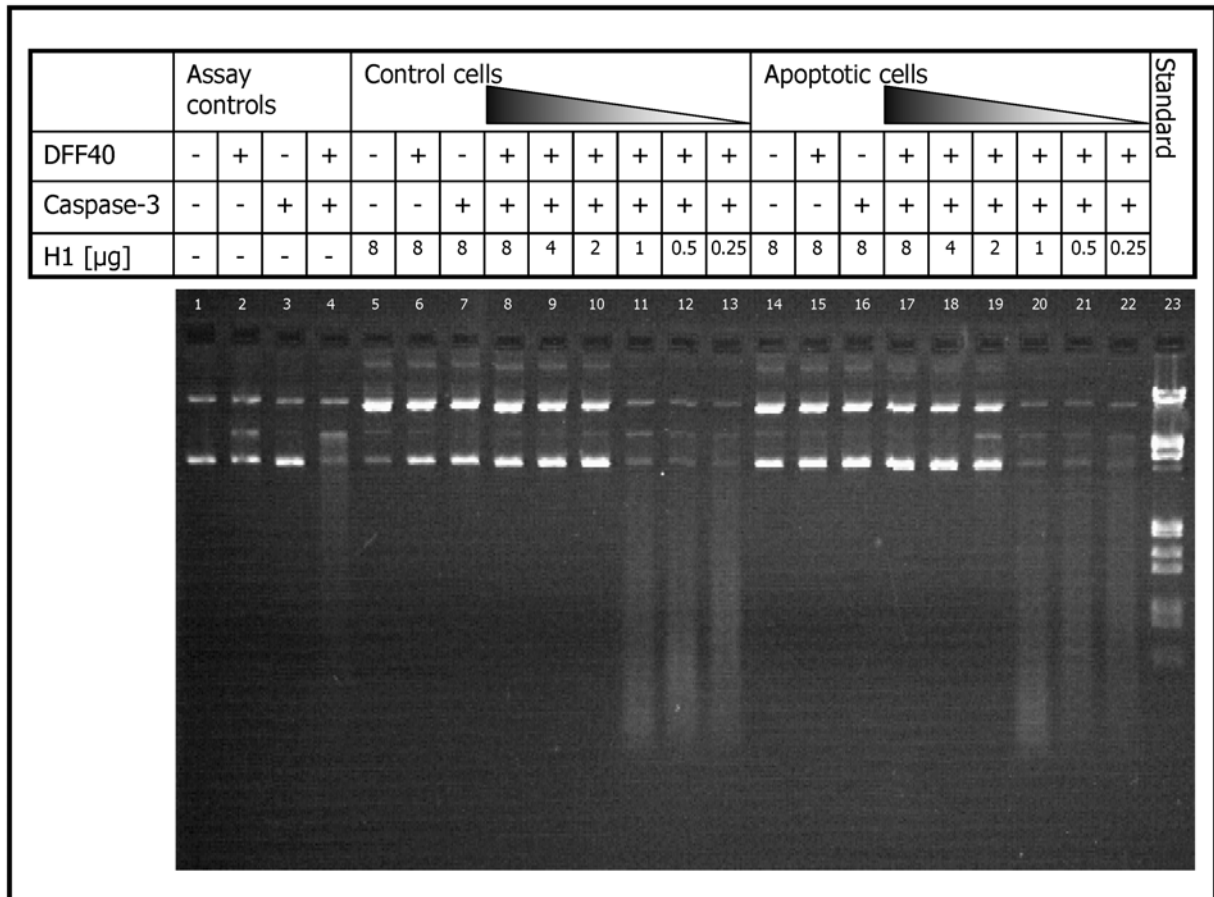


Figure 3-19: Effect of H1 histones from control and apoptotic HL60 cells on DFF40 activity

H1 histones were extracted from control and apoptotic HL60 cells as described in chapter 2.2.5.2.1, and different concentrations were used in the plasmid assay as indicated in the figure. No differences in the activation features of H1 histones from untreated control cells (lanes 5-13) compared with H1 histones from apoptotic cells (lanes 14-22) was seen. Assay controls (lanes 1-4) demonstrate specific activation of recombinant DFF40 by recombinant caspase-3.

Since a differential effect of differently modified H1 histones on DFF activity could be excluded, it remained to be determined whether the activating or the inhibiting effect of the H1 histones prevails under *in vivo* conditions. Furthermore, it seemed interesting to check other cellular components for their influence on DNA fragmentation during apoptosis. This question was particularly interesting because some cells show internucleosomal DNA cleavage during apoptosis (HL60 and Jurkat cells) whereas others do not (Raji cells).

3.1.5. EXPERIMENTS WITH CELLULAR PROTEINS

3.1.5.1. Effect of H1 histones on DFF40 activity on a chromatin substrate

The following experiment was carried out to approximate the experimental design to the *in vivo* conditions more accurately. The results obtained so far demonstrated an inhibiting effect of all H1 histone subtypes on the DFF40 activity at high concentrations. In contrast, lower H1 histone concentrations had an activating effect on DFF40, independently from the respective H1 subtype. However, the applied high concentration of H1 histones is hardly found in chromatin under *in vivo* conditions. So, it seemed interesting to test whether H1 histones also have an inhibiting effect if they are present on a natural chromatin substrate in addition to the endogenous H1 histones. Purified nuclei from HL60 cells were selected as a natural chromatin substrate because the nuclei contain native chromatin packaged by core histones and linker histones under *in vivo* conditions. These nuclei were incubated with DFF40, activated by caspase-3, and the recombinant subtype H1^o was added to some reactions. Subtype H1^o was chosen because former experiments in this study demonstrated activation of DFF40 activity by H1^o in a broad range of concentrations. Cytoplasm was added to some reactions to test for an additional activating or inhibiting effect of cytoplasmic extracts. Importantly, controlled nuclear transport processes do not affect this experimental system since the nuclear pore complexes of the purified nuclei are leaky. This leakyness results from both effects of Triton X 100 on the nuclear membrane (*Faiferman and Pogo, 1975*) and the mechanical disruption of the connections from the nuclei to the endoplasmic reticulum during ultracentrifugation.

A typical apoptotic DNA ladder was seen in lanes 8 to 13 of figure 3-20. This DNA ladder resulted from active DFF40, digesting preferably the linker DNA between the nucleosomes which is not protected by being packaged in the nucleosome. The cells from which the nuclei were purified were not apoptotic, as demonstrated by lacking DNA fragmentation in lane 1. Caspase-3 on its own was not able to cause DNA fragmentation in nuclei (lane 2); the same was true for the DFF40/DFF45 complex in the absence of activating caspase-3 (lane 3). As expected, no DNA fragmentation was seen with cytoplasm from non-apoptotic HL60 (lane 4). Caspase-3 was not able to activate endogenous DFF40 from the cytoplasm of HL60 cells in this assay (lanes 5 to 7). This was presumably due to degradation of the labile endogenous DFF40 in this cytoplasmic preparation since other experiments revealed activation of endogenous DFF40 by recombinant caspase-3 (see fig. 3-23). However, caspase-3 induced enhanced activity of recombinant DFF40 in the presence of cytoplasm (lanes 8 to 10)

compared with DFF40 activated in the absence of cytoplasm (lanes 11 to 13). Interestingly, addition of H1^o completely blocked DNA fragmentation in chromatin from nuclei. This result may indicate that additional present H1 histones on a DNA substrate generally inhibit DNA fragmentation. The results suggest that an unspecific deposition of H1 histones on chromatin may protect DNA from being digested by DFF40. Therefore, it may be concluded that the inhibiting effect of recombinant H1 on DFF40 is an artefact, caused by unphysiologically high H1 histone contents (see also chapter 3.1.2.5). Furthermore, the activating effect of all subtypes was seen at a concentration of 0.5 to 1.5 µg per µg plasmid DNA, conditions similar to those found under in vivo conditions in chromatin (discussed in chapter 4.2.1).

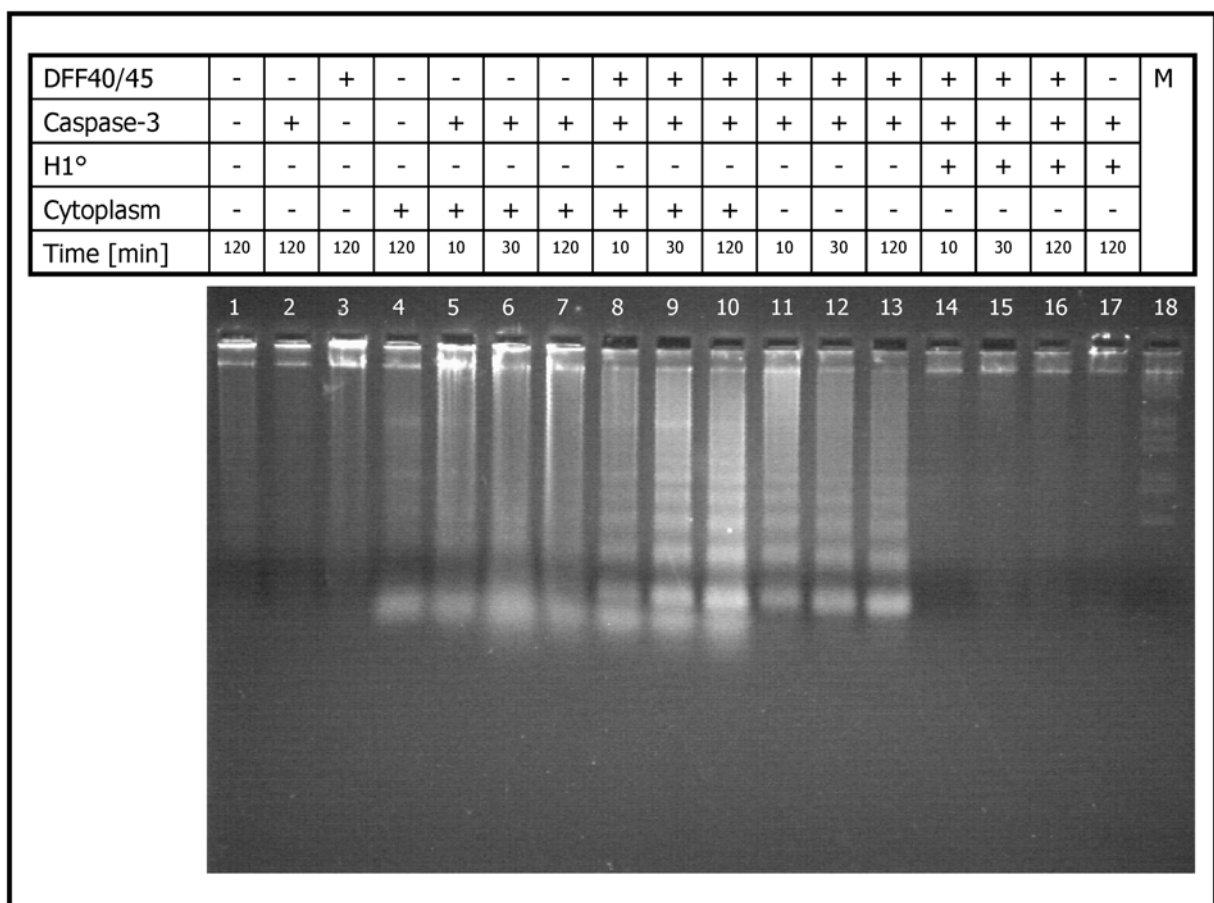


Figure 3-20: Effect of H1^o on the DFF40 activity in purified nuclei

Nuclei purified from HL60 cells were incubated with different proteins for different times as indicated in the figure. A typical apoptotic DNA ladder (generated by recombinant DFF40, after activation by cleavage of recombinant DFF45 by recombinant caspase-3) was seen in lanes 8 to 13. Lane 1 demonstrates that the cells from which the nuclei were purified, were not apoptotic as DNA fragmentation was lacking. Both caspase-3 (lane 2) or DFF40/DFF45 complex (lane 3) on their own were not able to cause DNA fragmentation, respectively. No DNA fragmentation was seen in the control lane with cytoplasm from non-apoptotic HL60 (lane 4). Caspase-3 was not able to activate endogenous DFF40 from the cytoplasm of HL60 cells in this assay (lanes 5 to 7) but resulted in an enhanced activity of activated DFF40 (lanes 8 to 10) compared with DFF40 activated in the absence of cytoplasm (lanes 11 to 13). Addition of H1^o completely blocked DNA fragmentation in nuclei. **M**: DNA standard λ -DNA cut by Eco R I and Hind III.

3.1.5.2. Effects of cytoplasm from different cell types on DFF40 activity

The results obtained with a natural chromatin substrate demonstrated an inhibiting effect of H1 histones present in excess on DNA which was already packaged by nucleosomes. Interestingly, cytoplasm was able to enhance the activity of caspase-3-activated DFF40 on this chromatin substrate. Thus, the question arose whether additional cytoplasmic factors may have an influence on the activity of DFF40. The following experiments were carried out with both cell types that easily undergoes apoptosis with concomitant DNA fragmentation (HL60 and Jurkat cells) and cytoplasm of a cell type (Raji) which is known to be quite resistant to apoptosis and in which DNA fragmentation can hardly be detected.

The following figure shows DNA extracted from HL60, Jurkat, and Raji cells induced for apoptosis with 150 ng/ml Topotecan. Whereas internucleosomal DNA cleavage was detected in HL60 cells and Jurkat cells, it was not observed in Raji cells. Nevertheless, all of the topotecan-treated cells were dying though the survival rates were different. Cell death resulting in internucleosomal DNA degradation was seen in HL60 cells after 3h and in Jurkat cells after 6h. In contrast, cell death in Raji cells was detected after 12 h of incubation with Topotecan. The concomitant random DNA cleavage resulted in a smear of genomic DNA rather than DNA laddering in these cells.

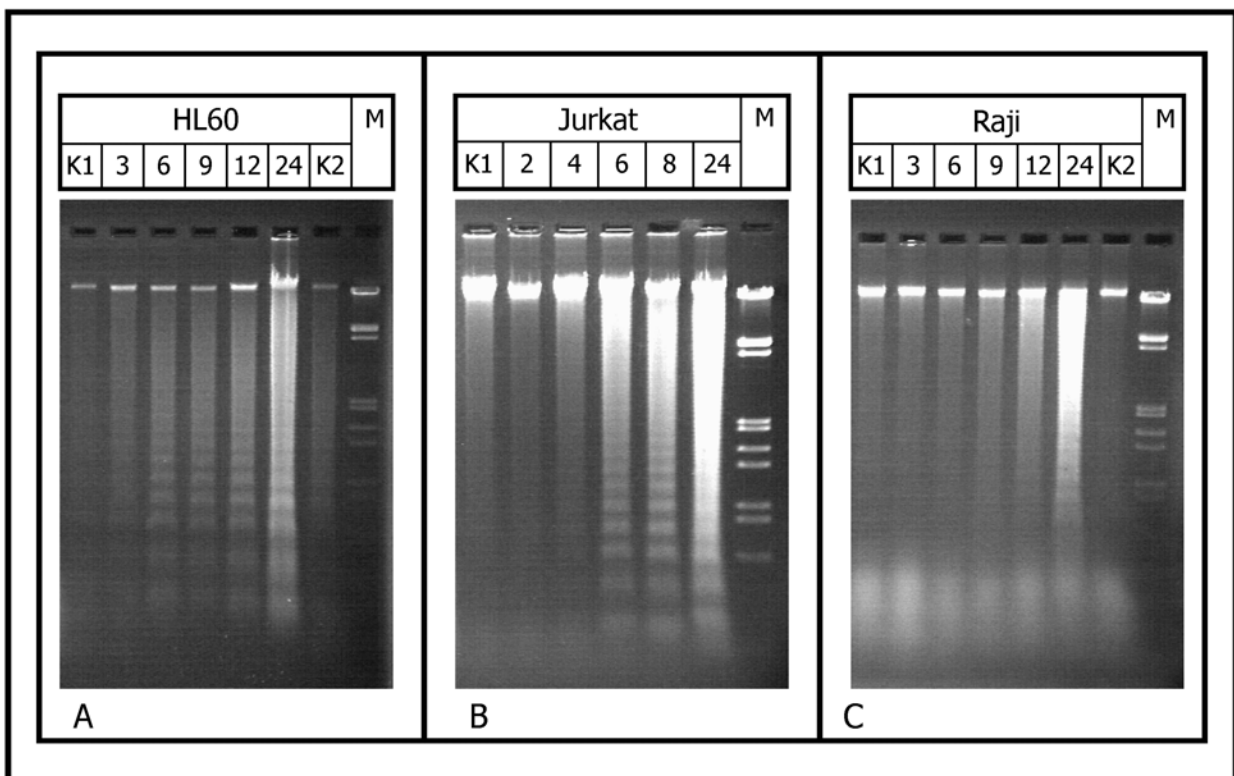


Figure 3-21: DNA fragmentation during apoptosis in HL60, Jurkat, and Raji cells

Figure 3-21: HL60, Jurkat, and Raji cells were induced to undergo apoptosis by adding 150 ng Topotecan per ml of culturing-media. Cells were harvested at differing times as indicated in the figure, and extracted DNA was subjected to electrophoresis on a TBE-agarose gel. The figure shows DNA fragments in the gel stained by ethidium bromide. **A:** Nucleosomal DNA fragmentation was present in HL60 cells **B:** Nucleosomal DNA fragmentation in Jurkat cells. **C:** Random DNA degradation, resulting in a smear of DNA in the gel, was seen in Raji cells rather than DNA laddering. Thus, all these topotecan-treated cells were dying, which was detectable by DNA degradation. However, Raji cells were markedly delayed in their response to Topotecan.

The effects of the respective cytoplasmic extracts from HL60 and Raji cells were tested by using nuclei from both HL60 cells and Raji cells. This experimental design was chosen to evaluate possible effects resulting from differentially expressed or modified nuclear proteins in the chromatin of these two cell lines, which also might have an effect on DFF40 activity. The results are depicted in fig. 3-22 and 3-23.

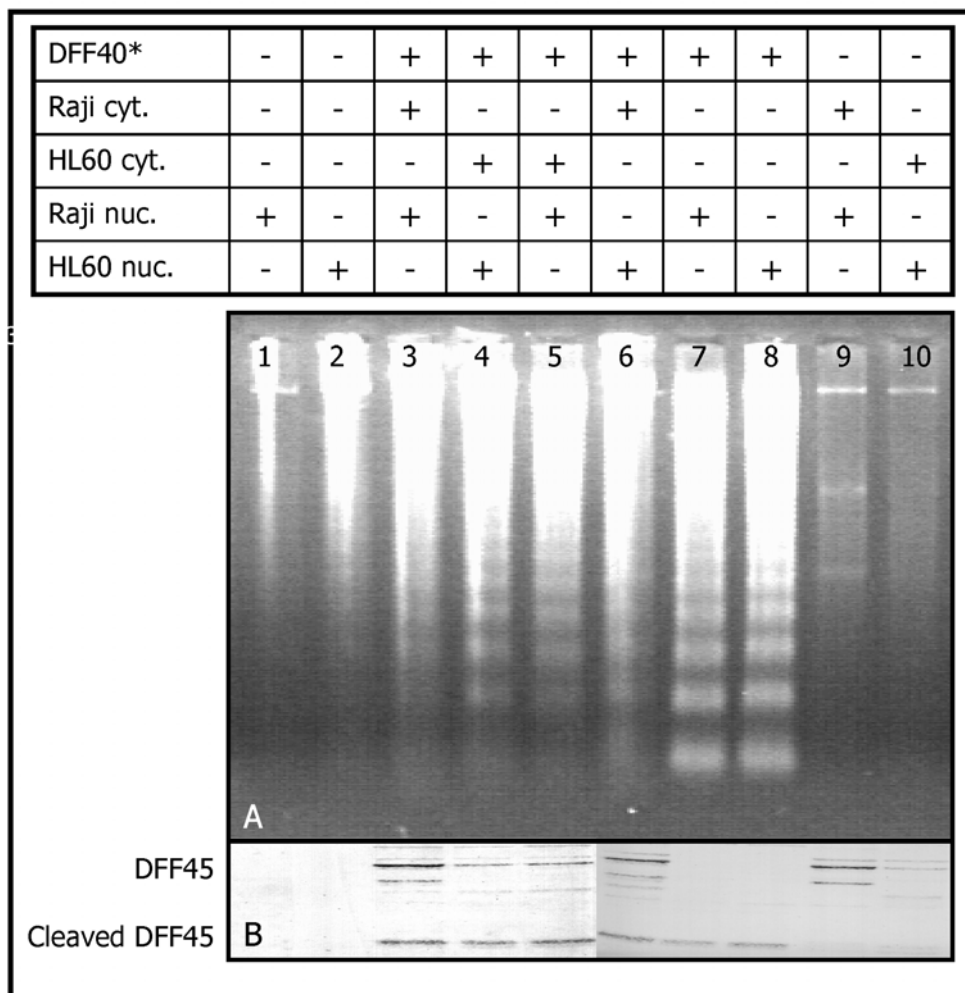


Figure 3-22: Effect of DFF40 and cytoplasm from HL60 and Raji cells on purified nuclei

This figure legend refers to figure 3-22 on the previous page.

Purified nuclei and cytoplasm, prepared from both HL60 and Raji cells were digested by recombinant caspase-activated DFF40, and DNA samples were prepared as described in chapter 2.2.4.10.6. Proteins were prepared for western blotting as described in chapter 2.2.5.2.4, and blotted proteins were detected with an antibody recognizing DFF45 and DFF35. **A:** DNA samples visualized by staining with ethidium bromide. No internucleosomal DNA degradation was seen in nuclei from Raji cells (lane 1) and HL60 cells (lane 2) incubated without DFF40, whereas incubation of Raji nuclei as well as HL60 nuclei in the presence of activated DFF40 led to internucleosomal DNA degradation. DNA laddering was still seen in nuclei from both cell types when digested in the presence of HL60 cytosol (lanes 4 and 5). In contrast to this, the presence of Raji cytosol led to less DNA degradation in both types of nuclei (lanes 3 and 6). **B:** Proteins were analyzed using a primary antibody directed against DFF45/DFF35 and using BCIP/NBT as a substrate for AP coupled to the secondary antibody. Cleaved DFF45 resulting from the caspase-3 mediated activation of the DFF40/45 complex was detected in all samples containing DFF40. Additionally, endogenous DFF45 from the respective cell type was detected. Nuclei prepared from both cell types did not contain DFF45, presumably due to the preparation conditions (lanes 1 and 2). Interestingly, Raji cytosol contained much more DFF45 than HL60 cytosol did (compare lanes 3, 6, 9 and lanes 4, 5, 10). **DFF40*:** Caspase-activated DFF40: DFF40 was activated from the DFF40/45 complex by an initial incubation step at 30°C for 30 min. Caspase activity was inhibited during the following experiment by adding a caspase-inhibitor. **cyt:** Cytoplasm, **nuc:** Nuclei.

Fig 3-22 and 3-23 demonstrate differences in the effects of the respective cytoplasmic extracts on the DFF40 activity in nuclei: In contrast to the cytoplasmic extract from HL60 cells, Raji cytoplasmic extract was able to reduce internucleosomal DNA degradation in nuclei. Obviously, there are no differences in the chromatin of these two cell types, which might have differentially affected DFF40 since DNA laddering was observed in both Raji nuclei and HL60 nuclei (details are explained in the figure legend of figure 3-22).

A similar experiment (depicted in fig. 3-23 on the next page) demonstrated that recombinant caspase-3 was able to generate a DFF40-like activity in HL60 cytoplasm but not in Raji cytoplasm. The activated DNase degraded DNA from purified nuclei by internucleosomal cleavage. In contrast, recombinant caspase-3 on its own or cytoplasm from either HL60 or Raji cells on its own was not able to induce internucleosomal DNA cleavage in both HL60 and Raji nuclei.

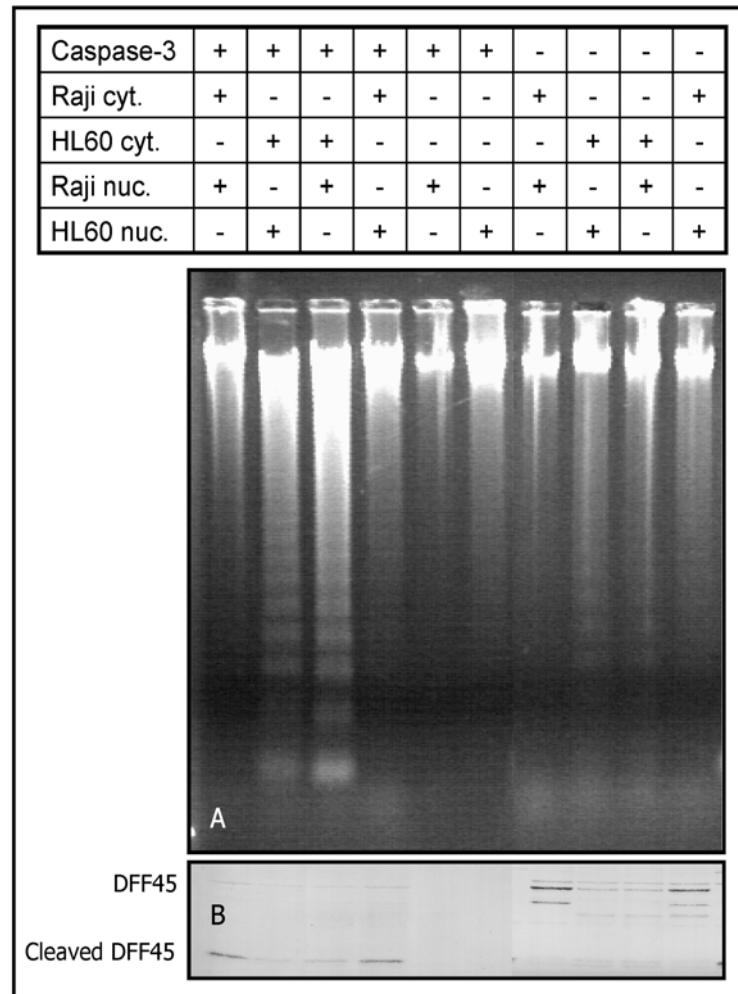


Figure 3-23: Effect of caspase-3 and cytoplasm from HL60 and Raji cells on purified nuclei

Purified nuclei and cytoplasm, prepared from both HL60 and Raji cells, were treated as already described in figure 3-22 but recombinant caspase-3 was added instead of recombinant activated DFF40. **A:** DNA samples after staining with ethidium bromide. **B:** blotted proteins assayed for DFF45. Recombinant caspase-3 was able to induce a DFF40-like DNase activity in HL60 cytoplasm (lanes 2 and 3) but not in Raji cytoplasm (lanes 1 and 4). Recombinant caspase-3 did not induce DFF40-like activity in nuclei in the absence of cytoplasm (lanes 5 and 6). Cytoplasm of HL60 induced slight DNA laddering in both HL60 and Raji nuclei (lanes 8 and 9), whereas Raji cytoplasm did not induce DNA laddering (lanes 7 and 10).

To confirm these results, and to further characterize the factors involved in the different behaviour of cytoplasmic extracts from HL60 and Raji cells, the extracts were further characterized. Attention was focused on DFF45 as a possible candidate responsible for the different features seen in the cytoplasmic extracts because the expression rates varied considerably between Raji and HL60 cells (see figure 3-24). Because DFF45 is a chaperone and therefore might be resistant to heat treatment (i.e. may retain its inhibitory effect), plasmid assays were performed in the presence of heat-treated or native cytoplasmic extracts prepared from both Raji and HL60 cells.

Dilution series of native and heat-treated cytosols were prepared ranking from 1:1 (corresponding to 100 mg/ml for native protein) to 1:32 (corresponding to 3.125 mg/ml

for native protein) by diluting them with the buffer used for preparation of the cytoplasmic extracts, and samples were analyzed by SDS-PAGE and western blotting. Western blotting revealed that Raji cytoplasmic extracts contained much more DFF45 and DFF35 than HL60 cytoplasmic extracts did. The heat-treated cytoplasmic extracts from both Raji and HL60 cells still contained DFF45, although at a lower level.

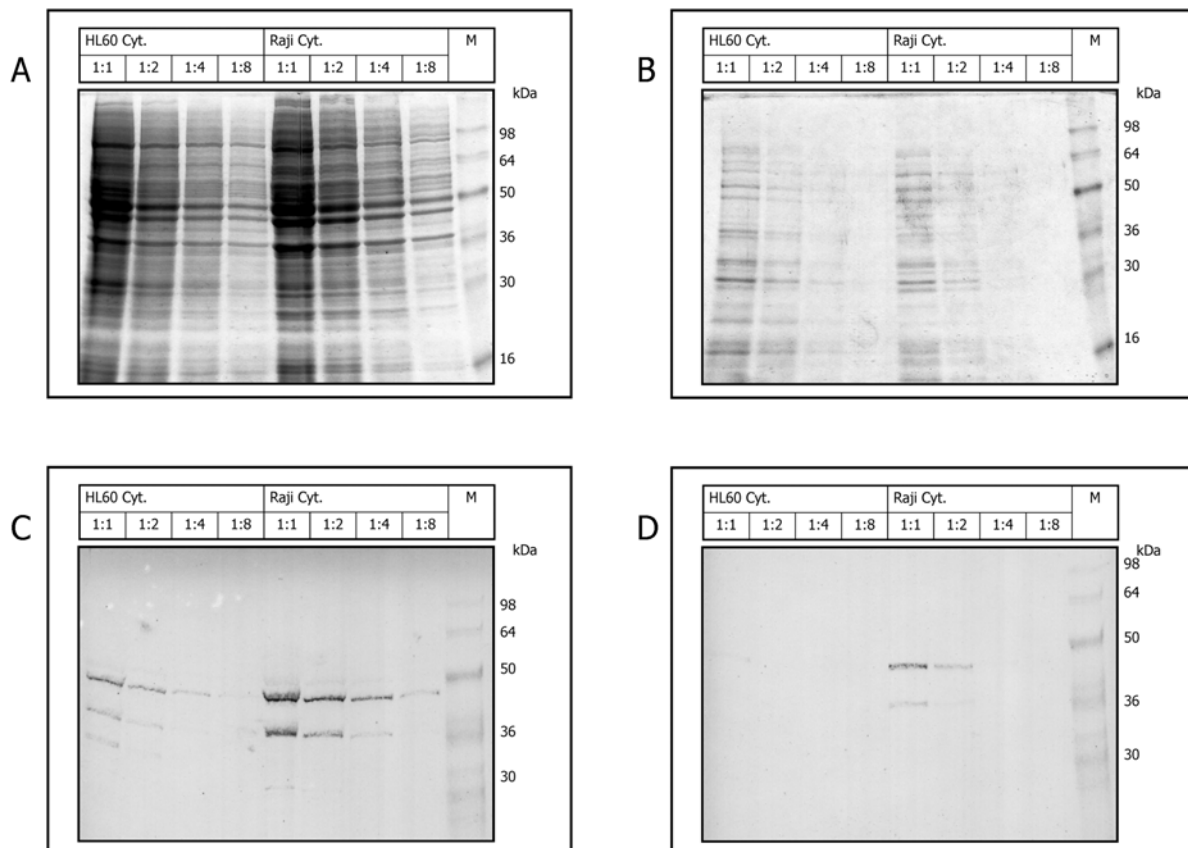


Figure 3-24: DFF45 in native and heat-treated cytoplasmic extracts from HL60 and Raji cells

Cytoplasmic extracts were prepared from HL60 and Raji cells as described in chapter 2.2.5.2.3. Aliquots were heat-treated by incubating them in a 97°C water-bath for 15 min. Precipitated proteins were pelleted by a centrifugation step at 13,000 g for 5 min at 4°C, supernatants were transferred to fresh tubes and used as 'heat-treated cytoplasmic extracts' in dilution series in the following experiments. **A:** SDS-PAGE of the native cytoplasmic extracts using a 12% gel; the first 4 samples of each dilution series are shown. **B:** SDS-PAGE of the heat treated cytoplasmic extracts using a 12% gel; the first 4 samples of each dilution series are shown. **C:** Western blot of native cytoplasmic extracts detected with an antibody recognizing both **DFF45** and **DFF35**. **D:** Western blot of heat-treated cytoplasmic extracts assayed for both **DFF45** and **DFF35**. Western blots were detected using an AP-coupled secondary antibody using BCIP/NBT as a colouring substrate. **M:** Seeblue prestained protein standard. **Note:** The DFF45-antibody used in this study recognizes both DFF45 and DFF35, therefore, two bands were detected in cellular protein preparations.

As demonstrated in fig. 3-24, DFF45 was still detectable in the cytoplasmic extracts of both HL60 cells and Raji cells even after heat treatment. Thus, the effect of DFF45

could now be tested without being affected by other active enzymes in the heat-treated cytoplasmic extracts. The inhibiting effect on the activity of DFF40 correlated well with the content of DFF45 in the extracts, as demonstrated in the following figure (3-25).

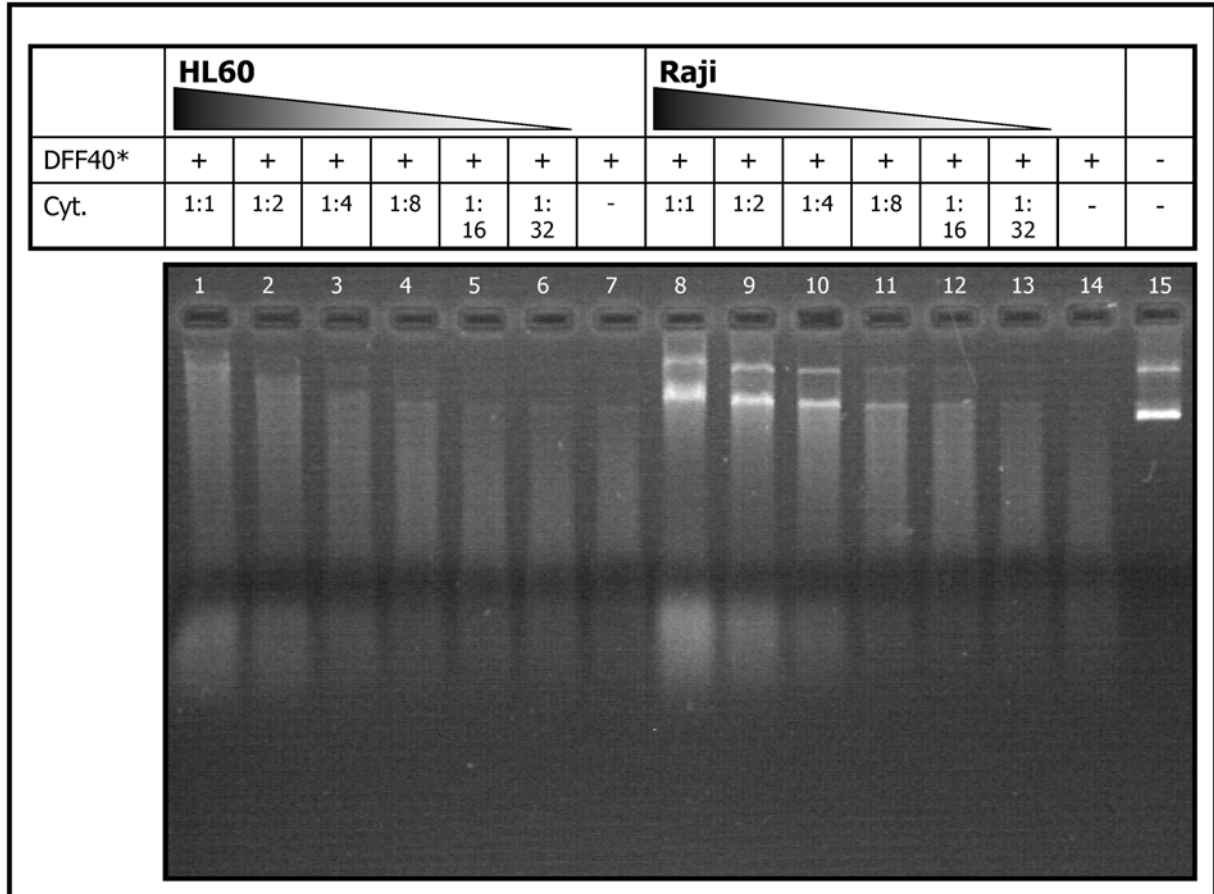


Figure 3-25: Plasmid assay with heat-treated cytoplasmic extracts from HL60 and Raji cells

The western blots of heat-treated cytoplasmic extracts used in this assay are shown in figure 3-24-B and 3-24-D. HL60 cytoplasmic extract had a slightly inhibiting effect (lane 1 to 3) whereas cytoplasm from Raji cells had a strongly inhibiting effect on DFF40 activity (lane 8 to 11). The inhibiting effect of the cytoplasmic extracts correlated well with the content of DFF45 in the corresponding sample (compare fig. 3-24). **Cyt:** Cytoplasmic extract. **DFF40*:** recombinant DFF40/DFF45 complex was preincubated (30 min, 37°C) with recombinant caspase-3 for activation. Note: All reactions initially contained 1 µg plasmid DNA (lane 15), DNA contents decreased only due to the activity of DFF40 in this assay.

In contrast to the effect of heat-inactivated cytoplasmic extracts, native extracts from HL60 cells and Raji cells had an opposite effect: Cytosols from HL60 cells activated DNA fragmentation by DFF40 whereas cytosol from Raji cells inhibited DFF40 activity. BSA is often used as a stabilising agent for nucleases (e.g. in restriction digest reactions), so BSA was used as a control for unspecific protein effects on DFF40.

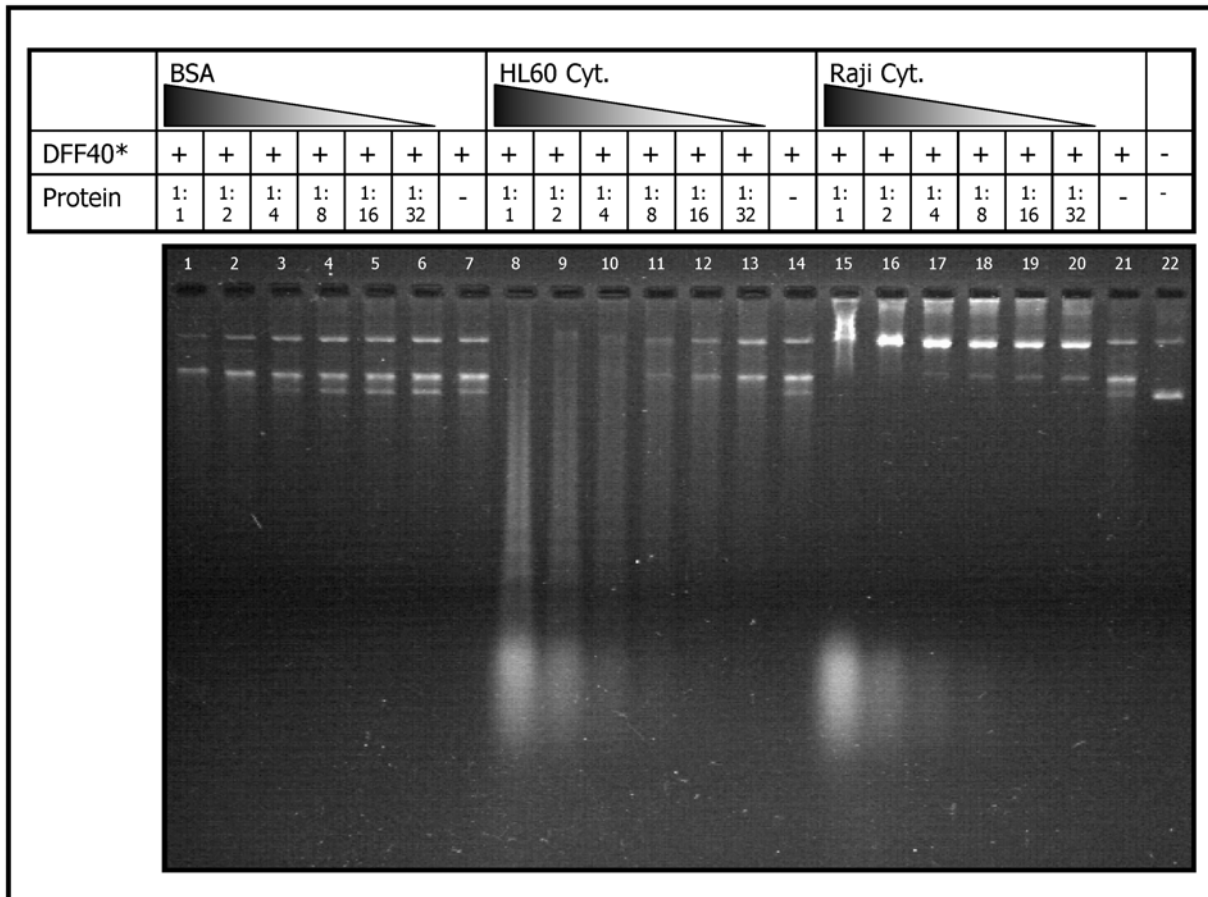


Figure 3-26: Plasmid assay with native cytoplasm from HL60 and Raji cells

The native cytoplasmic extracts used in this assay are shown in figure 3-24 A and C. HL60 cytoplasmic extract had a dose-dependent strongly activating effect (lane 8 to 13), whereas cytoplasm from Raji cells had a dose-dependent strongly inhibiting effect on DFF40 activity (lane 15 to 20). BSA, used as a control for the effect of an indifferent protein only had a slightly activating effect on DFF40 (lanes 1-7). The inhibiting effect of the Raji cytoplasmic extracts correlated well with the high amount of DFF45 in the samples. **Cyt**: Cytoplasmic extract, **DFF40***: Recombinant DFF40/DFF45 complex was preincubated (for 30 min at 37°C) with recombinant caspase-3 for activation.

A comparative western blot demonstrating the expression levels of caspase-3 and DFF45 in HL60 cells and Raji cells is shown in figure 3-27. Presumably, the activating effect of the native HL60 cytoplasmic extracts was not caused by an enhanced expression of caspase-3 in HL60 cells since similar amounts of this effector caspase, which activates DFF40 by cleaving the inhibitor DFF45, are expressed in HL60 cells and Raji cells. Though expression of DFF45 in Raji and HL60 cells was found to be considerably different, the expression of caspase-3 was at a comparable level. Therefore, it may be assumed that the same amount of caspase-3 may be ready to be activated from Raji and HL60 cytoplasm and the differential behaviour of both types of cytoplasm is more likely due to higher expression levels of DFF45 in Raji cells.

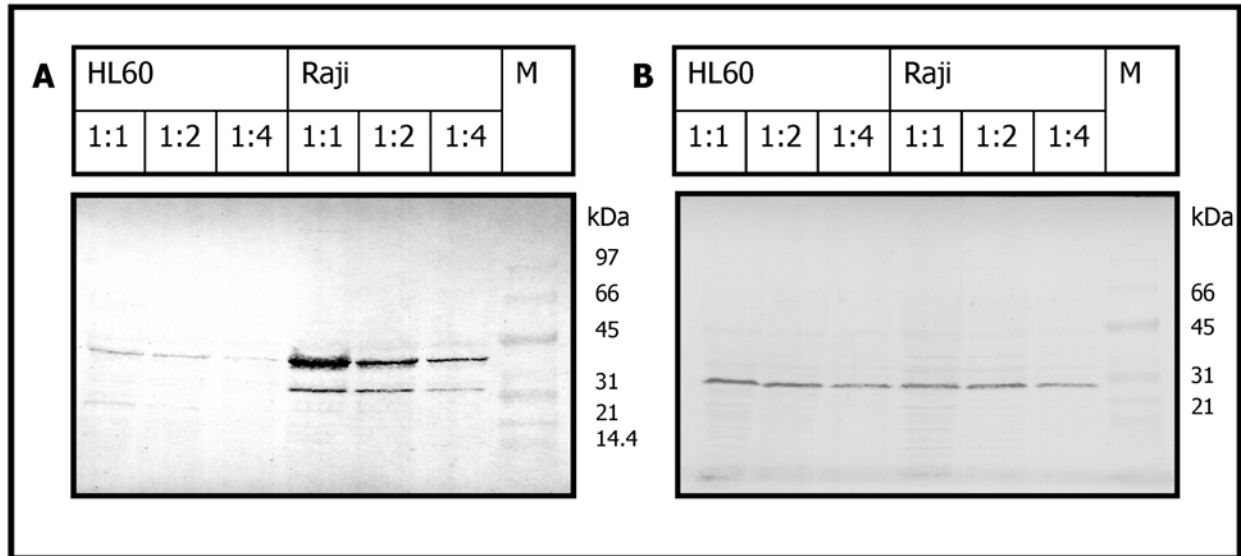


Figure 3-27: Expression levels of DFF45/DFF35 and caspase-3 in HL60 and Raji cells

Dilution series from cytoplasmic extracts of HL60 cells and Raji cells were subjected to SDS-PAGE and western blotting, applying 25, 12, and 6 μg protein in the respective lanes. **A:** Proteins on the blot were assayed for **DFF45** and **DFF35**. Expression of DFF45 (and DFF35) was much stronger in Raji cytoplasm than in HL60 cytoplasm. **B:** Proteins on the NC-membrane were assayed for **procaspase-3**. Comparable amounts of procaspase-3 were detected in HL60 cells and Raji cells. **Note:** The DFF45-antibody used in this study recognizes both DFF45 and DFF35, therefore, two bands were detected in cellular protein preparations.

3.2. SUMMARY: FACTORS INFLUENCING DFF40 ACTIVITY

Different subtypes and differently modified H1 histones were tested for their effects on the DNase activity of the apoptotic endonuclease DFF40 in an in vitro system with purified recombinant proteins and plasmid DNA. All H1 histone subtypes enhanced DFF40 activity on a plasmid substrate in a similar concentration range of 0.5 to 1.5 μg per μg of plasmid DNA. However, a comparatively larger activating range was found with the replacement histone H1^o which had an activating effect in a concentration range of 1.3 to 3.1 μg per μg plasmid DNA. Higher concentrations of H1 histones generally led to an inhibition of DFF40 activity on plasmid DNA.

Importantly, the enhancing effect on DFF40 activity seemed to be specific for H1 histones since it was not seen with the core histone H3 or BSA, whereas the inhibiting effect was found with core histone H3 as well. An inhibiting effect of H1 histones was seen with chromatin of purified nuclei as well when these were incubated with active DFF40 in the presence of additional H1 histone protein. Thus, inhibition may occur due to unspecific deposition of histones on DNA substrates in response to unphysiologically high H1 histone concentrations, e.g. in DNA from purified nuclei which was already packaged in nucleosomes.

Furthermore, the effect of H1 histones on DFF40 activity was not affected by *in vitro* phosphorylation of H1 histones and by posttranslational modifications on H1 histones occurring during apoptosis as demonstrated with *in vivo* modified H1 histones from untreated and apoptotic HL60 cells.

Extracted cellular proteins from different lymphoma cell lines were subsequently used to identify other factors which influence DFF40 activity *in vivo*. HL60 cells were chosen as a cell system containing optimal conditions for DFF40 activity since DNA fragmentation was generally detectable soon after induction of apoptosis in these cells. Raji cells were selected as a cell system containing inhibiting conditions for DFF40 activity since induction of apoptosis did not lead to nucleosomal DNA fragmentation in these cells. The factors responsible for this differential apoptotic DNA cleavage pattern in the different cell lines were found to be located in the cytoplasm rather than in the nuclei of the cells since digestion of purified nuclei from both Raji cells and HL60 cells with recombinant DFF40 generated DNA laddering. Indeed, the following experiments confirmed a cytoplasmic localization of the factors which are responsible for the different behaviour of the cells during apoptosis: Cytoplasm of HL60 cells had an activating effect on the activity of recombinant DFF40 on plasmid DNA whereas cytoplasm from Raji cells inhibited DFF40 activity on plasmid DNA. Furthermore, recombinant caspase-3 was able to induce a DFF40-like activity in HL60 cytoplasm but not in Raji cytoplasm which increased DFF40 activity on purified nuclei. Importantly, expression levels of endogenous caspase-3 did not differ significantly when comparing HL60 and Raji cells, and a similar amount of caspase-3 should be ready to be activated during apoptosis in both cell types. Hence, different expression levels of this crucial apoptotic executioner caspase are presumably not the reason for delayed progression of apoptosis in Raji cells. Since heat-treated cytosols from both cell types had an inhibiting effect on DFF40 activity, the protein responsible for this differential behaviour was supposed to be DFF45, the inhibitor of DFF40 since this heat-stable protein was still found in the supernatants of heat treated cytosol preparations. Furthermore, DFF45 was shown to be expressed in Raji cytoplasm at higher levels than in HL60 cytoplasm, and thus DFF45 may be the DNase-inhibiting factor which is completely cleaved by caspase-3 in HL60 cytoplasm but not in Raji cytoplasm for release of a DFF40-like activity during apoptosis. Thus, high amounts of DFF45 seemed to be correlated with less DFF40 activity *in vitro*.

3.3. DFF40 AS A PUTATIVE FACTOR PROMOTING APOPTOSIS

The results obtained in the first part of this work gave rise to a new working hypothesis: DFF40 may play a role in enhancing the apoptotic signal in the cellular signalling-cascade by causing DNA damages which in turn are additional signals for the cell to stop proliferation and to undergo apoptosis. Taken together, this may lead to a positive feed-back reaction enhancing apoptosis. On the other hand, expression levels of DFF45, the chaperone and inhibitor of DFF40, may alter the sensitivity of cells to apoptotic signals. High levels of DFF45 proteins were able to inhibit DFF40 activity under in vitro conditions, as concluded from the results obtained in the first part of this study.

The question now was whether altered levels of DFF40 or DFF45 in vivo affect the susceptibility of cells to undergo apoptosis. Raji cells were shown to express high levels of DFF45 and to undergo delayed cell death without internucleosomal DNA cleavage. In contrast, HL60 cells, which were shown to have comparatively lower DFF45 levels, readily undergo apoptosis with concomitant internucleosomal DNA cleavage. This supports a hypothesis in which the relative ratio between the protein levels of DFF40 and its inhibitor DFF45 may be at least one factor in determining the different readiness of these cells to undergo apoptosis since this ratio may determine the extent of apoptotic DNA damage. The extent of apoptotic DNA damage in turn may affect progression of apoptosis by generating additional pro-apoptotic signals.

3.3.1. CHARACTERIZATION OF APOPTOSIS IN DIFFERENT HUMAN CELL LINES

First steps in testing the hypothesis described above were a comparison of DFF40/DFF45 expression in HL60, Jurkat, and Raji cells, and a more detailed characterization of the apoptotic features of these cells. The spatial distribution of DFF40 and DFF45 in the cell might be important for performance of apoptosis as well since sequestering of pro- and anti-apoptotic proteins to different cellular compartments might exclude an interaction between activated proteins during apoptosis. So, the following experiments were conducted to define the cellular localization of several apoptotic actors. Total cell extracts, cytoplasm, and nuclei were prepared from different cell types as described in chapter 2.2.5.2. Proteins were subjected to SDS-PAGE followed by western blotting; finally, the blots were analyzed for the presence of DFF40 or DFF45, respectively. Furthermore, the cellular localization of the respective proteins was confirmed by immune fluorescence.

3.3.1.1. Expression and localization of DFF40 and DFF45

As shown in the following figure, all of the tested cell types expressed relatively low amounts of DFF40 (~30 µg proteins per lane were applied to the gel). Raji cells possessed noticeably more DFF45 than HL60 and Jurkat cells. A major part of both proteins, DFF40 and DFF45, was found in the nucleus in HL60 cells; this was in contrast to the distribution of these proteins seen in Jurkat and Raji cells. Both of the latter cell types showed a mostly cytoplasmic localization of DFF40 and DFF45. In Raji cells DFF40 expression was low in cytoplasm and it was even below the detection limit in nuclei; a mostly cytoplasmic localization of DFF40 was seen in Jurkat cells as well. An estimation of the respective DFF40 and DFF45 contents revealed an equal DFF45:DFF40 ratio in both HL60 and Jurkat cells (cells which easily undergo DNA laddering during apoptosis). Interestingly, the DFF40:DFF45 ratio was remarkably altered in Raji cells, suggesting that a comparatively higher amount of DFF45 is not bound to DFF40 in Raji cells. DFF35, an inhibitor but no chaperone of DFF35, was localized exclusively to the cytoplasm. It does not translocate to the nucleus since it lacks a nuclear localization signal due to alternative splicing (*Samejima and Earnshaw, 2000*).

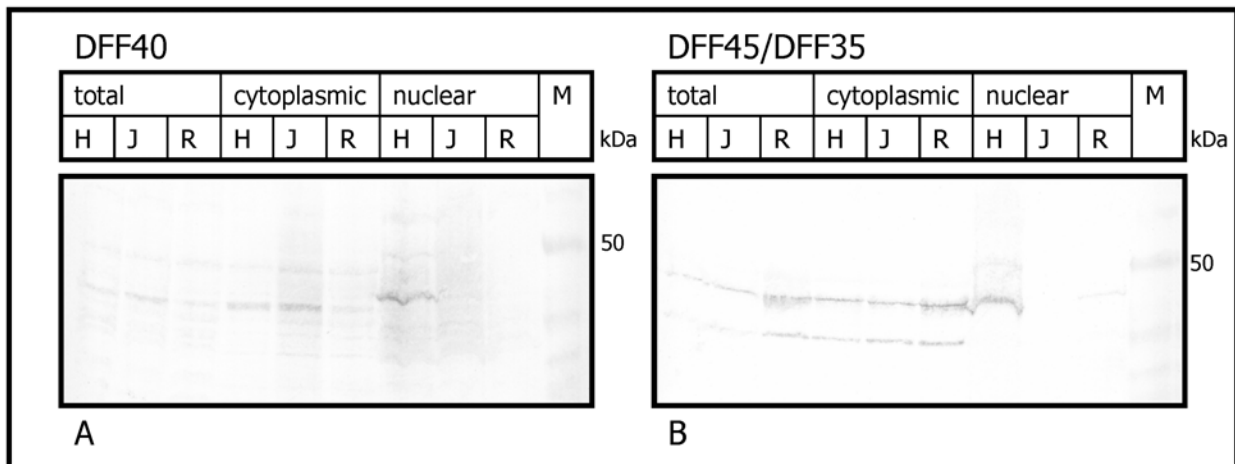


Figure 3-28: Expression and localization of DFF40 and DFF45 in different cell types

Total cell extracts, cytoplasm, and nuclei were prepared from HL60, Jurkat, and Raji cells as described in chapter 2.2.5.2. 30 µg of each protein preparation were subjected to SDS-PAGE followed by western blotting. **A:** Proteins on the blots were assayed for **DFF40**. **H:** HL60 cells, **J:** Jurkat cells, **R:** Raji cells, **M:** Seebue prestained protein standard. **B:** Blots assayed for **DFF45**. BCIP/NBT was used as a substrate for the alkaline-phosphate-coupled secondary antibody. **Note:** The DFF45 antibody used in this study recognizes both DFF45 and DFF35; therefore, up to two bands were detected in the samples.

Since HL60 cells showed a different distribution pattern of DFF40 and DFF45 in nucleus and cytosol compared with Raji cells, Jurkat cells were chosen as a more suitable cell system for the following experiments. The compartmental distribution of both proteins in Jurkat cells was similar to those in Raji cells, only the DFF40:DFF45 ratio varied

between Jurkat and Raji cells. Thus, the following experiments were carried out to characterize the features of both Raji and Jurkat cells during progression of apoptosis.

3.3.1.2. Different protein levels of proteins involved in apoptosis

As shown in figure 3-29 on the following page, Jurkat cells showed a typical DNA laddering which expectedly was lacking in Raji cells. A distinct DNA laddering was detectable in Jurkat cells 8 hours after having added Topotecan to the cells. After 24 hours both Jurkat and Raji cells showed a smeared DNA cleavage pattern which is typical for random cleavage of DNA, presumably catalyzed by other DNases than DFF40. This kind of DNA cleavage may indicate activation of other DNases than DFF40, which become active in dying cells only under cell culture conditions. Since *in vitro* cultured cells are not removed by surrounding cells, which is the most important feature of apoptosis *in vivo*, these surplus cells often undergo secondary necrosis. Therefore, other enzymes are activated in the later course of the dying process in cultured cells. Interestingly, DFF40 contents decreased during apoptosis in Jurkat cells, this may have resulted from secondary necrosis as well. However, DFF40 was still present during nucleosomal DNA fragmentation in Jurkat cells. In contrast to Jurkat cells, DFF40 was present at a rather low level in Raji cells, hardly detectable in this experiment.

The nuclear enzyme poly (ADP ribose) polymerase (PARP) is cleaved during both apoptosis and necrosis. However, apoptotic cleavage of PARP is catalyzed by apoptotic downstream caspases (e.g. caspase-3) and results in distinct fragment sizes specific for apoptosis. Intact PARP has a molecular weight of 119 kDa. Apoptotic cleavage of PARP by caspases generates two fragments by separating its DNA binding domain (~ 20 kDa) from the catalytic domain (~ 89kDa). In figure 3-2 only the resulting 89 kDa fragment is demonstrated. Apoptotic PARP cleavage was seen in both Jurkat and Raji cells. However, PARP cleavage in Raji cells was incomplete even 56 hours after induction of apoptosis whereas Jurkat cells showed a complete cleavage of PARP after 24 hours. This may have occurred due to lower caspase-3 activities; therefore, the levels of procaspase-3 were subsequently analyzed.

Procaspase-3 was detected in both Jurkat and Raji cells, though it was detectable at a lower level in Raji cells. Protein levels of procaspase-3 and DFF45 expectedly decreased in Jurkat cells in parallel with DNA fragmentation and PARP cleavage, indicating activation of caspase-3 by cleaving the precursor procaspase-3 (active, cleaved caspase-3 itself was not detected by the antibody used in this experiment). In contrast to Jurkat cells, cleavage of both procaspase-3 and DFF45 was incomplete in Raji cells. This suggests that activation of caspase-3 was less effective in Raji cells compared with Jurkat cells, which presumably led to lower caspase-3 activities in Raji cells.

Additionally, intact DFF45 was still present in late apoptosis in Raji cells which still may have interfered with DFF40 activity, leading to the suppression of its DNase activity. Taken together, the results showed a weak performance of apoptosis in Raji cells compared with Jurkat cells. This relatively weak performance of apoptosis prolonged survival of Raji cells but did not save all cells from being ultimately killed, as demonstrated by the DNA damage and the decreasing protein contents in the samples (compare the Ponceau-stained blots in figure 3-29).

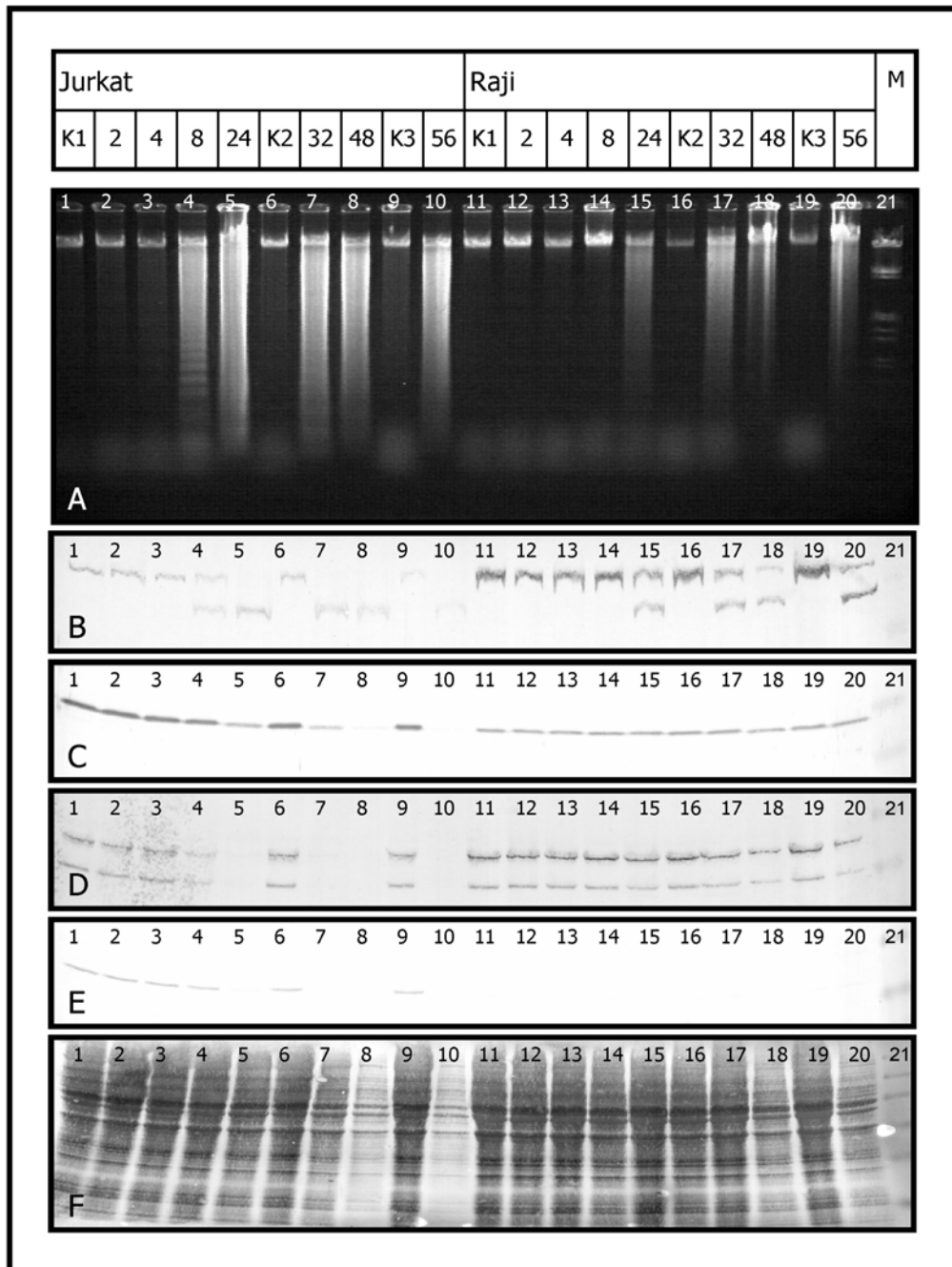


Figure 3-29: DNA fragmentation and concomitant changes in protein levels during apoptosis

Figure 3-29: Jurkat and Raji cells were induced to undergo apoptosis by adding 150 ng/ml Topotecan. Cells were harvested at the times indicated above in [h], **K1:** 0h control, **K2:** 24h control, **K3:** 48h control. **A:** Fragmented DNA visualized by UV illumination after agarose gel electrophoresis and staining with ethidium bromide. **B:** Proteins on the NC-membrane were detected with an antibody recognizing both cleaved and uncleaved **PARP**. **C:** Immunostaining for **procaspase-3**. **D:** Immunostaining for **DFF45/DFF35**. **E:** Immunostaining for **DFF40**. **F:** Ponceau-staining of total proteins in the cell lysates. Protein amounts corresponding to 1×10^7 cells were subjected to SDS-PAGE and western blotting. **M:** Marker for DNA samples: λ -DNA cut by Eco RI and HindIII, Marker for protein samples: See blue prestained protein standard. Untreated cells were used as controls.

3.3.1.3. Morphology of Jurkat and Raji cells during apoptosis

Laser scanning microscopy (LSM) was carried out to check for a similar compartmental distribution of caspase-3 and DFF45/DFF35 in Raji and Jurkat cells. Detection with an antibody recognizing the nuclear protein histone deacetylase-1 (HDAC-1) was conducted as a control for the detection of a protein which is localized in the nucleus.

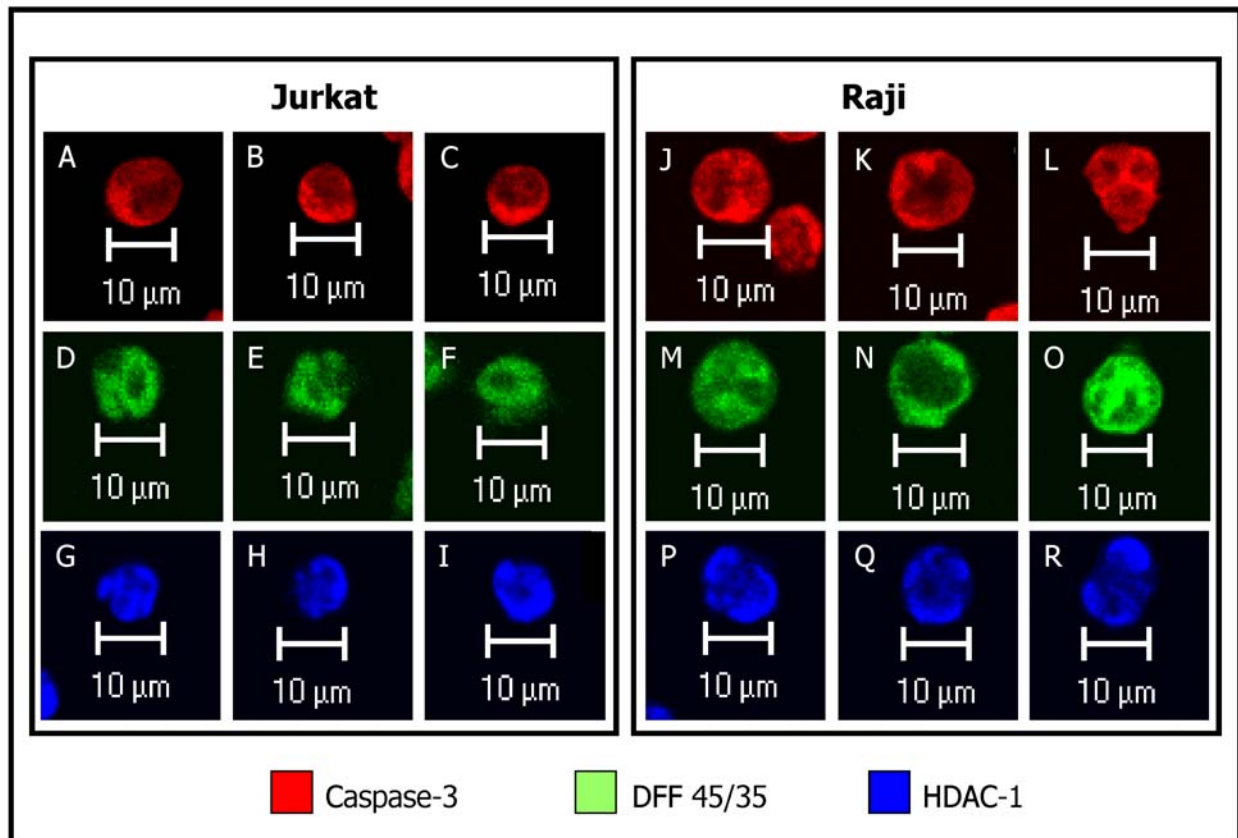


Figure 3-30: Localization of caspase-3, DFF45/DFF35, and HDAC-1 in Jurkat and Raji cells

Cells were fixed with PFA and subsequently immuno-stained for caspase-3, DFF45/DFF35, and HDAC-1, respectively, as described in chapter 2.2.5.6.4. Immuno-detection was carried out using a secondary antibody coupled to CY-3, which was detected by an argon laser during LSM. Respective colours seen in this figure do not correspond to the fluorescent colour of the dye CY-3 but were generated digitally by the software used for analysis by LSM. **Note:** Figure A to R show different random sampled cells.

As already concluded from western blotting experiments, LSM confirmed that caspase-3 was localized mainly in the cytoplasm of non-apoptotic cells. Only a small portion of caspase-3 was found in nuclei from both Jurkat (A,B,C in fig. 3-30) and Raji cells (J,K,L in fig. 3-30). In contrast to the localization of caspase-3, both DFF45/DFF35 and HDAC-1, were localized mainly in the nuclei of both cell types (fig. 3-30 D,E,F, and M,O). However, DFF45/DFF35 seemed to be exceptionally localized to the cytoplasm in a few Raji cells (N in fig. 3-30). As expected, HDAC-1 was localized in the nuclei of both Jurkat and Raji cells (fig. 3-30 G,H,I, and P,Q,R).

The cytoplasmic localization of caspase-3 was confirmed to occur all over the cell's diameter by taking a LSM series of scans corresponding to slices of 0.2 μm through one cell as depicted in the following representative figure (3-31).

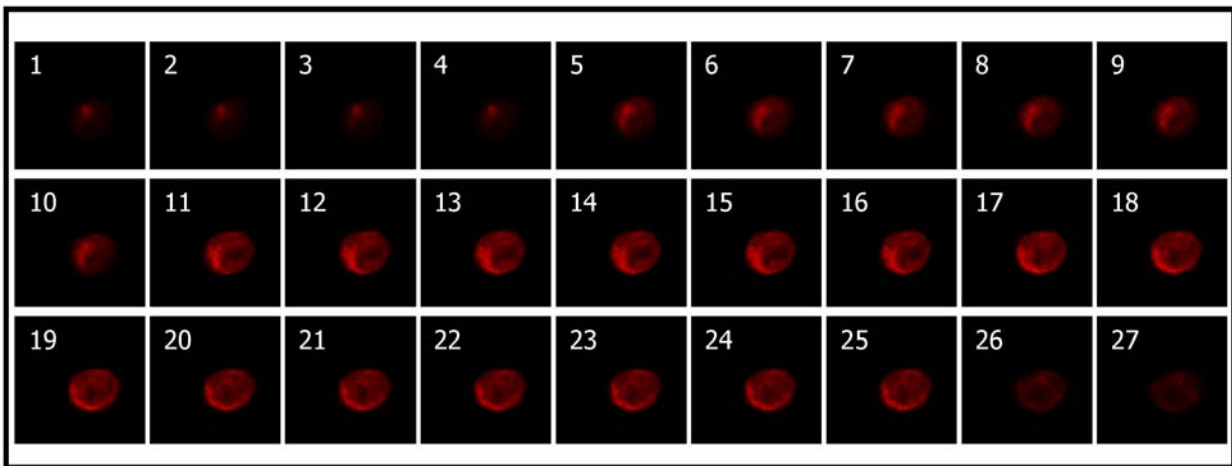


Figure 3-31: LSM series demonstrating a mostly cytoplasmic localization of caspase-3

Jurkat cells were fixed with PFA and subsequently immuno-stained for detection of caspase-3 as described in chapter 2.2.5.6.4. Immuno-detection was carried out using a secondary antibody coupled to CY-3, which was detected by an argon laser. A series of digital sections, 0.2 μm thick, was recorded for this figure. Red colour seen in this figure does not correspond to the colour of the fluorescence of CY-3 but were generated digitally by the software used with the laser scanning microscope.

As shown in figure 3-32, apoptotic Jurkat cells showed a typical chromatin condensation in the course of apoptosis which in contrast could not be detected in most Raji cells. Analysis of alterations in the cell sizes by using a Casy cell counter allowed an estimation of the viability in the cell population. Particles less than 7.5 μm in diameter are resulting from cellular debris and were therefore excluded from counting. Viable Jurkat cells are $\sim 15 \mu\text{m}$ in diameter whereas viable Raji cells are $\sim 12 \mu\text{m}$ in size, the latter showing a typical distribution balanced to the left of the median. 24 hours after having added Topotecan to the cells, the balance was shifted to the left side of the median in both Raji and Jurkat cell populations. Dying and dead cells resulted in an increase of the part of population ranking between 7.5 and 10 μm in diameter in both

Jurkat and Raji cell populations, and debris contents (less than 7.5 μm in diameter) increased markedly. Concomitantly, the amount of viable cells decreased markedly in both cell populations. A comparison of the microscopic features and the histograms obtained after counting the cell population in the Casy cell counter is shown in figure 3-32.

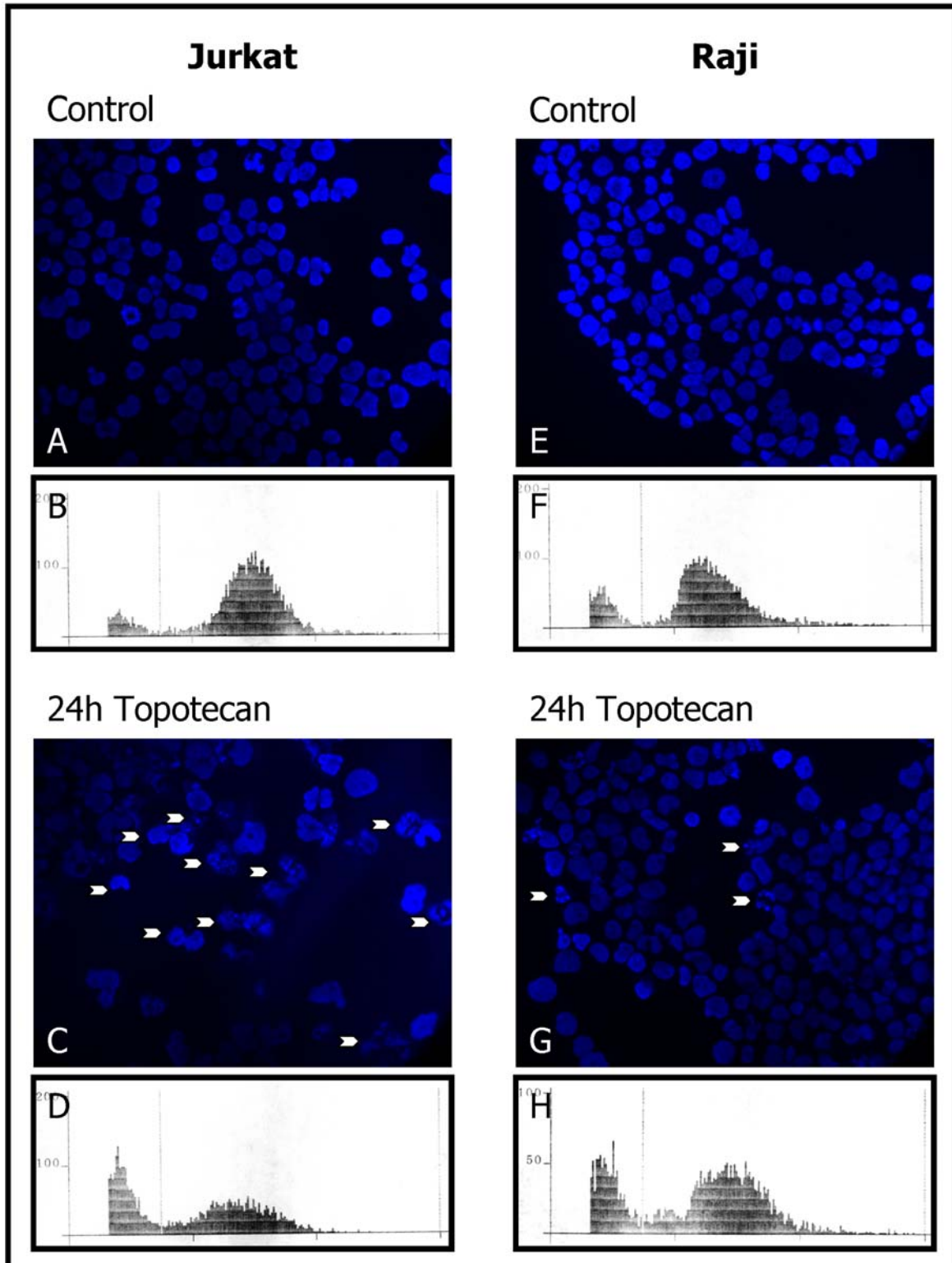


Figure 3-32: Morphologic features of Jurkat and Raji cells during apoptosis

This figure legend refers to fig. 3-32 on the previous page

Cells were induced to undergo apoptosis by adding 150 ng/ml Topotecan to the media. Untreated cells or apoptotic cells were stained with the dye Hoechst 33342 and photographed using a fluorescence microscope (enl. 400x; fig. A, C, E, G) or counted in a Casy cell counter (0-30 μm diameter; fig. B, D, F, H). White arrows: Nuclear fragments of apoptotic cells.

Additional informations about the cells health status can be obtained by using a combination of fluorescence and phase contrast microscopy. This allowed a simultaneous observation of changes in both cell shape and chromatin compaction during apoptosis. These features varied considerably between Jurkat and Raji cells and confirmed a delay in apoptosis in Raji as demonstrated in the following figures.

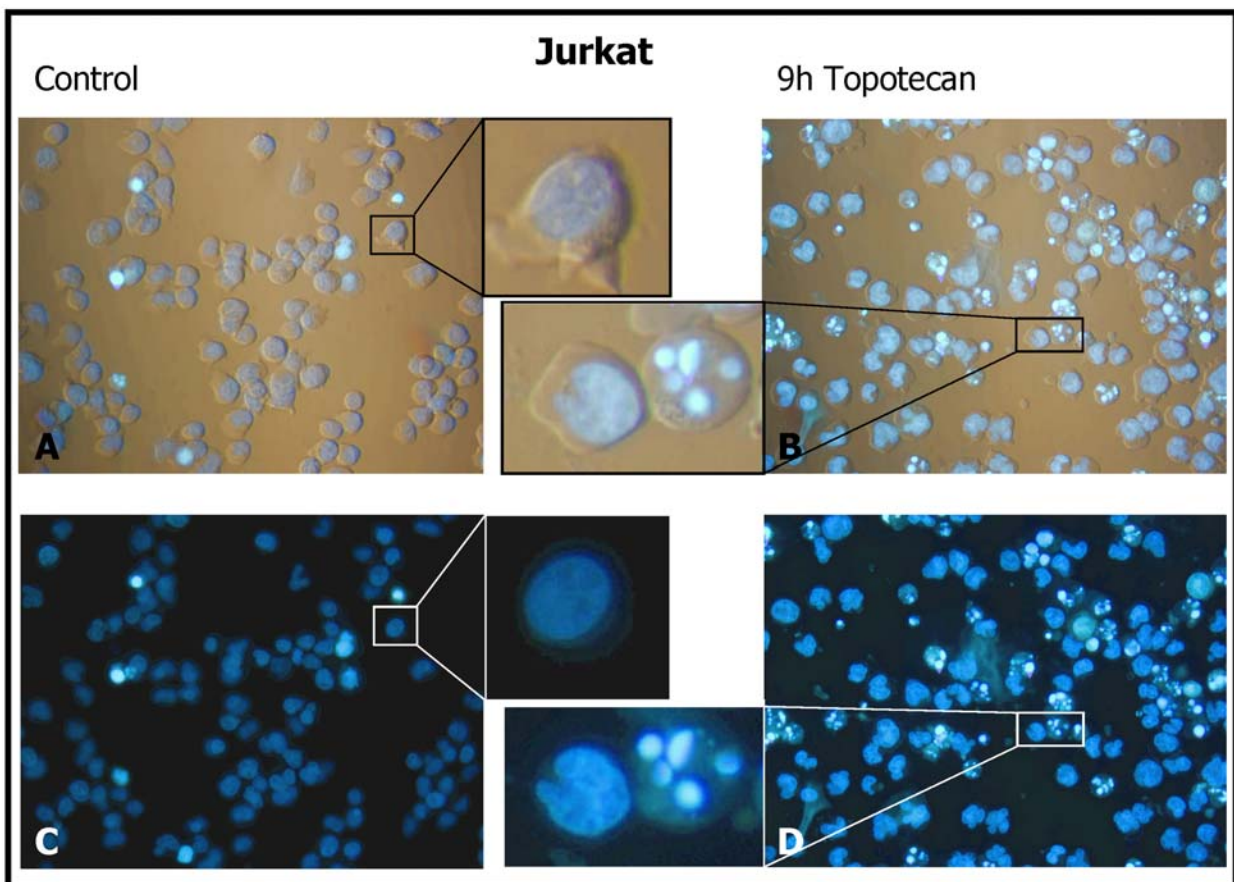


Figure 3-33: Phase contrast microscopy and Hoechst 33342 staining of Jurkat cells

Chromatin from untreated and apoptotic Jurkat cells (treated for 9h with 150 ng/ml Topotecan) was stained by using Hoechst 33342 and visualized by Fluorescence microscopy alone (**C** and **D**) or by using a combination of fluorescence and phase contrast microscopy (**A** and **B**). Magnification was 400x. A prevailing part of the cells showed apoptotic chromatin condensation and nuclear fragmentation after 9 h of treatment with Topotecan; the cells lost their typical branches too (compare enlargements of fig. A and fig. B). Note: Several markedly brighter stained cells are dead cells which lost membrane integrity and thus are stained more intensive by the dye Hoechst 33342, intensive staining in these cases was not caused by chromatin condensation (see fig. A and C) .

Whereas Jurkat cells showed characteristic chromatin condensation and nuclear fragmentation in the first 9 hours of treatment with Topotecan, this feature was lacking in Raji cells after 9 hours of treatment with Topotecan as demonstrated in figure 3-34.

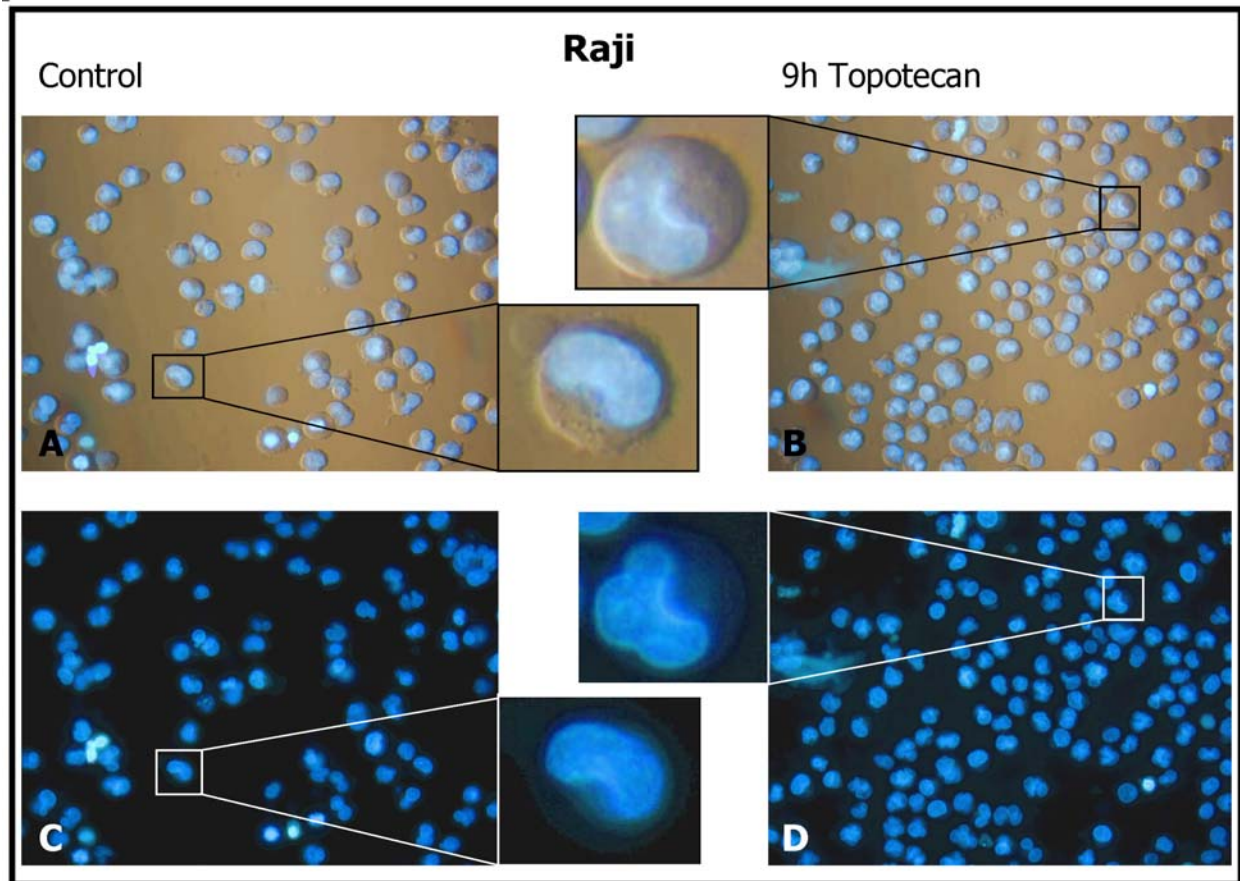


Figure 3-34: Phase contrast microscopy and Hoechst 33342 staining of Raji cells

Untreated and apoptotic Raji cells (treated for 9h with 150 ng/ml Topotecan) were stained by using Hoechst 33342 and visualized by fluorescence microscopy alone (**C** and **D**) or by using a combination of fluorescence and phase contrast microscopy (**A** and **B**). Magnification was 400x. Neither apoptotic chromatin condensation nor nuclear fragmentation was seen in Raji cells after 9 h of treatment with Topotecan. In contrast to Jurkat cells, morphology of Raji cells was mostly unaffected at this time of apoptosis (compare enlargements of fig. A and fig. B). Note: Several markedly brighter stained cells are dead cells which lost membrane integrity and thus are stained more intensively by the dye Hoechst 33342, intensive staining was not caused by chromatin condensation in these cases (compare fig 3-33 A and C).

3.3.1.4. Summary: Apoptotic features of Jurkat and Raji cells

Comparing the apoptotic features of Raji and Jurkat cells it seemed obvious that, apart from lacking DNA fragmentation in Raji cells, progression of apoptosis in Raji cell populations seemed to be delayed. This delay may be caused by less intensive caspase-like enzyme activities in these cells. Cleavage of procaspase-3 and concomitant cleavage of PARP and DFF45 occurred later and less intensively in the course of

apoptosis in Raji cells compared with Jurkat cells. Moreover, the cleavage of caspase-3 substrates was incomplete in Raji cells even 56 hours after induction of apoptosis. In Jurkat cells cleavage of caspase-3 was even enhanced as soon as DNA laddering occurred. This correlation between caspase-3 activity, DNA damage, and progression kinetics of apoptosis may support the hypothesis of a positive feedback mechanism induced by these DNA damages. Lacking DNA damage in Raji cells may therefore contribute to insufficient caspase activation since additional early DNA damage does not occur in the course of apoptosis in Raji cells.

Detectable differences furthermore occurred in the protein levels of caspase-3 and PARP, and the most obvious differences were found in the expression levels of DFF40 and DFF45. Raji cells showed an insufficient activation of procaspase-3 and incomplete cleavage of DFF45, an important caspase-3 substrate. This was not caused by a unfavourable localization of the effector-caspase caspase-3 or DFF45 in the cell since intracellular localization of caspase-3 and DFF45 in Raji cells did not differ significantly from the compartmental distribution of these proteins in Jurkat cells. Taken together, progression of apoptosis seemed to be delayed in Raji cells due to less caspase activity compared with Jurkat cells. Additionally, DFF40 activity seemed to be correlated with subsequent enhanced caspase-3 activity in Jurkat cells. Though protein expression levels of caspase-3 were lower in Raji cells than in Jurkat cells, this is presumably not the decisive factor for lower caspase-3 activities in Raji cells since HL60 cells, showing a caspase-3 expression level similar to that of Raji cells, readily undergo apoptosis and DNA fragmentation upon treatment with Topotecan. Since DNA damage can trigger apoptosis in many cell types, the question arose whether enhancing the activity of DFF40 in Raji cells, leading to more intensive DNA damages in the cell during apoptosis, would be sufficient to improve the performance of apoptosis in these cells by inducing enhanced caspase-activities. Stable transfection of both Raji and Jurkat cells, aiming at an enhanced expression of DFF40 in these cells, was chosen as a tool to test this hypothesis *in vivo*. Since an inhibiting effect of DFF45, the inhibitor of DFF40, may suppress DNA fragmentation in Raji cells as well, additional stable over-expression of DFF45 in both cell types was chosen to test the hypothesis that high cellular levels of DFF45 may act as an anti-apoptotic factor *in vivo*. If this assumption was correct, over-expression of DFF45 was supposed to cause enhanced resistance to apoptosis and lower levels of caspase-3 activities in these cells.

3.3.2. STABLE TRANSFECTION

Stable transfection of human cells was carried out using the vector pcDNA6 myc-his A (see chapter 2.1.13.3) supplied by Invitrogen. Raji and Jurkat cells were transfected in different experiments with a vector containing an insert with the DFF40 sequence or DFF45 sequence, respectively. Selection for stably transfected cells is possible by using Blasticidin as a selection agent since the vector confers resistance to this antibiotic. Blasticidin is quite a toxic substance, so non-transfected cells die faster than they do when using antibiotics similar to Neomycin. As a control for the following experiments, cells were 'mock'-transfected with an empty vector which confers resistance to the selection marker Blasticidin without expression of another recombinant protein driven by the CMV-promotor .

In some cell lines selection of stably transfected cells takes only one week. Nevertheless, establishing of a killing curve is necessary to determine the concentration of Blasticidin which reliably eliminates non-transfected cells.

3.3.2.1. Establishing a Blasticidin killing curve

Before cells can be selected for stable transfectants, the required concentration of the antibiotic should be determined in advance by establishing a killing curve for the cell line to be transfected. For this purpose, non-transfected cells were incubated with varied concentrations of the antibiotic used later for selection and cell growth was monitored e.g. by determining the increases of cell numbers in a defined time. A convenient and fast way to determine the cell numbers in large sets of samples is supplied by using the cell counter CASY. To establish a killing curve, cells were counted at day 3, day 6, and day 10 after administration of Blasticidin. If necessary, the cell cultures were splitted during this time to avoid cell death by unfavourable culture conditions. An example for a killing curve is shown in figure 3-35.

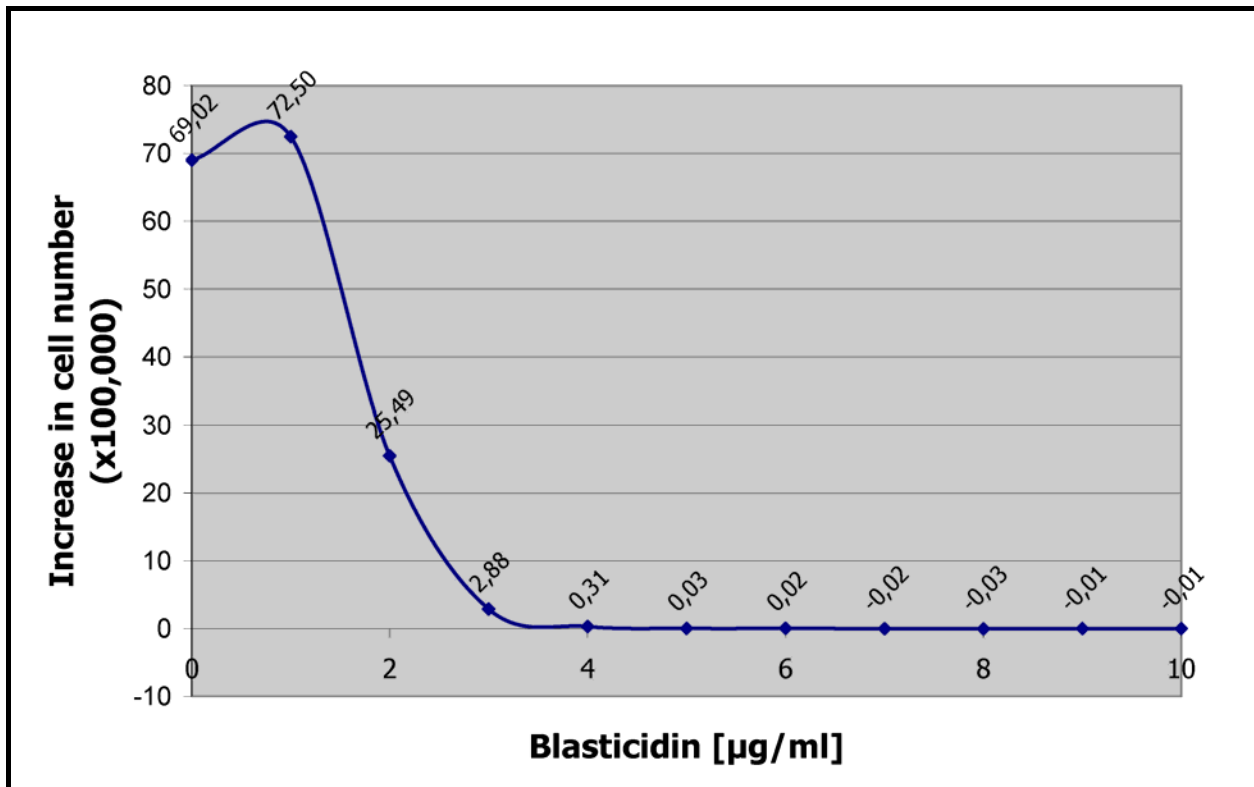


Figure 3-35: Example for a killing curve using Blasticidin on non-transfected Raji cells

Raji cells were incubated at standard culture conditions for 10 days with varying amounts of Blasticidin as indicated in the figure. Cell numbers were determined at day 6 and day 10 after addition of Blasticidin. Increase of cell numbers in the respective cultures was calculated by subtracting the values of day 6 from the respective values of day 10. Blasticidin concentrations were considered to be sufficient to kill all non-transfected cells when no more cell growth was recorded in the culture, this partly resulted in 'negative increase'-values as the cell number decreased. In a non-transfected culture 7 µg Blasticidin per ml medium were sufficient to kill all Raji cells (the concentration used later during selection of stable Raji-transfectants was 10 µg/ml).

3.3.2.2. Monitoring of cell growth during selection after stable transfection

Growth of transfected cells during selection with Blasticidin was initially retarded and a large amount of cells in the cultures died. This cell death was detectable by comparing the differing cell sizes occurring in the population. Dead cells appeared smaller in size than living cells and therefore caused a shift to the left in the population which was visible in the histograms of the cell sizes within 18 days ('day 18' in fig. 3-36). Growing cells were visible in the histograms as an increasing population at the positions corresponding to cell sizes expectable for viable cells. Generally, mock-transfected cells recovered faster than cells transfected with vectors which allowed expression of recombinant proteins. As expected, no cell growth was detectable under selective conditions in non-transfected cultures ('control' in fig. 3-36). The respective Casy histograms for differentially transfected Raji cells are shown in figure 3-36.

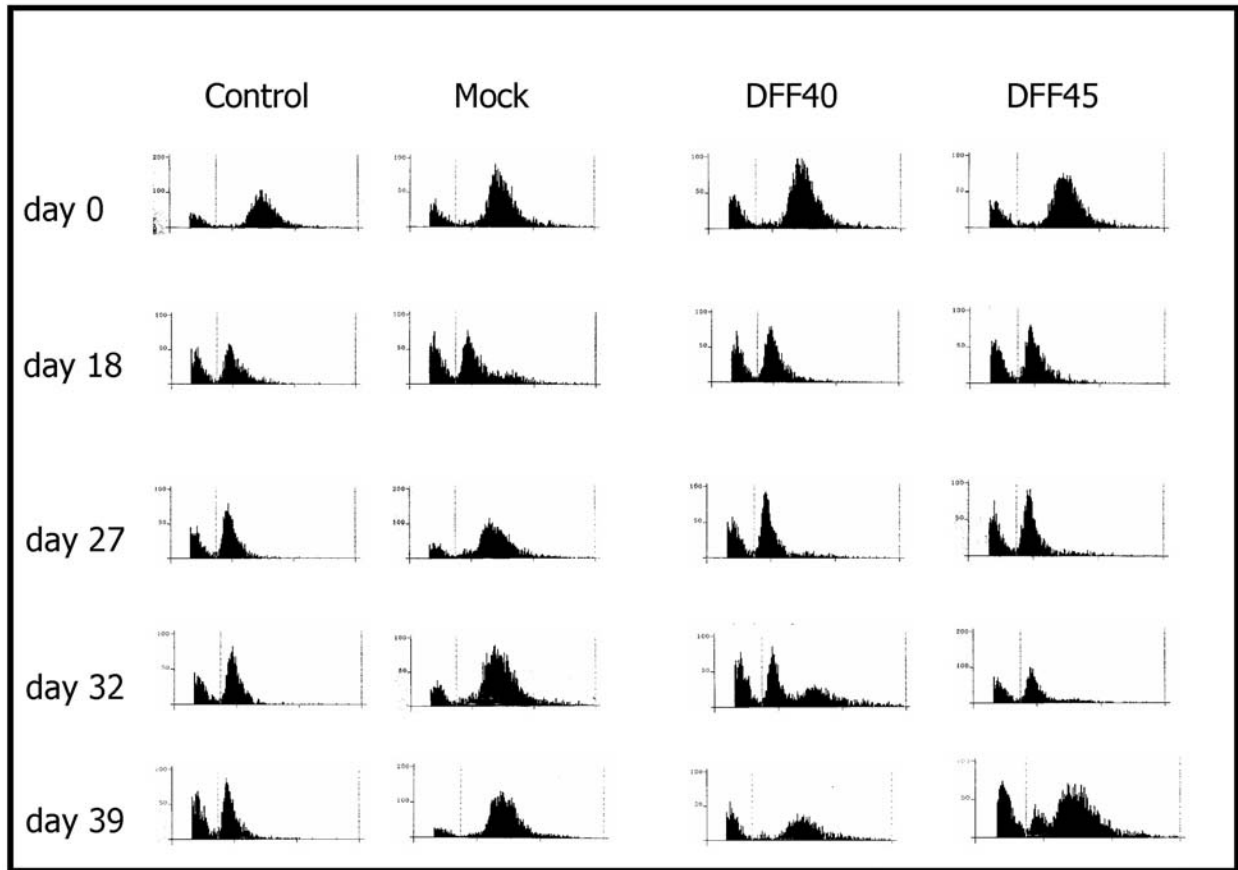


Figure 3-36: Growth of Raji cells during selection using 10 µg/ml Blasticidin

Raji cells were transfected using the Effectene-Kit (Qiagen) and kept under selective culture conditions starting 48 hours after transfection. Control cells received no vector, mock-transfected cells were transfected with empty vector, and the other cells were transfected with vector containing the genetic information for DFF40 or DFF45. The histograms, representing the sizes of the cells in the populations, were recorded at the indicated times using a Casy cell counter. Surviving, stably transfected cells were only detected in cells transfected with a vector conferring Blasticidin resistance. Control cells ('transfected' with H₂O instead of vector DNA) did not survive the selective conditions.

As demonstrated in fig 3-36, surviving cells were clearly detectable at day 27 in mock-transfected cells, at day 32 in DFF40-transfected cells, and at day 39 in DFF45-transfected cells. H₂O-'transfected' cells did not survive Blasticidin selection.

The same procedure of transfection and selection was subsequently conducted with Jurkat cells. Since the results obtained for the killing curve and for the histograms during selection with Blasticidin were very similar to those obtained for Raji cells, a presentation of the respective figures is omitted here.

3.3.3. EXPERIMENTS WITH TRANSFECTED RAJI CELLS

3.3.3.1. Detection of the tagged recombinant proteins

Recombinant DFF40 and DFF45 both carried a myc-epitope and a 6xhis-tag when these proteins were expressed from the vector pcDNA6 myc-his A. Therefore, the recombinant proteins were specifically detectable in cell lysates from transfected cells by an antibody recognizing the myc-epitope as shown in figure 3-37. The recombinant proteins DFF40 and DFF45 were detectable in the respective transfected cells due to their differential electrophoretic mobility during SDS-PAGE which resulted in bands differing in heights after immuno-detection on western blots using an anti-myc-antibody. No bands at the corresponding heights were visible in cell lysates from non-transfected or mock-transfected cells.

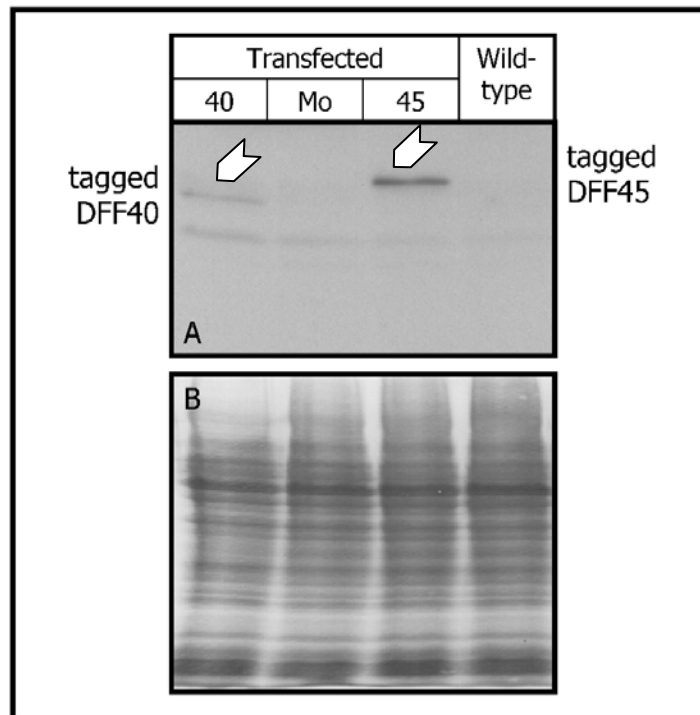


Figure 3-37: Detection of recombinant myc-tagged proteins in stably transfected Raji cells

A: Cell lysates from differently transfected Raji cell types were subjected to western blotting and analyzed for presence of the myc-epitope in the recombinant proteins. The blot was detected by using a primary anti-myc-antibody and a secondary antibody coupled to horseradish peroxidase. Blots were analyzed by ECL and subsequent exposure of a film to visualize the bands. **B:** Equal protein transfer was confirmed by Ponceau-staining of the membrane. **Note:** Unspecific staining with the anti-myc-antibody (lower bands), was seen in all lanes. The upper bands (marked with white arrowheads) correspond to the respective myc-tagged protein. **Note:** Subsequent westernblots for control of the expression of recombinant proteins were assayed with another antibody, respectively, since detection of the myc-tag did not allow a discrimination between recombinant proteins and the respective endogenous protein.

3.3.3.2. Morphological changes of transfected Raji cells

As shown in the following three figures, transfection with DFF40 led to morphological changes in apoptotic Raji cells which were comparable to those observed in Jurkat cells (fig. 3-33), whereas mock-transfected and DFF45-transfected Raji cells had similar apoptotic morphologies as already observed in non-transfected Raji cells (fig 3-34). However, chromatin condensation and nuclear fragmentation in apoptotic DFF40-transfected Raji cells was still less distinct than observed in Jurkat cells (compare chapter 3.3.1.3).

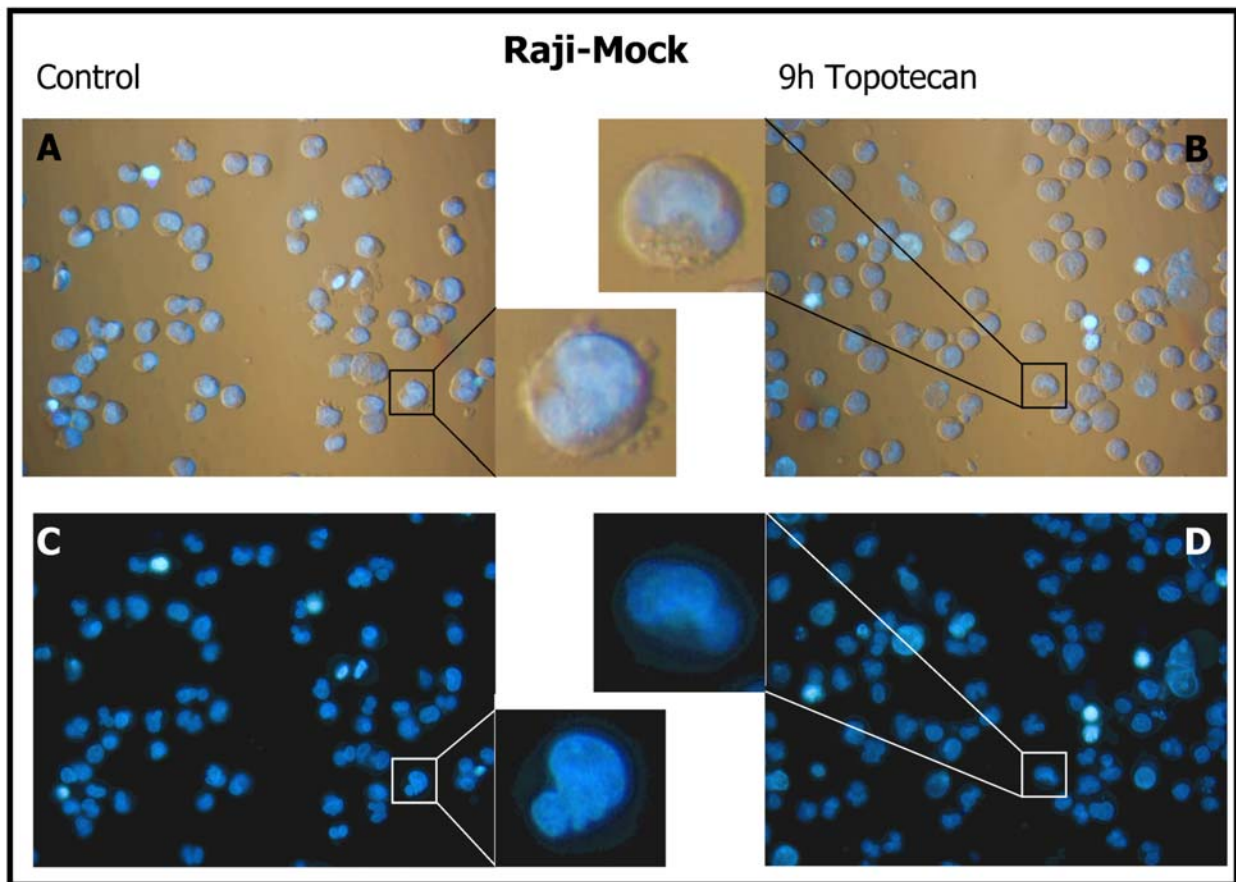


Figure 3-38: Apoptotic morphology of mock-transfected Raji cells

Untreated and apoptotic Raji cells (treated for 9 hours with 150 ng/ml Topotecan) were stained by using Hoechst 33342 and visualized by fluorescence microscopy alone (**C** and **D**) or by using a combination of fluorescence and phase contrast microscopy (**A** and **B**). Magnification was 400x. Neither apoptotic chromatin condensation nor nuclear fragmentation was seen in mock-transfected Raji cells after 9 hours of treatment with Topotecan. **Note:** Several markedly brighter stained cells are dead cells which lost membrane integrity and thus are stained more intensive by the dye Hoechst 33342; intensive staining in these cases was not caused by chromatin condensation (compare fig. 3-33 A and C)

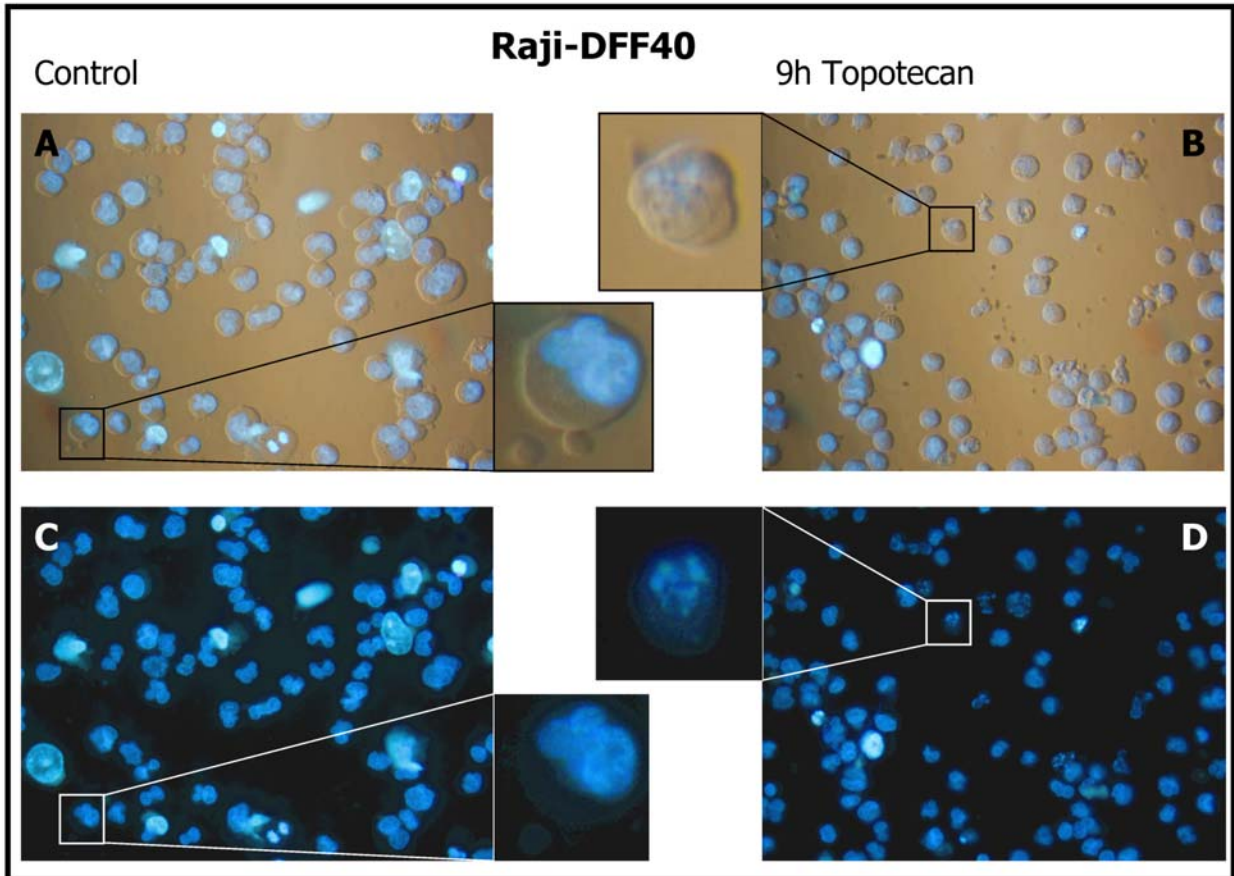


Figure 3-39: Apoptotic morphology of DFF40-transfected Raji cells

Untreated and apoptotic Raji cells (treated for 9 hours with 150 ng/ml Topotecan) were stained by using Hoechst 33342 and visualized by fluorescence microscopy alone (**C** and **D**) or by using a combination of fluorescence and phase contrast microscopy (**A** and **B**). Magnification was 400x. Weak apoptotic chromatin condensation and nuclear fragmentation was seen in DFF40-transfected Raji cells after 9 hours of treatment with Topotecan. Note: Several markedly brighter stained cells are dead cells which lost membrane integrity and thus are stained more intensive by the dye Hoechst 33342, intensive staining in these cases was not caused by chromatin condensation (compare fig. 3-33 A and C)

There were slight changes in the morphology of DFF40-transfected Raji cells, which may be due to the activity of recombinant DFF40 on chromatin in these cells.

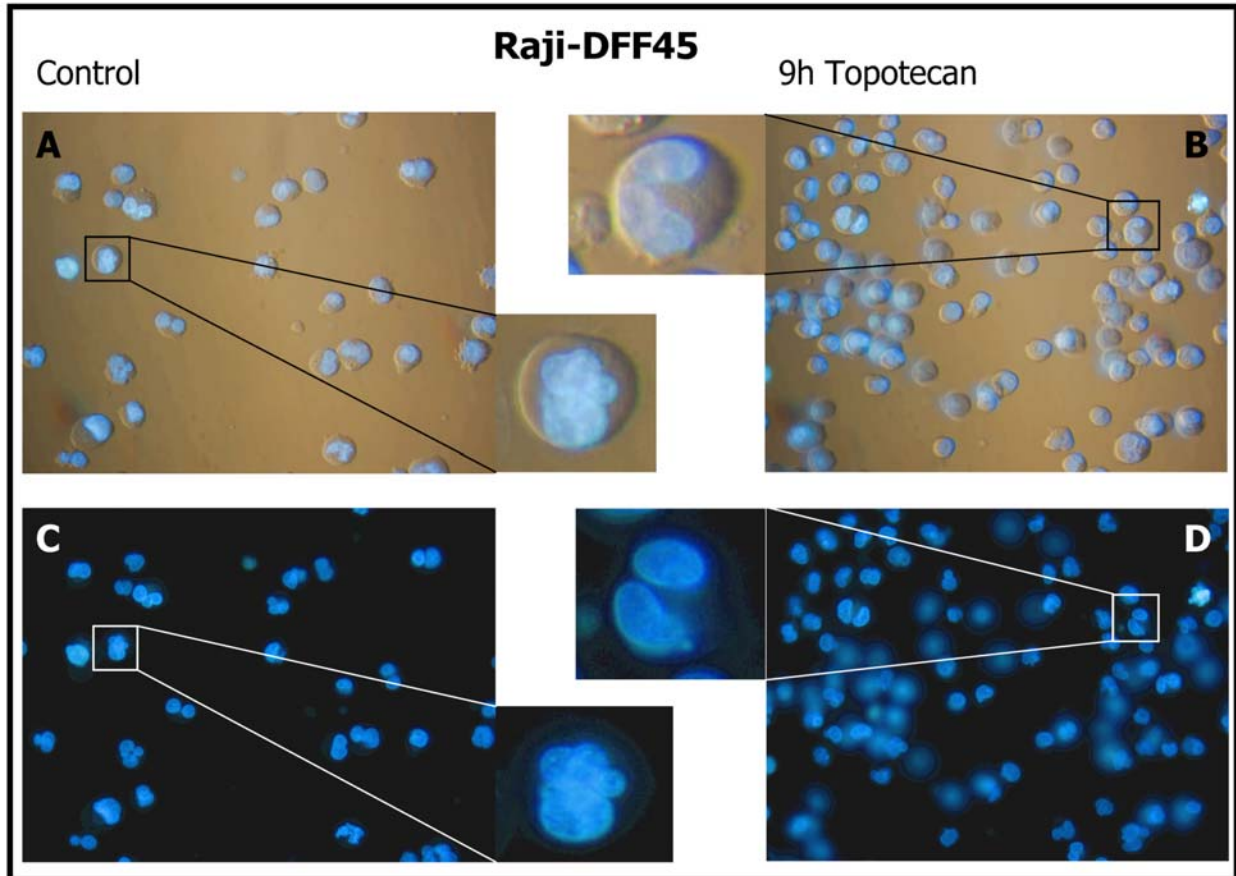


Figure 3-40: Apoptotic morphology of DFF45-transfected Raji cells

Untreated and apoptotic Raji cells (treated for 9 hours with 150 ng/ml Topotecan) were stained by using Hoechst 33342 and visualized by fluorescence microscopy alone (**C** and **D**) or by using a combination of fluorescence and phase contrast microscopy (**A** and **B**). Magnification was 400x. Neither apoptotic chromatin condensation nor nuclear fragmentation was seen in DFF45-transfected Raji cells after 9 hours of treatment with Topotecan.

3.3.3.3. Changes in protein levels during apoptosis in Raji cells

Transfected cells, expressing the recombinant proteins, and mock-transfected cells, transfected with the empty vector, were subsequently used for experiments which were designed to check for changes in the apoptotic features of the respective cells. Mock-transfected cells were included in the experimental design to evaluate a possible influence of the vector or of the selection process on the apoptotic features of the cells. Topotecan was used to induce apoptosis, and changes in the protein levels of DFF40 and DFF45 as well as in the extent of DNA fragmentation were analyzed. Since apoptosis is a process which depends on caspase activity, the extent of PARP-cleavage was monitored by using an antibody able to recognize both uncleaved PARP and cleaved PARP. The extent of PARP cleavage depends on the activity of effector caspases, mainly caspase-3. Therefore, the activity of caspase-3 is related to the extent of PARP cleavage; this was visualized in western blots.

Figure 3-41 demonstrates a less intensive PARP-cleavage in cells expressing recombinant DFF45 compared with those transfected for the expression of recombinant DFF40 or to those transfected with the empty vector.

Expression of the recombinant proteins can be distinguished easily from endogenous proteins since the 6xhis-tag and the myc-epitope present in the recombinant proteins caused a slightly higher molecular weight of the respective protein. This additional recombinant protein with a higher molecular weight led to the formation of an additional second band in western blots above the band of the respective endogenous protein. Unfortunately, there were endogenous proteins which migrated to similar positions in the gel and cross-reacted with the respective antibody. Nevertheless, the additionally expressed recombinant proteins were distinctly demonstrated since exactly these bands disappeared in western blots of proteins from cells which down-regulated expression of the respective protein during subsequent culturing (data not shown).

Expression of total DFF40 was considerably higher in the DFF40-transfected cells compared with both mock-transfected and DFF45-transfected cells. Obviously, DFF40 was degraded in all three cell types in late apoptosis (after 24 h), demonstrating that the final degradation process of the tagged recombinant protein itself was not altered in the cells. Degradation of DFF40 resulted in the formation of a third band which occurred below the band of endogenous DFF40 protein. Since this degradation of DFF40 generally occurred late (>24 h after induction with Topotecan see fig. 3-41) and was detected in experiments during this study with Jurkat cells too (data not shown), it presumably did not affect internucleosomal DNA cleavage. However, there were differences in the extent of degradation: Surprisingly, the extent of DFF40 cleavage correlated with the extent of PARP cleavage, suggesting that caspases are responsible for this degradation process.

DFF45-transfected cells showed an enhanced expression of total DFF45 compared with both DFF40-transfected and mock-transfected cells. Endogenous and recombinant DFF45, despite its tags, were cleaved in a similar extent, but expectedly they were not completely eliminated in the course of apoptosis in Raji cells. Higher amounts of DFF45 (endogenous and recombinant proteins) were still detectable in DFF45-transfected cells 30 hours after induction of apoptosis, presumably since the basal expression of DFF45 was higher in these cells. Interestingly, caspase-3 activity seemed to be lower in DFF45 transfected cells since PARP cleavage occurred less distinct in these cells 30 h after induction of apoptosis (fig 3-41 A).

Taken together, these results for the first time indicated a higher caspase activity in DFF40-transfected Raji cells compared with mock-transfected or DFF45-transfected Raji cells.

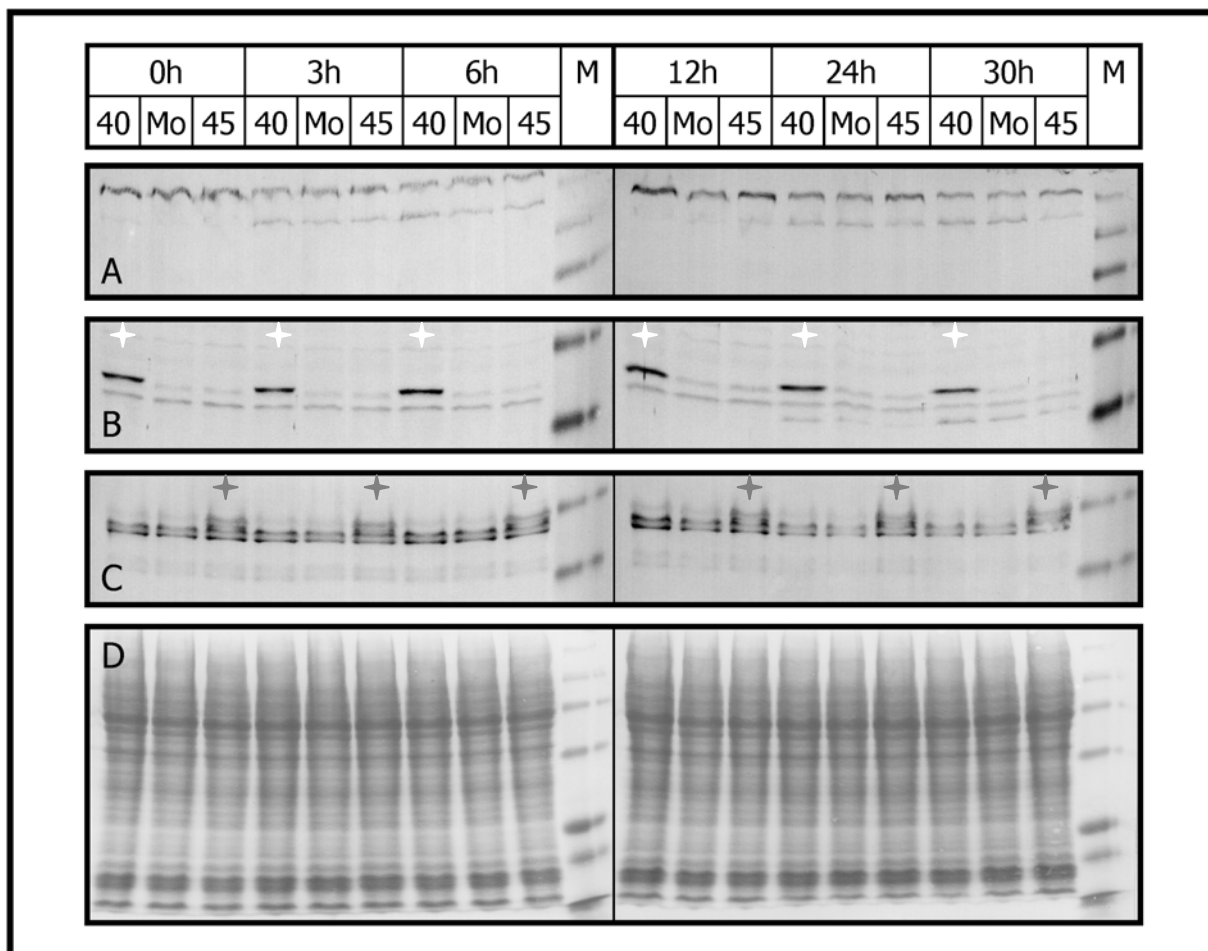


Figure 3-41: Detection of PARP, DFF40, and DFF45 in the course of apoptosis in Raji cells

Raji cells were induced to undergo apoptosis by adding 150 ng/ml Topotecan to the medium and aliquots were harvested at the times indicated in the figure above. 30 µg of proteins per sample were separated by SDS-PAGE and blotted onto nitrocellulose-membranes. Proteins were analyzed on the membrane by using different primary antibodies and a secondary antibody coupled to alkaline phosphatase; detection was carried out by using BCIP/NBT as a colouring substrate. **A:** Blots were analyzed for **PARP**-cleavage by an antibody detecting intact PARP (116 kDa) and cleaved PARP (89kDa). **B:** Immunostaining for **DFF40**; over-expressed tagged DFF40 migrated slightly above another endogenous cross-reacting protein. The same is true for **C:** immuno-detection of **DFF45**. Homogenous transfer and comparable concentrations of cellular proteins on the blots were confirmed by **D:** Ponceau-staining of the membrane. **40:** Stably transfected Raji cells showing distinct over-expression of DFF40, **Mo:** Mock-transfected Raji cells (stably transfected with the empty vector used for all transfections). **45:** Stably transfected Raji cells showing weak over-expression of DFF45. **M:** Prestained protein standard. **Note:** A cross-reacting endogenous protein, visible in all lanes, migrates just slightly below the recombinant DFF40 and DFF45 protein and should not be confused with it (compare figure 3-37 for authenticity of the recombinant proteins). Lanes containing recombinant DFF40 protein are marked with a 'white star', lanes containing recombinant DFF45 are marked with a 'grey star'.

3.3.3.4. Changes in the DNA fragmentation pattern in Raji cells

Stable transfection of Raji cells for over-expression of DFF40 enabled these cells to cleave their genomic DNA in a DFF40-like manner after induction of apoptosis, resulting in nucleosomal fragmentation. This also demonstrates that endogenous DFF45 in Raji cells was generally able to act as a chaperone on recombinant DFF40, allowing the

generation of a functional Dnase during apoptosis. On the other hand and for unknown reasons, mock-transfected cells showed nucleosomal DNA fragmentation as well. The type of DNA fragmentation in mock-transfected cells was less intensive and showed a slightly different pattern compared with that of DFF40-transfected cells. Interestingly, internucleosomal DNA cleavage was still lacking in DFF45-transfected cells, as depicted in figure 3-42. Nevertheless, the cells were dying and degraded their genomic DNA in a random fashion resulting in a smear of DNA rather than DNA laddering as visualized by agarose gel electrophoresis. However, DNA fragmentation in DFF40-transfected Raji cells was generally lower compared with that in other cell types (not shown in figure 3-42). A possible explanation for this observation is discussed later (see chapter 4.3.6).

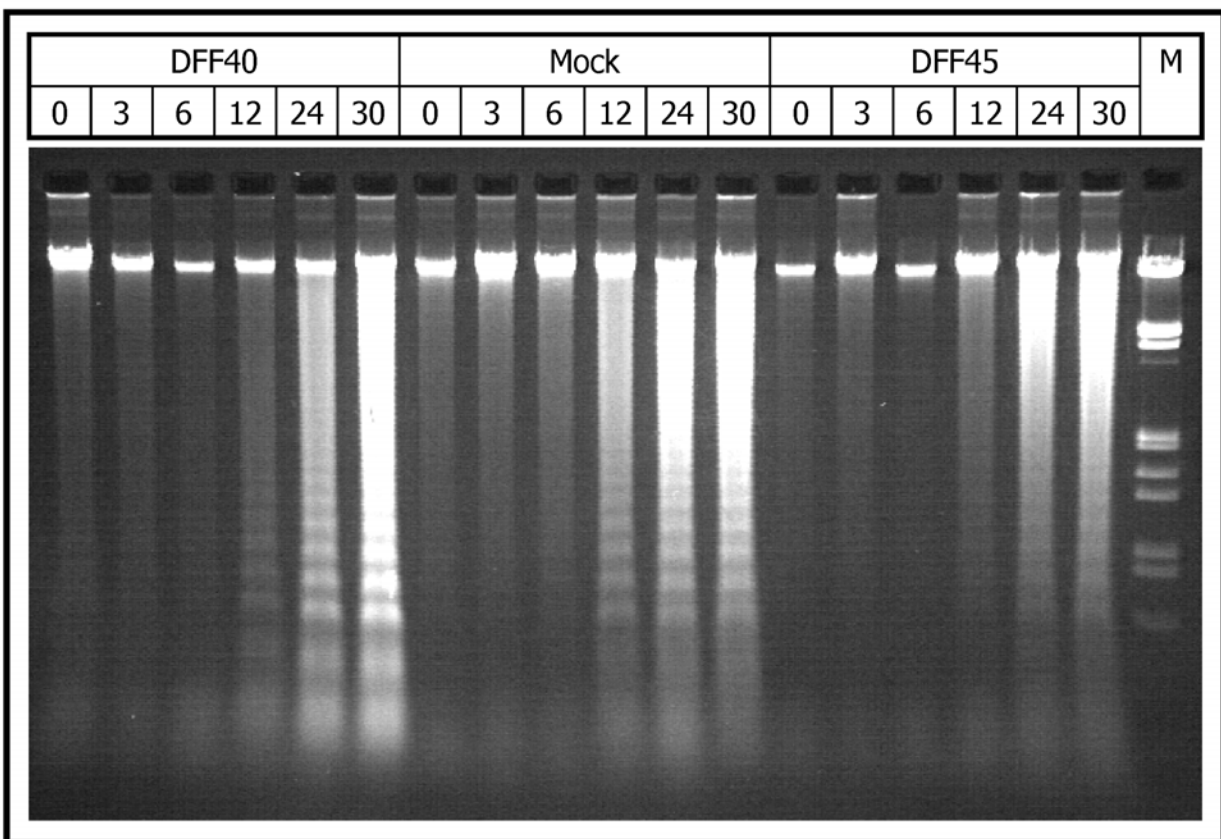


Figure 3-42: DNA fragmentation in stably transfected Raji cells

Stably transfected Raji cells were induced to undergo apoptosis by adding 150 ng Topotecan per ml of medium and aliquots from the cultures were harvested at the times indicated above (specifications are given in [h]). DNA was prepared from the cells, subjected to electrophoresis using a 1% agarose gel, and finally visualized on a UV-transilluminator after staining with ethidium bromide.

3.3.3.5. Single cell cloning

A possible explanation for the different features of apoptotic DNA degradation in transfected cells may be random genetic changes in the cells during the long lasting selection and culturing process after transfection. This may favour a process similar to

gene-drifting during evolution. A long lasting culturing of the cells was indispensable after transfection since the few surviving cells needed quite a long time for regeneration, and this time might have been sufficient to generate heterogeneous cultures. These altered cultures might contain subcultures of cells with slightly different apoptotic features at differing ratios. Therefore, the method of single-cell cloning was chosen to detect subcultures containing such random changes. The process of single-cell cloning means that cells are cultured in a way that allows the generation of a cell line which derives from one single cell. A comparison of non-transfected and mock-transfected cells after single cell cloning should reveal putative changes in the cultures which might be caused by long-time-culturing.

The clones obtained after single-cell cloning were subsequently tested for the expression of selected proteins involved in apoptosis and for the type of DNA fragmentation during apoptosis. Indeed, slight changes in the expression levels of selected proteins were seen in cultures obtained from different single-cell clones. A summary of representative blots is shown in figure 3-43.

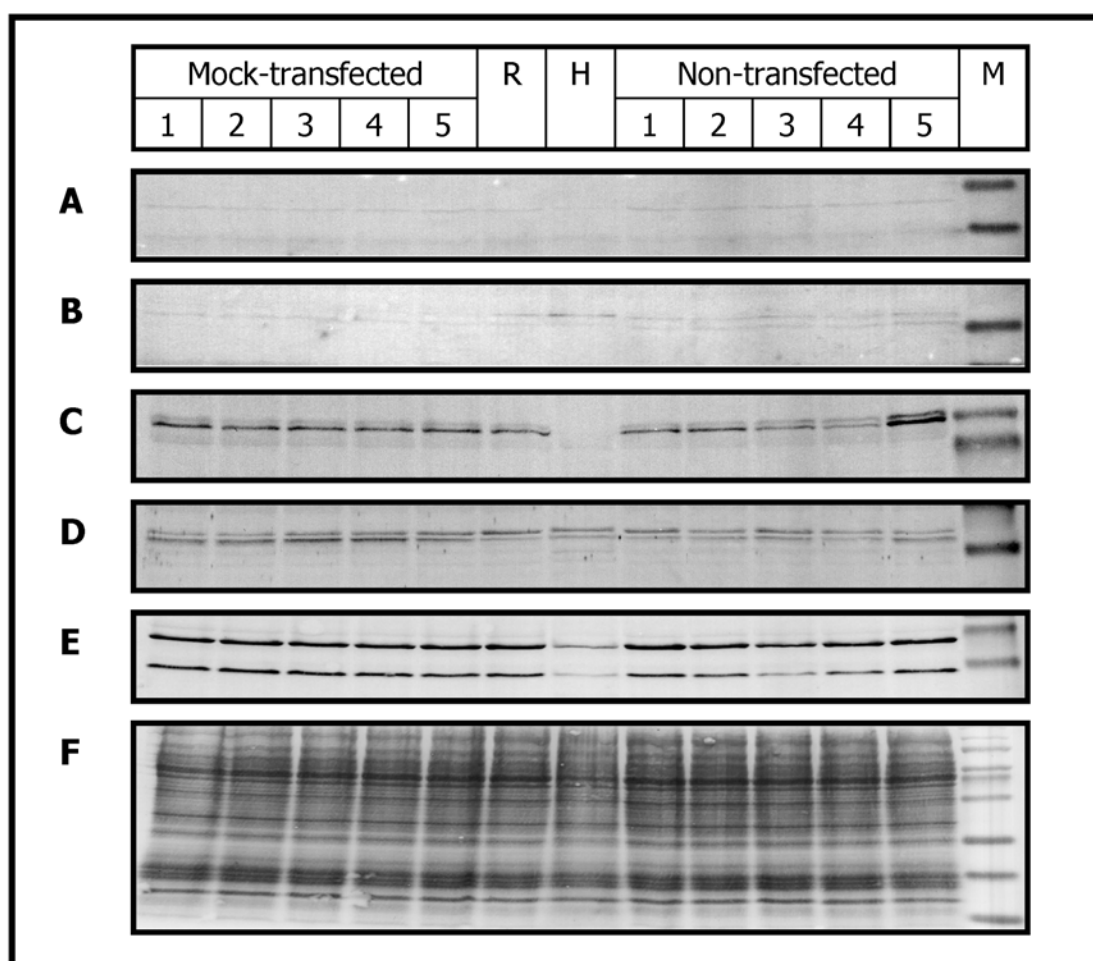


Figure 3-43: Expression levels of selected proteins in Raji single-cell clones

This figure legend refers to figure 3-43 on the previous page

Cell-extracts of mock-transfected and non-transfected Raji single cell clones were analyzed by western blotting for the expression levels of selected proteins, 25 µg total protein were applied per lane. Detection was carried out using an alkaline-phosphatase coupled secondary antibody and BCIP/NBT as a substrate. Numbers **1-5** indicate different clones obtained after single-cell cloning. **A**: Assayed for **bax**: Expression levels of pro-apoptotic bax slightly decreased in transfected Raji single cell clones **B**: Assayed for **bcl-2**: Expression levels of anti-apoptotic bcl-2 slightly decreased in transfected Raji cells. **C**: Assayed for **p53**. Expression levels were not affected in transfected single cell clones but they varied considerably in non-transfected single cell clones. **D**: Assayed for **DFF40**. **E**: Assayed for **DFF45/DFF35**. **F**: Ponceau-stained membrane containing blotted total proteins. **R**: Raji cells (< 10 splitting cycles), **H**: HL60 cells (< 10 splitting cycles), note that the levels of pro-apoptotic bax were low and levels of anti-apoptotic bcl-2 were high in this apoptosis-sensitive cell line. **M**: Prestained protein standard.

The results from the western blots and the extent of DNA fragmentation which was detectable after induction of apoptosis in these cells are summarized in the table below.

Type of cell	Clone No.	Expression of endogenous protein*					Nucleosomal DNA fragmentation* ²
		bax	bcl-2	p53	DFF40	DFF45	
Mock-transfected Raji single-cell clones	1	+	+	++	+	+++	-
	2	+	+	++	+	+++	+
	3	+	+	++	++	+++	+
	4	+	+	++	++	+++	+
	5	+	+	++	+	+++	+
Non-transfected Raji single-cell clones	1	++	++	++	++	+++	-
	2	++	+	++	+	+++	+
	3	++	++	+	++	++	-
	4	++	++	+	+	+++	-
	5	++	++	+++	++	+++	+
Wild-type cells	Raji	++	+	+	+	+++	-
	HL60	-+	+++	-	+	+	+++

- Not detectable; -+ hardly detectable, + weak; ++ moderate; +++ strong

* Results from two independent western blots

*² Results from three independent experiments

Table 3-1: Comparison of selected features in Raji single-cell clones

There were slight (bax, bcl-2, DFF40) to moderate (DFF45/DFF35, p53) changes detectable in the protein levels of the different sub-clones. However, these changes could not be reliably correlated to an enhanced or decreased sensitivity to nucleosomal

DNA fragmentation and apoptosis in the respective cell line as illustrated in the table above which summarizes the results from several experiments. Strikingly, HL60 cells which are more sensitive to induction of apoptosis than Raji cells expressed both lower levels of pro-apoptotic bax and higher levels of anti-apoptotic bcl-2. However, apoptotic nucleosomal DNA fragmentation in the mock-transfected single-cell clones, was always considerably weak as depicted in figure 3-42. Interestingly, even some of the single cell clones derived from non-transfected cells showed a weak nucleosomal DNA degradation pattern during apoptosis. This demonstrates that the reason for developing this feature is neither located in the vector used for transfection nor in the selection conditions for the transfectants using Blasticidin. The 'new acquisition' of nucleosomal DNA fragmentation in non-transfected and mock-transfected cells may therefore rather be the result of the long lasting culturing conditions which possibly allowed an alteration of the cells which presumably leads to changes in the overall ratio of pro- and anti-apoptotic proteins.

The fact that long-time culturing of cells obviously changed important features of the cells in a random manner made it more difficult to investigate the consequences of DFF40 activity or expression levels of DFF45 on apoptosis under cell culture conditions. It seemed quite probable that only the results of several repeated experiments were able to show a putative effect of DNA fragmentation on the progression of apoptosis. As demonstrated above, a slightly variable background of the apoptotic features had to be expected from the transfection experiments in different cells. Therefore, the effect was supposed to be found only by statistical means. A statistical comparison, an analysis of variance (ANOVA), seemed to be suitable to find the effects of over-expressing either DFF40 or DFF45 in Raji cultures mainly for one reason: A putative, directed, and non-random effect of over-expressed recombinant proteins should be able to outweigh random effects, caused by the non-directed changes of the apoptotic features in the cells during long-time-culturing.

Statistical analysis using ANOVA requires a quantifiable apoptotic parameter. An apoptotic parameter which can be quantitated easily and in a reasonable fashion by using a fluorimetric assay is the enzymatic activity of caspase-3. Therefore, several experiments were carried out and absolute enzymatic caspase-3-activities were determined by using a calibrated fluorimeter. The resulting values were subsequently tested for statistically significant differences by two-way-ANOVA.

3.3.4. COMPARISON OF CASPASE-3 ACTIVITIES IN TRANSFECTED RAJI CELLS

As already detailed above, the aim of this study was an evaluation of the effect of nucleosomal DNA fragmentation on the sensitivity of cells to apoptotic signals. Though

DFF40 activity generally occurs downstream of caspase-3-activity during apoptosis, the resulting DFF40-catalyzed DNA damage may serve to increase apoptotic signalling (compare chapter 1.3.3.2). DFF40 may thus contribute to progression of apoptosis by providing a positive feedback loop. On the other hand, high expression levels of DFF45 may counteract DFF40 activity in the course of apoptosis by directly inhibiting DFF40 activity. Thus DFF45 may interfere with a putative positive feedback loop when it is expressed at high levels in a cell.

Generally, it is difficult to find a reasonably quantifiable specific parameter to characterize the extent of apoptosis *in vivo*. Since apoptosis can be defined as a controlled cell death resulting from the enzymatic activity of caspases, the increasing activity of the effector-caspase caspase-3 was chosen as a quantifiable hallmark in cultured cells indicating both an effective induction of apoptosis and decreased cell viability.

In the following experiments non-transfected, mock-transfected, DFF40-transfected, and DFF45-transfected Raji cells were induced to undergo apoptosis by adding 150 ng/ml Topotecan and aliquots of the cell suspensions were harvested at different times, and controls were left untreated. After having collected all samples, caspase-3 activity was measured in the cell lysates by fluorimetric assays using DEVD-afc as a substrate for caspase-3 as described in chapter 2.2.3.11. Additionally, cells were examined for the type of DNA fragmentation, and protein expression patterns were analyzed by western blotting.

The results from several experiments, carried out with cells from several, independent transfection procedures, are summarized in the following representative figures. All those Raji cells which were transfected with DFF40 showed a nucleosomal DNA fragmentation; in contrast to previous experiments, the prevailing part of mock-transfected cells obtained in these experiments did not show nucleosomal DNA fragmentation, as illustrated in the following figure (3-44). Expectedly, non-transfected and DFF45-transfected cells did not show any nucleosomal DNA fragmentation as depicted in figure 3-44.

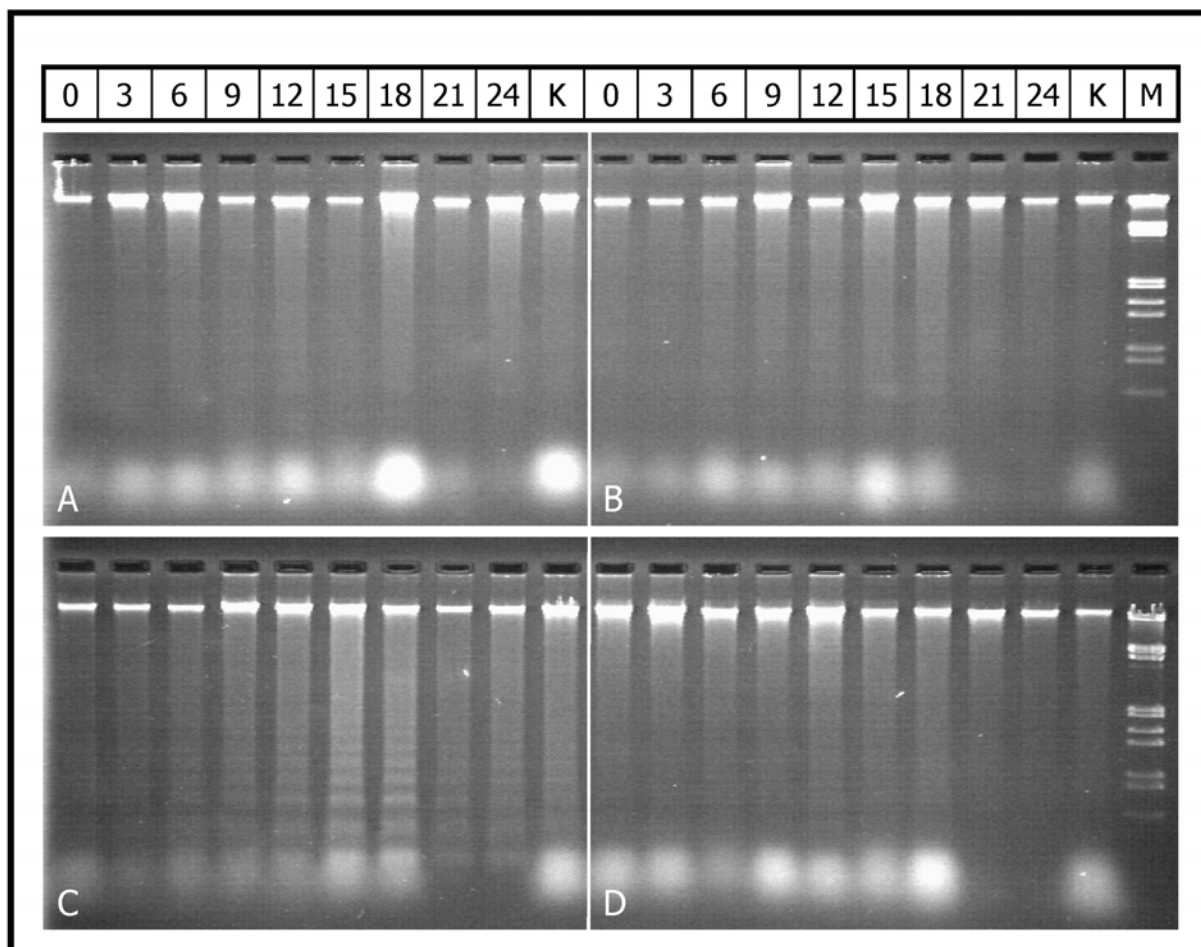


Figure 3-44: DNA fragmentation in the course of apoptosis in Raji cells

Transfected and non-transfected Raji cells were induced to undergo apoptosis by adding 150 ng/ml Topotecan. Aliquots of the cells were harvested at different times as indicated in the figure (specifications are in h) and the extracted DNA was subjected to agarose gel electrophoresis and visualized by UV-light after staining with ethidium bromide. **A:** DNA from non-transfected cells, **B:** DNA from mock-transfected cells (transfected with the empty vector), **C:** DNA from DFF40-transfected cells, **D:** DNA from DFF45-transfected cells. **K:** Untreated control cells. **M:** DNA marker (λ -DNA cut by EcoRI and Hind III).

DNA fragmentation in Raji cells was clearly correlated with the expression of recombinant DFF40, expressed in addition to endogenous DFF40, since recombinant DFF40 protein was detectable in western blots of the transfected cells. However, expression of recombinant DFF45 was comparatively low in DFF45-transfected Raji cells as shown in figure 3-45 on the next page. Later experiments with Jurkat cells revealed that expression of recombinant proteins under control of the CMV promotor was not stable in all transfection experiments since the activity of the promotor may be downregulated in some cell systems (discussed in chapter 4.3.4).

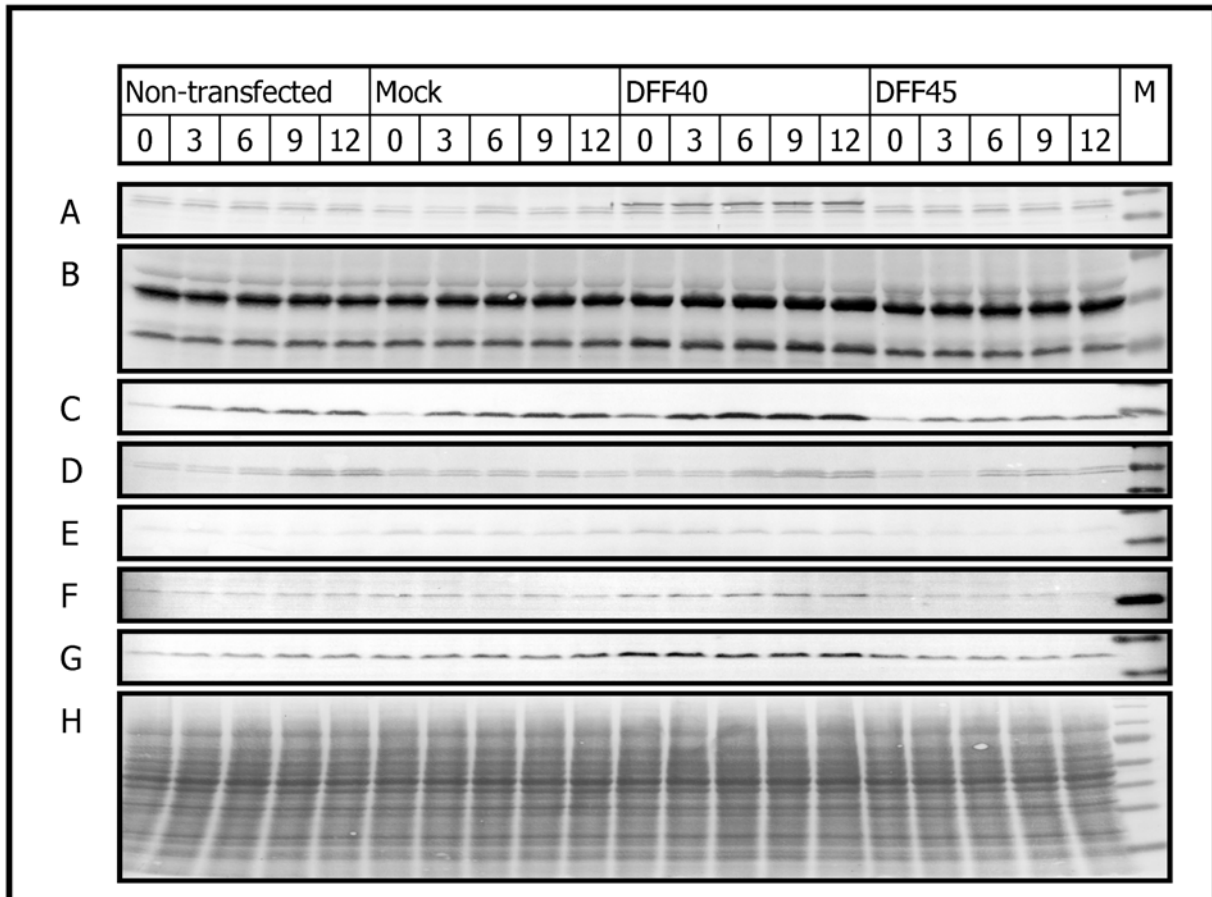


Figure 3-45: Changes in the protein levels in the course of apoptosis in Raji cells

Transfected and non-transfected Raji cells were induced to undergo apoptosis by adding 150 ng/ml Topotecan. Aliquots of the cells were harvested at different times as indicated in the figure (specifications are in h) and cell lysates were blotted onto NC-membranes and detected using different antibodies. Detection was by an alkaline phosphatase-coupled secondary antibody using BCIP and NBT as colouring substrates. **A:** Assayed for **DFF40**, additional recombinant DFF40 resulted in a band occurring above endogenous DFF40. **B:** Assayed for **DFF45/DFF35**, DFF45/DFF35 expression was slightly upregulated in DFF40-transfected cells. **C:** Assayed for **phosphorylated histone H2A.X**, increase of H2A.X phosphorylation was stronger in DFF40-transfected cells, indicating both enhanced HMW- and nucleosomal DNA fragmentation in these cells. In contrast, increase of H2A.X phosphorylation was decreased in DFF45-transfected cells, indicating both decreased HMW- and nucleosomal DNA fragmentation in DFF45-transfected cells. **D:** Assayed for **p53**, DNA damage generally resulted in up-regulation of p53 levels in Raji cells. **E:** Assayed for **WAF1** (p21), upregulation of p53 was unable to induce expression of WAF1, indicating a functional defect of p53 in Raji cells. **F:** Assayed for **bax**, bax expression was slightly upregulated in DFF40-transfected cells. **G:** Assayed for **bcl-2**, expression of bcl-2 was slightly upregulated in DFF40-transfected cells. **H:** Ponceau-stained proteins on the NC-membrane, confirming comparable amounts of proteins in the lanes. M: Prestained protein standard.

Generally, DNA damage in all of the dying cells was accompanied by increased phosphorylation of the core histone H2A.X. The core histone H2A.X is reported to be phosphorylated in all cells suffering from DNA damages (*Rogakou et al., 2000; Talasz et al., 2002; Huang et al., 2003*) since H2A.X is phosphorylated by ATM kinase in response to dsDNA damage. Thus, H2A.X phosphorylation may be expected to occur in response to the DNA damages induced by Topotecan as well. Importantly, HMW- and

nucleosomal DNA fragmentation obviously caused an even enhanced early phosphorylation of H2A.X in the course of apoptosis in DFF40-transfected cells, indicating both enhanced HMW- and nucleosomal DNA fragmentation during apoptosis in these cells. In contrast, H2A.X phosphorylation in DFF45-transfected cells was decreased compared with all the other cell types. This indicated less DNA damage in these cells, which supports the hypothesis that high levels of DFF45 inhibit DFF40 *in vivo*.

P53 is a protein sensor for DNA damage and thus involved in the genomic integrity surveillance network. Since the p53 gene is often mutated and therefore not functional or even lacking in tumor cells, it is generally regarded as a tumor suppressor gene. The expression of p53 was upregulated in the course of apoptosis in all of the examined Raji cells. However, **WAF1** levels (**w**ildtype p53-**a**ctivated **f**ragment **1**, also called p21 or CIP-1) were unaffected, indicating a presumably mutated defect p53 protein in this type of Raji cells. WAF1 (p21) is a protein regulated by p53, its expression is reported to increase with enhanced levels of active p53 (*Shiohara et al.1994; reviewed in Gartel and Tyner, 2002*). The expression levels of both pro-apoptotic bax and anti-apoptotic bcl-2 were slightly higher in DFF40-transfected cells compared with all of the other cell types. Nevertheless, the relative ratio of both pro-apoptotic bax and anti-apoptotic bcl-2 were unchanged in the four differently transfected cell types and provided equal apoptotic background conditions in the different cell types. As shown in figure 3-46 on the following page, there seemed to be differences in the mean caspase-3-activities in the course of apoptosis in the cells of the four groups. Compared with non-transfected cells, caspase-3-activities appeared to be higher in mock-transfected cells and even higher in DFF40-transfected cells. In contrast, caspase-3-activities in DFF45-transfected cells seemed to be comparably lower. Thus, since the standard errors of the means were considerably high, the point in question now was whether the observed differences in the enzymatic activities of caspase-3 in the four different experimental groups were statistically significant or not.

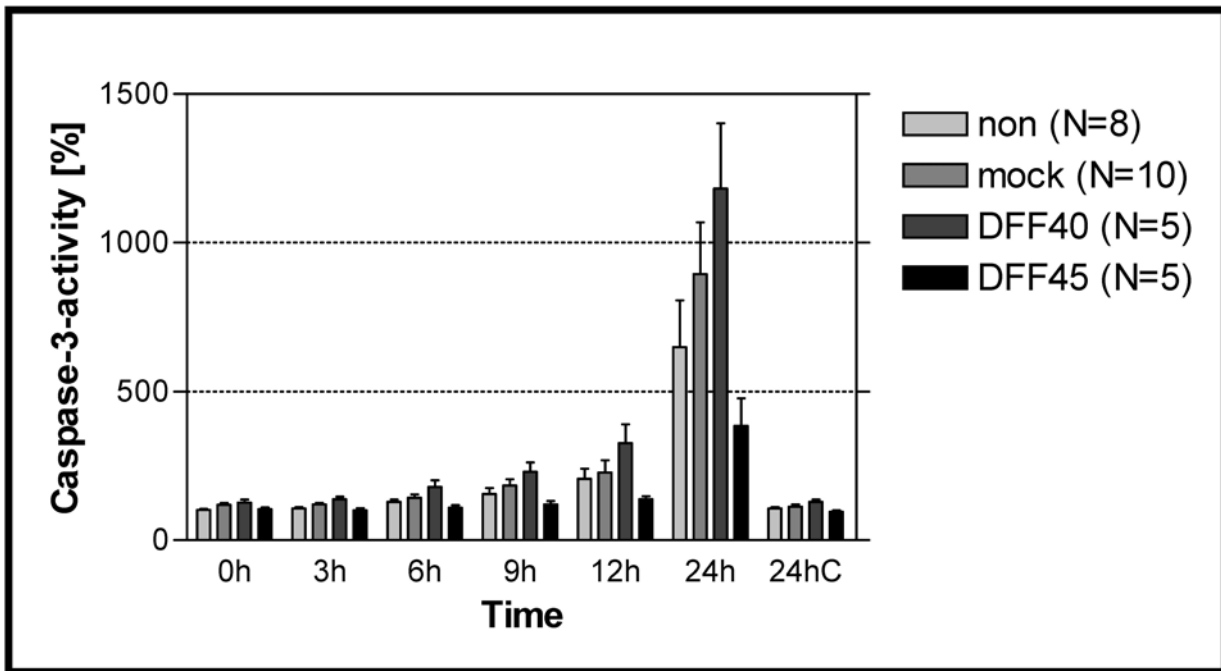


Figure 3-46: Caspase-3 activities in Raji cells after induction of apoptosis by Topotecan

Non-transfected, mock-transfected, DFF40-transfected, and DFF45-transfected Raji cells were induced to undergo apoptosis by adding 150 ng/ml Topotecan and harvested at different times as indicated in the abscissa of the graph. Caspase-3 activities were determined by measuring the fluorescence of DEVD-afc using a fluorimeter. Absolute caspase-3 activities were calculated using a fluorimeter-specific factor resulting in the unit μU per mg of protein (compare chapter 2.2.3.11). These values were finally converted into relative values resulting in the unit %, referring to the caspase-3 activity in the non-transfected 0h-control (ordinate of the graph). This graph depicts mean values with error bars, indicating the respective SEMs. **N**: Number of experiments used for calculation of the mean values. **C**: Control (no induction of apoptosis), **non**: Non-transfected Raji cells, **mock**: Raji cells transfected with empty vector only, **DFF40**: Raji cells transfected for additional expression of DFF40, **DFF45**: Raji cells transfected for additional expression of DFF45.

Interestingly, nucleosomal DNA fragmentation (detected after 12 h) preceded the major increase of caspase-3 activity (detected after 24 h) in DFF40-transfected cells (compare figure 3-44). Furthermore, enhanced HMW-DNA fragmentation (resulting in increased phosphorylation of H2A.X) was detected already 3 h after induction of apoptosis in DFF40-transfected cells, whereas increases of caspase-3 activities were detected 9 h to 12 h after induction of apoptosis. This observation supports the hypothesis of a positive feed back mechanism induced by DFF40-catalyzed DNA damages (both HMW- and nucleosomal DNA fragmentation) in the course of apoptosis. On the other hand, caspase-3 activities in DFF45-transfected cells seemed to be lower compared with all of the other cell types. Thus, less initial apoptotic DNA-damage seemed to be correlated with less caspase-3 activity in the course of apoptosis in DFF45-transfected cells.

Furthermore, figure 3-46 illustrates that caspase-3 activities were affected by two different factors. Caspase-3 activities increased with proceeding of apoptosis in the

course of the experiment in all groups, but the extent of the increase seemed to depend on the type of transfection. Thus, two parameters, namely 'time' (time after induction of apoptosis) and 'transfection' (type of recombinant protein expressed after transfection), obviously had an effect on the results, and this experimental design required statistical analysis by two-way-ANOVA.

Two-way-ANOVA is a statistical method for the analysis of variances which are supposed to be caused by two different factors. Additionally, this statistical method analyses the probability for an interaction between these two factors. Bonferroni post-tests were subsequently included in the analysis to compare the effects in the four different experimental groups to each other (see chapter 2.2.6 for details concerning the statistical analysis methods used in this study).

3.3.4.1. Two-way ANOVA with Bonferroni post-tests

Statistical analysis using two-way ANOVA with Bonferroni post-tests was performed using the software GraphPad Prism V.4.00 for Windows, GraphPad Software, San Diego California, USA (www.graphpad.com). Groups were defined by the parameter 'transfection' in the different columns and by the parameter 'time' in the respective rows (for details see chapter 2.2.6).

As expected, there were significant differences ($p < 0.001$) caused by the parameter 'time' in all four groups. Differences were caused by increasing amounts of apoptotic cells (with higher caspase-3 activities) in the population. The changes due to the parameter 'transfection' observed in the caspase-3 activities in these four groups after treatment with Topotecan for 24 h were of varied significances as depicted in the following figure. This was supposed to reflect a differential susceptibility of the cells towards induction of apoptosis. The respective Bonferroni post-test results (see chapter 2.2.6) are summarized in figure 3-47.

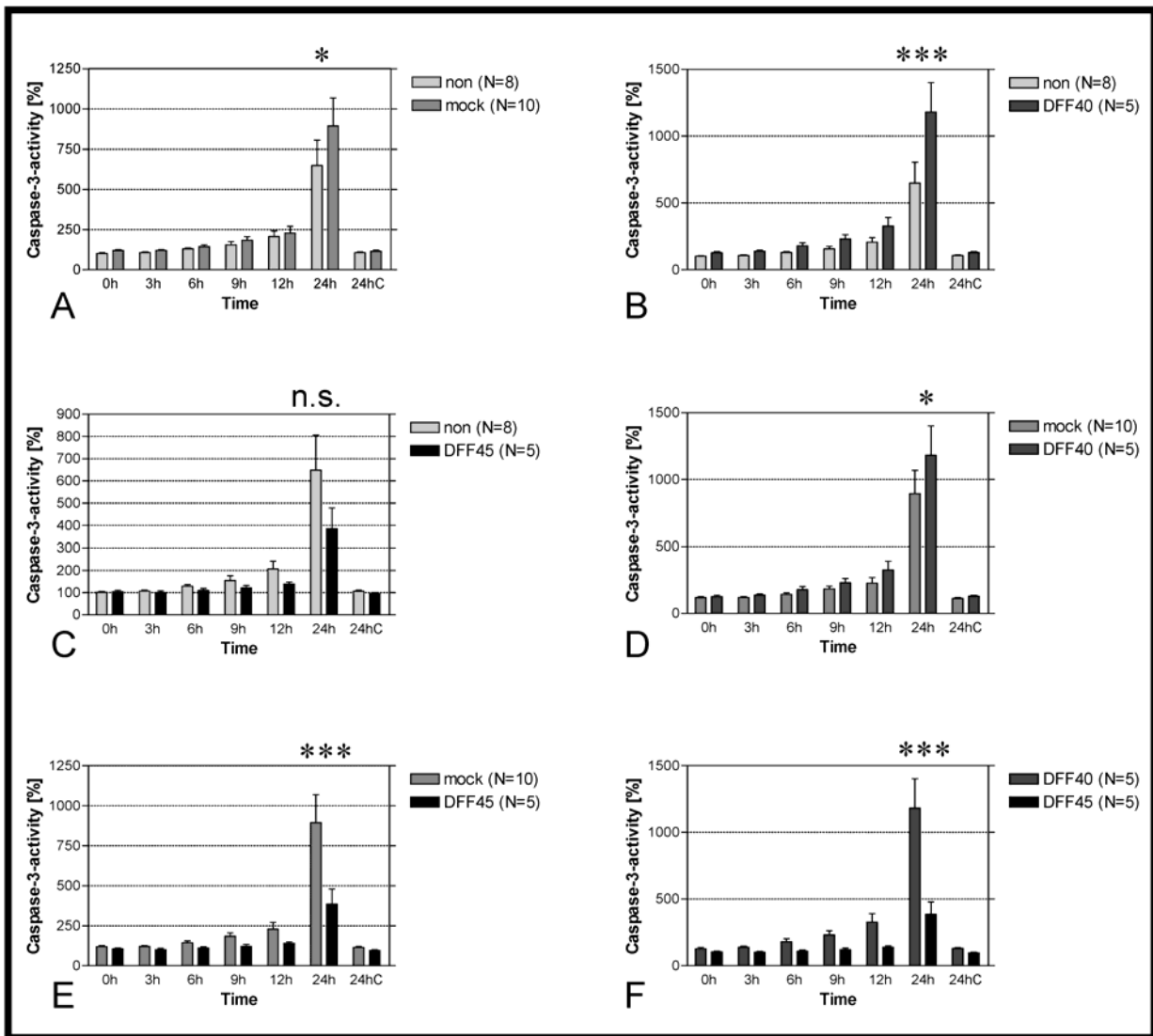


Figure 3-47: Caspase-3 activities in Raji cells: Two-way ANOVA with Bonferroni post-tests

Values resulting from the calculation of caspase-3 activities after induction of apoptosis in transfected and non-transfected Raji cells were subjected to two-way ANOVA with Bonferroni-post-tests to evaluate significant differences between the groups (compare chapter 2.2.6). Test results for the 24 h-values, obtained by comparing all four groups simultaneously, are depicted as follows: **A: Non-transfected Raji cells vs. mock-transfected Raji cells** (transfected with the empty vector). **B: Non-transfected Raji cells vs. DFF40-transfected Raji cells.** **C: Non-transfected Raji cells vs. DFF45-transfected Raji cells.** **D: Mock-transfected Raji cells vs. DFF40-transfected Raji cells.** **E: Mock-transfected Raji cells vs. DFF45-transfected Raji cells.** **F: DFF40-transfected Raji cells vs. DFF45-transfected Raji cells.** **n.s.:** $p > 0.05$ (not significant); *****: $p < 0.05$ (significant); ******: $p < 0.01$ (significant); *******: $p < 0.001$ (significant). Statistical analysis was performed with GraphPad Prism.

The differences in caspase-3 activities due to transfection were significant ($p < 0.001$) when comparing:

1. Non-transfected cells to DFF40-transfected cells.
2. Mock-transfected cells to DFF45-transfected cells.
3. DFF40-transfected cells to DFF45-transfected cells.

Caspase-3 activities showed significant changes ($p < 0.05$) due to transfection in a comparison of:

1. Non-transfected cells to mock-transfected cells
2. Mock-transfected cells to DFF40-transfected cells

The changes, caused by transfection, observed in a comparison of the caspase-3 activities of non-transfected cells and DFF45-transfected cells were not statistically significant ($p > 0.05$).

However, the overall interaction between the two parameters 'time' and 'transfection' was significant between the four groups ($p < 0.01$) which generally makes the p-values, resulting from this two-way ANOVA, difficult to interpret. In this case a significant interaction may indicate that the parameter transfection had a differential effect on the caspase-3-activities in the course of the experiments (compare chapter 2.2.6). This may be a consequence of the experimental design because differences in the inducible caspase-3 activity in the differently transfected cell populations became evident only in the course of apoptosis. Interaction presumably occurred because caspase-3 activities increased in a differential extent in the different cell types. Thus, interaction was supposed to occur mainly in comparisons of the different cell types with DFF40-transfected Raji cells. However, this two-way ANOVA analysis did not allow to locate the exact source of interaction since this type of analysis indicated just an overall interaction when comparing all four experimental groups simultaneously. Thus, another type of two-way ANOVA was performed to locate the groups with significant interaction.

3.3.4.2. Analysis of interaction by two-way ANOVA on column pairs

Analysis by two-way ANOVA with Bonferroni post tests (see chapter 2.2.6 and 3.3.4.1) allowed a statistical comparison of all four experimental groups, but indicated just an overall interaction, without showing the exact source of the interaction when comparing all of the four groups in one analysis. Thus, another 6 independent two-way ANOVAs were conducted, comparing all possible combinations of column pairs, respectively. This allowed analysis of the interaction in every analyzed column pair, but resulted in slightly different p-values, compared with the values obtained in the former analysis (see chapter 3.3.4.1), which compared all four groups at a time.

Indeed, interaction was only found to be statistically significant in those cell types with high differences in the inducible caspase-3 activity. Significant interaction was detected only in a comparison of non-transfected to DFF40-transfected cells, DFF40-transfected to DFF45-transfected cells, and mock-transfected to DFF45-transfected cells, respectively (see table 3-2). Thus, the significant interaction is presumably a consequence of differential susceptibility to induction of caspase-3 activity in these cells

and should not interfere with the interpretation of the p-values obtained during two-way ANOVA (compare chapter 2.2.6).

Expectedly, the parameter 'time' always had a statistical significant effect because this reflects the apoptotic reaction in the course of the experiments. Response to Topotecan treatment occurred in all cells and was indicated by time-dependent increases in the activity of caspase-3. Importantly, statistical analysis supported the hypothesis that internucleosomal DNA cleavage by DFF40 increases the susceptibility of cells to undergo apoptosis since there were significantly higher caspase-3 activities in cells undergoing internucleosomal DNA cleavage. Furthermore, higher caspase-3 activities were detected as a consequence of DFF40 activity since caspase-3 activity only increased after internucleosomal DNA degradation had started in these cells. Thus, the statistical significant differences could be correlated with biological significant data in these experiments. DFF40-catalyzed DNA-damages seemed to enhance apoptotic signalling in the cells by contributing to a positive feedback loop. Furthermore, there was statistical evidence for an even lower caspase-3 activity in DFF45-transfected cells, which was correlated with initial less DNA-damage as analyzed by the phosphorylation state of H2A.X (compare figure 3-45). This could support the hypothesis that DFF45 is able to counteract a putative positive feedback loop by inhibiting DFF40 activity.

	Parameter	Non	Mock	DFF40
Mock	<i>Time</i>	***		
	<i>Transfection</i>	n.s.		
	<i>Interaction</i>	n.s.		
DFF40	<i>Time</i>	***	***	
	<i>Transfection</i>	**	n.q.s.	
	<i>Interaction</i>	**	n.s.	
DFF45	<i>Time</i>	***	***	***
	<i>Transfection</i>	n.q.s.	**	***
	<i>Interaction</i>	n.s.	**	***

Table 3-2: Two-way ANOVA of caspase-3 activities in Raji cells (analysis of interaction)

n.s.: $p > 0.1$ (not significant), **n.q.s.:** $p < 0.1$ (not [quite] significant), *: $p < 0.05$ (significant) ** $p < 0.01$ (significant), ***: $p < 0.0001$ (significant). Analysis by pairwise two-way ANOVA resulted in slightly different p-values compared to the p-values obtained by two-way ANOVA with Bonferroni post tests. This test was performed to check for significant interactions: These were only detected in a comparison of: **1.** DFF40-transfected cells vs non-transfected cells, **2.** DFF40-transfected cells vs DFF45-transfected cells **3.** mock-transfected cells to DFF45-transfected cells.

Since the results obtained so far indicated a role for DFF40 in enhancing the apoptotic signalling by adding DNA damage in an apoptotic system with Raji cells (reflected in higher caspase-3 activities in cells undergoing internucleosomal DNA cleavage), it seemed interesting to test this hypothesis in other cell types. So, the expression-experiments were carried out with Jurkat cells. Moreover, the effect of over-expressed DFF45 could not yet be tested in a satisfying manner in Raji cells since the expression levels of recombinant DFF45 in these cells was quite low. Thus, the question was still open whether an excess of DFF45 was able to inhibit DFF40 activity *in vivo*, thereby impairing the progress of apoptosis by decreasing the DFF40-catalyzed DNA damages. In contrast to Raji cells, Jurkat cells show a nucleosomal DNA fragmentation pattern after induction of apoptosis which is caused by activated DFF40. Therefore, the expression experiments were carried out with Jurkat cells to test the consequences of an over-expression of DFF45 in these cells (chapter 3.3.6 and 3.3.7).

3.3.5. SUMMARY: APOPTOSIS IN STABLY TRANSFECTED RAJI CELLS

Raji cells stably transfected for expression of additional recombinant DFF40 showed high expression levels of recombinant DFF40, and internucleosomal DNA cleavage was restored in these cells. HMW-DNA damage (detected by increased phosphorylation of H2A.X) occurred within 3 h after induction of apoptosis and was even increased in DFF40-transfected cells compared with all of the other Raji cell types. In contrast, HMW-DNA damage in DFF45-transfected cells was lower than in all the other Raji cell types. Furthermore, DNA damage generally preceded the major increase of caspase-3 activity in all Raji cell types. Importantly, caspase-3 activity in the course of apoptosis was significantly higher in DFF40-transfected cells, and caspase-3 activity in the course of apoptosis was significantly lower in DFF45-transfected cells compared with the other cell types. This supports the hypothesis that DFF40-catalyzed DNA damage during apoptosis contributes to a positive feedback loop which finally enhances progression of apoptosis. Furthermore, the results demonstrated that DFF45, the inhibitor of DFF40, may counteract this putative positive feedback mechanisms in Raji cells by directly inhibiting the activity of DFF40, thus limiting apoptotic DNA damage.

3.3.6. EXPERIMENTS WITH TRANSFECTED JURKAT CELLS

3.3.6.1. Changes in protein levels during apoptosis in Jurkat cells

Transfection and selection of stably transfected Jurkat cells was carried out as already described for Raji cells. Jurkat cells were transfected with recombinant DFF40 as well since this protein was already expressed successfully in Raji cells and served as a control for successful transfection and expression under control of the CMV promotor in Jurkat cells. As shown below, expression of recombinant DFF40 in Jurkat cells was successful, though the expression levels were not as high as in Raji cells. Furthermore, expression of recombinant DFF40 protein down-regulated expression of endogenous DFF40 protein by about 20% in Jurkat cells (see figure 3-48 A) as estimated by quantitative densitometry (see chapter 2.2.7). Thus, the content of total DFF40 in the different Jurkat cell types was not increased by the expression of recombinant DFF40 in Jurkat cells. This displacing effect of recombinant DFF40 was not observed in Raji cells (compare fig. 3-45) and may indicate a differential regulation process for the DFF40 protein levels in different cell types. As already observed in Raji cells, Jurkat cells cleaved DFF40 in the later course of apoptosis, therefore it may be concluded that this late cleavage of DFF40 does not impair the ability for nucleosomal DNA fragmentation which occurs earlier during apoptosis.

In contrast to DFF40, recombinant DFF45 could not be expressed in Jurkat cells (see figure 3-48-B). Thus, effects of DFF45 over-expression *in vivo* unfortunately could not be analyzed in this study. Furthermore, transfection experiments for the expression of DFF45 in HL60 cells failed because none of these cells survived the transfection and selection procedure (data not shown).

Expression-levels of bax and bcl-2 were not affected by transfection in Jurkat cells. As already described by other authors, p53 was not detectable in Jurkat cells (the corresponding blot is not shown in figure 3-48 since there were no bands visible).

H2A.X phosphorylation increased in the course of apoptosis in all Jurkat cell types. This was caused by increasing DNA damages as already detailed above for the experiments with Raji cells. Unexpectedly, H2A.X phosphorylation seemed to be decreased in the course of apoptosis in DFF40-transfected cells compared with all the other Jurkat cells. This could be supposed to occur due to less DNA fragmentation in DFF40-transfected cells.

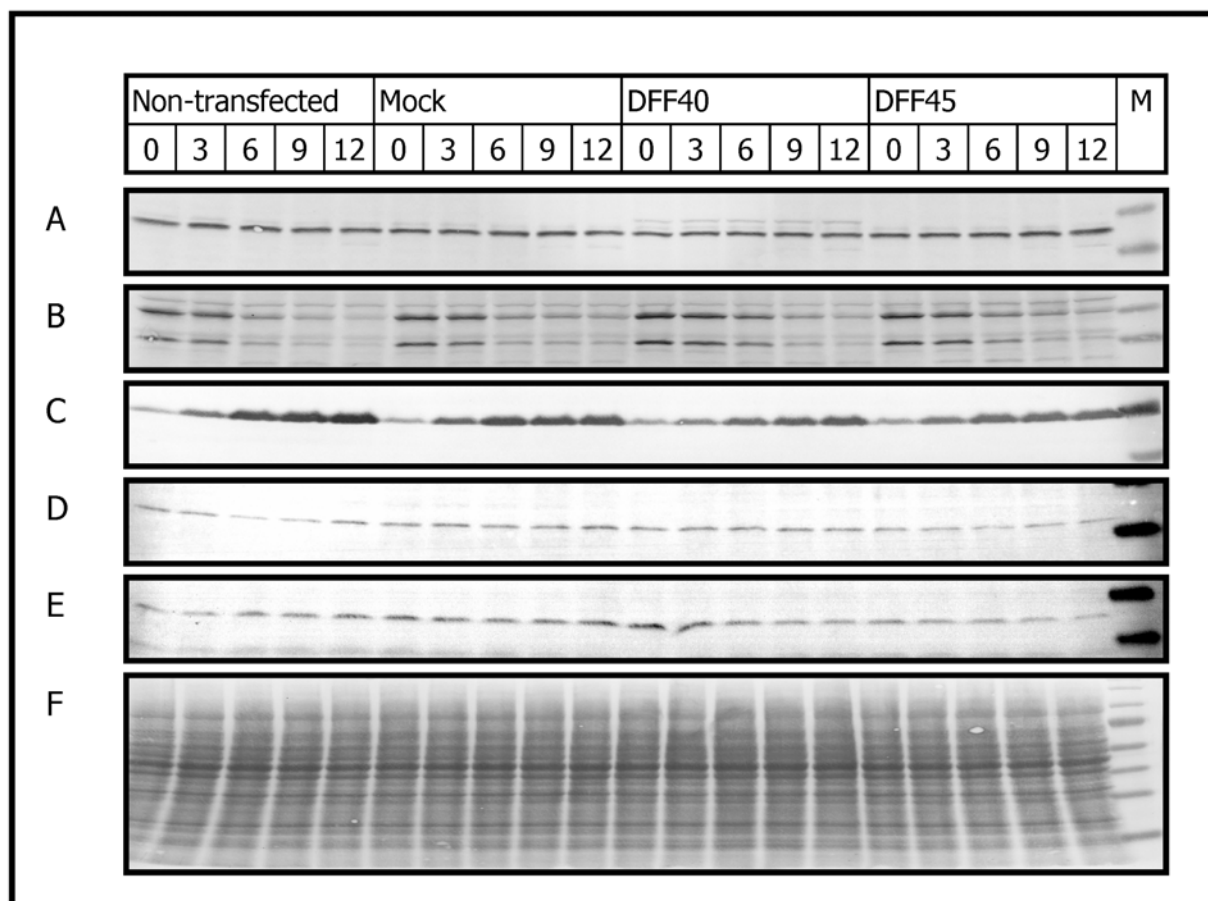


Figure 3-48: Changes in the protein levels during the course of apoptosis in Jurkat cells

Transfected and non-transfected Jurkat cells were induced to undergo apoptosis by adding 150 ng/ml Topotecan. Aliquots of the cells were harvested at different times as indicated in the figure (specifications are in h) and cell lysates were blotted onto NC-membranes and detected using different antibodies. Detection was done by using alkaline phosphatase-coupled secondary antibody and BCIP/NBT as colouring substrates. **A:** Assayed for **DFF40**: Recombinant DFF40 was detectable in DFF40-transfected Jurkat cells (upper band). Mean values for Gaussian integrated densities in the lower bands (corresponding to endogenous protein) were: Non-transfected: 1189 (± 77), Mock: 1149 (± 91), DFF40: 946 (± 28), DFF45: 1239 (± 88). **B:** Assayed for **DFF45/DFF35**: expression of DFF45/DFF35 was slightly upregulated in DFF40-transfected cells, expression of recombinant DFF45 in DFF45-transfected cells was not detectable. **C:** Assayed for **phosphorylated histone H2A.X**: Less H2A.X phosphorylation was observed in the course of apoptosis in DFF40-transfected cells, **D:** Assayed for **bax**: No changes were detectable, **E:** Assayed for **bcl-2**: No changes were detectable, **F:** Ponceau-stained proteins on the NC-membrane confirming equal protein amounts. **M:** Prestained protein standard.

3.3.6.2. Changes in the DNA fragmentation pattern in Jurkat cells

DNA samples were subjected to electrophoresis to evaluate the extent of DNA damage. Interestingly, less H2A.X phosphorylation in DFF40-transfected Jurkat cells was correlated with an initial less intensive DNA fragmentation in these cells as shown in figure 3-49 on the next page. Less DNA fragmentation was visible in DFF40-transfected cells within 6h after adding Topotecan to the cells (lane 6 in figure 3-49 A, B, C, and D). Recombinant DFF40 obviously replaced up to 20% of endogenous DFF40 (compare

figure 3-48) and expression of recombinant DFF40 resulted in decreased DFF40 activity in Jurkat cells. Thus, it was likely that the tag of recombinant DFF40 interfered with the activation of recombinant DFF40 (see chapter 4.3.6). DFF40-transfected Jurkat cells contained a mixture of both endogenous and recombinant DFF40, and had a comparably lower nuclease activity than all the other Jurkat cell types. Therefore, it may be concluded that recombinant DFF40 indeed had a lower enzymatic activity than endogenous DFF40. Thus, total DFF40 activity could be decreased in DFF40-transfected cells since total expression of DFF40 did not change in Jurkat cells. Nevertheless, the cells were dying and later on degraded their DNA to an extent which was indistinguishable from that of the other cells.

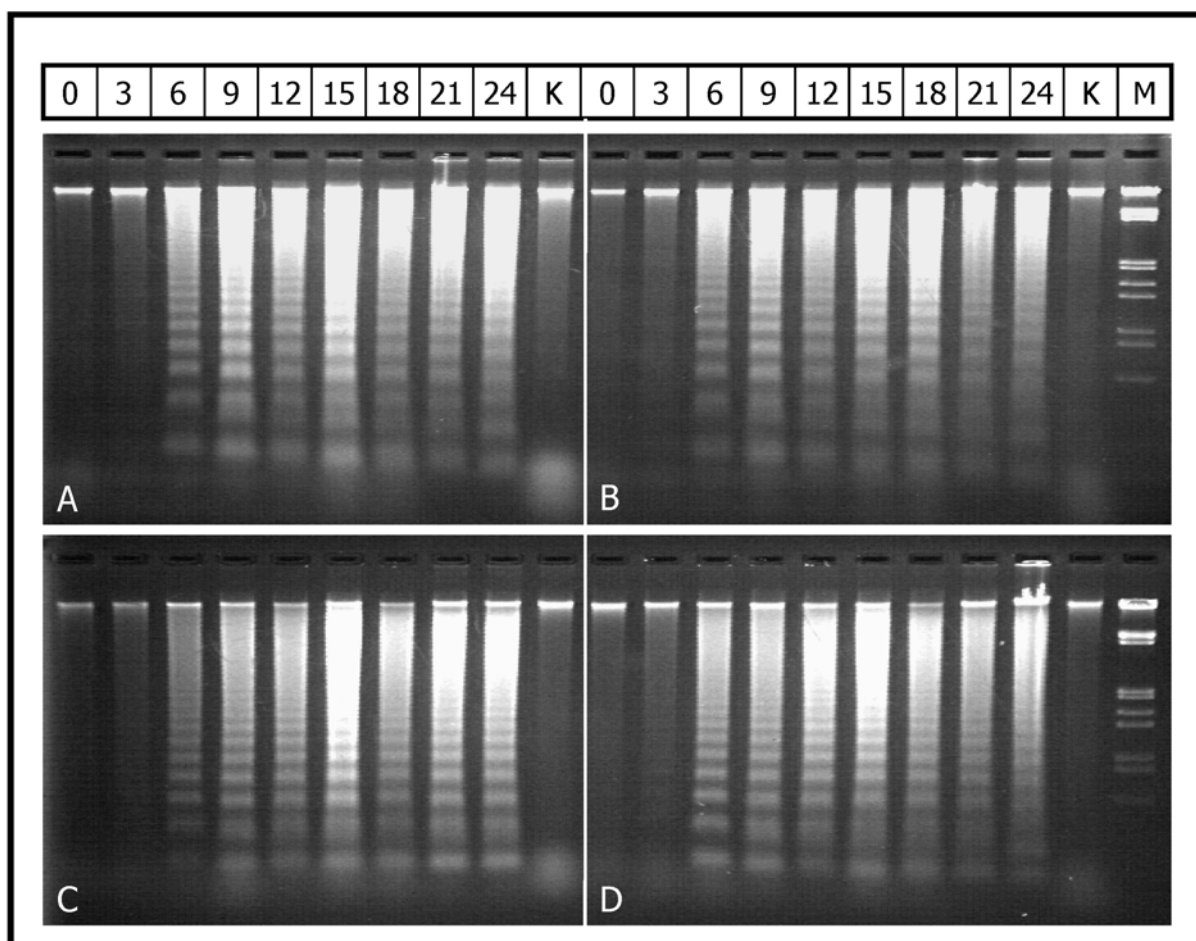


Figure 3-49: DNA fragmentation in the course of apoptosis in Jurkat cells

Stably transfected Jurkat cells were induced to undergo apoptosis by adding 150 ng Topotecan per ml of medium and aliquots from the cultures were harvested at the times indicated above (specifications are in [h]). DNA was prepared from the cells, subjected to electrophoresis using a 1% agarose gel, and visualized on a UV-transilluminator after staining with ethidium bromide. **A:** DNA from non-transfected cells, **B:** DNA from mock-transfected cells (transfected with the empty vector), **C:** DNA from DFF40-transfected cells, **D:** DNA from DFF45-transfected cells. **K:** untreated control cells. **M:** DNA marker (λ -DNA cut by EcoRI and Hind III). **Note:** Less DNA fragmentation was visible 6 h after induction of apoptosis in DFF40-transfected Jurkat cells compared with the other cell types. Nevertheless, all cells were dying as can be concluded by progression of DNA fragmentation in all cells.

3.3.7. COMPARISON OF CASPASE-3 ACTIVITIES IN TRANSFECTED JURKAT CELLS

It should be mentioned in advance that only two experiments could finally be evaluated by statistical analysis since Jurkat cells often rapidly down-regulated the expression levels of recombinant DFF40. After several transfection experiments, only two experiments, in which tagged DFF40 was detected, were efficient for further experiments, and expression of recombinant DFF45 even failed completely as already detailed above (chapter 3.3.6.1). However, it was particularly interesting to analyze the remaining three differently transfected Jurkat cell types for differences in their caspase-3 activities during apoptosis since there were already differences detected in the extent of apoptotic DNA damage. Would there be a correlation between DNA damage and increase in caspase-3 activity in these cells as it was already observed in Raji cells?

However, these results obtained with transfected Jurkat cells have to be regarded as preliminary because they are based on only two transfection experiments. However, they finally supported the hypothesis which was derived from experiments with Raji cells, though the obtained results were contradictory at a first glance as detailed in the following.

Those Jurkat cells which were transfected with the expression vector for recombinant DFF45 were named 'DFF45-transfected' cells in the following since they were transfected with another vector than the mock-transfected cells and thus differ genetically from mock-transfected cells, although expression of the recombinant protein was not detectable in western blots. Interestingly, in contrast to DFF40-transfected Raji cells, DFF40-transfected Jurkat cells seemed to have reduced caspase-3 activities in the course of apoptosis, even 24 h after induction of apoptosis as illustrated by the following figure (figure 3-50). This slightly reduced caspase-3 activity fitted well with the observation that DFF40-transfected Jurkat cells had less intensive DNA damages in the beginning of apoptosis. In contrast to Raji cells, in which all types of DNA fragmentation generally preceded the main increase in caspase-3 activity, caspase-3 activities in Jurkat cells increased in parallel with internucleosomal DNA cleavage. However, DFF40-catalyzed HMW DNA fragmentation in Jurkat cells preceded the main increase of caspase-3 activities (compare the differential phosphorylation state of H2A.X in figure 3-48 with the increases of caspase-3 activities in figure 3-50). Statistical analysis was carried out subsequently to test for significant differences of caspase-3 activities as already described for Raji cells (see chapters 3.3.4.1, 3.3.4.2, and 2.2.6).

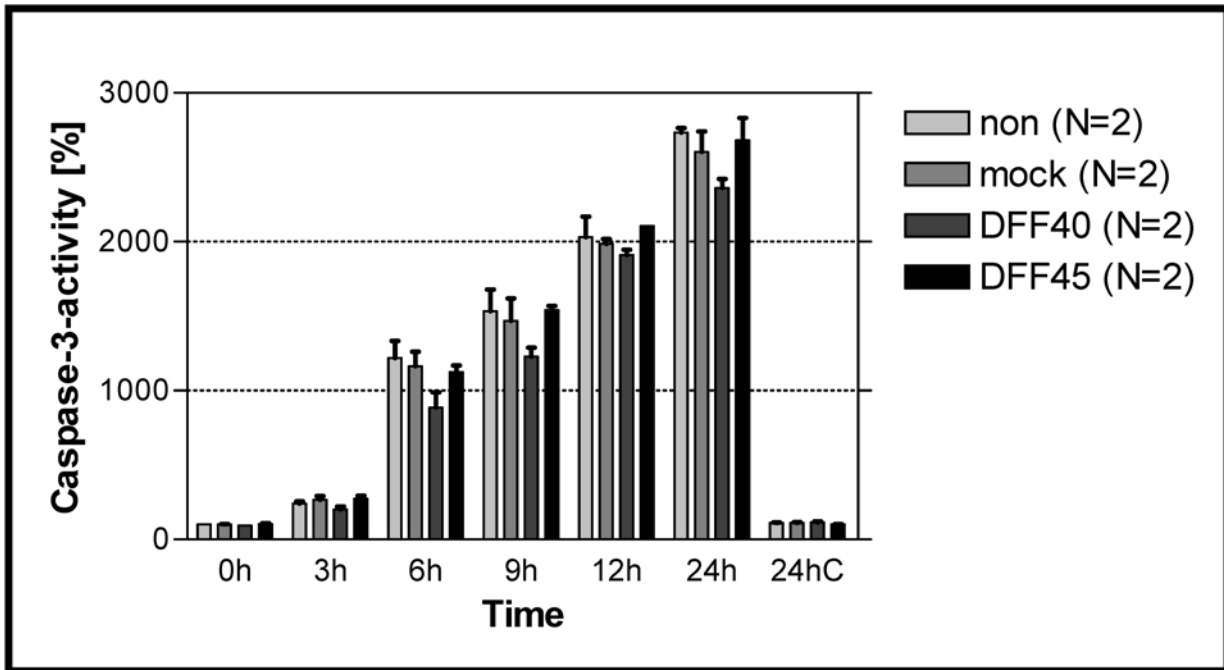


Figure 3-50: Caspase-3 activities in Jurkat cells after induction of apoptosis by Topotecan

Non-transfected, mock-transfected, DFF40-transfected, and DFF45-transfected Jurkat cells were induced to undergo apoptosis by adding 150 ng/ml Topotecan and harvested at different times as indicated in the graph's x-axis. Expression of recombinant protein was only detectable in DFF40-transfected cells. Caspase-3 activities were determined by measuring the fluorescence of DEVD-afc using a fluorimeter. Absolute caspase-3 activities were calculated using a fluorimeter-specific factor resulting in the unit μU per mg of protein. These values were finally converted into relative values resulting in the unit %, referring to the caspase-3 activity in the non-transfected 0h-control. This graph depicts mean values with error bars, indicating the respective SEMs. **N**: Number of experiments used for calculation of the mean values. **C**: Control (no induction of apoptosis), **non**: Non-transfected Jurkat cells, **mock**: Jurkat cells transfected with empty vector only, **DFF40**: Jurkat cells transfected for additional expression of DFF40, **DFF45**: Jurkat cells transfected for additional expression of DFF45. **Note**: These data are preliminary data since they are based on only two different transfection experiments.

3.3.7.1. Two-way ANOVA with Bonferroni post-tests

Statistical analysis of the results was carried out as already described for Raji cells (see chapter 3.3.4.1, 3.3.4.2 and 2.2.6). As already detailed in chapter 2.2.6, two-way ANOVA allows statistical analysis of even unreplicated values (by assuming that there is no interaction) since the data are finally arranged in column and rows during statistical analysis. However, even interaction could be tested in this analysis since there was at least one replicate experiment. Groups were defined by the parameter 'transfection' in the different columns and by the parameter 'time' in the respective rows. However, as already mentioned above, the results from statistical analysis are based on only two different transfection experiments, and thus the data should be regarded as preliminary. The cogency of the statistical analysis is low with this number of experiments.

As expected, there were significant differences ($p < 0.001$) caused by the parameter 'time' in all four groups and were caused by increasing amounts of apoptotic cells (with a higher enzymatic activity of caspase-3) in the population.

The changes due to the parameter 'transfection' observed in the caspase-3 activities in these four groups after treatment with Topotecan for 24 h were of differing significance as depicted in figure 3-51 on the following page. In contrast to Raji cells, transfection of DFF40 into Jurkat cells resulted in a significant decrease - instead of an increase - of caspase-3 activities compared with non-transfected cells ($p < 0.01$) or DFF45-transfected cells ($p < 0.05$). Nevertheless, since DFF40 activity obviously decreased due to transfection with recombinant DFF40 (resulting in less internucleosomal DNA degradation and thus less DNA damage), less DNA damage in Jurkat cells was correlated with less caspase-3 activity as already seen in Raji cells. This decrease in DFF40 activity in Jurkat cells may be due to less activity of the recombinant DFF40 protein which possesses two tags which might generally affect a protein's biological activity. Importantly, this less active DFF40 enzyme was obviously sufficient to restore DFF40 activity in Raji cells which express only low levels of endogenous DFF40. In contrast, such a less active recombinant DFF40 protein might impair internucleosomal DNA cleavage in Jurkat cells since it displaced some of the endogenous DFF40 protein in these cells.

Preliminary statistical analysis (see chapter 2.2.6 for cogency of two-way ANOVA with replicated or unreplicated values) revealed significant differences ($p < 0.01$) in the caspase-3 activities of non-transfected and DFF40-transfected Jurkat cells. Still significant differences ($p < 0.05$) were detectable when comparing the caspase-3 activities of DFF40- and DFF45-transfected cells.

The changes, caused by transfection, observed in a comparison of the caspase-3 activities were not statistically significant ($p > 0.05$) when comparing:

1. Non-transfected cells to mock-transfected cells.
2. Non-transfected cells to DFF45-transfected cells.
3. Mock-transfected cells to DFF40-transfected cells.
4. Mock-transfected cells to DFF45-transfected cells.

However, it cannot be excluded that no statistical significant changes were detectable only due to the low number of experiments used in this preliminary statistical analysis.

As already observed in Raji cells, the overall interaction between the two parameters 'time' and 'transfection' was significant, which generally makes the p-values, resulting from two-way ANOVA, difficult to interpret (see chapter 2.2.6). As already detailed for Raji cells, this may be a consequence of the experimental design since differences in

the inducible caspase-3 activity in the differently transfected cell populations only became evident in the course of apoptosis.

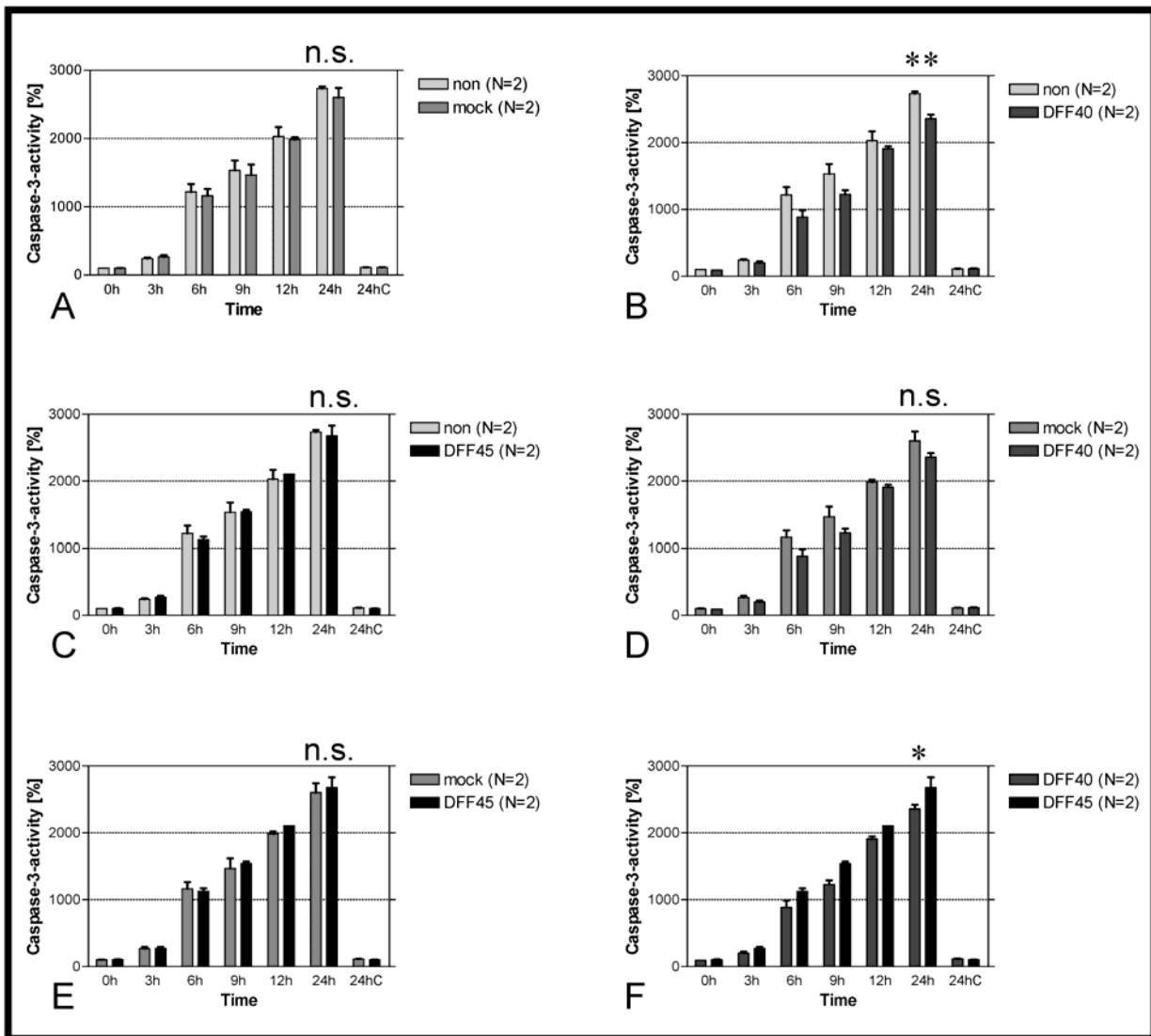


Figure 3-51: Caspase-3 activities in Jurkat cells: Two-way ANOVA with Bonferroni post-tests

Values resulting from the determination of caspase-3 activities after induction of apoptosis in transfected and non-transfected Jurkat cells were subjected to two-way ANOVA with Bonferroni-post-tests to evaluate significant differences between the groups (see chapter 2.2.6). Test results, obtained by comparing all four groups simultaneously, are depicted as follows: **A:** Non-transfected cells vs. mock-transfected cells (transfected with the empty vector). **B:** Non-transfected cells vs. DFF40-transfected cells. **C:** Non-transfected cells vs. DFF45-transfected cells. **D:** Mock-transfected cells vs. DFF40-transfected cells. **E:** Mock-transfected cells vs. DFF45-transfected cells. **F:** DFF40-transfected cells vs. DFF45-transfected cells. **n.s.:** $p > 0.05$ (not significant); *****: $p < 0.05$ (significant); ******: $p < 0.01$ (significant); *******: $p < 0.001$ (significant). Calculations were performed using the software GraphPad Prism 4.0. **Note:** These data are preliminary data since they are based on only two different transfection experiments.

3.3.7.2. Analysis of interaction by two-way ANOVA on column pairs

Since the analysis used so far indicated just an overall interaction, without showing the exact source of the interaction when comparing all of the four groups at a time, another 6 independent two-way ANOVAs were conducted comparing all combinable column pairs of two groups, respectively (see chapter 2.2.6). This allowed analysis of the interaction in every analyzed column pair, but resulted in slightly different p-values, compared with the values obtained in the former analysis, which compared all four groups at a time (compare chapters 3.3.4.1., 3.3.4.2, and 2.2.6). A significant interaction was found only in a comparison of the caspase-3 activities in DFF40-transfected Jurkat cells and DFF45-transfected Jurkat cells. The results are summarized in the following table (3-3).

	Parameter	Non	Mock	DFF40
Mock	<i>Time</i>	***		
	<i>Transfection</i>	n.s.		
	<i>Interaction</i>	n.s.		
DFF40	<i>Time</i>	***	***	
	<i>Transfection</i>	***	**	
	<i>Interaction</i>	n.q.s.	n.s.	
DFF45	<i>Time</i>	***	***	***
	<i>Transfection</i>	n.s.	n.s.	***
	<i>Interaction</i>	n.s.	n.s.	*

Table 3-3: Two-way ANOVA of Jurkat cells including analysis of interaction

n.s. $p > 0.1$ (not significant) **n.q.s.** $p < 0.1$ (not [quite] significant), *****: $p < 0.05$ (significant) ******: $p < 0.01$ (significant), *******: $p < 0.0001$ (significant). Analysis by pairwise two-way ANOVA resulted in slightly different p-values compared to the p-values obtained by two-way ANOVA with Bonferroni post tests. This test was performed to check for significant interactions: These were only detected in a comparison of DFF40-transfected cells vs DFF45-transfected cells **Note**: These data are preliminary data since they are based on only two different transfection experiments.

3.4. SUMMARY: APOPTOSIS IN STABLY TRANSFECTED CELLS

Analysis of apoptosis in stably transfected Jurkat and Raji cells indicated that the prerequisites for apoptosis vary considerably between different cell lines. At a first glance, the results obtained from experiments with the transfected cell lines seemed to be contradictory: Expression of recombinant DFF40 resulted in an increase of both DNA

fragmentation and caspase-3 activity in Raji cells, and just the opposite happened in transfected Jurkat cells. However, considering the background of endogenous proteins in Raji and Jurkat cells, may explain the differential behaviour of the cells which may be finally based on the same principle as detailed in the following.

The transfection experiments with Raji cells clearly demonstrated that recombinant DFF40, despite its tags, was principally able to act as a DNase, specifically catalyzing HMW- and nucleosomal DNA fragmentation during apoptosis. However, the enzymatic activity of recombinant DFF40 may have been slightly affected due to the attached tags. This may have resulted in lower enzymatic activities of the recombinant DNase compared with endogenous, native DFF40 in Jurkat cells. Transfection of Jurkat cells with recombinant DFF40 resulted in reduced endogenous DFF40 levels and less DNA damage in the course of apoptosis in these cells. Thus, overall DFF40 levels did not change in Jurkat cells. Just the opposite happened in Raji cells. Expression of endogenous DFF40 was generally low in Raji cells and therefore expression of additional, recombinant DFF40 in these cells did not displace endogenous DFF40. Consequently, recombinant DFF40, though possessing a comparably lower enzymatic activity, was able to restore previously lacking nucleosomal DNA fragmentation during apoptosis in Raji cells.

Interestingly, caspase-3 activities were correlated with the extent of DNA fragmentation in both cell lines. DNA fragmentation in Raji cells markedly preceded the strong increase of caspase-3 activity. This effect was less distinct, but still present, in Jurkat cells. These results suggest a cellular positive feedback loop which is induced by DNA damages in the cells during apoptosis. They support the hypothesis that an apoptotic downstream event (DNA fragmentation) contributes to progression of apoptosis presumably by enhancing pro-apoptotic signalling in cells due to the induced DNA damage. Occurrence of apoptotic HMW DNA was demonstrated in both Raji and Jurkat cells by increased phosphorylation of H2A.X, presumably induced by ATM kinase in response to apoptotic ds DNA damage.

Though caspase-3 activity was correlated with nucleosomal DNA fragmentation in Jurkat cells as well, an increase in both features occurred concomitantly and not consecutively as observed in Raji cells. However, HMW DNA fragmentation also preceded the major increase in caspase-3 activity in Jurkat cells, thus ATM-induced pathways may also contribute to enhanced apoptotic signalling in a positive feedback loop in Jurkat cells. Thus, it may be concluded that this positive feedback mechanism contributes to a varying extent to the progression of apoptosis in different cell types. Importantly, this feed back mechanism may enhance progression of apoptosis in cells which are delayed in progression of apoptosis.

4. DISCUSSION

The understanding of the molecular process of apoptosis is still a field of increasing interest in biology. To date, it is a commonly accepted fact that a multicellular organism cannot exist without a tight regulation of divisions, growth, differentiation, and death in its cells. An important player in this game is apoptosis: A process involved both in the physiological and silent removal of excess cells, e.g. during development, and in pathological processes e.g. during certain diseases. The latter may be caused by either too much or too little apoptosis.

The main focus in recent and current studies on apoptosis was generally directed to the activation of caspase and the resulting consequences. Indeed, this is a major feature of apoptosis, though in recent years other caspase-independent but evolutionary conserved signalling pathways to apoptosis emerged. Nevertheless, an understanding of more subtle details of apoptosis may elucidate some of the processes during pathological conditions due to lacking or excess apoptosis. These lacking 'pieces in a giant puzzle' may finally help to solve relevant clinical problems e.g. during the therapy of diverse cancers types. Little is known about the apoptotic processes going on during cancer therapy in vivo and about the reasons for developing or pre-existing resistance which may finally determine success or failure of the chosen therapy (*Fulda and Debatin, 2004; Dai et al., 2004; Longley and Johnston, 2005*).

Cultured lymphoma cell lines are a commonly used model to study apoptosis. However, the results have to be interpreted with caution since it is an in vitro model which does not reflect the possible interactions of different cells in an organism. Most of the apoptotic cells studied in this cell system would not even exist under physiological conditions since they would be readily engulfed by phagocytic cells in vivo. However, the conditions during pathological excess of apoptosis in vivo may be more similar to the cell culture system because phagocytic cells may be overcharged by masses of dying cells. Persisting dead cells may finally induce an inflammatory or autoimmune response in vivo. Thus, an in vitro observed process called secondary necrosis may also contribute to pathological conditions in some types of diseases involving excess apoptosis.

DNA fragmentation during apoptosis is often regarded as an event at the end of the apoptotic signalling cascade (an 'apoptotic downstream event') which does not affect the course of apoptosis. Unquestionable, DNA fragmentation is not necessary to kill the apoptotic cell, and most of the physiologically occurring apoptotic events proceed in a

speed which does not even allow DFF40-catalyzed DNA fragmentation before the cell disappears by being engulfed from surrounding cells. Probably, in most physiological apoptotic processes the cell is already engulfed and digested by other enzymes before DFF40 can start its DNA-destroying activities. So, why has this evolutionary conserved and even redundant mechanism (i.e. caspase-independent DNA fragmentation by EndoG) for apoptotic DNA inactivation been developed at all? The matter is not as simple as it seems in this case, and other environmental factors presumably contributed to the evolution of apoptotic DNA-degrading enzymes. Examples for such environmental factors are e.g. parasites or viruses. Since they are specialized on escaping the immune systems of their hosts, these biological factors contributed considerably to the development of adequate defense strategies in their hosts which may subsequently have been interwoven into the cellular apoptotic signalling net work. Some cellular parasites are able to escape lysosomal DNA degradation in the lysosomes of macrophages, e.g. during tuberculosis. These parasites are even safe from other immune responses because they propagate in an immune-privileged compartment. This is just one example demonstrating that there is obviously a strong selective pressure to optimize the strategies in dealing with potentially dangerous 'biological waste' DNA since a commonly used pathway may fail. Regarding the high amount of potentially dangerous DNA which may be included in a dying cell, e.g. by transposons from viral DNA or oncogenes, it is easy to see that evolutionary selection will favour such organisms that are able to cope with this potentially pathogenic DNA by developing adequate strategies. One of these strategies may be a cell-autonomous and fast inactivation of DNA in dying cells. Internucleosomally cleaving enzymes like DFF40 or EndoG are enzymes that may be regarded as specialists for a fast inactivation of DNA because they cleave the DNA into regular 200 bp fragments, irrespective of the DNA sequence, which will inactivate most genes immediately, thus also silencing any hazardous DNA.

Furthermore, DNA fragmentation may enhance apoptotic signalling in 'borderline cells', which received only a weak pro-apoptotic signal or which contain high amounts of anti-apoptotic 'veto'-molecules, e.g. bcl-2 or IAPs. Such 'borderline cells' are really to be regarded as cells persisting at the borderline to apoptosis: Just a little tip in the balance might either rescue or kill the cell ultimately. Since many human cancer types are quite resistant to apoptosis as a consequence of an enhanced expression of anti-apoptotic proteins (prominent and often cited example: Bcl-2 overexpression in B cell lymphoma cells) or decreased expression or lack of pro-apoptotic proteins (e.g. lack of functional caspase-3 in some cancer cell types), there is a need for understanding the basic

networks and the search for mechanisms which may override the anti-apoptotic effects of these molecules.

One way to enhance progression of apoptosis may be an enhancement of the initial apoptotic signalling. Since DNA damage contributes to apoptotic signalling, it may be beneficial to promote an effective DNA cleavage in cells which lack DFF40 activity and do not undergo internucleosomal DNA degradation during apoptosis. Therefore, it is useful to further characterize the conditions which affect DFF40 activity. Former studies already demonstrated a role for HMG-1, HMG-2, HSP-70, topoisomerase I, and histone H1 in enhancing DFF40 activity in vitro. However, it was not yet clear if different H1 subtypes or differentially modified H1 histones have diverse effects on DFF40 activity. In particular, the differentially modified H1 histones were initially supposed to affect DFF40 activity differently because a dephosphorylation of H1 histones was seen prior to DNA degradation during apoptosis in HL60 cells (*Kratzmeier et al., 2000*).

The experiments in the present study were carried out using plasmid DNA as a substrate for recombinant DFF40. This experimental design does not reflect the in vivo conditions in a correct manner because it did not include the complex structure of chromatin, and furthermore, they were carried out with recombinant proteins. However, the experimental approach using plasmid DNA is well characterized and reliable because it had already been used to test the DNase activity of DFF40 in vitro (*e.g. Enari et al., 1998*). The use of recombinant proteins provides a reproducible experimental protein background and controlled experimental conditions as a first approach. Subsequently, cellular proteins were integrated into the experimental design to confirm the previously obtained results with recombinant proteins.

4.1. CHARACTERIZING THE RECOMBINANTLY EXPRESSED PROTEINS

4.1.1. PURIFICATION OF H1 HISTONE SUBTYPES FROM YEAST

The family of histone proteins is an evolutionary conserved group of basic proteins and includes 5 classes: H1, H2A, H2B, H3, and H4. Comprising the major protein component of chromatin in eukaryotic cells, histones are essential for the formation of the chromosomal fiber since they are responsible for the nucleosomal organization of DNA in eukaryotes. Thus, histones arrange the first and the second level of packaging DNA into chromatin. The core histones H2A, H2B, H3, and H4 form the core octamer which is formed by two of each core histones and serves to spool up ~ 146 bp of DNA on this 'core of a coil'. DNA is wrapped twice around the octamer, thus forming an intermediate structure which is called the chromatosome (*Simpson, 1978*). Histone H1 'seals' this

chromatosome by associating to a part of the linker DNA, ~20 bp in length, at its entry/exit site on the outside of the core histone octamer (*Allan et al., 1986*). Core particle, linker DNA, and linker histone H1 form a structure called nucleosome which is the basic repeat structure of eukaryotic DNA. The nucleosomes are arranged like beads on a string in an environment of low ionic strength, forming the 10 nm fiber. They are connected by a linker DNA strand (the 'string') which is generally more susceptible to nuclease digestion than the DNA which is wrapped around the core particle (the 'bead') (*reviewed in Olins and Olins, 2003*). The association of H1 histones to the linker DNA and to adjacent nucleosomes leads to a further 'second level' compaction of DNA, resulting in the formation of the 30 nm fiber.

H1 histones are the most divergent class of histones (*Cole, 1984; Doenecke et al., 1997*). The complete set of seven subtypes of H1 histones has been characterized, and they may be readily expressed in transformed yeast cells from which they are selectively extractable by using 5% PCA (*Johns and Butler, 1962*). Though yeast presumably possesses H1 histone-like proteins (*Ushinsky et al., 1997; Conconi and Wellinger, 2003*), these endogenous yeast proteins are obviously not extractable using 5% PCA.

Consistent with the data obtained before, the expression levels of the recombinant H1 histone proteins in yeast varied considerably in the present study. Expression of subtype H1^o was higher than that of H1.1 and H1t; expression of the latter was very low (see figure 3-9 on page 120). This may be explained by the higher lysine content of H1^o or the higher arginine content in H1t, respectively, when comparing these H1 histone subtypes to the other ones (*Albig et al., 1998; Wellman et al., 1997; Gerchman et al., 1994*). Consistent with former results, the PCA-extracted H1 histones, heterologously expressed in yeast, were very pure as demonstrated by SDS-PAGE (see figure 3-9 on page 120).

In contrast to other groups who described rapid yeast cell death as a consequence of even low level expression of exogenous H1 histones from sea urchin (*Miloshev et al., 1994*), the yeast cells used in this study were quite viable and seemed not to be affected by the expressed recombinant human H1 histones. However, mammalian H1 histones are obviously less toxic than sea urchin H1 histones since *Linder and Thoma (1994)* observed survival of yeast expressing mammalian H1 histones at low levels. However, high levels of recombinant H1 histones also affected survival of the yeast cells.

4.1.2. PURIFICATION OF CASPASE-3 FROM YEAST

Caspase-3 is a potent effector caspase in mammalian cells and rapidly induces apoptosis in these cells as soon as it is activated. In contrast to its deadly effects in mammalian cells, expression of caspase-3 in yeast is obviously possible without instantly killing the yeast cells as demonstrated in this study: It was observed that the yeast cells were only retarded in cell growth. This may be a general feature of *S. cerevisiae* since a delay in cell growth but no cell death in yeast upon expression of caspase-3 was described by *Wright et al. (1999)*.

Furthermore, purification of caspase-3 from yeast generally yields the active caspase enzyme. This may be due to a yeast enzyme which perhaps cleaves recombinant caspase-3 in the required manner or by auto-activation. The latter was previously demonstrated: Under in vivo conditions caspase-3 does not auto-activate because activated caspase-3 does not cleave procaspase-3. However, high concentrations of the enzyme during high-level expression in yeast may result in an artificial auto-activation procedure of caspase-3 which is not likely to occur in mammalian cells (*Sun et al., 1997*).

The caspase-3 preparations obtained after Ni-NTA chromatography were quite pure, and contaminating proteins were hardly detectable in SDS-PAGE (see figure 3-5 on page 116). The presence of both cleaved and uncleaved caspase-3 in the purified preparations was additionally confirmed in western blots (see figure 3-6 on page 117).

4.1.3. PURIFICATION OF DFF40/DFF45 COMPLEX FROM BACTERIA

Expression of catalytically active DFF40 is only possible in the presence of its chaperone and inhibitor DFF45. DFF45 is obviously able to exert its chaperone activity by itself during expression of DFF40 in *E. coli* and does not need the assistance of HSP-70 and HSP-40, which was described to assist correct folding of DFF40 in vitro (*Nagata et al., 2002*) to generate a functional DNase. Though the enzyme complex purified by Ni-NTA chromatography still was not very pure as demonstrated by SDS-PAGE (see figure 3-3 on page 114), it contained DFF40 without any doubt since DFF40 was detected in western blots (see figure 3-4 on page 115). The main issue of this study was the purification of a functional DFF40 enzyme, which is a tricky procedure since DFF40 is a labile enzyme which rapidly degrades in vitro and loses its DNase activity. Indeed, the enzyme's rapid loss of activity was the reason why experiments conducted by Liu et al. initially failed to prove its DNase activity (*Liu et al., 1997; Nagata, 2003*). Therefore, the main concern of the purification experiments during the study in hand was to prove a DNase activity specific for DFF40 in the preparations, in the first instance. Since bacteria

contain various endonucleases, a contamination with these abundant enzymes would be fatal for the interpretation of the following experiments and thus had to be excluded carefully.

DFF40-specific DNase activity in the experiments was demonstrated by including controls for specific activation of the DNase by caspase-3 in the experimental design. Plasmid DNA incubated with DFF40/DFF45 complex in the absence of caspase-3 was not degraded, whereas addition of caspase-3 generated a DNase activity. Importantly, caspase-3 on its own did not cause DNA degradation either. Therefore, only co-incubation of caspase-3 and DFF40/DFF45 complex was able to generate the DNase activity as demonstrated e.g. in figure 3-7 on page 118 and in figure 3-8 on page 119. As already mentioned before, caspase-3 cleaves the inhibitor DFF45 and releases active DFF40. Since no caspase-activated DNases exist in bacteria, the DNase activity released by co-incubation of recombinant DFF40/DFF45 complex with recombinant caspase-3 may be regarded as specifically and exclusively caused by DFF40. Furthermore, the recombinant DFF40 protein was able to generate the characteristic DNA ladder when degrading DNA from purified nuclei (see figure 3.20 on page 135).

4.2. FACTORS INFLUENCING THE ACTIVITY OF DFF40 IN VITRO

4.2.1. EFFECT OF DIFFERENT H1 HISTONE SUBTYPES

As already mentioned above, H1 histones are the most variable members of an evolutionary conserved histone protein family. H1 histones are proteins with a molecular weight of ~21 kDa and may be subdivided in two groups: The main types H1.1, H1.2, H1.3, H1.4, and H1.5, and the germ cell specific subtype H1t and replacement subtype H1^o which do not depend on DNA replication for expression. (*reviewed in Doenecke et al., 1997*).

All H1 histones possess three domains: A conserved DNA-binding central globular domain (*Allan et al., 1980*), a lysine-rich and highly variable N-terminal domain which is involved in positioning the respective H1 histone at its binding site (*Allan et al., 1986*), and a C-terminal domain which is presumably essential for the formation of higher order chromatin structures (*Thoma et al., 1983*).

As demonstrated in the study in hand, H1 histone subtypes affected DFF40 activity in different ways. High concentrations of linker histones generally inhibited DFF40 activity, whereas lower concentrations enhanced DFF40 activity. The effects were clearly dependent on the H1 histone concentration (see chapter 3.1.2). The activating effect presumably reflects the *in vivo* features in a correct manner since the inhibiting concentrations of linker histones are presumably not found in natural chromatin.

Strikingly, most efficient activation of DFF40 was seen in a concentration range of 0.5 to 1.5 μg histone per μg of DNA, which is a DNA/histone ratio quite similar to that presumably found in vivo. This approximation is based on the assumption that one bp of DNA has an average molecular weight of 650 grams per mol, and each nucleosome binds one linker histone. Thus, the DNA from one nucleosome has a molecular weight of ~ 13 kDa (200bp), and the corresponding H1 histone has a molecular weight of ~ 21 kDa (one mol nucleosomal DNA binds one mol H1 histone). Consequently, the expected physiological DNA/H1 histone ratio would be ~ 0.5 μg H1 histone per μg DNA.

It is likely that the H1 histones bind to the plasmid DNA by their globular DNA-binding domain even under in vitro conditions. As DFF40 directly interacts with H1 histones (*Liu et al., 1999*), binding of H1 histone to the plasmid DNA may enhance DFF40 activity by targeting the DNase to the plasmid DNA. In contrast, at high concentrations of H1 histones in the in vitro assay, the plasmid DNA may be covered all over with H1 histones. In this scenario DFF40 is targeted to the plasmid as before, but it does not reach its substrate because it is covered by H1 histones. An inhibition of DFF40 activity to this extent by H1 histones using a plasmid substrate was not described before, though *Widlak et al. (2000)* reported that H1 histones activated DFF40 on chromatin substrates much less intensive than it did on plasmid substrates. Accordingly, the study in hand demonstrated inhibition of DFF40 DNase activity in purified nuclei when high amounts of H1 histones were present in the reactions (see figure 3-20 on page 135). It is likely that high concentrations of H1 histones in this experiment prevented DFF40 from being targeted to the H1 histones of the chromatin substrate and thus prevented DFF40 from digesting the nuclear DNA.

Concerning the different H1 histone subtypes, there were no significant differences in activating or inhibiting DFF40 activity in vitro in the study in hand when comparing the main subtypes H1.2, H1.3, and H1.4 (see chapter 3.1.2). This may be due to the chemical similarity of these proteins. The five main type H1 histones possess an overall sequence similarity of 60 to 85% (*Drabent et al., 1995*), and their chemical features are presumably quite similar to each other since e.g. only refined electrophoretic methods are able to separate the different subtypes (*Lindner et al., 1993, 1995*). However, activation characteristics of H1^o on DFF40 differed considerably from that of H1.2, H1.3 and H1.4. H1^o activated DFF40 in a broader concentration range (~ 1 to 3 μg per μg DNA). This difference may be caused by the different molecular structure of H1^o compared with the main H1 subtypes. It differs from the other H1 histone subtypes since it has an even higher lysin content and an overall length of 193 amino acids (instead of 210 to 225 amino acids for the other H1 subtypes) (*reviewed in Doenecke et al., 1994*).

Interestingly, H1 histones are clearly different in their effect on DFF40 compared with the core histone H3. Only an inhibiting but no activating effect of H3 histone was seen in the study in hand (see figure 3-14 on page 126). This inhibiting effect at high concentrations may have the reason already discussed above for high concentrations of H1 histones: High amounts of histone H3 are likely deposited on the plasmid DNA and thus may hide the substrate from the DNase. It may be concluded that H3 does not interact with DFF40 and thus is unable to target DFF40 to the plasmid substrate *in vivo*. However, since histone H3 is located inside the core of the nucleosome *in vivo*, this inhibiting effect is presumably of no biological significance.

4.2.2. EFFECT OF PHOSPHORYLATED H1 HISTONES ON THE ACTIVITY OF DFF40

Phosphorylation of H1 histones plays a major role in the structural organization and functions of chromatin *in vivo* (*reviewed in Th'ng, 2001*). A correlation between histone phosphorylation and mitosis is commonly observed (*Hendzel et al., 1997; Sauve et al., 1999*), and phosphorylation of histone H1 and histone H3 is thought to allow mitotic chromatin condensation because phosphorylation presumably interrupts histone-DNA interactions (*Kaplan et al., 1984*) and thus allows interaction with chromatin condensing proteins. This way, phosphorylation contributes to the reorganization of chromatin during mitosis. The protease involved in phosphorylation of H1 during mitosis was reported to be p34^{cdc-2} kinase, and activation of this kinase was reported to occur during cell death in various cell lines. From these results it was initially concluded that apoptotic cells were dying by premature mitosis, but other reports did not support this idea since activation of p34^{cdc-2} is not a general prerequisite for apoptosis (*reviewed in Th'ng, 2001*).

Phosphorylation of H1 histones was demonstrated during thymocyte apoptosis (*Lee et al., 1999; Enomoto et al., 2001*). However, phosphorylation may have occurred in these cells due to increased phosphorylation of nuclear proteins as a consequence of the apoptosis inducer used in the experiments (a phosphatase inhibitor). Interestingly, a kinase was later identified which changed its substrate specificity during apoptosis: Upon cleavage by caspase-3, the mammalian sterile twenty (MstI) kinase catalyzed phosphorylation of H2B at serine 14 both *in vitro* and *in vivo* (*Cheung et al., 2003*). Perhaps, there are even more kinases which change their substrates after being cleaved by caspase-3 or another caspase. Such a putative kinase may be responsible for other to date unsettled phosphorylation events during apoptosis. The opposite scenario, i.e. cleavage of a phosphatase may change its substrate affinity, thus leading to dephosphorylation of certain proteins during apoptosis, may be also imaginable.

In contrast to these reports, it has been described in several reports that H1 histones are dephosphorylated during apoptosis (*Kratzmeier et al., 2000; Talasz et al., 2002*). Dephosphorylation of H1 histones may generally result from a response to DNA damages because it was reported to occur in irradiated cells by an ATM-dependent signalling transduction pathway (*Guo et al., 1999*; compare chapter 1.3.3.2.). Two different and independent impacts are imaginable: DNA damage, e.g. by irradiation or DNA-damaging agents, or DNA damage by apoptotic DNases, e.g. DFF40. Dephosphorylation of H1 histones was recently shown to occur as a consequence of the cell cycle arrest in response to apoptotic DNA damage (*Happel et al., 2005*). Interestingly, H1 histone dephosphorylation was observed in cells undergoing apoptosis induced by both TNF α and Topotecan. Since Topotecan causes DNA damages, a dephosphorylation of H1 histones may be expected to be a consequence of the DNA damage caused by the apoptosis inductor in this apoptosis system. Importantly, concomitantly with DNA HMW fragmentation, dephosphorylation of H1 histones also occurred in the receptor-mediated, extrinsic pathway after induction with TNF α (*Talasz et al., 2002*). Thus, it may be concluded that apoptotic DNases have an important part in generating the DNA damage which finally results in cell cycle arrest and dephosphorylation of H1 histones. Furthermore, even early HMW DNA damage is sufficient to trigger cell cycle arrest and dephosphorylation of H1 histones during apoptosis. Thus, dephosphorylation of H1 histones may precede internucleosomal DNA cleavage as already observed by *Kratzmeier et al. (2000)*. Dephosphorylation of H1 histones induced by irradiation is thought to be the result of both inhibiting regulation of cyclin dependent kinase activities and activation of H1 histone phosphatase activities (*Guo et al., 1999*)

Since phosphorylation of proteins introduces considerably high amounts of negative charges into the respective protein, this might subsequently affect interactions with other proteins. So, the next issue of the study in hand was to check whether phosphorylation or dephosphorylation of H1 histones affects the interaction with DFF40 and thus influences the catalytic activity of DFF40. Subtype H1.2 was chosen as a substrate for cdc2 kinase since cdc2-like kinases readily phosphorylate H1 histones (*Sweet et al., 1997*). Furthermore, H1.2, as well as H1.4, is one of the two most abundant H1 histone subtypes which are found in almost all mammalian tissues (*Doenecke et al., 1997*). Though histone H1.2 was even hyperphosphorylated by cdc2 kinase, as demonstrated by its differential migration features in SDS-PAGE compared with unphosphorylated H1.2 (see figure 3-15 on page 127), there were no differences detectable in the effects on DFF40 using plasmid DNA as a substrate (see figure 3-16 on page 128). This may indicate that phosphorylation of H1.2 by cdc2 occurs at sites of

H1.2 which are obviously indifferent for the interaction with DFF40 or DNA or, alternatively, that phosphorylation of H1.2 itself does not affect binding of DFF40 or DNA. However, the latter is not very likely since phosphorylation of H1 histones is generally thought to regulate activity of chromatin by destabilizing H1-DNA interactions, resulting in a more open chromatin structure which facilitates both the access and the activity of the replication and transcription machineries (*Chadee et al., 1995; Chadee et al., 1997; Halmer and Gruss, 1996*). Thus, increased phosphorylation of H1 histones leads to relaxation of active chromatin whereas dephosphorylation condenses and thus inactivates chromatin structures.

Recently, another kinase, CDK2, was reported to regulate H1 histone mobility in chromatin (*Contreras et al., 2003*); hence, phosphorylation of H1.2 by other kinases might have yielded other results than those obtained in this study using cdc2-hyperphosphorylated H1.2. Since H1.2 contains only four cyclin dependent kinase phosphorylation consensus sites which are phosphorylated in vivo (*Talasz et al., 1996*), in-vivo phosphorylated H1.2, containing four phosphate groups or less, does not change its migration features during conventional SDS-PAGE as observed in this study. Since different phosphorylation sites or even other posttranslational modifications might affect DFF40 activity in vivo, the following experiments were carried out with cellular H1 histones extracted from both control HL60 cells and HL60 cells induced for apoptosis with Topotecan. (In this study apoptosis in human lymphoma cells was generally induced by the topoisomerase I inhibitor Topotecan. Topotecan as an inducer of apoptosis is discussed in chapter 4.3.2).

4.2.3. EFFECT OF H1 HISTONES FROM APOPTOTIC AND CONTROL HL60 CELLS

The advantage of using H1 histones modified in vivo during apoptosis is obvious: It allows a statement concerning the effects of any in vivo occurring posttranslational modification of linker histones on DFF40 activity. Since in vivo modified H1 histones do not change their migration features during conventional SDS-PAGE, CZE was used to confirm H1 histone modifications due to phosphorylation because this method was already established for histone from HL60 cells by *Kratzmeier et al. (2000)*. They demonstrated dephosphorylation of H1 histones in cells by a decrease in the incorporation of ^{32}P into H1 histones from apoptotic HL60 cells compared with control HL60 cells and confirmed this result by CZE. As demonstrated by independent studies, changes in the total net charges of a protein due to phosphorylation are sufficient to separate differently phosphorylated forms of a molecule by CZE (*Dawson et al., 1994; Wei et al., 1998; Gamble et al., 1999*). The ability of CZE to separate phosphorylated H1 histones variants has been initially demonstrated by *Lindner et al. (1992)*.

Furthermore, *Kratzmeier et al. (1999)* were able to separate differently phosphorylated H1.2 histone subtypes by CZE and to relate the peaks of in vitro phosphorylated H1 histone subtypes to the peaks obtained from the different subtypes of in vivo phosphorylated/dephosphorylated H1 histones from HL60 cells. Changes in the respective peak heights indicated a decrease of the relative amounts of phosphorylated subtypes which were concomitantly observed with increases in the relative amounts of the respective dephosphorylated subtypes.

As demonstrated by CZE in the study in hand, the H1 histones purified from both control and apoptotic HL60 cells were differently modified as demonstrated by their respective phosphorylation state. As expected, H1 histones from apoptotic HL60 cells showed the typical changes in the peak pattern due to dephosphorylation compared with H1 histones from control HL60 cells (see figure 3-18 on page 132). However, other putative posttranslational modifications (poly ADP ribosylation) on the cellular H1 histones could not be detected in the separation system used. Yet, they might have affected the results obtained with these H1 histones in the in vitro assays. Clearly, there were no differences in the activating and inhibiting effect on DFF40 activity detectable in the plasmid assay when comparing the cleavage pattern obtained by co-incubation with H1 histones from apoptotic or control HL60 cells, respectively (see figure 3-19 on page 133).

Taken together, it may be concluded that modifications of H1 histones, despite obvious changes in the net protein charges by phosphorylation, do not affect DFF40 activity in vitro. However, the substrate used in the in vitro assay clearly differs from the in vivo substrate of DFF40 since the latter is a highly ordered structure with several levels of packaging which is not present in the plasmid DNA used in the in vitro assays. Nevertheless, it may be concluded that posttranslational modifications of H1 histone play a minor part, if any, in affecting DFF40 activity in vivo. Caspase activity or even caspase-independent pathways generally lead to marked overall structural changes in the nucleus which presumably have much more dramatic consequences for apoptotic chromatin fragmentation. These marked apoptotic structural changes occur e.g. by caspase-catalyzed cleavage of specific proteins in the nuclear matrix and may thus override any putative effects of posttranslational modifications on the participating proteins, e.g. on the chromatin 'packaging materials'. Work from another study supports this hypothesis. *Schliephacke et al. (2004)* reported exclusion of the telomeric region and random cleavage of bulk chromatin during apoptotic DNA fragmentation in various cell lines. The telomeric region may be protected by being packaged more densely than the bulk chromatin, thus leaving 'footprints' of undigested chromatin regions during early apoptotic DNA degradation since the DNA is protected by higher

order structures. Furthermore, since HMW DNA fragmentation frequently occurs at sites which are obviously determined by the attachment regions of DNA to the nuclear matrix (*Gromova et al., 1995; Khodarev et al., 1998; Schoenlein et al., 1999*). This is one more hint suggesting that higher order structures of the nuclear architecture influence apoptotic DNA degradation rather than single proteins and their posttranslational modifications. As already mentioned in chapter 1.3.4.2.1, active oligomerized DFF40 has a deep cleft which presumably recognizes the overall structure of nucleosomes rather than single linker histones.

4.2.4. EFFECT OF OTHER CELLULAR PROTEINS ON THE ACTIVITY OF DFF40

The following experiments were carried out in search for a presumably cytoplasmic factor which was supposed to contribute to the enhanced resistance of the Burkitt lymphoma B-cell line Raji towards induction of apoptosis compared with other lymphoma cell lines, e.g. promyelocytic HL60 cells or the T-cell line Jurkat.

Apoptosis plays an important role in shaping the B-cell repertoire of the immune system and is involved in three steps during B-cell maturation. Firstly, non-productive V(D)J rearrangement of the antibody heavy-chain and light-chain genes at the pro and pre B-cell stages results in the failure to produce an effective immunoglobulin receptor. This receptor is indispensable for survival of the immature B-cells because it saves the B-cell from being killed by lacking positive selection. Secondly, those cells that successfully rearranged their antibody genes but present an autoreactive B-cell receptor on their membrane are probably deleted by apoptosis during negative selection (unless they are saved by receptor editing). Thirdly, mature, antigen-activated B-cells are stringently selected for improved antigen affinity during clonal expansion in the germinal center, and less 'effective' B-cells die by apoptosis (*reviewed in Janeway and Travers, 1999*).

Thus, apoptosis may be readily induced in B-cells, and these cells are often used to investigate mechanisms for induction of apoptosis or resistance to apoptosis. As cancer cells often change their susceptibility to induction of apoptosis, many B-cell lymphoma cell lines have been established for cell culture.

The B-cell lymphoma cell line Raji is often reported to be either resistant to apoptosis induced by various apoptotic stimuli or to be at least delayed in cell death which is accompanied by lacking apoptotic internucleosomal DNA cleavage in this cell line (*Macklis et al., 1993; Kawabata et al., 1999; Hirokawa et al., 2002; Luciano et al., 2002*). In contrast, the promyelocytic cell line HL60 was reported to undergo apoptosis readily with concomitant internucleosomal DNA cleavage upon treatment with various apoptosis inducers (*Walker et al., 1994; Dubrez et al., 1995; Shimizu and Pommier, 1996*). Work of other groups as well as the study in hand demonstrated a comparable

susceptibility of purified nuclei from both HL60 and Raji cells to apoptotic DNA fragmentation (see figure 3-22 on page 137, and figure 3-23 on page 139), suggesting that there are no differences in the nuclei themselves which affect the susceptibility to DNA degradation: Cytoplasmic extracts from apoptotic HL60 cells induced DNA fragmentation in Raji nuclei whereas cell lysates from apoptotic Raji cells failed to induce DNA fragmentation in both Raji and HL60 nuclei (*Kawabata et al., 1999*). Accordingly, by using recombinant DFF40, the study in hand demonstrated that Raji cytoplasm inhibited DFF40 activity in both HL60 and Raji nuclei (see figure 3-22 on page 137) or on plasmid DNA (see figure 3-26 on page 142). In contrast, DFF40-catalyzed DNA degradation in both types of nuclei was still observed in the presence of cytoplasm from HL60 cells; and HL60 cytoplasm even enhanced DFF40 activity on plasmid DNA (see figure 3-26 on page 142).

Furthermore, recombinant caspase-3 was able to induce a DFF40-like DNase activity in HL60 cytoplasm which resulted in DNA laddering in both HL60 and Raji nuclei, whereas caspase-3 failed to induce this nuclease activity in Raji cytoplasm (see figure 3-23 on page 139).

In contrast to the DFF40-activating effect of native HL60 cytoplasm, heat-treated cytoplasm from both HL60 and Raji cells had an inhibitory effect on DFF40 catalytic activity when digesting plasmid DNA (see figure 3-25 on page 141). This indicates that the inhibitory effect is caused by a heat-stable protein whereas the activating effect may be caused by a heat-labile protein. Interestingly, the inhibitory effect of HL60 cytoplasm was less distinct than the inhibitory effect of Raji cytoplasm and correlated well with the expression levels of DFF45 in these cell lines: High levels of DFF45 were expressed in Raji cells and comparatively lower levels were detectable in HL60 cells (see figure 3-27 on page 143). Thus, it may be assumed that DFF45 is the heat stable factor which inhibits DNA fragmentation in the presence of Raji cytoplasm. On the other hand, the heat labile factor which may be responsible for enhanced DNA degradation in the presence of native HL60 cytoplasm may even be the heat-labile DFF40 itself in this experiment since relatively high levels of DFF40 were detectable in HL60 cytoplasm and only minute amounts of DFF40 were found in Raji cytoplasm. Thus, it may be concluded that a factor (e.g. DFF40) responsible for DNA fragmentation in HL60 cytoplasm is activated as a consequence of caspase-3 activity and that this factor is either heat-labile (a known feature of DFF40) or inhibitable by a heat stable factor (a known feature of DFF45) or that even even both factors contribute to the results. In contrast, caspase-3 was unable to induce a DNA fragmentation activity in Raji cytoplasm which rather inhibited caspase-induced DNA fragmentation. Interestingly, cytoplasm of Raji cells contains large amounts of DFF45 and this heat-stable protein

was still detectable in both Raji and HL60 cytoplasm after heat treatment, suggesting that DFF45 is responsible for the inhibiting effect on DNA fragmentation in Raji cytoplasm and heat-treated HL60 cytoplasm.

Furthermore, cleaved DFF45 was detectable in apoptotic Raji cells indicating that the pathway to apoptosis is defective downstream of caspase-3 in Raji cells, and this was observed also by *Kawabata et al. (1999)*. However, the study in hand demonstrated still residual amounts of intact DFF45 in Raji cells during late stages of apoptosis. Importantly, endogenous DFF45 in Raji cells was able to act as a chaperone on recombinant DFF40, and endogenous DFF45 was obviously able to release functional recombinant DFF40 during apoptosis in DFF40-transfected Raji cells. Hence, it may be concluded that DFF45 from Raji cells is cleaved at both caspase-3-consensus sites during apoptosis and that Raji DFF45 is generally cleavable in the required way to release active DFF40 from the complex. Thus, Raji DFF45 presumably does not differ in its functions from DFF45 protein of other cells which readily undergo DNA fragmentation during apoptosis, and incomplete cleavage of Raji DFF45 may have occurred rather due to high expression levels of DFF45 and/or low caspase-3-like enzymatic activities in Raji cells.

Since p53 levels were reported to be normal in Raji cells, and bcl-2 levels were reported to be even lower in Raji cells compared with HL60 cells (*Kuroki et al., 1996*), another cytoplasmic factor downstream of caspase-3 activity was suggested to contribute to the enhanced resistance to apoptosis in Raji cells compared with other cell types. *Kawabata et al. (1999)* supposed a functional defect in the DFF40 protein as a reason for lacking internucleosomal DNA cleavage. However, a functional defect in the DFF40 protein can be excluded from data obtained in the course of the study in hand during generation of the transfection vector. Sequence analysis was conducted to confirm the correct sequence of the respective insert DNA for the transfection vector. It furthermore revealed no differences in the Raji DFF40 mRNA sequence, obtained by RT-PCR, compared with both Jurkat and HeLa DFF40 (data not shown). Thus, it is more likely that low expression levels of DFF40 may be a sufficient reason for lacking apoptotic DNA fragmentation in Raji cells. Since the expression levels of the inhibitor DFF45 were comparably high in Raji cells compared with cell types which undergo DNA laddering during apoptosis, it may further be concluded that uncleaved DFF45 has additional inhibitory effects on residual DFF40 activity in Raji cells during apoptosis. This may explain why in the study in hand cytosolic preparations from Raji cells inhibited activity of recombinant DFF40 on plasmid DNA whereas cytosolic preparations of HL60 cells enhanced DFF40 activity on plasmid DNA (see figure 3-26 on page 142).

Since Raji cells, which lack apoptotic DNA degradation, are more resistant to apoptosis than HL60 or Jurkat cells, which readily undergo chromatin cleavage during apoptosis, these cells were considered to be suitable to test a new hypothesis: Does DFF40 activity contribute to the performance of apoptosis by inducing additional DNA damage in the cells or, alternatively, does lacking DNA fragmentation during apoptosis in Raji cells contribute to the delayed progression of apoptosis in these cells?

Furthermore, the question arose whether DFF45 is also generally able to inhibit DFF40 activity in vivo and might thus contribute to apoptosis resistance or delayed progression of apoptosis in cells which express the inhibitor at high levels. So, large amounts of DFF45 expressed in Raji cells were supposed to contribute to lacking DNA fragmentation and delayed progression of apoptosis in Raji cells. Though Raji DFF45 was shown to be generally cleavable by caspase-3, residual DFF45 was still present at late stages of apoptosis in Raji cells, and might thus still inhibit the small amount of activated DFF40 in Raji cells. Hence, the following experiments were conducted to alter the ratio of DFF40 and DFF45 protein in the cells, and to look for concomitant changes in the progression or extent of apoptosis.

4.3. FACTORS AFFECTING PROGRESSION OF APOPTOSIS IN VIVO

As already detailed in the introduction, DNA damage is a potent inducer of apoptosis via p53-dependent or p53-independent signalling pathways. Therefore, it may be supposed that DNA damage caused e.g. by DFF40 even may enhance apoptosis in vivo, or that lacking DNA damage, caused e.g. by too little DFF40 activity or enhanced expression of the inhibitor DFF45, might contribute to apoptosis resistance in some cell types. However, it should be mentioned in advance that the results from these studies presumably apply only to the conditions during weak pro-apoptotic signalling (i.e. conditions in cells at the borderline to apoptosis). Progression of full-blown apoptosis caused by administration of strong apoptosis inducers is a fast process which leads to a functional shut-down of the cell within 30 to 60 minutes (see chapter 1.3.1.2). DNA fragmentation in those cells is clearly a downstream event, and it is dispensable for cell death itself since the cell usually dies from other cellular malfunctions or is removed by phagocytosis. Clearly, this process cannot be enhanced by inducing enhanced DNA damage. In almost all cases of physiological apoptosis, e.g. during development, it may be supposed that the presentation of eat-me signals is sufficient to eliminate the condemned cell since it is subsequently engulfed and digested by phagocytes or surrounding cells without 'ifs' or 'buts'. This may be the reason why DFF40- or DFF45-deficient mice are generally viable. They do not even suffer from diseases due to

undigested DNA because the DNA is digested by other DNases, presumably from the lysosomes of the engulfing cell.

Yet, the cellular reaction may differ considerably if the initial apoptotic signal is too weak to kill the cell instantly. This may be the case during pathological conditions, and induction of insufficient apoptosis plays a major role in several diseases and e.g. in the failure of cancer therapies of certain cancer types. In these cases DNA damage induced by DFF40 might serve to enhance pro-apoptotic signalling in the target cells as detailed above.

Since the spatial distribution and expression patterns of proteins might have a considerable effect on apoptosis, a selected set of features was characterized in the cells used later for stable transfection before the transfection experiments were carried out.

4.3.1. EXPRESSION AND CELLULAR LOCALIZATION OF DFF40 AND DFF45

The exact localization of DFF40/DFF45 complex in a cell is still controversially discussed (see chapter 1.3.4.2.1); however, a recently published review concluded a nuclear localization from the available data (*Widlak and Garrard, 2005*). Since the cellular localization as well as the expression levels of both DFF40 and DFF45 were supposed to affect cellular responses to apoptotic stimuli, immunofluorescence microscopy and western blots were carried out to characterize the localization in the cell types used later for stable transfection experiments. Furthermore, the cellular 'protein background' should be comparable in the cells used for the transfection experiments. Since HL60 cells were subsequently demonstrated to have a mostly (though not exclusively) nuclear localization of DFF40 and DFF45, as analyzed by western blots (see figure 3-28 on page 146), Jurkat cells were chosen for the subsequent transfection experiments. Localization of DFF40 and DFF45 in Jurkat cells seemed to be mainly cytoplasmic, similar to the spatial distribution found in Raji cells in a comparison of the expression levels by western blotting. Furthermore, Jurkat cells readily undergo DNA fragmentation and apoptosis in response to Topotecan and thus seemed to be suitable to investigate the consequences of enhanced expression of DFF45.

In contrast to the results obtained from the western blots, DFF45 seemed to be localized mostly (though not exclusively) in the nucleus in both Jurkat and Raji cells when analyzed by LSM (see figure 3-30 on page 149). However, the magnification and resolution of LSM was not sufficient to distinguish between a possible nuclear or perinuclear localization in the cells. Interestingly, these contradictory results, regarding western blots with cell extracts and fluorescence microscopy, were reported from other groups before, and they are so far in agreement with the results from this study

because a prevailing cytoplasmic localization was always concluded from the western blots of cytoplasmic extraction protocols (*Liu et al., 1997; Enari et al., 1998; Mitamura et al., 1998; Xerri et al., 2000*), whereas a predominant nuclear localization was generally reported in experiments involving immunostaining or fluorescence-tagged DFF45 (*Samejima and Earnshaw, 1998; Xerri et al., 2000; Lechardeur et al., 2000*), and never conversely. So, it may be supposed that either the nuclei become leaky for DFF45 during the cytoplasmic extraction protocols used in the experiments, or that DFF45 is indeed partially localized in the cytoplasm loosely attached to the nuclear membrane, this way only mimicking a mostly nuclear localization during fluorescence microscopy. Alternatively, since both DFF40 and DFF45 carry an NLS (*Lechardeur et al., 2000*), it could be assumed that a portion of the protein complex is 'caught in the act' of transferring into the nucleus when analyzed by immunofluorescence staining. DFF45 is expressed at relatively high levels in a cell, and a considerably large portion of DFF45, alone or complexed with DFF40, could be localized in the nuclear pore complex (NPC) from which it may be easily eluted during cytoplasmic extraction protocols, thus resulting in a seemingly cytoplasmic localization. However, to date it is not known whether the non-ionic detergent (NP-40, Igepal) used in the preparation protocol for the cytoplasmic extracts solubilizes transported proteins from the NPC, but interestingly proteins from the central channel in the NPC are generally extractable by other non-ionic detergents, so e.g. in the presence of 0.1% Triton X 100 (*Unwin and Milligan 1982; Akey, 1989*).

A different ratio of DFF40 to DFF45 was observed in the study in hand by comparing Jurkat cells, HL60 cells, and Raji cells (see figure 3-28 on page 146 and figure 3-29 on page 148). Different expression levels suggest different regulation mechanisms which would allow varied expression levels of DFF40 and DFF45 in specific cell types. Indeed, differential regulation of DFF40 and DFF45 levels may be probable in human tissues provided that gene regulation is similar to the regulation mechanism in mice. Mouse CAD and ICAD genes were reported to be localized in a corresponding chromosomal region compared to the gene locations of DFF40 and DFF45 in humans, and both CAD and ICAD genes were demonstrated to be regulated by different promoters in mice (*Kawane et al., 1999*).

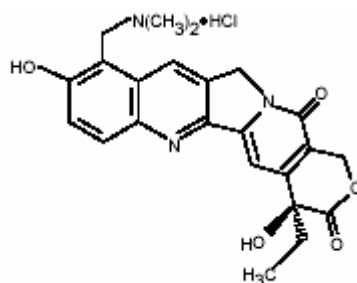
In the study in hand, the DFF40/DFF45 ratio was markedly altered in Raji cells because this cell line expressed lower amounts of DFF40 but higher levels of DFF45 and DFF35 compared to both HL60 and Jurkat cells. This result was confirmed independently and in parallel to the the study in hand by *Luciano et al. (2002)* who demonstrated low or undetectable expression levels of DFF40 and relatively high expression levels of DFF45 in B leukemic cell lines (SKW 6.4, RPMI 88.66, and Raji) compared to T cell lymphoma

lines (Jurkat, HP Ball, and CEM). In accordance with the data obtained for induction of apoptosis with Topotecan in the study in hand, *Luciano et al. (2002)* found no internucleosomal DNA cleavage in Raji cells undergoing cell death induced by death receptor ligands and staurosporine.

In the present study, Topotecan was used to induce apoptosis. Therefore, this inducer of apoptosis is discussed in the following chapter.

4.3.2. TOPOTECAN AS AN INDUCER OF APOPTOSIS IN LYMPHOMA CELLS

Topotecan is a semi-synthetic derivative of the plant alkaloid Camptothecin and a potent inhibitor of topoisomerase I (*Eng et al., 1988; Lorence et al., 2004; Cowan, 1999*). Its structural formula is depicted in figure 4-1.



(Source: GlaxoSmithKline)

Figure 4-1: Structural formula of Topotecan-hydrochloride (trademark name: Hycamtin[®])

Topotecan is e.g. used for intravenous chemotherapy of metastatic ovarian cancers or small cell lung cancer, but due to its high cytotoxicity it is indicated only if other therapies failed. It was reported that the number of white blood cells decreased by up to 90% during treatment with Topotecan. Bone marrow suppression with concomitant neutropenia, anemia, and thrombocytopenia is the dose-limiting cytotoxic factor in the treatment of cancers by Topotecan (*reviewed in the prescribing informations, GlaxoSmithKline*). Due to its apoptosis-inducing effect on haematopoietic cells, Topotecan is commonly used for in vitro induction of apoptosis in cultured lymphoma cells. Therefore, Topotecan was chosen to induce apoptosis in the lymphoma cells used in the present study.

The physiological task of the enzyme targeted by Topotecan, topoisomerase I, is to relieve torsional tractions within the DNA molecule, which occur during replication or transcription. Introduction of reversible, transient single strand breaks in the DNA by topoisomerase I allows rotation of the broken strand around its intact complementary strand and thus relaxes the super-coiled DNA double helix (*Wang, 1996*). Topotecan mimics a DNA basepair and intercalates with the DNA at sites of DNA single-strand

cleavage. The ability to intercalate with DNA may be facilitated by its chemical structure since it is similar to highly aromatic planar quaternary alkaloids (*see figure above and data reviewed in Cowan, 1999*). Thus, Topotecan prevents religation of the single strand breaks which have been generated by topoisomerase I but initially causes no damage to the DNA. Since Topotecan binds to the enzyme-substrate-complex, the mode of enzymatic inhibition is uncompetitive (*Staker et al., 2002*). However, cytotoxicity of Topotecan is thought to be due to double strand breaks. Because Topotecan inhibits topoisomerase I by irreversibly binding to it, these double strand breaks are most likely generated mechanically during the S-Phase of the cell cycle by collision of the multienzyme complex of the replication machinery at the replication fork with the trapped ternary complex formed by topoisomerase I, Topotecan, and DNA (*Bjornsti et al., 1989; Li and Liu, 2001*). Therefore, it may be concluded that Topotecan is not a DNA-damaging agent by itself but rather converts topoisomerase I into a DNA-damaging agent during S-phase of the cell cycle. The double strand breaks generated during this 'accident' are sufficient to cause cellular responses typical for DNA damage signalling in the affected cell which finally leads to cell cycle arrest and/or apoptosis.

4.3.3. EXPRESSION PATTERNS OF SELECTED PROTEINS DURING APOPTOSIS

Only the expression of a few selected proteins could be analyzed by western blots. Since **caspase-3** is the apoptotic activator of DFF40, its localization was analyzed in both Jurkat and Raji cells. Cellular localization of caspase-3 in the cytoplasm did not differ in Jurkat and Raji cells (see figure 3-30 on page 149). However, after induction of apoptosis in Jurkat cells, levels of procaspase-3 decreased markedly within 24 hours with no detectable precursor after 48 hours in Jurkat cells, whereas procaspase-3 was still detectable, though at a slightly lower level, in Raji cells even 56 hours after induction of apoptosis (see figure 3-29 on page 148). Furthermore, by comparing the results from western blots, the expression levels of procaspase-3 seemed to be lower in Raji cells than in Jurkat cells. However, the staining intensities of cells during immunofluorescence experiments detecting procaspase-3 were more intense in Raji cells than in Jurkat cells. Since caspase-3 was reported to be generally expressed and cleaved during apoptosis in Raji cells (*Kawabata et al., 1999; Dudich et al., 1999; Pique et al., 2000; Hirokawa et al., 2002; Lu et al., 2004*), the procaspase-3 level found in Raji cells is presumably not the decisive factor for delayed progression of apoptosis in this cell line. Furthermore, HL60 cells were demonstrated to have similar expression levels of procaspase-3 compared with Raji cells (see figure 3-27 on page 143). Other groups also reported reduced caspase-3 activity and no DNA fragmentation in Raji cells during

conditions which induce apoptosis in other cells e.g. Jurkat or HL60 (*Kawabata et al., 1999; Yanokura et al., 2000; Hirokawa et al., 2002*).

Expression levels of the nuclear enzyme **PARP** were higher in Raji cells than in Jurkat cell as analyzed by western blots (see figure 3-29 on page 148). PARP is a nuclear zinc-finger DNA-binding protein and acts as a DNA damage sensor which is involved in DNA metabolism and repair, thus contributing to genomic stability and mammalian longevity. It catalyzes the polymerization of up to 200 ADP ribose units at sites of DNA strand breaks by using NAD⁺ as a substrate to generate branched homopolymers of ADP ribose which are linked by glycosidic bonds and bound to chromatin proteins (*e.g. reviewed in D'Amours et al., 1999; Oliver et al., 1999; Bürkle 2001*). PARP is a typical substrate of caspase-3, and thus PARP cleavage yielding the 89 kDa fragment is commonly associated with caspase-3 activity and occurs downstream of caspase-3 as a hallmark event of apoptosis in the apoptotic cascade. Necrotic cleavage of PARP, presumably by lysosomal enzymes, was reported to occur as well in some dying cells, but it generates fragments clearly different in sizes from those generated during apoptosis (*Shah et al., 1996; D'Amours et al., 2001; Soldani et al., 2001; Gobeil et al., 2001; Soldani and Scovassi, 2002*).

In contrast to Jurkat cells, which showed complete apoptotic cleavage of PARP within 24 hours after induction of apoptosis, residual intact PARP was still detectable in Raji cells even 56 hours after induction of apoptosis in the study in hand. Cleavage of PARP started concomitantly with detectable DNA damage in both Jurkat and Raji cells and even before a distinct decrease of procaspase-3 was detectable in both cell lines (see figure 3-29 on page 148). This may indicate that even minute amounts of cleaved procaspase-3 are sufficient to generate a caspase-3-like enzyme activity. Thus, it may be concluded that complete cleavage of procaspase-3 is presumably not necessary in cells to generate enough active tetrameric enzymes for cleavage of some apoptotic downstream substrates. Though at a low level, PARP cleavage in Raji cells demonstrates the presence of a functional procaspase-3 in these cells in the present study. It resulted in the generation of the PARP fragments which are specific for apoptosis but indicated weak apoptotic signalling because residual intact PARP could be detected even 56 h after induction with Topotecan.

High expression levels and insufficient cleavage of PARP may be just one out of several possible reasons for the occurrence of necrotic cell death rather than apoptosis in Raji cells after treatment with various cytotoxic substances. Necrotic cell death was observed in Raji cells by several authors under conditions which induced apoptosis in other cell lines (*Macklis et al., 1993; Finstad et al., 1998, 2000; Heimli et al., 2001; Into et al., 2002*). Since PARP utilizes large amounts of NAD⁺ to generate the protein-bound

poly ADP ribose chains in response to DNA damage, the energy resources of Raji cells may be depleted faster than in other cells as a consequence of PARP activity. On the other hand, efficient PARP cleavage by caspases may contribute to a 'proper apoptotic cell death' in cells which undergo apoptosis rather than necrosis, because energy depletion by activated PARP is avoided, and thus a switch from apoptotic to necrotic cell death due to failing energy metabolism is prevented under conditions supplying enough effector caspase activity.

Importantly, since PARP cleavage in the present study generated the fragments typical for apoptosis in both Jurkat and Raji cells, an early shift to necrosis may be excluded in Raji cells under the experimental conditions chosen in the study in hand. However, inhibition of cell growth in Raji cells by inducing cell cycle arrest instead of apoptosis was reported by *Kuroki et al. (1996)*, and this scenario seems more probable for the Raji cells used in the study in hand because they are delayed by about 16 hours in progression of cell death compared to Jurkat cells when regarding the DNA degradation patterns after electrophoresis. Nevertheless, cell death in Raji cells was clearly evident since the DNA was degraded in a random fashion resulting in a smear of DNA in agarose gels in the course of apoptosis.

Expression levels of **DFF45** decreased markedly within 8 hours in apoptotic Jurkat cells, and DFF45 was completely cleaved and thus undetectable 24 hours after induction of apoptosis in these cells (see figure 3-29 on page 148). In contrast uncleaved DFF45 was still detectable in apoptotic Raji cell populations even 56 h after induction of apoptosis.

Since DFF45 is not only the chaperone of DFF40 but also its inhibitor, it may contribute to the absence of internucleosomal DNA cleavage in Raji cells because uncleaved DFF45 may still have an inhibitory effect on the small amounts of activated DFF40. This hypothesis is supported by recently published data which demonstrated that uncleaved DFF45 was principally able to disassemble and thus inactivate the activated DFF40 dimers (*Woo et al., 2004*). Other authors reported that nuclease activity of activated oligomerized DFF40 may be inhibited by association of DFF45 with these complexes without mediating its disassembly (*Widlak et al., 2003*).

The model diagram in figure 4-2 summarizes some of the conditions for apoptosis in Jurkat and Raji cell populations as derived from the experimental results in this study.

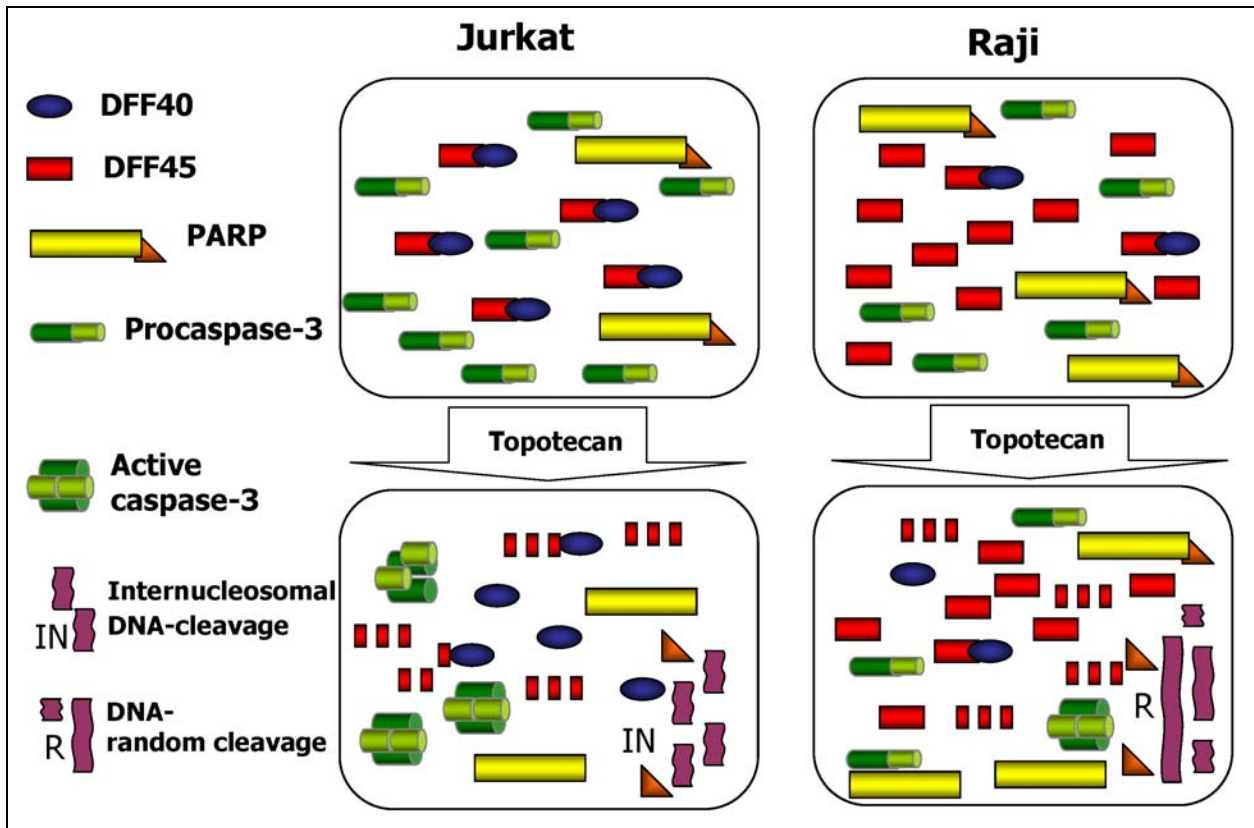


Figure 4-2: Apoptotic events in Jurkat and Raji cell populations

This diagram summarizes some of the events during apoptosis induced by Topotecan in Jurkat and Raji cell populations as observed in the present study. **Jurkat cells** readily undergo apoptosis induced by Topotecan, and apoptosis is accompanied by complete activation of caspase-3. Active caspase-3 in these cells cleaves downstream substrates, e.g. PARP and DFF45, completely, thus releasing a DFF40-like DNase activity which generates internucleosomally cleaved DNA fragments. In contrast, **Raji cells** induced by Topotecan do not activate caspase-3 completely and cleavage of downstream substrates, such as DFF45 and PARP is also incomplete. Importantly, PARP is cleaved in a caspase-3-specific manner, indicating principally active effector caspases in Raji cells. Since obviously less DFF40 is activated in Raji cells, DNA fragmentation occurs in a random manner, presumably by lysosomal nucleases in the dying cells. Note: The DFF40:DFF45 ratio in Jurkat and Raji cells varies considerably: Thus, it may be concluded that intact DFF45 contributes to the absence of DNA fragmentation in Raji cells because it may inhibit a substantial amount of DFF40 during progression of cell death in Raji cells. To sum it up, the events observed in this study rather suggest a delay in progression of apoptosis than a switch to necrotic events in Topotecan-treated Raji cells.

4.3.4. STABLE TRANSFECTION PROCEDURE

The generation of stably transfected cell lines seemed useful in this study because Raji cells were generally delayed in their response to apoptotic signals by about 16 hours compared with Jurkat cells. Thus, the expression of a recombinant protein from a transiently transfected vector may be downregulated in parallel to the apoptotic response in Raji cells and lead to a wrong interpretation of the results. Both Raji and Jurkat cells were used for a stable transfection procedure to generate cell lines expressing either recombinant DFF40 or DFF45. The use of Blasticidin as a selective

antibiotic for the transfected cells allowed a relatively fast selection of stably transfected cells compared with other antibiotics, e.g. Neomycin. Blasticidin was demonstrated to be a suitable antibiotic for selection of stably transfected mammalian cells by several groups before (*Kimura et al., 1994; Kudo et al., 1994; Frengen et al., 2000*).

Expression of recombinant DFF40 was possible in both Raji and Jurkat cells, but Jurkat cells downregulated expression of recombinant DFF40 within a few cell generations. Expression of recombinant DFF45 was only successful in Raji cells. Jurkat cells were obviously able to either regulate cellular levels of DFF45 posttranslationally, perhaps by targeting excess DFF45 to the proteasome, or they rapidly downregulated expression of DFF45 under control of the the CMV promotor. However, since no traces of recombinant DFF45 protein were detectable in western blots of Jurkat cells, the latter seems more probable.

The viral CMV promotor used for the expression of recombinant proteins in the study in hand is known for its robust function in a variety of human cell lines and allows high expression levels of the desired protein (*Muller et al., 1990; Doll et al., 1996*). However, both silencing (*Gopalkrishnan et al., 1999; Teschendorf et al., 2002*) and enhancement of the CMV promotor activity (*Yano et al., 1994*) in transfected cell has been reported. Enhancement of the CMV promotor activity was e.g. dependent on the gene product of the ras oncogene, and silencing was supposed to occur as a consequence of changes in cell physiology, e.g. in differentiating cells. This suggests that there are presumably even more silencing and enhancing elements which may affect transfection experiments in general. Thus, it may be concluded that successful expression of a recombinant protein depends on the protein to be expressed and the type of cell line to be transfected.

A still unknown mechanism may have led to a fast down-regulation of the CMV promotor in DFF45-transfected Jurkat cells in the present study. Interestingly, in contrast to recombinant DFF45, recombinant DFF40 could initially be expressed under control of the CMV promotor in Jurkat cells. Hence, it may be concluded that the CMV promotor is not generally silenced in Jurkat cells but may be rather silenced dependent on the expressed protein. A posttranslational regulation mechanism regulating the levels of DFF40 protein may be supposed in Jurkat cells because recombinant DFF40 obviously replaced a portion of the endogenous protein. Thus, overall DFF40 levels could not be altered in Jurkat cells by stable transfection. This regulation mechanism was either not present in Raji cells or it at least allowed expression of recombinant DFF40 since endogenous DFF40 levels were below the 'specified' physiological levels. Because Raji cells readily expressed recombinant DFF45 additionally to already high

levels of endogenous DFF45 levels, it could be assumed that lacking posttranslational regulation in Raji cells may contribute to the enhanced levels of DFF45 protein.

4.3.5. MORPHOLOGY OF APOPTOTIC JURKAT AND RAJI CELLS

Changes in the nuclear morphology of apoptotic cells are the most obvious features observable during apoptosis. Morphological changes in the nucleus during apoptosis may be caused by three independently acting factors (compare chapter 1.3.4 for details):

- Mitochondrial factors (Endo G, AIF) which induce chromatin condensation, nuclear fragmentation, and HMW DNA fragmentation
- Caspase-catalyzed cleavage of proteins in the nuclear matrix, i.e. by caspase-3 and caspase-6
- HMW DNA fragmentation by DFF40

The exact timing of HMW chromatin fragmentation, internucleosomal DNA cleavage, and chromatin condensation has been controversially discussed in the existing literature. Initial experiments suggested that both DNA fragmentation and chromatin condensation are caused by DFF40 itself. (*Liu et al., 1998*). However, experiments with DFF40 knockout chicken cells revealed still proceeding HMW DNA cleavage and early chromatin condensation in the nuclear periphery during apoptosis in these cells (*Samejima et al., 2001*). Internucleosomal DNA cleavage and late stage chromatin condensation was not detectable in these cells, demonstrating that the latter is dependent on DFF40 activity in these cells. *Walker et al. (1999)* reported that neither caspase-3 nor DFF40 is required for apoptotic HMW DNA degradation. HMW DNA fragmentation but no internucleosomal DNA cleavage was detectable during apoptosis in human cancer cells containing a mutated caspase-3 gene. Hence, active caspase-3 was dispensable in these cells for the generation of HMW DNA fragments. Another cell line was reported to undergo HMW DNA fragmentation but no internucleosomal DNA cleavage, thus demonstrating that HMW DNA degradation occurs independently from the enzyme responsible for internucleosomal DNA degradation.

Samejima et al. (1999) demonstrated in an in vitro system using purified nuclei and cytosolic extracts from cells in various stages of apoptosis that internucleosomal DNA cleavage and chromatin condensation appear downstream from caspase activities. It may be summarized that the current point of view is that DFF40 induces both early HMW- and internucleosomal DNA cleavage in a caspase-dependent manner. Furthermore, DFF40 activity may be either supported or replaced by caspase-independent mechanisms which depend on AIF and EndoG. Chromatin condensation is thought to occur due to HMW DNA fragmentation, caspase-independent actions of AIF,

and activated downstream caspases which cleave proteins of the nuclear matrix (see chapter 1.3.4).

In contrast to Jurkat cells, which showed distinct apoptotic chromatin condensation in the course of apoptosis (see figure 3-33 on page 152), these changes were not observed in non-transfected, mock-transfected, and DFF45-transfected Raji cells. Interestingly, expression of recombinant DFF40 changed the apoptotic morphology of Raji cells. Non-transfected, mock-transfected, and DFF45-transfected Raji cells did not show chromatin condensation after treatment with Topotecan for 9h, whereas DFF40 transfected cells showed membrane blebbing and chromatin condensation at the same time (compare chapter 3.3.3.2). However, chromatin condensation in DFF40-transfected Raji cells was less intensive than in Jurkat cells, but it was clearly correlated with DFF40 activity. Increased HMW DNA fragmentation preceded chromatin condensation in DFF40 transfected Raji cells as shown by increased phosphorylation of H2A.X (discussed in chapter 4.3.7).

Since caspase-3 activities were comparably low at this time of apoptosis (see figure 3-46 on page 172), apoptotic chromatin fragmentation in DFF40-transfected Raji cells occurred independently from caspase-3, and DFF40 activity obviously contributed considerably to apoptotic chromatin condensation by inducing HMW DNA damage. Thus, lacking chromatin condensation may be caused in Raji cells rather by lacking DFF40 activity downstream of caspase-3 activity than by lacking caspase-3 activity itself. However, since chromatin condensation was less distinct in DFF40-transfected Raji cells than in Jurkat cells, it may be assumed that mitochondrial factors or other caspases contribute to this process as well. Thus, it may be concluded that chromatin condensation is an apoptotic event which may be influenced by multiple factors, but DFF40 seems to play an important part in this process.

4.3.6. DNA FRAGMENTATION PATTERNS IN TRANSFECTED LYMPHOMA CELLS

Raji cells expressing recombinant DFF40 showed distinct internucleosomal DNA cleavage in the course of apoptosis which did not occur in non-transfected and DFF45-transfected Raji cells. However, some of the mock-transfected cells produced a weak DNA ladder too after induction of apoptosis, whereas the majority of the mock-transfected cells did not change their DNA cleavage pattern during apoptosis (see figure 3-44 on page 169). Internucleosomal DNA cleavage in a minority of mock-transfected cells may be caused by other DNases in these cells, e.g. EndoG released from mitochondria in the course of apoptosis. Since the selection of stably transfected cells required several generation times of the cultured cells, it was assumed to reflect a random process. Presumably, slight changes in the expression levels of anti- or pro-

apoptotic proteins are sufficient to affect the apoptotic signalling conditions in the respective cells.

These changes may occur by random processes, and they are not restricted to cultured cells and may even contribute to the persistence of cancer cells *in vivo*. Thus, tumor cells may be intrinsically drug resistant, or they acquire resistance to chemotherapy during treatment (*reviewed in Longley and Johnston, 2005*). Acquired drug resistance may target apoptotic pathways which change their signalling due to random processes, which possibly generates a selective advantage of the affected cells. Presumably, changes in the individual expression patterns of genes contribute considerably to the generation of cancer cell types which are resistant to multiple inducers of apoptosis (acquired multiple drug resistance) in the course of cancer therapy, (*Shain and Dalton, 2001; Wittig et al., 2002; Shi et al., 2002*). All cancer therapies induce a considerable selective pressure on cancer cells, and certain cancer types are more prone to genetic changes by mutations since various cell cycle checkpoints may be inactivated. Lacking genomic surveillance results in genomic instability, and mutations in oncogenes or tumor suppressor genes in some cell types will favour the propagation of cells which are resistant to apoptosis.

Importantly, since the majority of the mock-transfected cells were not affected in their apoptotic DNA fragmentation features, a direct effect on apoptotic features in the transfected cells caused by the vector used for stable transfection or by the selection conditions using the antibiotic Blasticidin may be excluded. This hypothesis is further supported by the apoptotic features of Raji cells stably transfected for expression of DFF45: These cells never showed any internucleosomal DNA cleavage during apoptosis even in cells with only low expression levels of additional DFF45. However, expression of recombinant DFF45 presumably contributed to delayed progression of apoptosis in these cells (see chapter 4.3.8) and thus might counteract a possible putative lower viability of transfected cells.

Interestingly, expression of recombinant DFF40 reduced initial DNA fragmentation during apoptosis in DFF40-transfected Jurkat cells compared with the other Jurkat cell types (see figure 3-49 on page 180). This surprising observation may have resulted from less DNase activity due to the tags of the recombinant DFF40 protein. Importantly, a residual DNase activity of the recombinant DFF40 protein was clearly demonstrated in Raji cells. In contrast to the expression in Raji cells, expression levels of DFF40 seemed to be tightly regulated in Jurkat cells since expression of recombinant DFF40 decreased expression of endogenous DFF40 by up to 20% (see figure 3-48 on page 179). Thus, a portion of endogenous DFF40 was obviously replaced by less active recombinant DFF40. This may explain less intensive internucleosomal DNA cleavage during early

apoptosis in DFF40-transfected Jurkat cells. Though a 6xhis tag alone presumably does not interfere with the enzymatic activity of endonucleases (*e.g. demonstrated by Moncke-Buchner et al., 2004*) a combination of the 6xhistag and a myc-epitope yet may slightly decrease the enzymatic activity of recombinant DFF40 since it could interfere with its activation mode which presumably requires oligomerization and formation of a 'pair of molecular scissors' (*Woo et al., 2004*; compare chapter 1.3.4.2.1).

4.3.7. PROTEIN EXPRESSION LEVELS IN TRANSFECTED LYMPHOMA CELLS

DFF40

Successful expression of recombinant DFF40 protein in Raji cells and Jurkat cells was confirmed by western blotting and resulted in an additional band occurring above the band of endogenous DFF40 protein since the molecular weights of the recombinant proteins are slightly higher due to the tags than those of endogenous proteins (see figure 3-45 on page 170 and figure 3-48 on page 179). Thus, endogenous DFF45 of Raji cells was obviously able to act as a chaperone on recombinant DFF40, and DFF45 from Jurkat cells allowed expression of recombinant DFF40 in DFF40-transfected Jurkat cells. Since endogenous DFF45 was present to act as a chaperone, expression of the recombinant DFF40 protein was generally possible in cells transfected with a vector containing only the ORF of DFF40 but no ORF for DFF45.

As already discussed in chapter 4.3.6, DFF40 total protein amounts did not increase in Jurkat cells despite a successful expression of the recombinant DFF40 protein. This may also indicate that there is just enough DFF45 to allow expression of a fixed amount of DFF40 in Jurkat cells. In contrast, expression of recombinant DFF40 in Raji cells increased DFF40 contents in these cells substantially, and this was obviously possible since Raji cells express large amounts of DFF45 which can act as a chaperone to create a functional DFF40 enzyme.

DFF45

Interestingly, the expression of recombinant DFF40 even seemed to slightly upregulate expression levels of endogenous DFF45 in DFF40 transfected Raji cells and Jurkat cells (see figure 3-45 on page 170 and figure 3-48 on page 179). Thus, it could be assumed that the expression of DFF40 also induces expression of its chaperone and inhibitor DFF45. Regarding the potential hazard of activated DFF40, a tight regulation of the expression of its inhibitor appears to be useful. Interestingly, this result was confirmed by recent data of *Kimura et al. (2004)* who found that mouse fibroblasts which were transiently transfected with a CAD expression vector induced endogenous ICAD at higher expression levels than did non-transfected cells or cells transfected with the empty control vector.

Since expression of recombinant DFF45 protein generally failed in Jurkat cells, it may be concluded that expression of DFF45 is regulated differently compared with Raji cells which expressed recombinant DFF45 in addition to already existing high levels of endogenous DFF45. Thus, a large excess of DFF45 did not prevent expression of additional recombinant DFF45 in Raji cells. These results suggest a possible posttranslational regulation mechanism which may be additionally affected by DFF40 and may be responsible for maintaining cell type-specific expression levels of DFF45. However, the exact regulation mechanism remains to be determined. *Rogakou et al. (2000)* reported successful expression of mouse ICAD in transiently transfected Jurkat cells, and they obviously circumvented a putative regulation mechanism by using a related but clearly different protein. So, it should be mentioned that the mouse ICAD used by this group was resistant to caspase cleavage and had a flag tag. Thus, its *in vivo* interactions with other proteins could have been different from those of the recombinant DFF45 protein used in the study in hand. Furthermore, human DFF45 and mouse ICAD are clearly different proteins since their sequence identity at the protein level is only 76.1%. Nevertheless, DFF45 and ICAD are encoded by orthologous genes (*Liu et al., 1997*).

Bcl-2, bax, p53, and WAF1

Levels of pro-apoptotic bax and anti-apoptotic bcl-2 were similar in transfected and non-transfected Jurkat cells (see figure 3-48 on page 179) whereas bax and bcl-2 levels in DFF40 transfected Raji cells seemed to be increased compared to non-, mock-, and DFF45-transfected Raji cells (see figure 3-45 on page 170). The reason for this observation is not clear, but may be explained by random changes in the cultured cells due to the long cultivation times. Moreover, compared with the expression in Raji cells, expression levels of pro-apoptotic bax were low and those of anti-apoptotic bcl-2 were high in HL60 cells, a cell line which is particularly sensitive to induction of apoptosis (*Shimizu and Pommier, 1997; Schliephacke et al., 2004*). Thus, the observed changes did not necessarily affect the results of the experiments. Furthermore, the slightly decreased quotient from the bax/bcl-2 ratio (due to increased relative bcl-2 levels) in DFF40-transfected Raji cells might be expected to contribute rather to increased apoptosis resistance. In fact, it did not prevent these cells from increased activities of both DFF40 and caspase-3 upon induction of apoptosis (compare chapter 4.3.6).

P53 was only detectable in Raji cells since Jurkat cells do not express p53 due to several mutations as reported by several groups (*e.g. Vigorito et al., 1999; Chowdhury et al., 2003*). Expression of p53 was upregulated within 9 h in the course of apoptosis in Raji cells and indicated a response to DNA damage in these cells. However, increased p53 levels failed to induce WAF1 in Raji cells (see figure 3-45 on page 170), and thus, it

may be concluded that Raji p53 is not functional presumably due to a point mutation. Mutated p53 was reported to be expressed in Raji cells before (*Duthu et al., 1992; Buttgereit et al., 2001; Kroger et al., 2001*). Thus, it may be concluded that p53 presumably does not contribute to the delay in progression of apoptosis in Raji cells compared with Jurkat cells. A shift from apoptosis to cell cycle arrest was reported to occur occasionally in cancer cells with intact p53. In these cells p53 contributed rather to a persistence of cells with limited DNA damage by inducing cell cycle arrest and DNA repair than inducing apoptotic cell death (*Scott et al., 2003*). Furthermore, p53-dependent expression of WAF1 was able to block apoptosis in cells with limited DNA damage (*Han et al., 2002*). However, since WAF1 levels did not increase in the course of apoptosis in Raji cells, the delay in the apoptotic response of Raji cells is presumably caused by other factors in the present study.

Phosphorylation state of H2A.X

Phosphorylation of histone H2A.X at serine 139 was initially reported to occur in response to DNA double-strand breaks by ionizing radiation (*Rogakou et al., 1999*). However, it seems to be a general cellular response to ds DNA breaks, and it was detected both in lymphoid cells during V(D)J recombination (*Chen et al., 2000b*) and during meiotic recombination processes in mice (*Mahadevaiah et al., 2001*). Furthermore, phosphorylation of H2A.X is an early event in apoptosis which parallels HMW DNA fragmentation and precedes both externalization of phosphatidylserine on the outer membrane and internucleosomal DNA cleavage during apoptosis (*Rogakou et al., 2000*). These results indicate that phosphorylation of H2A.X occurs as a consequence of the double strand breaks generated during HMW DNA fragmentation. These double strand breaks are e.g. detected by ATM (see chapter 1.3.3.2) which subsequently phosphorylates a number of targets, among them H2A.X (*Burma et al., 2001*).

H2A.X phosphorylation increased within the first 3 h after induction of apoptosis in both Jurkat and Raji cells, indicating early presence of HMW DNA fragmentation during apoptosis in both cell lines. Furthermore, there was a correlation between the extent of internucleosomal DNA cleavage and the increase in H2A.X phosphorylation in both cell lines. Thus, enhanced DNA damage in Raji cells expressing recombinant DFF40 was confirmed by an enhanced H2A.X phosphorylation in this cell type compared to non-, mock-, and DFF45 transfected Raji cells (see figure 3-45 on page 170) whereas the slight decrease of DFF40 activity in early apoptotic (induction for 3 h) Jurkat cells was accompanied by a slight decrease in H2A.X phosphorylation (see figure 3-48 on page 179).

The expression level of recombinant DFF45 in DFF45-transfected Raji cells was obviously sufficient to cause a slight decrease in HMW DNA fragmentation in Raji cells as demonstrated by a slightly less distinct increase in H2A.X phosphorylation compared with non- and mock-transfected Raji cells. Accordingly, *Rogakou et al. (2000)* reported decreased H2A.X phosphorylation in Jurkat cells which were transiently transfected with recombinant mouse ICAD. However, mouse ICAD used in that study was caspase-resistant and thus not cleavable in the course of apoptosis. Importantly, the extent of DNA ds breaks as detected by gel electrophoresis and H2A.X phosphorylation seemed to be correlated with the inducible capacity of caspase-3 activities in both Raji and Jurkat cells (compare chapter 4.3.8).

Furthermore, HMW- and internucleosomal DNA cleavage in the apoptotic systems used in this study were caused rather by DFF40 than by other apoptotic DNases since transfection with recombinant DFF40 caused changes in the DNA fragmentation kinetics in both Jurkat and Raji cells. Yet, contribution of other DNases cannot be entirely excluded in this apoptotic system although the impact of those DNases seemed to be low.

Additionally expressed recombinant DFF45 seemed to reduce DNA ds breaks and caspase-3 activities in stably transfected Raji cells as observed in the study in hand (see chapter 3.3.4). Together with the observation of decreased phosphorylation of H2A.X in Jurkat cells transiently expressing uncleavable mouse ICAD (*Rogakou et al., 2000*), it may be concluded that uncleaved DFF45 is presumably able to inhibit activated DFF40 in vivo and thus contributes to enhanced resistance to apoptosis in cell types with increased expression levels of DFF45. This increased apoptosis resistance may be reflected by lower caspase-3 activity and less DNA damage in the cell population upon induction of apoptosis.

Unfortunately, to date this hypothesis could neither be confirmed nor disproved with DFF45-transfected Jurkat cells because additional recombinant DFF45 was not expressible in these cells. However, transient expression of mouse ICAD in Jurkat cells seemed to be possible as reported by *Rogakou et al. (2000)*. Thus, future experiments could be carried out using mouse ICAD instead of human DFF45 to alter the ratio between DFF40 and its inhibitor in Jurkat cells. Since mouse ICAD was able to inhibit human DFF40 activity in purified nuclei in vitro (*Enari et al., 1998*), it may be concluded that mouse ICAD can replace human DFF45 in inhibiting DFF40 in vivo as well. Alternatively, firstly a vector containing the DFF35 ORF sequence could be used because the protein levels of DFF35 might be regulated otherwise. As detailed in chapter 1.3.4.2.2, DFF35 has only inhibitory but no chaperone activity on DFF40 and might thus be used to check for consequences of enhanced expression of a DFF40-

inhibitory protein in Jurkat cells. Or, secondly, a vector with another promotor could be used because a down-regulation of the CMV promotor could have been the reason for lacking expression of DFF45 in Jurkat cells.

4.3.8. COMPARISON OF CASPASE-3 ACTIVITIES IN TRANSFECTED LYMPHOMA CELLS

Caspase-3-like activities were measured in cell lysates using the fluorescent substrate DEVD-afc. This substrate is commonly used, i.e. it was already used by other groups for comparative quantitative analysis of caspase-3 activities in different sources (*Sun et al., 1997; Martins et al., 1997; Marti et al., 2000; Meergans et al., 2000; Weng et al., 2002*).

The activity of caspase-3 increased with progression of apoptosis in all cell types analyzed in the study in hand, and it was always correlated with cell death as may be concluded from both DNA gel electrophoresis, which demonstrated degradation of DNA in the dying cells, and changes in the morphology of the dying cells. Thus, high caspase activities were correlated with early apoptotic cell death. Generally, caspase-3 activities were higher in Jurkat cells compared with Raji cells. This fact confirmed the earlier results from the study in hand, which included complete and early cleavage of caspase-3 substrates in Jurkat cells and delayed, incomplete cleavage of these substrates in Raji cells. Thus, fast and marked increases in caspase-3 activities were generally correlated with low cell viability.

The two major questions which were addressed in this part of the present study were: Does DFF40 activity contribute to the progression of apoptosis by inducing additional DNA damage, thus enhancing the apoptotic signalling state of the cell and decreasing cell viability? And if so, does DFF45 contribute to the resistance of some cell types by suppressing additional DNA damage, thus increasing cell viability?

As already discussed in chapter 4.3.7, it may be concluded from the presented results that apoptotic DNA damage was correlated rather with DFF40 activity than with the activity of other apoptotic DNases in the apoptotic systems used. Furthermore, DNA damage caused an increase in caspase-3 activity of Raji cells (and not conversely) because HMW- and internucleosomal DNA cleavage preceded the main increase in caspase-3 activity: Enhanced H2A.X phosphorylation (indicating HMW DNA damage) in those cells occurred within 3 h and internucleosomal DNA cleavage was demonstrated within 12 to 15 h whereas the main increase of caspase-3 was detectable after 24 h (see chapter 3.3.4). Importantly, increase of DNA damage was more pronounced in DFF40-transfected Raji cells since enhanced phosphorylation of H2A.X was detected compared with non-, mock-, and DFF45 transfected Raji cells. Furthermore, the

resulting caspase-3 activity in DFF40- transfected Raji cells was significantly higher than in all the other Raji cell types. Since caspase-3 activities are correlated with cell death, it may be concluded that DNA ds breaks contributed to progression of apoptosis by enhancing the apoptotic signalling state in Raji cells, and thus contribute to a positive feedback mechanism. These results are in contrast to the statement of *Luciano et al. (2002)* who concluded that the 'very low ratio of DFF40 vs DFF45 in B cell lymphomas is unlikely to explain by itself the lack of DNA fragmentation observed in certain B cell lines'. They found no correlation between DFF40/DFF45 expression, DNA fragmentation, caspase-3 activity, and apoptosis in B lymphoma cells. In contrast, the study in hand demonstrated 'restored' DNA fragmentation by altering the DFF40:DFF45 ratio in a B cell lymphoma line via stable transfection, and enhanced progression of apoptosis by demonstrating significantly increased caspase-3 activities. Interestingly, and consistent with a part of the results from the study in hand, *Luciano et al. (2002)* demonstrated a correlation of caspase-3 activity, DFF40/DFF45 expression and DNA fragmentation in other cell lines. A positive feedback mechanism of DNA damage during apoptosis was suggested in parallel by work of other authors as well. DFF40 and PARP presumably contribute to an amplification loop during TNF α induced apoptosis in primary mouse fibroblasts (*Boulares et al., 2001, 2002*).

Thus, a positive feedback mechanism might generally contribute to progression of apoptosis in cells which show enhanced resistance to apoptosis. It may be one factor (lacking) for the tip in the balance which finally determines a cell's fate: Death or survival. This even may have clinical relevance for treatment of certain cancer types which show insufficient apoptosis during various therapies. Indeed, a recent paper supported this relevance: *Kimura et al. (2004)* evaluated the therapeutic potential of a combination of CAD overexpression and cisplatin in mouse squamous cell carcinoma for cancer chemotherapy in vivo: They demonstrated both enhanced arrest in tumor cell growth and increase of apoptosis by CAD transfection in vitro and in vivo. CAD gene transfer enhanced cisplatin-induced cell killing in cultured mouse fibroblasts, and a combination of cisplatin and an in vivo CAD gene therapy using a Gene Gun System in combination with cisplatin led to enhanced tumor regression compared with mice transfected with control vector and treated with cisplatin.

The statistical data obtained with the Jurkat cells in the study in hand should be regarded as preliminary results since only two transfection experiments could be taken into consideration. The number of successful transfection experiments was low because transfected Jurkat cells rapidly downregulated expression of recombinant DFF40 in contrast to Raji cells (see chapter 4.3.4). However, expression of recombinant DFF40 in Jurkat cells decreased caspase-3 activity significantly compared with non-transfected

and cells transfected with a 'DFF45' expression plasmid (which did not express recombinant DFF45) (see figure 3-50 on page 182 and figure 3-51 on page 184).

The detection of even lower levels of caspase-3 activity in DFF40-transfected Jurkat cells in the study in hand was surprising in the first instance and seemed to be a contradiction to the results obtained with DFF40-transfected Raji cells at a first glance.

Importantly, as discussed in chapter 4.3.6 and 4.3.7, expression of recombinant DFF40 in Jurkat cells decreased total DFF40 activity in these cells as detected by decreased initial H2A.X phosphorylation and less distinct internucleosomal DNA cleavage. Thus, DNA fragmentation and caspase-3 activity were correlated in this cell line too, and, despite opposite effects of DFF40 transfection in Jurkat cells, the preliminary data obtained so far with this cell line supported the positive feedback loop hypothesis.

Surprisingly, expression of even low amounts of additional recombinant DFF45 in Raji cells was sufficient to decrease caspase-3 activities, and it was likely that this decrease was a consequence of less DNA damage in DFF45-transfected Raji cells. A decrease in internucleosomal DNA cleavage was not observable in DFF45-transfected Raji cells because non-transfected Raji cells do not undergo internucleosomal DNA cleavage, but there was a decrease in residual HMW DNA cleavage which could be concluded from less H2A.X phosphorylation compared to non-, mock-, and DFF40-transfected Raji cells; (*Rogakou et al. 2000*; compare chapter 4.3.7). Initial appearance of HMW DNA fragments was shown to be correlated with H2A.X phosphorylation. Both HMW DNA cleavage and phosphorylation of H2A.X were found to be early apoptotic events since they precede the appearance of internucleosomal DNA cleavage and even the externalization of phosphatidylserine to the outer leaflet of the cell membrane (*Rogakou et al., 2000*).

Expression of recombinant DFF45 in Raji cells in the present study could have decreased HMW DNA cleavage by inhibiting the responsible DNase. Interestingly, this decrease in HMW DNA cleavage was correlated with a marked decrease in the inducible caspase-3 activity during apoptosis.

4.3.9. FUTURE EXPERIMENTS

A major disadvantage of the study in hand is the fact that the experiments carried out so far analyzed parameters in a cell population and do not analyze the conditions in a single cell. Thus, single cell analysis should be carried out to confirm the results of this study which represent only the 'average state' in the respective cell populations. This would e.g. allow to exactly correlate HMW DNA cleavage, H2A.X phosphorylation, and caspase-3 activity at the 'single cell level' e.g. by FACS-analysis. Furthermore, the correlated cell viability could be monitored more reliably, e.g. by Annexin V/propidium

iodide labelling for the detection of apoptotic and necrotic cells. FACS analysis would additionally allow to elucidate the signalling pathway from DNA damage to increased caspase-3 activity which may be supposed to involve the mitochondria (see chapter 1.3.3.2 and figure 1-2 on page 26). This could be revealed by FACS analysis detecting the cells for breakdown of the mitochondrial inner membrane potential with fluorescent dyes.

Supposing, expression of an DFF40 inhibitory protein (by strategies already detailed in chapter 4.3.7) in Jurkat cells failed, a functional knockout of DFF40 by RNAi transfection methods could be the method of choice to alter the DFF40:DFF45 ratio in these cells by decreasing the expression of DFF40. And finally, since the experiments in the study in hand were carried out with only one apoptosis inductor (Topotecan), the experiments should be repeated with another apoptosis inductor, preferably an inductor which activates the extrinsic pathway to apoptosis and does not cause DNA damage itself.

4.3.10. PERSPECTIVES

The results from the studies in hand together with the published data of other groups indicate that DFF40-catalyzed DNA damage during apoptosis contributes to an enhanced progression of apoptosis in some apoptotic systems. Furthermore, the inhibitor of DFF40, DFF45, seems to be at least one factor which contributes to a delay of apoptosis or to apoptosis resistance by decreasing the apoptotic DNA damage. As already discussed above, this is certainly of no biological significance during physiological cell death, which proceeds fast and eliminates a cell within 30 to 60 min by phagocytic cells without leaving any traces of the executed cell. However, during pathological conditions, an acceleration of apoptosis and the inactivation of potentially dangerous DNA from cancer cells or virus-infected cells may be beneficial. Comparing the cells analyzed in the present study, it is obvious that cells which are delayed in progression of apoptosis have much more time and opportunity to spread cancer-associated genes or viral DNA elements both in vitro and in vivo. Thus, an acceleration of apoptosis which concomitantly contributes to the destruction of potentially dangerous DNA may e.g. contribute to improved cancer therapies e.g. in those cases where apoptosis induced by chemotherapy or radiation is insufficient.

Beyond that, apoptosis is a process which is certainly affected by many interacting factors which may enhance or delay progression of apoptosis, depending on the cellular context. Thus, the results of the experiments in this study clearly contribute only a tiny part in a giant puzzle.

5. SUMMARY

In the first part of this study, an *in vitro* system using plasmid DNA or purified nuclei was established using recombinant proteins, which finally allowed checking for the effect of defined protein on the activity of the apoptotic endonuclease DFF40.

DFF40/DFF45 complex, expressed in transformed *E. coli* and purified by Ni-NTA chromatography as well as recombinant caspase-3, expressed in yeast and purified by Ni-NTA chromatography, were yielded as recombinant enzymes with specific enzyme activity, respectively. Recombinant H1 histone subtypes were selectively extracted from differentially transformed yeast and yielded pure preparations as confirmed by SDS-PAGE. The study demonstrated inhibition of DFF40 activity both on plasmid substrates and in purified nuclei from HL60 cells at high concentrations of H1 histones, irrespective from the subtype. In contrast, lower, presumably physiological, concentrations generally enhanced DFF40 activity on plasmid DNA in a dose-dependent manner. Except a broader activating concentration range of H1°, there were no significant differences in activating DFF40 between the different subtypes detectable in the system used. The same results, i.e. no differences in the activating or inhibiting effect on DFF40 activity, were obtained using both *in vitro*-phosphorylated and unphosphorylated H1.2 histones, or H1 histones extracted from either control or apoptotic HL60 cells.

The aim of the second part of this study was to identify factors which contribute to the resistance to apoptotic DNA fragmentation in Raji cells compared with cell lines which readily undergo internucleosomal DNA cleavage in the course of apoptosis (HL60 and Jurkat cells). A heat-stable factor in Raji cytoplasm was found to inhibit DFF40 activity on purified nuclei from both HL60 and Raji nuclei, whereas a heat-labile factor could be activated by recombinant caspase-3 in HL60 cytoplasm which subsequently degraded plasmid DNA or DNA from both Raji and HL60 nuclei. From these experiments it was concluded that the factor responsible for enhanced resistance to apoptotic DNA fragmentation in Raji cells was presumably not localized in the chromatin and that DNA fragmentation is catalyzed by a heat-labile, caspase-3 activated protein, presumably DFF40, whereas inhibition of DNA fragmentation was mediated by a heat-stable protein which was found to be DFF45.

Since further results from this study revealed a different ratio of DFF40 and DFF45 in apoptosis-sensitive cell lines (HL60 and Jurkat) compared with cells undergoing delayed apoptosis (Raji), the question arose whether these different protein ratios may influence progression of apoptosis *in vivo* in these cells. The two major working-hypotheses were:

1. Does DFF40 contribute to the progression of apoptosis by inducing additional DNA damage, which induces an apoptotic amplification loop?
2. Does DFF45 contribute to a delayed progression of apoptosis by inhibiting additional DFF40-catalyzed DNA damage, thus counteracting an apoptotic amplification loop?

After having characterized the apoptotic features of the lymphoma cells later used in the experiments, stable transfection was carried out to alter the DFF40/DFF45 ratio in both Raji and Jurkat cells. Stable expression of both recombinant DFF40 and DFF45 proteins was successful in Raji cells, whereas expression of recombinant DFF45 in Jurkat cells failed, and expression of recombinant DFF40 was generally down-regulated within a few cell generations in Jurkat cells.

Experiments with the transfected cells revealed that both internucleosomal DNA cleavage and HMW DNA cleavage could be restored in DFF40-transfected Raji cells, though the recombinant DFF40 protein was presumably less active than endogenous DFF40 protein as shown in DFF40-transfected Jurkat cells. In contrast to Raji cells, increased expression of total DFF40 protein was not possible in Jurkat cells because recombinant DFF40 replaced a portion of endogenous DFF40 in Jurkat cells. This resulted in a slightly decreased DFF40-activity and less apoptotic DNA damage in DFF40-transfected Jurkat cells.

Apoptotic DFF40-catalyzed DNA damage in both transfected Jurkat and Raji cells was generally correlated with the inducible amount of caspase-3 activity during apoptosis: DFF40-transfected Jurkat cells with slightly less apoptotic DNA damage had less caspase-3 activity, and DFF40-transfected Raji cells with markedly more apoptotic DNA damage had significantly higher caspase-3 activity. HMW DNA damage and internucleosomal DNA cleavage even preceded the marked increase of caspase-3 activity in Raji cells. Thus, DFF40 presumably contributes to an amplification loop in cells with delayed apoptosis by adding additional DNA damage.

Expression of additional recombinant DFF45 in Raji cells decreased apoptotic DNA damage in these cells and was correlated with significantly decreased caspase-3 activity in the course of apoptosis. Thus, DFF45 presumably contributes to delayed progression of apoptosis in cells expressing high levels of this protein by directly inhibiting DFF40 activity *in vivo*, and decreased apoptotic DNA damage in cell types which express high levels of this protein may counteract a possible apoptotic amplification loop during apoptosis.

The results of this study could be of interest in cancer research because they indicate that malignancy of tumor cells and resistance to cancer therapies may be enhanced in tumor cells with insufficient internucleosomal DNA-degradation during apoptosis.

6. REFERENCES

Adams JM, Cory S (1998)

The bcl-2 protein family: Arbiters of cell survival
Science **281**: 1322-1326

Adrain C, Slee EA, Harte MT, Martin SJ (1999)

Regulation of apoptotic protease factor-1 oligomerization and apoptosis by the WD-40 repeat region
J Biol Chem **274**: 20855-20860

Akao Y, Otsuki Y, Kataoka S, Ito Y, Tsujimoto Y (1994)

Multiple subcellular localization of bcl-2: detection in nuclear outer membrane, endoplasmic reticulum membrane, and mitochondrial membranes
Cancer Res **54**: 2468-2471

Akey CW (1989)

Interactions and structure of the nuclear pore complex revealed by cryo-electron microscopy
J Cell Biol **109**: 955-970

Albig W (1989)

Die Rolle der Hexosephosphorylierung bei der Glucoserepression in der Hefe
PhD thesis, University of Tübingen

Albig W, Runge DM, Kratzmeier M, Doenecke D (1998)

Heterologous expression of human H1 histones in yeast
FEBS Letters **435**: 245-250

Alderson MR, Tough TW, Davis-Smith T, Braddy S, Falk B, Schooley KA, Goodwin RG, Smith CA, Ramsdell F, Lynch DH (1995)

Fas ligand mediates activation-induced cell death in human T lymphocytes
J Exp Med **181**: 71-77

Allan J, Hartman PG, Crane-Robinson C, Aviles FX (1980)

The structure of histone H1 and its location in chromatin
Nature **288**: 675-679

Allan J, Mitchell T, Harborne N, Bohm L, Crane-Robinson C (1986)

Roles of H1 domains in determining higher order chromatin structure and H1 location
J Mol Biol **187**: 591-601

Ameisen JC (2002)

On the origin, evolution, and nature of programmed cell death: A timeline of four billion years
Cell Death Differ **9**: 367-393

Arnoult D, Akarid K, Grodet A, Petit PX, Estaquier J, Ameisen JC (2002)

On the evolution of programmed cell death: Apoptosis of the unicellular eukaryote *Leishmania major* involves cystein proteinase activation and mitochondrion permeabilization
Cell Death Differ **9**: 65-81

Ashkenazi A, Dixit VM (1998)

Death receptors: Signalling and modulation
Science **281**: 1305-1308

Ausubel, FM, Brent R, Kingston RE, Moore DD, Seidman JG, Smith JA, Struhl K (eds., 1987)

Current protocols in molecular biology
John Wiley & Sons, New York

Avery L, Horvitz HR (1987)

A cell that dies during wild-type *C. elegans* development can function as a neuron in a *ced-3* mutant
Cell **51**: 1071-1078

Banin S, Moyal L, Shieh S, Taya Y, Anderson CW, Chessa L, Smorodinsky NI, Prives C, Reiss Y, Shiloh Y, Ziv Y (1998)

Enhanced phosphorylation of p53 by ATM in response to DNA damage
Science **281**: 1674-1677

Becker DM, Guarente L (1991)

High-efficiency transformation of yeast by electroporation
Methods Enzymol **194**: 182-187

Beere HM, Chresta CM, Alejo-Herberg A, Skladanowski A, Dive C, Larsen AK, Hickman JA (1995)

Investigation of the mechanism of higher order chromatin fragmentation observed in drug-induced apoptosis
Mol Pharmacology **47**: 986-996

Beers EP (1997)

Programmed cell death during plant growth and development
Cell Death Differ **4**: 649-661

Bellairs R (1961)

Cell death in chick embryos as studied by electron microscopy
J Anat **95**: 54-60

Benditt JO, Meyer C, Fasold H, Barnard FC, Riedel N (1989)

Interaction of a nuclear location signal with isolated nuclear envelopes and identification of signal-binding proteins by photoaffinity labelling
Proc Natl Acad Sci USA **86**: 9327-9331

Benedict MA, Hu Y, Inohara N, Nunez G (2000)

Expression and functional analysis of apaf-1 isoforms. Extra WD-40 repeat is required for cytochrome c binding and regulated activation of caspase-9
J Biol Chem **275**: 8461-8468

Bjornsti MA, Benedetti P, Viglianti GA, Wang JC (1989)

Expression of human DNA topoisomerase I in yeast cells lacking yeast DNA topoisomerase I: restoration of sensitivity of the cells to the antitumor drug camptothecin
Cancer Res **49**: 6318-6323

Boise LH, Gonzalez-Garcia M, Posteme CE, Ding L, Lindsten T, Turka LA, Mao X, Nunez G, Thompson CB (1993)

Bcl-x, a bcl-2 related gene that functions as a dominant regulator of apoptotic cell death
Cell **74**: 597-608

Boldin MP, Goncharov TM, Goltsev YV, Wallach D (1996)

Involvement of MACH, a novel MORT1/FADD-interacting protease in FAS/Apo-1 and TNF receptor-induced cell death
Cell **85**: 803-815

Boulares AH, Zoltoski AJ, Yakovlev A, Xu M, Smulson ME (2001)

Roles of DNA fragmentation factor and poly(ADPribose) polymerase in an amplification phase of tumour necrosis factor induced apoptosis
J Biol Chem **276**: 38185-38192

Boulares AH, Zoltoski AJ, Sherif ZA, Yakoviev A, Smulson ME (2002)

Roles of DNA fragmentation factor and poly (ADP-ribose) polymerase-1 in sensitization of fibroblasts to tumor necrosis factor-induced apoptosis
Biochem Biophys Res Comm **290**: 796-801

Boya P, Roques B, Kromer G (2001)

Viral and bacterial proteins regulating apoptosis at the mitochondrial level
EMBO J **20**: 4325-4331

Boyce M, Degterev A, Yuan J (2004)

Caspases: An ancient cellular sword of Damocles
Cell Death Differ **11**: 29-37

Broach JR, Li Y, Wu LC, Jayaram M (1983)

In: Experimental manipulation of gene expression (Inouye M, Editor)
Academic press New York: 83-117

Brunner T, Mogil RJ, LaFace D, Yoo NJ, Mahboubi E, Echeverri F, Martin SJ, Force WR, Lynch DH, Ware CF, et al. (1995)

Cell-autonomous Fas (CD95)/Fas-ligand interaction mediates activation-induced apoptosis in T-cell hybridomas
Nature **373**: 441-444

Bürkle A (2001)

PARP-1: A regulator of genomic stability linked with mammalian longevity
Chembiochem **2**: 725-728

Burma S, Chen BP, Murphy M, Kurimasa A, Chen DJ (2001)

ATM phosphorylates histone H2AX in response to DNA double-strand breaks
J Biol Chem **276**: 42462-42467

Buttgereit P, Schakowski F, Marten A, Brand K, Renoth S, Ziske C, Schottker B, Ebert O, Schroers R, Schidt-Wolf IG (2001)

Effects of adenoviral wildtype p53 transfer in p53-mutated lymphoma cells
Cancer Gene Ther **8**: 430-439

Candé C, Cecconi F, Dessen P, Kroemer G (2002)

Apoptosis-inducing factor (AIF): key to the conserved caspase-independent pathways of cell death?

J Cell Sci **115**: 4727-4734

Cecconi F (2001)

Apaf1 is no longer single

Cell Death Differ **8**: 773-775

Cerretti DP, Kozlosky CJ, Mosley B, Nelson N, van Ness K, Greenstreet TA, March CJ, Kronheim SR, Druck T, Cannizzaro LA, Huebner K, Black RA (1992)

Molecular cloning of the interleukin-1 β converting enzyme

Science **256**: 97-100

Chadee DN, Allis CD, Wright JA, Davie JR (1997)

Histone H1b phosphorylation is dependent upon ongoing transcription and replication in normal andras-transformed mouse fibroblasts

J Biol Chem **272**: 8113-8116

Chadee DN, Taylor WR, Hurta RA, Allis CD, Wright JA, Davie JR (1995)

Increased phosphorylation of histone H1 in mouse fibroblasts transformed with oncogenes or constitutively active mitogen-activated protein kinase kinase

J Biol Chem **270**: 20098-20105

Chauveau J, Moule Y, Rouiller C (1956)

Isolation of pure and unaltered liver nuclei morphology and biochemical composition

Exp Cell Res **11**: 317-321

Chen HT, Bhandoola A, Difillipantonio MJ, Zhu J, Brown MJ, Tai X, Rogakou EP, Brotz TM, Bonner WM, Ried T, Nussenzweig A (2000b)

Response to RAG mediated V(D)J cleavage by NBS1 and H2AX

Science **290**: 1962-1964

Chen D, Stetler A, Guodong C, Pei W, O'Horo C, Yin XM, Chen J (2000)

Characterization of the rat DNA fragmentation factor 35/Inhibitor of caspase-activated DNase (short form): The endogenous inhibitor of caspase-dependent DNA fragmentation in neuronal apoptosis

J Biol Chem **275**: 38508-38517

Chen P, Abrams JM (2000)

Drosophila apoptosis and Bcl-2 genes: Outliers fly in

J Cell Biol **148** (4): 625-627

Chen P, Nordstrom W, Gish B, Abrams JM (1996)

Grim, a novel cell death gene in Drosophila

Genes Dev **10** (14): 1773-1782

Cheung WL, Ajiro K, Samejima K, Kloc M, Cheung P, Mizzen CA, Beeser A, Etkin LD, Chernoff J, Earnshaw WC, Allis CD (2003)

Apoptotic phosphorylation of H2B is mediated by mammalian sterile twenty kinase

Cell **113**: 507-517

Chittenden T, Harrington EA, O'Connor R, Flemington C, Lutz RJ, Evan G, Guild BC (1995)

Induction of apoptosis by the bcl-2 family homologue bak
Nature **374**: 733-736

Chowdhury IH, Farhadi A, Wang XF, Robb ML, Birx DL, Kim JH (2003)

Human T cell leukemia virus type 1 activates cyclin dependent kinase inhibitor p21/Waf1/Cip1 expression through a p53 independent mechanism: Inhibition of cdk2
Int J Cancer **107**: 603-611

Clarke PG and Clarke S (1996)

Nineteenth century research on naturally occurring cell death and related phenomena
Anat Embryol **193**: 81-99

Claveria C, Albar JP, Serrano A, Buesa JM, Barbero JL, Martinez-A C, Torres M (1998)

Drosophila grim induces apoptosis in mammalian cells
EMBO J **17**: 7199-7208

Clem RJ (2001)

Baculoviruses and apoptosis: The good, the bad, and the ugly
Cell Death Differ **8**: 137-143

Cohen GM (1997)

Caspases: The executioner of apoptosis
Biochem J **326**: 1-16

Cohen GM, Sun XM, Fearnhead H, MacFarlane M, Brown DG, Snowden RT, Dinsdale D (1994)

Formation of large molecular weight fragments of DNA is a key committed step of apoptosis in lymphocytes
J Immunol **153**: 507-516

Cole RD (1984)

A minireview of microheterogeneity in H1 histones and its possible significance
Anal Biochem **136**: 24-30

Cole, TCH (1995)

Taschenwörterbuch der Zoologie, A Pocket Dictionary of Zoology
Thieme Verlag, Stuttgart

Collins SJ, Gallo RC and Gallagher RE. (1977)

Continuous growth and differentiation of human myeloid leukaemic cells in suspension culture
Nature **270**: 347-9

Colussi PA, Quinn LM, Huang DCS, Coombe M, Read SH Richardson H, Kumar S (2000)

Debcl, a proapoptotic Bcl-2 homologue is a component of the *Drosophila melanogaster* cell death machinery
J Cell Biol **148** (4): 703-714

Conconi A, Wellinger RJ (2003)

A new link for a linker histone

Mol Cell **11**: 1421-1423

Conradt B, Horvitz HR (1998)

The *C. elegans* protein EGL-1 is required for programmed cell death and interacts with the Bcl-2-like protein CED-9

Cell **93**: 519-529

Contreras A, Hale TK, Stenoien DL, Rosen JM, Mancini MA, Herrera R (2003)

The dynamic mobility of histone H1 is regulated by Cyclin/CDK phosphorylation

Mol Cell Biol **23**: 8626-8636

Cote J, Ruiz-Carrillo A (1993)

Primers for mitochondrial DNA replication generated by endonuclease G

Science **261**: 765-769

Cowan MM (1999)

Plant products as antimicrobial agents

Clin Microbiol Rev **12**: 564-582

Crook NE, Clem RJ, Miller LK (1993)

An apoptosis-inhibiting baculovirus gene with a zinc finger-like motif

J Virol **67**: 2168

Croxton R, Ma Y, Song L, Haura EB, Cress WD (2002)

Direct repression of the Mcl-1 promoter by E2F1

Oncogene **21**: 1359-1369

Cryns V, Yuan J (1998)

Proteases to die for

Genes Dev **12**: 1551-1570, published erratum in **13**: 371

Dai Z, Huang Y, Sadee W (2004)

Growth factor signaling and resistance to cancer chemotherapy

Curr Top Med Chem **4**: 1347-1356

D'Amours D, Desnoyers S, D'Silva I, Poirier GG (1999)

Poly(ADP-ribose)ylation reactions in the regulation of nuclear functions

Biochem J **342**: 249-268

D'Amours D, Sallmann FR, Dixit VM, Poirier GG (2001)

Gain-of-function of poly(ADP-ribose) polymerase-1 upon cleavage by apoptotic proteases: implications for apoptosis

J Cell Sci **114**: 3771-3778

Daugas E, Nochy D, Ravagnan L, Loeffler M, Susin SA, Zamzani N, Kroemer G (2000)

Apoptosis-inducing factor (AIF): a ubiquitous mitochondrial oxidoreductase involved in apoptosis

FEBS Letters **476**: 118-123

Dawson JF, Boland MP, Holmes CF (1994)

A capillary electrophoresis-based assay for protein kinases and protein phosphatases using peptide substrates

Anal Biochem **220**: 340-345

De la Taille, A, Chen MW, Burchardt M, Chopin DK, Buttyan R (1999)

Apoptotic conversion: Evidence for exchange of genetic information between prostate cancer cells mediated by apoptosis

Cancer Res **59**: 5461-5463

Desagher S, Osen-Sand A, Nichols A, Eskes R, Montessuit S, Lauper S, Maundrell K, Antonsson B, Martinou JC (1999)

Bid induced conformational change of Bax is responsible for mitochondrial cytochrome c release during apoptosis

J Cell Biol **144**: 891-901

Deveraux QL, Reed JC (1999)

IAP family proteins suppressors of apoptosis

Genes Dev **13**: 239-252

Deveraux QL, Roy N, Stennicke HR van Arsdale T, Zhou Q, Srinivasula SM, Alnemri ES, Salvesen GS, Reed JC (1998)

IAPs block apoptotic events induced by caspase-8 and cytochrome c by direct inhibition of distinct caspases

EMBO J **17**(8): 2215-2223

Dhein J, Walczak H, Bäumlner C, Debatin KM, Krammer PH (1995)

Autocrine T-cell suicide mediated by APO-1 (Fas/CD95)

Nature **373**: 438-441

Doenecke D, Albig W, Bouterfa H, Drabent B (1994)

Organization and expression of H1 histone and H1 replacement histone genes

J Cell Biochem **54**: 423-431

Doenecke D, Albig W, Bode C, Drabent B, Franke K, Gavenis K, Witt O (1997)

Histones: Genetic diversity and tissue-specific gene expression

Histochem Cell Biol **107**: 1-10

Doll, RF, Crandall JE, Dyer CA, Aucoin JM, Smith FI (1996)

Comparison of promoter strengths on gene delivery into mammalian brain cells using AAV vectors

Gene Ther **3**: 437-447

Dorstyn L, Read S, Cakouros D, Huh JR, Hay BA, Kumar S (2002)

The role of cytochrome c in caspase activation in *Drosophila melanogaster* cells

J Cell Biol **156**: 1089-1098

Drabent B, Franke K, Bode C, Kosciessa U, Bouterfa H, Hameister H, Doenecke D (1995)

Isolation of two murine H1 histone genes and chromosomal mapping of the H1 histone gene complement

Mamm Genome **6**: 505-511

Du CY, Fang M, Li YC, Li L, Wang XD (2000)

Smac, a mitochondrial protein that promotes cytochrome c-dependent caspase activation by eliminating IAP inhibition

Cell **102**:33-42

Dubrez L, Goldwasser F, Genne P, Pommier Y, Solary E (1995)

The role of cell cycle regulation and apoptosis triggering in determining the sensitivity of leukemic cells to topoisomerase I and II inhibitors

Leukemia **9**: 1013-1024

Dudich E, Semenkova L, Dudich I, Gorbatova E, Tochtamisheva N, Tatulov E, Nikolaeva M, Sukhikh G (1999)

α -Fetoprotein causes apoptosis in tumor cells via a pathway independent of CD95, TNFR1 and TNFR2 through activation of caspase-3-like proteases

Eur J Biochem **266**: 750-761

Durrieu F, Samejima K, Fortune JM, Kandels-Lewis S, Osheroff N, Earnshaw WC (2000)

DNA topoisomerase II α interacts with CAD nuclease and is involved in chromatin condensation during apoptotic execution

Curr Biol **10**: 923-926

Duthu A, Debuire B, Romano J, Ehrhardt JC, Fiscella M, May E, Appella E, May P (1992)

P53 mutations in Raji cells: Characterization and localization relative to other Burkitt's lymphomas

Oncogene **7**: 2161-2167

Earnshaw WC (1995)

Nuclear changes in apoptosis

Curr Biol **7**: 337-343

Earnshaw WC (1999)

A cellular poison cupboard

Nature **397**: 387-389

Earnshaw WC, Martins LM, Kaufmann SH (1999)

Mammalian caspases: Structure, activation, substrates and functions during apoptosis

Annu Rev Biochem **68**: 383-424

Ellis HM, Horvitz HR (1986)

Genetic control of programmed cell death in the nematode *C. elegans*

Cell **44**: 817-829

Enari M, Hase A, Nagata S (1995)

Apoptosis by a cytosolic extract from Fas-activated cells
EMBO J **14**: 5201-5208

Enari M, Sakahira H, Yokoyama H, Okawa K, Iwamatsu A, Nagata S (1998)

A caspase-activated DNase that degrades DNA during apoptosis, and its inhibitor ICAD
Nature **391**: 43-50

Enari M, Talanian RV, Wong WW, Nagata S (1996)

Sequential activation of ICE-like and CPP32-like proteases during Fas-mediated apoptosis
Nature **380**: 723-726

Eng WK, Faucette L, Johnson RK and Sternglanz R (1988)

Evidence that DNA topoisomerase I is necessary for the cytotoxic effects of camptothecin
Mol Pharmacol **34**: 755-60.

Engelberg-Kulka H, Glaser G (1999)

Addiction molecules and programmed cell death and antideath in bacterial cultures
Annu Rev Microbiol **53**: 43-70

Enomoto R, Koyamazaki R, Maruta Y, Tanaka M, Takuma K, Mori K, Lee E (2001)

Phosphorylation of histones triggers DNA fragmentation in thymocyte undergoing apoptosis induced by protein phosphatase inhibitors
Mol Cell Biol Res Comm **4**: 276-281

Evan G and Littlewood T (1998)

A matter of life and death
Science **281**: 1317-1322

Fadok VA, Bratton DL, Rose DM, Pearson A, Alan R, Ezekewitz B, Henson PM (2000)

A receptor for phosphatidylserine-specific clearance of apoptotic cells
Nature **405**: 85-90

Fadok VA, Voelker DR, Campbell PA, Cohen JJ, Bratton DL, Henson PM (1992)

Exposure of phosphatidylserine on the surface of apoptotic lymphocytes triggers specific recognition and removal by macrophages
J Immunol **148**: 2207-2216

Falck J, Coates J, Jackson SP (2005)

Conserved modes of recruitment of ATM, ATR, and DNA PKcs to sites of DNA damage
Nature **434**: 605-611

Feiferman I, Pogo AO (1975)

Isolation of a nuclear ribonucleoprotein network that contains heterogeneous RNA and is bound to the nuclear envelope
Biochemistry **14**: 3808-3816

Fernandes-Alnemri T, Armstrong RC, Krebs J, Srinivasula SM, Wang L, Bullrich F, Fritz LC, Trapani JA, Tomaselli KJ, Litwack G, Alnemri ES (1996)

In vitro activation of CPP32 and Mch3 by Mch4, a novel apoptotic cysteine protease containing two FADD-like domains
Proc Natl Acad Sci **93**: 7464-7469

Ferri KF, Kroemer G (2000)

Control of apoptotic DNA degradation
Nature Cell Biol **2**: E63-E64

Fesik SW, Shi Y (2001)

Controlling the caspases
Science **294**: 1477-1478

Filipski J, Leblanc J, Youdale T, Sikorska M, Walker PR (1990)

Periodicity of DNA folding in higher order chromatin structures
EMBO J **9**: 1319-1327

Finstad HS, Myhrstad MC, Heimli H, Lomo J, Blomhoff HK, Kolset SO, Drevon CA (1998)

Multiplication and death type of leukemia cell lines exposed to very long-chain polyunsaturated fatty acids
Leukemia **12**: 921-929

Finstad HS, Dyrendal H, Myhrstad MC, Heimli H, Drevon CA (2000)

Uptake and activation of eicosapentaenoic acid are related to accumulation of triacylglycerol in Ramos cells dying from apoptosis
J Lipid Res **41**: 554-563

Fischer U, Jänicke RU, Schulze-Osthoff K (2003)

Many cuts to ruin: a comprehensive update of caspase substrates
Cell Death Differ **10**: 76-100

Formigli L, Papucci L, Tani A, Schiavone N, Tempestini A, Orlandini GE, Capaccioli S, Zecchi Orlandini S. (2000)

Aponecrosis: morphological and biochemical exploration of a syncretic process of cell death sharing apoptosis and necrosis
J Cell Physiol **182**:41-49.

Frade JM, Michaelidis TM (1997)

Origin of eukaryotic programmed cell death A consequence of aerobic metabolism?
Bioessays **19**: 827-832

Fraser AG, Evan GI (1997)

Identification of a *Drosophila melanogaster* ICE/CED-3-related protein drICE
EMBO J **16**: 2805-2813

Frengen E, Zhao B, Howe S, Weichenhan D, Osoegava K, Gjernes E, Jessee J, Prydz H, Huxley C, de Jong PJ (2000)

Modular bacterial artificial chromosome vectors for transfer of large inserts into mammalian cells
Genomics **68**: 118-126

Fuentes-Prior P, Salvesen GS (2004)

The protein structures that shape caspase activity, specificity, activation and inhibition
Biochem J **384**: 201-232

Fulda S, Debatin KM (2004)

Signaling through death receptors in cancer therapy
Curr Opin Pharmacol **4**: 327-332

Fukushima T, Takat M, Morrison C, Araki R, Fujimori A, Abe M, Tatsumi K, Jasin M, Dhar PK, Sonoda E, Chiba T, Takeda S (2001)

Genetic analysis of the DNA dependent protein kinase reveals an inhibitory role of Ku in late S-G₂ phase DNA double strand break repair
J Biol Chem **276**: 44413-44418

Furukawa Y, Nishimura N, Satoh M, Endo H, Iwase S, Yamada H, Matsuda M, Kano Y, Nakamura M (2002)

Apaf-1 is a mediator of E2F-1-induced apoptosis
J Biol Chem **277**: 39760-39768

Gallagher R et al. (1979)

Characterization of the continuous differentiating myeloid cell line (HL60) from a patient with acute promyelocytic leukaemia
Blood **54**: 713-733

Gamble TN, Ramachandran C, and Bateman KP (1999)

Phosphopeptide isomer separation using capillary zone electrophoresis for protein kinases and phosphatases
Anal Chem **71**: 3469-3476

Gartel AL, Tyner AL (2002)

The role of the cyclin dependent kinase inhibitor p21 in apoptosis
Mol Cancer Ther **1**: 639-649

Gately DP, Hittle JC, Chan GK, Yen TJ (1998)

Characterization of ATM expression, localization, and associated DNA-dependent protein kinase activity
Mol Biol Cell **9**: 2361-2374

Gerchman SE, Graziano V, Ramakrishnan V (1994)

Expression of chicken linker histones in E. coli: sources of problems and methods for overcoming some of the difficulties
Protein Expr Purif **5**: 242-251

Gerschenson LE, Rotella RJ (1992)

Apoptosis: a different type of cell death
Faseb J **6**: 2450-2455

Gey GO, Coffman WD, Kubicek MT (1952)

Tissue culture studies of the proliferative capacity of cervical carcinoma and normal epithelium
Cancer Res **12**: 264

Glantz SA, Slinker BL (1990)

Primer of applied regression and analysis of variance
McGraw-Hill New York

Glucksmann A (1951)

Cell deaths in normal vertebrate ontogeny
Biol Rev **26**: 59-86

Gobeil S, Boucher CC, Nadeau D, Poirier GG (2001)

Characterization of the necrotic cleavage of poly(ADP-ribose) polymerase (PARP-1):
Implications of lysosomal proteases
Cell Death Differ **8**: 588-594

Goldbeter A, Koshland DE Jr (1981)

An amplified sensitivity arising from covalent modification in biological systems
Proc Natl Acad Sci USA **78**: 6840-6844

Gopalkrishnan RV, Christiansen KA, Goldstein NI, DePinho RA, Fisher PB (1999)

Use of the human EF1 α promoter for expression can significantly increase success in
establishing stable cell lines with consistent expression: a study using the tetracycline-
inducible system in human cancer cells
Nucleic Acids Res **27**: 4775-4782

Gottlieb E, van der Heiden MG, Thompson CB (2000)

Bcl-x(L) prevents the initial decrease in mitochondrial membrane potential and subsequent
reactive oxygen species production during tumor necrosis factor alpha-induced apoptosis
Mol Cell Biol **20**: 5680-5689

Green DR, Kroemer G (2004)

The pathophysiology of mitochondrial cell death
Science **305**: 626-629

Green DR, Reed JC (1998)

Mitochondria and apoptosis
Science **281**: 1309-1311

Greenberg JT (1996)

Programmed cell death: A way of life for plants
Proc Natl Acad Sci USA **93**: 12094-12097

Greenberg JT, Guo A, Klessig D, Ausubel FM (1994)

Programmed cell death in plants: A pathogen-triggered response activated co-ordinately with
multiple defense functions
Cell **77**: 551-563

Grether ME, Abrams JM, Agapite J, White K, Steller H (1995)

The head involution defective gene of *Drosophila melanogaster* functions in programmed cell
death
Genes Dev **9** (14): 1694-1708

Gromova II, Nielsen EF, Razin SF (1995)

Long-range fragmentation of the eukaryotic genome by exogenous and endogenous nucleases proceeds in a specific fashion via preferential DNA cleavage at matrix attachment sites

J Biol Chem **270**: 18685-18690

Gross A, Jockel J, Wei MC, Korsmeyer SJ (1998)

Enforced dimerization of Bax results in its translocation, mitochondrial dysfunction and apoptosis

Embo J **17**: 3878-3885

Gross A, McDonnell JM, Korsmeyer SJ (1999)

Bcl-2 family members and the mitochondria in apoptosis

Genes Dev **13**: 1899-1911

Gross A, Yin XM, Wang K, Wei MC, Jockel J, Milliman C, Erdjument-Bromage H, Tempst P, Korsmeyer SJ (1999b)

Caspase-cleaved Bid targets mitochondria and is required for cytochrome c release, while Bcl-xL prevents this release but not tumor necrosis factor R1/Fas death

J Biol Chem **274**: 1156-1163

Grudkowska M, Zagdanska B (2004)

Multifunctional roles of plant cysteine proteases

Acta Biochim Pol **51**: 609-624

Gu J, Dong RP, Zhang C, McLaughlin DF, Wu MX, Schlossman SF (1999)

Functional interaction of DFF35 and DFF45 with caspase-activated DNA fragmentation nuclease DFF40

J Biol Chem **274**: 20759-20762

Guo, CY, Wang Y, Brautigan DL, Larner JM (1999)

Histone H1 dephosphorylation is mediated through a radiation induced signal transduction pathway dependent on ATM

J Biol Chem **274**: 18715-18720

Haining WN, Carboy-Newcomb CC, Wei CL, Steller H (1999)

The proapoptotic function of Drosophila Hid is conserved in mammalian cells

Proc Natl Acad Sci **96**: 4936-4941

Halenbeck R, MacDonald H, Roulsten A, Chen TT, Conroy L, Williams LT (1998)

CPAN, a human nuclease regulated by the caspase-sensitive DFF45

Curr Biol **8**: 537-540

Hall-Jackson CA, Cross DA, Morrice N, Smythe C (1999)

ATR is a caffeine sensitive, DNA-activated protein kinase with a substrate specificity distinct from DNA-PK

Oncogene **18**: 6707-6713

Halmer L, Gruss C (1996)

Effects of cell cycle dependent histone H1 phosphorylation on chromatin structure and chromatin replication

Nucleic Acids Res **24**: 1420-1427

Han Z, Wei W, Dunaway S, Darnowski JW, Calabresi P, Sedivy J, Hendrickson EA, Balan KV, Pantazis P, Wyche JH (2002)

Role of p21 in apoptosis and senescence of human colon cancer cells treated with camptothecin

J Biol Chem **277**: 17154-17160

Happel N, Sommer A, Hänecke K, Albig W, Doenecke D (2005)

Topoisomerase inhibitor induced dephosphorylation of H1 and H3 histones as a consequence of cell cycle arrest

J Cell Biochem **in press**

Harris MH, Thompson CB (2000)

The role of the bcl-2 family in the regulation of outer mitochondrial membrane permeabilization

Cell Death Differ **7**: 1182-1191

Haupt Y, Maya R, Kazaz A, Oren M (1997)

MDM2 promotes the rapid degradation of p53

Nature **387**: 296-299

Heath MC (2000)

Hypersensitivity response-related death

Plant Mol Biol **44** (3) 321-334

Hedgecock EM, Sulston JE, Thomson JN (1983)

Mutations affecting programmed cell deaths in the nematode *Caenorhabditis elegans*

Science **220**: 1277-1279

Heimli H, Finstad HS, Drevon CA (2001)

Necrosis and apoptosis in cell lines exposed to eicosapentaenoic acid and antioxidants

Lipids **36**: 613-621

Henzel MJ, Wei Y, Mancini MA, van Hooser, A, Ranalli T, Brinkley BR, Bazett-Jones DP, Allis CD (1997)

Mitosis-specific phosphorylation of histone H3 initiates primarily within pericentromeric heterochromatin during G2 and spreads in an ordered fashion coincident with mitotic chromosome condensation

Chromosoma **106**: 348-360

Hengartner MO (2000)

The biochemistry of apoptosis

Nature **407**: 770-776

Hengartner MO (2001)

DNA destroyers

Nature **412**: 27-28

Hengartner MO, Ellis RE, Horvitz HR (1992)

C. elegans gene *ced-9* protects cells from programmed cell death

Nature **356**: 494-499

Hengartner MO, Horvitz HR (1994)

C. elegans cell survival gene *ced-9* encodes a functional homolog of the mammalian proto-oncogene *bcl-2*

Cell **76**: 665-676

Herrmann M, Voll RE, Zoller OM, Hagenhofer M, Ponner BB, Kalden JR, (1998)

Impaired phagocytosis of apoptotic cell material by monocyte derived macrophages from patients with systemic lupus erythematosus

Arthritis Rheumatism **41**: 1241-1250

Heusel JW, Wesselschmidt RL, Shresta S, Russell JH, Ley TJ (1994)

Cytotoxic lymphocytes require granzyme B for the rapid induction of DNA fragmentation and apoptosis in allogeneic target cells

Cell **76**: 977-987

Hewish DR, Burgoyne LA (1973)

Chromatin-substructure. The digestion of chromatin DNA at regularly spaced sites by a nuclear deoxyribonuclease

Biochem Biophys Res Comm **52**: 504-510

Hirada H, Takahashi A, Kobayashi S, Yonehara S, Sawai H, Okazaki T, Yamamoto K, Sasada M (1998)

Caspases are activated in a branched protease cascade and control distinct downstream processes in Fas-induced apoptosis

J Exp Med **187**: 587-600

Hirokawa M, Kawabata Y, Miura AB (2002)

Dysregulation of apoptosis and a novel mechanism of defective apoptotic signal transduction in human B-cell neoplasms

Leuk Lymphoma **43**: 243-249

Horvitz HR (2002)

Worms, life and death

in: *Nobel lecture* Dec 8, 2002

Horvitz HR, Ellis HM, Sternberg PW (1982)

Programmed cell death in the nematode development

Neurosci Comment **1**: 56-65

Horvitz HR, Sternberg PW, Greenwald IS, Fixsen W, Ellis HM (1983)

Mutations that affect neuronal cell lineages and cell fates during the development of the nematode *Caenorhabditis elegans*

Cold Spring Harb Symp Quant Biol **48 Pt 2**: 453-463

Horvitz HR, Sulston JE (1990)

"Joy of the worm" Anecdotal, historical and critical commentaries on genetics

Genetics **126**: 287-292

Howell DM, Martz E (1988)

Nuclear disintegration induced by cytotoxic T lymphocytes

J Immunol **140**: 689-692

Hsu SY, Kaipia A, McGee, E, Lomdi M, Hsueh AJ (1997)

Bok is a proapoptotic bcl-2 protein with restricted expression in reproductive tissues and heterodimerizes with selective anti-apoptotic bcl-2 family members
Proc Natl Acad Sci USA **94**: 12401-12406

Hu Y, Ding L, Spencer DM, Nunez G(1998)

WD-40 repeat region regulates apaf-1 self-association and procaspase-9 activation
J Biol Chem **273**: 33489-33494

Huang LC, Clarkin KC, Wahl GM (1996)

Sensitivity and selectivity of the DNA damage sensor responsible for activating p53-dependent G1-arrest
Proc Natl Acad Sci USA **93**: 4827-4832

Huang X, Traganos F, Darzynkiewicz Z (2003)

DNA damage induced by DNA topoisomerase I- and topoisomerase II-inhibitors detected by histone H2AX phosphorylation in relation to the cell cycle phase and apoptosis
Cell Cycle **2**: 614-619

Hug H(2000)

Apoptose: Die Selbstvernichtung der Zelle als Überlebensschutz
Biologie in unserer Zeit **30**(3): 128-135

Igaki T, Kanuka H, Inohara N, Sawamoto K, Nunez G, Okano H, Miura M (1999)

Drob-1, a Drosophila member of the Bcl-2/CED-9 family that promotes cell death
Proc Natl Acad Sci **97**: 662-667

Igaki T, Miura M (2004)

Role of Bcl-2 family members in invertebrates
Biochim Biophys Acta **1644** (2-3): 73-81

Ikeda S, Ozaki K (1997)

Action of endonuclease G on DNA damaged by L-ascorbic acid, peplomycin, and cis-diaminedichloroplatinum II
Biochem Biophys Res Comm **235**: 291-294

Into T, Nodasaka Y, Hasebe A, Okuzawa T, Nakamura J, Ohata N, Shibata K (2002)

Mycoplasmal lipoproteins induce toll-like receptor 2- and caspases-mediated cell death in lymphocytes and monocytes
Microbiol Immunol **46**: 265-276

Irmeler M, Thome M, Hahne M, Schneider P, Hofmann K, Steiner V, Bodmer JL, Schroter M, Burns K, Mattmann C, Rimoldi D, French LE, Tschopp J (1997)

Inhibition of death receptor signals by cellular FLIP
Nature **388**: 190-195

Itaya M, Yamaguchi I, Kobayashi K, Endo T, Tanaka T (1990)

The Blasticidin S resistance gene (bsr) selectable in a single copy status in the Bacillus subtilis chromosome
J Biochem **107**: 799-801

Ito H, Fukuda Y, Murata K, Kimura A (1983)

Transformation of intact yeast cells treated with alkali cations
J Bact **153**: 163-168

Izumi M, Miyazawa H, Kamakura T, Yamaguchi I, Endo T, Hanaoka F (1991)

Blasticidin S resistance gene (bsr): a novel selectable marker for mammalian cells
Exp Cell Res **197**: 229-233

James ER, Green DR (2002)

Infection and the origins of apoptosis
Cell Death Differ **9**: 355-357

Janeway and Travers (1999)

Immunologie
Spektrum Akademischer Verlag

Janicke RU, Sprengart ML, Wati MR, Porter AG (1998)

Caspase-3 is required for DNA fragmentation and morphological changes associated with apoptosis
J Biol Chem **273**: 9357-9360

Jiang CG, Baehrecke EH, Thummel CS (1997)

Steroid regulated programmed cell death during *Drosophila* metamorphosis
Development **124**: 4673-4683

Jiang X, Wang X (2000)

Cytochrome c promotes caspase-9 activation by inducing nucleotide binding to Apaf-1
J Biol Chem **275**: 31199-31203

Johns EW, Butler JA (1962)

Further fractionation of histones from calf thymus
Biochem J **82**: 15-18

Jones AM (2001)

Programmed cell death in development and defense
Plant Phys **125**: 94-97

Ju ST, Panka DJ, Cui H, Ettinger R, el-Khatib M, Sherr DH, Stanger BZ, Marshak-Rotstein A (1995)

Fas(CD95)/FasL interactions required for programmed cell death after T-cell activation
Nature **373**: 444-448

Kaplan LJ, Bauer R, Morrison E, Langan TA, Fasman GD (1984)

The structure of chromatin reconstituted with phosphorylated H1. circular dichroism and thermal denaturation studies
J Biol Chem **259**: 8777-8785

Kawabata Y, Hirokawa M, Kitabayashi A, Horiuchi T, Kuroki J, Miura AB (1999)

Defective apoptotic signal transduction pathway downstream of caspase-3 in human B-lymphoma cells: A novel mechanism of nuclear apoptosis resistance
Blood **94**: 3523-3530

Kawane K, Fukuyama H, Adachi M, Sakahira H, Copeland NG, Gilbert DJ, Jenkin NA, Nagata S (1999)

Structure and promoter analysis of murine CAD and ICAD genes
Cell Death Differ **6**: 745-752

Kawane K, Fukuyama H, Kondo G, Takeda J, Ohsawa Y, Uchiyama Y, Nagata S (2001)

Requirement of DNase II for definitive erythropoiesis in the mouse fetal liver
Science **292**: 1546-1549

Kawane K, Fukuyama H, Yoshida H, Nagase H, Ohsawa Y, Uchiyama Y, Okada K, Iida T, Nagata S (2003)

Impaired thymic development in mouse embryos deficient in apoptotic DNA degradation
Nature Immunol advance online publication Jan 13th doi:10.1083/ni881

Kerr JF, Wyllie AH, Currie AR (1972)

Apoptosis: a basic biological phenomenon with wide-ranging implications in tissue kinetics
Br J Cancer **26**: 239-257

Khanna KK, Lavin MF, Jackson SP, Mulhern TD (2001)

ATM, a central controller of cellular responses to DNA damage
Cell Death Differ **8**: 1052-1065

Khodarev NN, Sokolova IA, Vaughan AT (1998)

Association between DNA cleavage during apoptosis and regions of chromatin replication
J Cell Biochem **70**: 604-615

Khodarev NN, Bennett T, Shearing N, Sokolova I, Koudelik J, Walter S, Villalobos M, Vaughan AT (2000)

LINE L1 retrotransposable element is targeted during the initial stages of apoptotic DNA fragmentation
J Cell Biochem **79**: 486-495

Khodarev NN, Sokolova IA, Vaughan ATM

Mechanisms of induction of apoptotic DNA fragmentation
Int J Radiat Biol **73**: 455-467

Kidd JV, Lahti JM, Teitz T (2000)

Proteolytic regulation of apoptosis
Sem Cell Dev Biol **11**: 191-201

Kimura M, Kamakura T, Tao QZ, Kaneko I, Yamaguchi I (1994)

Cloning of the Blastidicin S deaminase gene (BSD) from *Aspergillus terreus* and its use as a selectable marker for *Schizosaccharomyces pombe* and *Pyricularia oryzae*
Mol Gen Genet **242**: 121-129

Kimura M, Takatsuki A, Yamaguchi I (1994)

Blasticidin S deaminase gene from *Aspergillus terreus* (BSD): a new drug resistance gene for transfection of mammalian cells
Biochim Biophys Acta **1219**: 653-659

Kimura Y, Sugimoto C, Matsukawa S, Sunaga H, Igawa H, Yamamoto H, Izo T, Saito H, Fujieda S (2004)

Combined treatment of cisplatin and overexpression of caspase-activated deoxyribonuclease (CAD) promotes apoptosis in vitro and in vivo
Oral Oncol **40**: 390-399

Kluck RM, Bossy-Wetzel E, Green DR, Newmeyer DD (1997)

The release of cytochrome c from mitochondria: a primary site for bcl-2 regulation of apoptosis
Science **275**: 1132-1136

Koonin EV, Aravind L (2002)

Origin and evolution of eukaryotic apoptosis: the bacterial connection
Cell Death Differ **9**: 394-404

Korn C, Scholz SR, Gimatdudinow O, Pingoud A, Meiss G (2002)

Involvement of conserved histidine, lysine and tyrosine residues in the mechanism of DNA cleavage by the caspase-3 activated DNase CAD
Nucleic Acids Res **30**: 1325-1332

Kozela C, Regan S (2003)

How plants make tubes
Trends Plant Sci **8**: 159-164

Krajewski S, Tanaka S, Takayama S, Schibler MJ, Fenton W, Reed JC (1993)

Investigation of the subcellular distribution of the bcl-2 oncoprotein: residence in the nuclear envelope, endoplasmic reticulum, and outer mitochondrial membranes
Cancer Res **53**: 4701-4714

Krammer PH (1999)

CD95 (APO-1/Fas)-mediated apoptosis: live and let die
Adv Immunol **71**: 163-210

Krammer PH (2000)

CD95's deadly mission in the immunessystem
Nature **407**: 789-795

Kratzmeier M, Albig W, Hänecke K, Doenecke D (2000)

Rapid dephosphorylation of H1 histones after apoptosis induction
J Biol Chem **275** (39): 30478-30586

Kratzmeier M, Albig W, Meergans T, Doenecke D (1999)

Changes in the protein patterns of H1 histones associated with apoptotic DNA fragmentation
Biochem J **337**: 319-327

Kroger LA, DeNardo GL, Gumerlock PH, Xiong CY, Winthrop MD, Shi XB, Mack PC, Leshchinsky T, DeNardo SJ (2001)

Apoptosis-related gene and protein expression in human lymphoma xenografts (Raji) after low dose rate radiation using ⁶⁷Cu-2IT-BAT-Lym-1 radioimmunotherapy
Cancer Biother Radiopharm **16**: 213-225

Kubbutat MH, Jones SN, Vousen KH (1997)

Regulation of p53 stability by MDM2
Nature **387**: 299-303

Kudo T, Saeki H, Katayose Y, Yasui A (1994)

Construction of a human B cell line, TKHMY, suitable for production of stable human hybridomas
J Immunol Methods **177**: 17-22

Kumar (1999)

Mechanisms mediating caspase activation in cell death
Cell Death Differ **6**: 1060-1066

Kumar S, Vaux DL (2002)

A Cinderella caspase takes center stage
Science **297**: 1290-1291

Kuriyama H, Fukuda H (2002)

Developmental programmed cell death in plants
Curr Opin Plant Biol **5** (6): 568-573

Kuroki J, Hirokawa M, Kitabayashi A, Lee M, Miura AB (1996)

Cell-permeable ceramide inhibits the growth of TNF α resistant B lymphoma cells by inducing G0/G1 arrest but not apoptosis: a new model for dissecting cell-cycle arrest and apoptosis
Leukemia **10**: 1950-1958

Lagarkova MA, Iarovaia OV, Razin SV (1995)

Large-scale fragmentation of mammalian DNA in the course of apoptosis proceeds via excision of chromosomal DNA loops and their oligomers
J Biol Chem **270**: 20239-20241

Lakin ND, Hann BC, Jackson SP (1999)

The ataxia telangiectasia related protein ATR mediates DNA-dependent phosphorylation of p53
Oncogene **18**: 3989-3995

Lam E (2004)

Controlled cell death, plant survival and development
Nat Rev Mol Cell Biol **5**: 305-315

Lam E, Kato N, Lawton M (2001)

Programmed cell death, mitochondria and the plant hypersensitivity response
Nature **411**: 848-853

Lechardeur D, Drzymala L, Sharma M, Zylka D, Kinach R, Pacia J, Hicks C, Usmani N, Rommens JM, Lukacs GL (2000)

Determinants of the nuclear localization of the heterodimeric DNA fragmentation factor (ICAD/CAD)
J Cell Biol **150**: 321-334

Lee CY, Baehrecke E (2000)

Genetic regulation of programmed cell death in *Drosophila*
Cell Res **10**: 193-204

Lee E, Nakatsuma A, Hiraoka R, Ishikawa E, Enomoto R, Yamauchi A (1999)

Involvement of histone phosphorylation in thymocyte apoptosis by protein phosphatase inhibitors
IUBMB Life **48**: 79-83

Letai A, Bassik MC, Walensky LD, Sorcinelli MD, weiler S, Korsmeyer SJ (2002)

Distinct BH3 domains either sensitize or activate mitochondrial apoptosis, serving as prototype cancer therapeutics
Cancer Cell **2**: 183-199

Levin PA, Grossman AD (1998)

Cell cycle and sporulation in *Bacillus subtilis*
Curr Opin Microbiol **1**: 630-635.

Levrero M, De Laurenzi V, Costanzo A, Sabatini S, Gong J, Wang JYJ, Melino G (2000)

The p53/p63/p73 family of transcription factors: overlapping and distinct functions
J Cell Sci **113**: 1661-1670

Lewis K (2000)

Programmed death in bacteria
Microbiol Mol Biol Rev **64**: 503-514

Li H, Zhu H, Xu C, Yuan J (1998)

Cleavage of BID by caspase 8 mediates the mitochondrial damage in the Fas pathway of apoptosis.
Cell **94**: 491-501

Li LY, Luo X, Wang X (2001)

Endonuclease G is an apoptotic DNase when released from mitochondria
Nature **412**: 95-99

Li TK, Liu LF (2001)

Tumor cell death induced by topoisomerase-targeting drugs
Annu Rev Pharmacol Toxicol **41**: 53-77

Liang SH, Clarke MF (2001)

Regulation of p53 localization
Eur J Biochem **268**: 2779-2783

Linder C, Thoma F (1994)

Histone H1 expressed in *Saccharomyces cerevisiae* binds to chromatin and affects survival, growth, transcription, and plasmid stability but does not change nucleosomal spacing
Mol Cell Biol **14**: 2822-2835

Lindner H, Helliger W, Dirschlmeier A, Talasz H, Wurm M, Sarg B, Jaquemar M, Puschendorf B (1992)

Separation of phosphorylated histone H1 variants by high performance capillary electrophoresis

J Chromatogr **608**: 211-216

Lindner H, Wurm M, Dirschlmeier A, Sarg B, Helliger W (1993)

Application of high-performance capillary electrophoresis to the analysis of H1 histones

Electrophoresis **14**: 480-485

Lindner H., Helliger W, Sarg B, and Meraner C. (1995)

Effect of buffer compositions on the migration order and separation of histone H1 subtypes

Electrophoresis **16**: 604-610

Lithgov T, van Driel R, Bertram JF, Strasser A (1994)

The protein product of the oncogene bcl-2 is a component of the nuclear envelope, the endoplasmic reticulum, and the outer mitochondrial membrane

Cell Growth Differ **5**: 411-417

Liu X, Kim CN, Yang J, Jemmerson R, Wang X (1996)

Induction of apoptotic program in cell-free extracts: requirement for dATP and cytochrome c

Cell **86**: 147-157

Liu X, Li P, Widlak P, Zou H, Luo X, Garrard WT, Wang X (1998)

The 40 kDa subunit of DNA fragmentation factor induces DNA fragmentation and chromatin condensation during apoptosis

Proc Natl Acad Sci USA **95**: 8461-8466

Liu X, Zou H, Slaughter C, Wang X (1997)

DFF, a heterodimeric protein that functions downstream of caspase-3 to trigger DNA fragmentation during apoptosis

Cell **89**:175-184

Liu X, Zou H, Widlak P, Garrard W, Wang X (1999)

Activation of the apoptotic endonuclease DFF40 (caspase-activated DNase or nuclease): Oligomerization and direct interaction with histone H1 (1999)

J Biol Chem **274** (20): 13836-13840

Lockshin R, Williams C (1964)

Programmed cell death. II. Endocrine potentiation of the breakdown of the intersegmental muscles of silkworms

J Insect Physiol **10**: 643-649

Lockshin RA (1997)

The early modern period in cell death

Cell Death Differ **4**: 347-351

Longley DB, Johnston PG (2005)

Molecular mechanisms of drug resistance

J Pathol **205**: 275-292

Lorence A, Medina-Bolivar F, Nessler CL (2004)

Camptothecin and 10-hydroxycamptothecin from *Camptotheca acuminata* hairy roots
Plant Cell Rep **22**: 437-441

Lu D, Bai XC, Gui L, Su YC, Deng F, Liu B, Li XM, Zeng WS, Cheng BL, Luo SQ (2004)

Hydrogen peroxide in the Burkitt's lymphoma cell line Raji provides protection against arsenic trioxide-induced apoptosis via the phosphoinositide-3 kinase signalling pathway
Br J Haematol **125**: 512-520

Luciano F, Ricci JE, Herrant M, Bertolotto C, Mari JL, Cousin JL, Auberger P (2002)

T and B leukemic cell lines exhibit different requirements for cell death: correlation between caspase activation, DFF40/DFF45 expression, DNA fragmentation and apoptosis in T cell lines but not in Burkitt's lymphoma
Leukemia **16**: 700-707

Luo X., Budihardjo I, Zou H, Slaughter C, Wang X (1998)

Bid, a Bcl-2 interacting protein, mediates cytochrome c release from mitochondria in response to activation of cell surface death receptors
Cell **94**: 481-490

Macklis RM, Beresford BA, Palayoor S, Sweeney S, Humm JL (1993)

Cell cycle alterations, apoptosis, and response to low-dose-rate radioimmunotherapy in lymphoma cells
Int J Radiat Oncol Biol Phys **27**: 643-650

Madigan MT, Martinko JM, Parker J (1997)

Brock: Biology of microorganisms, 8th edition
Prentice-Hall International Editions

Mahadevaiah SK, Turner JMA, Baudat F, Rogakou EP, de Boer P, Blanco-Rodriguez J, Jasin M, Keeney S, Bonner WM, Burgoyne PS (2001)

Recombinational DNA double strand breaks in mice precede synapsis
Nat Genet **27**: 271-276

Martinon F, Burns K, Tschopp J (2002)

The inflammasome: a molecular platform triggering activation of inflammatory caspases and processing of proIL-beta
Mol Cell **10**(2): 417-426

Martins LM, Mesner PW, Kottke TJ, Basi GS, Sinha S, Tung JS, Svingen PA, Madden BJ, Takahashi A, McCormick D, Earnshaw WC, Kaufmann SH (1997)

Comparison of caspase activation and subcellular localization in HL60 and K562 cells undergoing etoposide-induced apoptosis
Blood **90**: 4283-4296

Maynard Smith J, Szathmary E (1997)

The major transitions in evolution
Oxford University Press

McCarthy JV, Dixit VM (1998)

Apoptosis induced by Drosophila Reaper and Grim in a human system
J Biol Chem **273**: 24009-24015

McIlroy D, Sakahira H, Talanian RV, Nagata S (1999)

Involvement of caspase-3 activated DNase in internucleosomal DNA cleavage induced by diverse apoptotic stimuli
Oncogene **18**: 4401-4408

McIlroy D, Tanaka M, Sakahira H, Fukuyama H, Suzuki M, Yamamura KI, Ohsawa Y, Uchiyama Y, Nagata S (2000)

An auxiliary mode of apoptotic DNA fragmentation provided by phagocytes
Genes Dev **14**: 549-558

McLaughlin B (2004)

The kinder side of killer proteases: Caspase activation contributes to neuroprotection and CNS remodelling
Apoptosis **9**: 111-121

Macklis RM, Beresford BA, Palayoor S, Sweeney S, Humm JL (1993)

Cell cycle alterations, apoptosis, and response to low-dose-rate radioimmunotherapy in lymphoma cells
Int J Radiat Oncol Biol Phys **27**: 643-650

Marti A, Graber H, Lazar H, Ritter PM, Baltzer A, Srinivasan A, Jaggi R (2000)

Caspases: decoders of apoptotic signals during mammary involution. Caspase activation during involution.
Adv Exp Med Biol **480**: 195-201

Meergans T, Hildebrandt AK, Horak D, Hanisch D, Wendel A (2000)

The short prodomain influences caspase-3 activation in HeLa cells
Biochem J **349**: 135-140

Meier P, Finch A, Evan G (2000)

Apoptosis in development
Nature **407**: 796-801

Meiss G, Scholz SR, Korn C, Gimatdudinow O, Pingoud A (2001)

Identification of functionally relevant histidine residues in the apoptotic nuclease CAD
Nucleic Acids Res **29**: 3901-3909

Merriam Webster's Inc. - Publisher Llewellyn WA (1987)

Webster's Ninth New Collegiate Dictionary, a Merriam-Webster®
Merriam Webster's Inc., Springfield Massachusetts, USA

Messinger H (1987)

Langenscheidts Großes Schulwörterbuch Deutsch-Englisch, 17. Auflage
Langenscheidt KG, Berlin und München

Messinger H, Rüdemberg W (1991)

Langenscheidts Großes Schulwörterbuch Englisch-Deutsch, 22. Auflage
Langenscheidt KG, Berlin und München

Micheau O, Tschopp J (2003)

Induction of TNF Receptor I-mediated apoptosis via two sequential signalling complexes
Cell **114**: 181-190

Miloshev G, Venkov P, van Holde K, Zlatanova J (1994)

Low levels of exogenous histone H1 in yeast cause cell death
Proc Natl Acad Sci USA **91**: 11567-11570

Minn AJ, Velez P, Schendel SL, Liang H, Muchmore SW, Fesik SW, Fill M, Thompson CB (1997)

Bcl-xL forms an ion channel in synthetic lipid membranes
Nature **385**: 353-357

Mirkes PE (2002)

2001 Warkany Lecture: To die or not to die, the role of apoptosis in normal and abnormal mammalian development
Teratology **65**: 228-239

Mitamura S, Ikawa H, Mizuno N, Kaziro Y, Itoh, H (1998)

Cytosolic nuclease activated by caspase-3 and inhibited by DFF-45
Biochem Biophys Res Commun **243**: 480-484

Miura M, Zhu H, Rotello R, Hartwig EA, Yuan J (1993)

Induction of apoptosis in fibroblasts by interleukin-1 β converting enzyme, a mammalian homolog of the *C. elegans* cell death gene *ced-3*
Cell **5**: 653-660

Moncke-Buchner E, Mackeldanz P, Kruger DH, Reuter M (2004)

Overexpression and affinity chromatography purification of the type III restriction endonuclease EcoP15I for use in transcriptome analysis
J Biotechnol **114**: 99-106

Moroni MC, Hickman ES, Denchi EL, Caprara G, Colli E, Cecconi F, Muller H, and Helin K (2001)

Apaf-1 is a transcriptional target for E2F and p53
Nat Cell Biol **3**: 552-558

Mortier-Barriere I, de Saizieu A, Claverys JP, Martin B (1998)

Competence-specific induction of *recA* is required for full recombination proficiency during transformation in *Streptococcus pneumoniae*
Mol Microbiol **27**:159-170

Mukae N, Yokoyama H, Yokokura T, Sakoyama Y, Sakahira H, Nagat S (2000)

Identification and developmental expression of inhibitor of caspase-activated DNase (ICAD) in *Drosophila melanogaster*
J Biol Chem **275**: 21402-21408

Muller SR, Sullivan PD, Clegg DO, Feinstein SC (1990)

Efficient transfection and expression of heterologous genes in PC12 cells
DNA Cell Biol **9**: 221-229

Muzio M, Chinnaiyan AM, Kischkel FC, O'Rourke K, Shevchenko A, Ni J, Scaffidi C, Bretz JD, Zhang M, Gentz R, Mann M, Kreammer PH, Peter ME, Dixit VM (1996)

FLICE, a novel FADD homologous ICE/CED-3-like protease, is recruited to the CD95 (Fas/Apo-1) death-inducing signalling complex

Cell **85**: 817-827

Nagata S, Nagase H, Kawane K, Mukae N, Fukuyama H (2003)

Degradation of chromosomal DNA during apoptosis

Cell Death Differ **10**: 108-116

Nagata T, Kishi H, Liu QL, Matsuda T, Imanaka T, Tsukada K, Kang D, Muraguchi A (2002)

The regulation of DNase activities in subcellular compartments of activated thymocytes

Immunology **105**: 399-406

Nahle Z, Polakoff J, Davuluri RV, McCurrach ME, Jacobson MD, Narita M, Zhang MQ, Lazebnik Y, Bar-Sagi D, and Lowe SW (2002)

Direct coupling of the cell cycle and cell death machinery by E2F

Nat Cell Biol **4**: 859-864

Neter J, Wassermann W, Kutner MH (1990)

Applied linear statistical methods models 3rd edition pp 741-744 and 771

Richard D. Irwin Chicago Homewood Illinois

Nguyen M, Branton PE, Walton PA, Oltvai ZN, Korsmeyer SJ, Shore GC (1994)

Role of membrane anchor domain of Bcl-2 in suppression of apoptosis caused by E1B-defective adenovirus

J Biol Chem **269**: 16521-16524

Nicholson DW (1999)

Caspase structure, proteolytic substrates, and function during apoptotic cell death

Cell Death Differ **6**: 1028-1042

Nicholson DW (2000)

From bench to clinic with apoptosis-based therapeutic agents

Nature **407**: 810-816

Nicotera P, Leist M (1997)

Intracellular ATP, mitochondrial function and the decision between apoptosis and necrosis

Cell Death Differ **4**: 435-442

Nicotera P, Leist M, Ferrando-May E (1999)

Apoptosis and necrosis: different execution of the same death

Biochem Soc Symp **66**:69-73.

Nordstrom W, Chen P, Steller H, Abrams J (1996)

Activation of the reaper gene during ectopic cell killing in *Drosophila*

Dev Biol **180**: 213-226

O'Connor L, Strasser A, O'Reilly L, Hausmann G, Adams JM, Cory S, Huang DCS (1998)

Bim: a novel member of the bcl-2 family that promotes apoptosis
Embo J **17**: 384-395

Oberhammer F, Wilson JW, Dive C, Morris ID, Hickman JA, Wakeling AE, Walker PR, Sikorska M (1993)

Apoptotic death in epithelial cells: cleavage of DNA to 300 and/or 50kb fragments prior to or in the absence of internucleosomal fragmentation
EMBO J **12**: 3679-3684

Oda, E, Ohki R, Murasawa H, Nemoto J, Shibue T, Yamashita T, Tokino T, Taniguchi T, Tanala N (2000)

Noxa, a BH3-only member of the Bcl-2 family and candidate mediator of p53-induced apoptosis
Science **288**: 1053-1058

Odaka C, Mizuochi T (2002)

Macrophages are involved in DNA degradation of apoptotic cells in murine thymus after administration of hydrocortisone
Cell Death Differ **9**: 104-112

Okayama H, Ueda K, Hayaishi O (1978)

Purification of ADP-ribosylated nuclear proteins by covalent chromatography on dihydroxyboryl polyacrylamide beads and their characterization
Proc Natl Acad Sci USA **75**: 1111-1115

Olins DE, Olins AL (2003)

Chromatin history: our view from the bridge
Nature Rev Mol Cell Biol **4**: 809-814

Oliver FJ, Menissier-de Murcia J, de Murcia G (1999)

Poly(ADP-ribose) polymerase in the cellular response to DNA damage, apoptosis, and disease
Am J Human Genet **64**: 1282-1288

Oltvai ZN, Korsmeyer SJ (1994)

Checkpoints of duelling dimers foil death wishes
Cell **79**: 189-192

Oltvai ZN, Milliman CL, Korsmeyer SJ (1993)

Bcl-2 heterodimerizes in vivo with a conserved homolog, bax, that accelerates programmed cell death
Cell **74**: 609-619

Orth K, Chinnaiyan AM, Garg M, Froelich CJ, Dixit VM ((1996)

The CED-3/ICE-like protease Mch2 is activated during apoptosis and cleaves the death substrate lamin
J Biol Chem **271**: 16443-16446

Parrish J, Li L, Klotz K, Ledwich D, Wang X, Xue D (2001)

Mitochondrial endonuclease G is important for apoptosis in *C. elegans*
Nature **412**: 90-94

Pediconi N, Ianari A, Costanzo A, Belloni L, Gallo R, Cimino L, Porcellini A, Screpanti I, Balsano C, Alesse E, Gulino A, Levrero M (2003)

Differential regulation of E2F1 apoptotic target genes in response to DNA damage
Nat Cell Biol **5**: 552–558

Perez-Gonzalez JA, Ruiz D, Esteban JA, Jimenez A (1990)

Cloning and characterization of the gene encoding a Blasticidin S acetyltransferase from *Streptoverticillium* sp.
Gene **86**: 129-134

Peter ME, Krammer PH (2003)

The CD95(APO-1/Fas) DISC and beyond
Cell Death Differ **10**: 26-35

Philchenkov (2004)

Caspases: potential targets for regulating cell death
J Cell Mol Med **8** (4): 432-444

Pique M, Barragan M, Dalmau M, Bellosillo B, Pons G, Gil J (2000)

Aspirin induces apoptosis through mitochondrial cytochrome c release
FEBS L **480**: 193-196

Pulvertaft JV (1964)

Cytology of Burkitt's tumour (African Lymphoma)
Lancet Feb 1 **39**: 238-240

Putcha GV, Johnson Jr. EM (2004)

"Men are but worms:" Neuronal cell death in *C. elegans* and vertebrates
Cell Death Differ **11**: 38-48

Puthalakath H, Huang DC, O'Reilly LA, King SM, Strasser A (1999)

The proapoptotic activity of the Bcl-2 family member Bim is regulated by interaction with the dynein motor complex
Mol Cell **3**: 287-296

Quinn L, Coombe M, Mills K, Daish T, Colussi P, Kumar S, Richardson H (2003)

Buffy, a *Drosophila* Bcl-2 protein, has anti-apoptotic and cell cycle inhibitory functions
EMBO J **22**: 3568-3579

Quinn LM, Dorstyn L, Mills K, Colussi PA, Chen P, Coombe M, Abrams, J, Kumar S, Richardson H (2000)

An essential role for the caspase Dronc in developmentally programmed cell death
J Biol Chem **275**: 40416-40424

Rao L, Perez D, White E (1996)

Lamin proteolysis facilitates nuclear events during apoptosis
J Cell Biol **135**: 1441-1455

Reed JC (1997)

Double identity for proteins of the Bcl-2 family
Nature **387**: 773–776

Ren Y, Savill J (1998)

Apoptosis: the importance of being eaten
Cell Death Differ **5**: 563- 568

Rich T, Allen RL, Wyllie AH (2000)

Defying death after DNA-damage
Nature **407**: 777-783

Rodriguez A Oliver H, Zou H, Chen P, Wang X, Abrams JM (1999)

Dark is a Drosophila homologue of Apaf-1/CED-4 and functions in an evolutionary conserved death pathway
Nat Cell Biol Sep **1** (5): 272-279

Rodriguez J, Lazebnik Y (1999)

Caspase-9 and Apaf-1 form an active holoenzyme
Genes Dev **13**: 3179-3184

Rogakou EP, Boon C, Redon C, Bonner WM (1999)

Megabase chromatin domains involved in DNA double-strand breaks in vivo
J Cell Biol **146**: 905-916

Rogakou EP, Nieves-Neira W, Boon C, Pommier Y, Bonner WM (2000)

Initiation of DNA fragmentation during apoptosis induces phosphorylation of H2AX histone at serine 139
J Biol Chem **275**: 9390-9395

Rotonda J, Nicholson DW, Fazil KM, Gallant M, Gareau Y, Labelle M, Peterson EP, Rasper DM, Ruel R, Vallaincourt JP, Thornberry NA, Becker JW (1996)

The three-dimensional structure of apopain /CPP32, a key mediator of apoptosis
Nature Struct Biol **3**: 619-625

Rothstein R (1985)

Cloning in yeast, in: DNA Cloning Vol II (ed. Glover DM)
IRL Press Oxford/Washington 45-66

Roy N, Deveraux QL, Takahashi R, Salvesen GS, Reed JC (1997)

The c-IAP-1 and c-IAP-2 proteins are direct inhibitors of specific caspases
EMBO J **16** (23): 6914-6925

Rubinstein B (2000)

Regulation of cell death in flower petals
Plant Mol Biol **44** (3): 303-318

Ruiz-Carrillo A, Renaud J (1987)

Endonuclease G: a (dG)n x (dC)n-specific DNase from higher eukaryotes
EMBO J **6**: 401-407

Sahara S, Aoto M, Eguchi Y, Imamoto N, Yoneda Y, Tsujimoto Y (1999)

Acinus is a caspase-3-activated protein required for apoptotic chromatin condensation
Nature **401**: 168-172

Sakahira H, Enari M, Nagata S (1998)

Cleavage of CAD inhibitor in CAD activation and DNA degradation during apoptosis
Nature **391**: 96-99

Sakahira H, Enari M, Nagata S (1999)

Functional differences of two forms of the inhibitor of caspase-activated DNase, ICAD-L and ICAD-S
J Biol Chem **274**: 15740-15744

Sakahira H, Enari M, Ohsawa Y, Uchiyama Y, Nagata S (1999b)

Apoptotic nuclear morphological change without DNA fragmentation
Curr Biol **9**: 543-546

Sakahira H, Nagata S (2002)

Co-translational folding of caspase-activated DNase with HSP-70 and HS-40 and inhibitor of caspase-activated DNase
J Biol Chem **277**: 3364-3370

Sakahira H, Takemura Y, Nagata S (2001)

Enzymatic active site of caspase-activated DNase (CAD and its inhibition by inhibitor of CAD
Arch Biochem Biophys **388**: 91-99

Salvesen, GS, Dixit, VM (1999)

Caspase-activation: The induced-proximity model
Proc Natl Acad Sci USA **96**: 10964-10967

Samali A, Zhivotovsky B, Jones D, Nagata S, Orrenius S (1999)

Apoptosis: Cell death defined by caspase activation
Cell Death Differ **6**: 495-496

Samejima K, Earnshaw WC (1998)

ICAD/DFF regulator of apoptotic nuclease is nuclear
Exp Cell Res **243**: 453-459

Samejima K, Earnshaw WC (2000)

Differential localization of ICAD-L and ICAD-S in cells due to removal of a C-terminal NLS from ICAD-L by alternative splicing
Exp Cell Res **255**: 314-320

Samejima K, Tone S, Earnshaw WC (2001)

CAD/DFF40 nuclease is dispensable for high molecular weight DNA cleavage and stage I chromatin condensation in apoptosis
J Biol Chem **276**: 45427-45432

Samejima K, Villa P, Earnshaw WC (1999)

Role of factors downstream of caspases in nuclear disassembly during apoptotic execution
Phil Trans R Soc Lond B **354**: 1591-1599

Sauve DM, Anderson HJ, Ray JM, James WM, Roberge M (1999)

Phosphorylation-induced rearrangement of the histone H1 NH2-terminal domain during mitotic chromosome condensation
J Cell Biol **145**: 225-235

Savill J, Fadok V (2000)

Corpse clearance defines the meaning of cell death
Nature **407**: 784-788

Scaffidi C, Fulda S, Srinivasan A, Friesen C, Li F, Tomaselli KJ, Debatin KM, Krammer PH, Peter ME (1998)

Two CD-95 (Apo-1, Fas) signalling pathways
Embo J **17**: 1675-1687

Schlegel (1985)

Allgemeine Mikrobiologie 6. Auflage
Thieme Verlag Stuttgart New York

Schlesinger PH, Gross A, Yin XM, Yamamoto K, Saito M, Waksman G, Korsmeyer SJ (1997)

Comparison of the ion channel characteristics of proapoptotic BAX and antiapoptotic BCL-2
Proc Natl Acad Sci USA **94**: 11357-11362

Schliephacke T, Meinl A, Kratzmeier M, Doenecke D, Albig W (2004)

The telomeric region is excluded from nucleosomal fragmentation during apoptosis, but the bulk nuclear chromatin is randomly degraded
Cell Death Differ **11**: 693-703

Schneider U, Schwenk HU, Bornkamm G (1977)

Characterization of EBV genome negative "null" and "T" cell lines derived from children with acute lymphoblastic leukemia and leucemic transformed non Hodgkin- lymphomas
Int J Cancer **19** (5): 621-626

Schoenlein PV, Barrett JT, Welter D (1999)

The degradation profile of extrachromosomal circular DNA during cisplatin-induced apoptosis is consistent with preferential cleavage at matrix attachment regions
Chromosoma **108**: 121-131

Scott SL, Earle JD, Gumerlock PH (2003)

Functional p53 increases prostate cancer cell survival after exposure to fractionated doses of ionizing radiation
Cancer Res **63**: 7190-7196

Shah GM, Shah RG, Poirier GG (1996)

Different cleavage pattern for poly(ADP-ribose) polymerase during necrosis and apoptosis in HL60 cells
Biochem Biophys Res Comm **229**: 838-844

Shain KH, Dalton WS (2001)

Cell adhesion is a key determinant in de novo multidrug resistance (MDR): new targets for the prevention of acquired MDR
Mol Cancer Ther **1**: 69-78

Sharif-Askari E, Alam A, Rheaume E, Beresford PJ, Scotto C, Sharma K, Lee D, DeWolf WE, Nuttall ME, Lieberman J, Sekaly RP (2001)

Direct cleavage of the human DNA fragmentation factor 45 by granzyme B induces caspase-activated DNase release and DNA fragmentation

EMBO J **20**: 3101-3113

Shi X, Liu S, Kleeff J, Friess H, Buchler MW (2002)

Acquired resistance of pancreatic cancer cells towards 5-Fluorouracil and gemcitabine is associated with altered expression of apoptosis-regulating genes

Oncology **62**: 354-362

Shieh SY, Ikeda M, Taya T, Prives C (1997)

DNA damaged-induced phosphorylation of p53 alleviates inhibition by MDM2

Cell **91**: 325-334

Shimizu S, Matsuoka Y, Shinohara Y, Yoneda Y, Tsujimoto Y (2001)

Essential role of voltage-dependent anion channel in various forms of apoptosis in mammalian cells

J Cell Biol **152** (2): 237-250

Shimizu T, Pommier Y (1996)

DNA fragmentation induced by protease activation in p53-null human leukemia HL60 cells undergoing apoptosis following treatment with the topoisomerase I inhibitor camptothecin: cell free system studies

Exp Cell Res **226**: 292-301

Shimizu T, Pommier Y (1997)

Camptothecin-induced apoptosis in p53-null human leukemia HL60 cells and their isolated nuclei: effects of the protease inhibitor Z-VAD-fmk and dichloroisocoumarin suggest an involvement of both caspases and serine proteases

Leukemia **11**: 1238-1244

Shiuhara M, el-Deiry WS, Wada M, Nakamaki T, Takeuchi S, Yang R, Chen DL, Vogelstein B, Koeffler HP (1994)

Absence of WAF1 mutations in a variety of human malignancies

Blood **84**: 3781-3784

Shresta S, Heusel JW, Macivor DM, Wesselschmidt RL, Russell JH and Ley TJ (1995)

Granzyme B plays a critical role in cytotoxic lymphocyte-induced apoptosis

Immunol Rev **146**: 211-221

Simpson RT (1978)

Structure of the chromatosome, a chromatin particle containing 160 base pairs of DNA and all the histones

Biochemistry **17**: 5524-5531

Skulachev VP (2001)

The programmed death phenomena, aging, and the Samurai law of biology

Exp Gerontol **36**: 995-1024

Smith GC, Cary RB, Lakin ND, Hann BC, Teo SH, Chen DJ, Jackson SP (1999)
Purification and DNA binding properties of the ataxia-teleangiectasia gene product ATM
Proc Natl Acad Sci USA **96**: 1134-1139

Smith TJ, Foster SJ (1995)
Characterization of the involvement of two compensatory autolysins in mother cell lysis during sporulation of *Bacillus subtilis*
J Bacteriol **177**:3855–3862

Sogame N, Kim M, Abrams JM (2003)
Drosophila p53 preserves genomic stability by regulating cell death
Proc Natl Acad Sci **100**: 4696-4701

Soldani C, Lazze MC, Bottone MG, Tognon G, Biggiogera M, Pellicciari CE, Scovassi AI (2001)
Poly(ADP-ribose) polymerase cleavage during apoptosis: When and where?
Exp Cell Res **269**: 193-201

Soldani C, Scovassi AI (2002)
Poly(ADP-ribose) polymerase-1 cleavage during apoptosis: An update
Apoptosis **7**: 321-328

Srinivasula SM, Ahmad M, Fernandes-Alnemri, Alnemri ES (1998)
Autoactivation of procaspase-9 by apaf-1 mediated oligomerization
Mol Cell **1**: 949-957

Srinivasula SM, Poyet JL, Razmara M, Datta P, Zhang Z, Alnemri ES (2002)
The PYRIN-CARD protein ASC is an activating adaptor for caspase-1
J Biol Chem **277**(24): 21119-21122

Staker BL, Hjerrild K, Feese MD, Behnke CA, Burgin AB, Stewart L (2002)
The mechanism of topoisomerase I poisoning by a camptothecin analog
Proc Natl Acad Sci USA **99**: 15387-15392

Stergiou L, Hengartner MO (2004)
Death and more: DNA damage response pathways in the nematode *C. elegans*
Cell Death Differ **11**: 21-28

Stroh S, Schulze-Osthoff K(1998)
Death by a thousand cuts: an ever increasing list of caspase substrates
Cell Death Differ **5**: 997-1000

Stryer L (1995)
Biochemie, 4. Auflage
Spektrum Akademischer Verlag GmbH, Heidelberg, Berlin, Oxford

Sulston JE (1976)
Post-embryonic development in the ventral cord of *Caenorhabditis elegans*
Philosoph Trans Roy Soc Lond Series B: Biological Sci **275**: 287-297

Sun J, Bottomley SP, Kumar S, Bird PI (1997)

Recombinant caspase-3 expressed in *Pichia pastoris* is fully activated and kinetically indistinguishable from the native enzyme
Biochem Biophys Res Commun **238**: 920-924

Susin SA, Lorenzo HK, Zamzami N, Marzo I, Snow BE, Brothers GM, Mangion J, Jacotot E, Costantini P, Loeffler M, Larochette N, Goodlett DR, Aebersold R, Siderovski DP, Penninger JM, Kroemer G (1999)

Molecular characterization of mitochondrial apoptosis-inducing factor (AIF)
Nature **397**: 441-446

Sweet MT, Carlson G, Cook RG, Nelson D, Allis CD (1997)

Phosphorylation of linker histones by a protein kinase A-like activity in mitotic nuclei
J Biol Chem **272**: 916-923

Takahashi A, Alnemri ES, Lazebnik YA, Fernandes-Alnemri T, Litwack G, Moir RD, Goldman RD, Poirier GG, Kaufman SH, Earnshaw WC (1996)

Cleavage of lamin A by Mch2 alpha but not CPP32: Multiple interleukin-1 β -converting enzyme-related proteases with distinct substrate recognition properties are active in apoptosis
Proc Natl Acad Sci USA **93**: 8395-8400

Takeuchi S, Hirayama K, Ueda K, Sakai H, Yonehara H (1958)

Blasticidin S, a new antibiotic
J Antibiotics **A11**: 1-5

Talasz H, Helliger W, Puschendorf B, Lindner H (1996)

In vivo phosphorylation of histone H1 variants during the cell cycle
Biochemistry **35**: 1761-1767

Talasz H, Helliger W, Sarg B, Debbage PL, Puschendorf B, Lindner H (2002)

Hyperphosphorylation of histone H2A.X and dephosphorylation of histone H1 subtypes in the course of apoptosis
Cell Death Differ **9**: 27-39

Talasz H, Sapojnikova N, Helliger W, Lindner H, and Puschendorf B (1998)

In vitro binding of H1 histone subtypes to nucleosomal organized mouse mammary tumour virus long terminal repeat promoter
J Biol Chem **273**: 32236-32243

Tang D, Kidd VJ (1998)

Cleavage of DFF45/ICAD by multiple caspases is essential for its function during apoptosis
J Biol Chem **273**: 28549-28552

Taylor WR, Stark GR (2001)

Regulation of the G2/M transition by p53
Oncogene **20**: 1803-1815

Teschendorf C, Warrington KH Jr, Siemann DW, Muzyezka N (2002)

Comparison of the EF-1 alpha and the CMV promoter for engineering stable tumor cell lines using recombinant adeno-associated virus
Anticancer Res **22**(6A): 3325-3330

Th'ng JPG (2001)

Histone modifications and apoptosis: Cause or consequence?
Biochem Cell Biol **79**: 305-311

Thoma F, Losa R, Koller T (1983)

Involvement of the domains of histone H1 and H5 in the structural organization of soluble chromatin
J Mol Biol **167**: 619-640

Thomas DA, Du C, Xu M, Wang X, Ley T (2000)

DFF45/ICAD can be directly processed by granzyme B during the induction of apoptosis
Immunity **12**: 621-632

Thomas H, Thomas HM, Ougham H (2000)

Annuality, perenniality and cell death
J Exp Bot **51** (352): 1781-1788

Thome M, Schneider P, Hofmann K, Fickenscher H, Meinel E, Neipel F, Mattmann C, Burns K, Bodmer JL, Schroter M, Scaffidi C, Krammer PH, Peter ME, Tschopp J (1997)

Viral FLICE-inhibitory proteins (FLIPs) prevent apoptosis induced by death receptors
Nature **386**:517-521

Thornberry NA, Bull HG, Calaycay JR, Chapman KT, Howard AD, Kostura MJ, Miller DK, Moulineaux SM, Weidner JR, Aunins J, Elliston KO, Ayala JM, Casano FJ, Chin J, Ding GJF, Egger LA, Gaffney EP, Limjuco G, Palyha OC, Raju SM, Rolando AM, Salley JP, Yamin TT, Lee TD, Shively JE, MacCross M, Mumford RA, Schmidt JA, Tocci MJ (1992)

A novel heterodimeric cysteine protease is required for interleukin-1 β processing in monocytes
Nature **356**: 768-774

Thornberry NA, Lazebnik Y (1998)

Caspases: Enemies within
Science **281**: 1312-1316

Tittel JN, Steller H (2000)

A comparison of programmed cell death between species
Genome Biol **1**(3): reviews 00003.1-00003.6

Toh SY, Wang X, Li P (1998)

Identification of the nuclear factor HMG2 as an activator for DFF nuclease activity
Biochem Biophys Res Comm **250**: 598-601

Troy CM, Shelanski ML (2003)

Caspase-2 redux
Cell Death Differ **10**: 101-107

Tsujimoto Y (1997)

Apoptosis and necrosis: Intracellular ATP as a determinant for cell death modes
Cell Death Differ **4**: 429-434

Tsujimoto Y, Finger LR, Yunis J, Nowell PC, Croce CM (1984)

Cloning of the chromosome breakpoint of neoplastic B cells with the t(14;18) chromosome translocation

Science **226**(4678):1097-1099

Unwin PNT, Milligan RA (1982)

A large particle associated with the perimeter of the nuclear pore complex

J Cell Biol **93**: 63-75

Ushinsky SC, Bussey H, Ahmed AA, Wang Y, Friesen J, Williams BA, Storms RK (1997)

Histone H1 in *Saccharomyces cerevisiae*

Yeast **13**: 151-161

Utz PJ, Anderson P (2000)

Life and death decisions: regulation of apoptosis by proteolysis of signaling molecules

Cell Death Differ **7**: 589-602

Van der Heiden MG, Chandel NS, Schumacker PT, Thompson CB (1999)

BCL-xL prevents cell death following growth factor withdrawal by facilitating mitochondrial ATP/ADP exchange

Mol Cell **3**: 159-167

Van Loo G, Schotte P, van Gurp M, Demol H, Hoorelbeke B, Gevaert K, Rodriguez I, Ruiz-Carillo A, Vandekerckhove J, Declercq W, Beyaert R, Vandenberghe P (2001)

Endonuclease G: a mitochondrial protein released in apoptosis and involved in caspase-independent DNA degradation

Cell Death Differ **8**: 1136-1142

Van Nieuwenhuijze AEM, van Lopik T, Smeenk, RJT, Aarden LA (2003)

Time between onset of apoptosis and release of nucleosomes from apoptotic cells: putative implications for systemic lupus erythematosus

Ann Rheum Dis **62**: 10-14

Van Sloun PPH, Jansen JG, Weeda G, Mullenders LHF, vanZeeland AA, Lohmann PHM, Vrieling H (1999)

The role of nucleotide excision repair in protecting embryonic stem cells from genotoxic effects of UV-induced DNA damage

Nucleic Acids Res **27**: 3276-3282

Varfolomeev EE, Schuchmann M, Luria V, Chiannikulchai N, Beckmann, J S, Mett IL., Rebrikov D, Brodianski VM, Kemper OC, Kollet O, Lapidot T, Soffer D, Sobe T, Avraham KB, Goncharov T, Holtmann H, Lonai P, Wallach D (1998).

Targeted disruption of the mouse Caspase 8 gene ablates cell death induction by the TNF receptors, Fas/Apo1 and DR3 and is lethal prenatally

Immunity **9**: 267-276.

Vaux DL (2002)

Apoptosis Timeline

Cell Death Differ **9**: 349-354

Vaux DL, Cory S, Adams JM (1988)

Bcl-2 gene promotes haematopoietic cell survival and cooperates with c-myc to immortalize pre-B cells

Nature **355**: 440-442

Vaux DL, Haecker G, Strasser A (1994)

An evolutionary perspective on apoptosis

Cell **76**: 777-779

Vaux DL, Korsmeyer SJ (1999)

Cell death in development

Cell **96**: 245-254

Vaux DL, Weissman IL, Kim SK (1992)

Prevention of programmed cell death in *Caenorhabditis elegans* by human bcl-2

Science **258**: 1955-1957

Verhagen AM, Ekert PG, Pakusch M, Silke J, Connolly LM, Reid GE, Moritz RL, Simpson RJ, Vaux DL (2000)

Identification of DIABLO, a mammalian protein that promotes apoptosis by binding to and antagonizing IAP proteins.

Cell **102**:43-53

Verma S, Zhao L, Chinnadurai G (2001)

Phosphorylation of the pro-apoptotic protein bik. mapping of phosphorylation sites and effect on apoptosis

J Biol Chem **276**: 4671-4676

Vernooy SY, Copeland J, Ghaboosi N, Griffin EE, Yoo SJ, Hay BA (2000)

Cell death in *Drosophila*: Conservation of mechanism and unique insights

J Cell Biol **150**: F69-F75

Vigorito E, Plaza S, Mir L, Mongay L, Vinas O, Serra-Pages C, Vives J (1999)

Contribution of p53 and PMA to gamma-irradiation induced apoptosis in Jurkat cells

Hematol Cell Ther **41**: 153-161

Vincenz C and Dixit VM (1997)

Fas-associated death domain proteininterleukin-1 b converting enzyme 2 (FLICE2), an ICE/Ced-3 homologue, is proximally involved in CD95- and p55-mediated death signalling

J Biol Chem **272**: 6578-6583

Vogt C (1842)

Untersuchungen über die Entwicklungsgeschichte der Geburtshelferkröte (*Alytes obstetricians*)

Solothurn: Jent und Gassmann, pp130

Wajant H (2002)

The Fas signalling pathway: more than a paradigm

Science **296**: 1635-1636

Walker NPC, Talanian RV, Brady KD, Dang LC, Bump NJ, Ferenz CR, Franklin S, Ghayur T, Hackett MC, Hammill LD, Herzog L, Hugunin M, Houy W, Mankovich JA, McGuinness L, Orlewicz E, Paskind M, Pratt CA, Reis P, Summani A, Terranova M, Welch JP, Xiong L, Möller A, Tracey DE, Kamen R, Wong WW (1994)

Crystal structure of the cysteine protease interleukin-1 β converting enzyme: a (p20/p10)₂ homodimer

Cell **78**: 343-352

Walker PR, Leblanc J, Carson C, Ribecco M, Sikorska M (1999)

Neither caspase-3 nor DNA fragmentation factor is required for high molecular weight DNA degradation in apoptosis

Ann NY Acad Sci **887**: 48-59

Walker PR, Weaver PM, Lach B, LeBlanc J, Sikorska M (1994)

Endonuclease activities associated with high molecular weight and internucleosomal DNA fragmentation in apoptosis

Exp Cell Res **213**: 100-106

Wang J, Lenardo MJ (2000)

Roles of caspases in apoptosis, development, and cytokine maturation revealed by homozygous gene deficiencies

J Cell Sci **113**: 753-757

Wang JC (1996)

DNA topoisomerases

Annu Rev Biochem **65**: 635-692

Wang K, Yin XM, Chao DT, Milliman CL, Korsmeyer SJ (1996)

Bid, a new BH3-domain only death agonist

Genes Dev **10**: 2859-2869

Watanabe M, Hitomi M, van der Wee K, Rothenberg F, Fisher SA, Zucker R, Svoboda KKH, Goldsmith EC, Heiskanen KM, Nieminen AL (2002)

The pros and cons of apoptosis assays for use in the study of cells, tissues, and organs

Microsc Microanal **8**: 375-391

Waxman DJ, Schwartz PS (2003)

Harnessing apoptosis for improved anticancer gene therapy

Cancer Res **63**: 863-8572

Wei J, Yang L, Harrata HK, Lee CS (1998)

High resolution analysis of protein phosphorylation using capillary isoelectric focusing – electrospray ionization – mass spectrometry

Electrophoresis **19**: 2356-2360

Wei MC, Zong WX, Cheng EH, Lindsten T, Paneutskakopoulou V, Ross MJ, Roth KA, MacGregor GR, Thompson CB, Korsmeyer SJ (2001)

Proapoptotic bax and bak: a prerequisite gateway to mitochondrial dysfunction and death

Science **292**: 727-730

Wellman SE, Song Y, Su D, Mamoon NM (1997)

Purification of mouse H1 histones expressed in Escherichia coli
Biotechnol Appl Biochem **26**: 117-123

Weng SL, Taylor SL, Morshedi M, Schuffner A, Duran EH, Beebe S, Oehninger S (2002)

Caspase activity and apoptotic markers in ejaculated human sperm
Mol Hum Reprod **8**: 984-991

White K, Tahaoglu E, Steller H (1996)

Cell killing by the Drosophila gene reaper
Science **271**: 805-807

Whitten JM (1969)

Cell death during early morphogenesis: Parallels between insect limb and vertebrate limb development
Science **163**: 1456-1457

Widlak P, Garrard WT (2001)

Ionic and cofactor requirement for the activity of the apoptotic endonuclease DFF40/CAD
Mol Cell Biochem **218**: 125-130

Widlak P, Li LY, Wang X, Garrard WT (2001b)

Action of recombinant human apoptotic endonuclease G on naked DNA and chromatin substrates: cooperation with exonuclease and DNase I
J Biol Chem **276**: 48404-48409

Widlak P, Li P, Wang X, Garrard WT (2000)

Cleavage preferences of the apoptotic endonuclease DFF40 (caspase-activated DNase or nuclease) on naked DNA and chromatin structures
J Biol Chem **275** (11): 8226-8232

Widlak P, Lanuszewska J, Cary RB, Garrard WT (2003)

Subunit structures and stoichiometries of human DNA fragmentation factor proteins before and after induction of apoptosis
J Biol Chem **278**: 26915-26922

Widlak P, Garrard WT (2005)

Discovery, regulation, and action of the major apoptotic nucleases DFF40/CAD and Endonuclease G
J Cell Biochem **94**: 1078-1087

Williams JR, Little JB, Shipley WU (1974)

Association of mammalian cell death with a specific endonucleolytic degradation of DNA
Nature **252**: 754-755

Wilson KP, Black JAF, Thomson JA, Kim EE, Griffith JP, Navia MA, Murcko MA, Chambers SP, Aldape RA, Raybuck SA, Livingston DJ (1994)

Structure and mechanism of interleukin-1 β converting enzyme
Nature **370**: 270-275

Wittig R, Nessling M, Will RD, Mollenhauer J, Salowsky R, Munstermann E, Schick M, Helmbach H, Gschwendt B, Korn B, Kioschis P, Lichter P, Schadendorf P, Poustka A (2002)

Candidate genes for cross-resistance against DNA-damaging drugs
Cancer Res **62**: 6698-6705

Wolf BB, Schuler M, Echeverri F, Green DR (1999)

Caspase-3 is the primary activator of apoptotic DNA fragmentation via DNA fragmentation factor 45/inhibitor of caspase-activated DNase activation
J Biol Chem **274**: 30651-30656

Wolter KG, Hsu YT, Smith CL, Nechushtan A, Xi XG, Youle RJ (1997)

Movement of Bax from the cytosol to mitochondria during apoptosis
J Cell Biol **139**: 1281-1292

Woo EJ, Kim YG, Kim MS, Han WD, Shin S, Robinson H, Park SY, Oh BH (2004)

Structural mechanism for inactivation and activation of CAD/DFF40 in the apoptotic pathway
Mol Cell **14**: 531-539

Wright ME, Han DK, Carter L, Fields S, Schwartz SM, Hockenbery DM (1999)

Caspase-3 inhibits growth in *Saccharomyces cerevisiae* without causing cell death
FEBS Lett **446**: 9-14

Wyllie AH (1980)

Glucocorticoid-induced thymocyte apoptosis is associated with endogenous endonuclease activation
Nature **284**: 555-556

Wyllie AH, Golstein P (2001)

More than one way to go
Proc Natl Acad Sci **98**: 11-13

Xerri L, Palmerini F, Devilard E, Defrance T, Bouabdallah R, Hassoun J, Birg F (2000)

Frequent nuclear localization of ICAD and and cytoplasmic coexpression of caspase-8 and caspase-3 in human lymphomas
J Pathol **192**: 194-202

Xue D, Shaham S, Horvitz HR (1996)

The *Caenorhabditis elegans* cell death protein CED-3 is a cystein protease with substrate specificities similar to those of the human CPP32 protease
Genes Dev **10**: 1073-1083

Yamaguchi H, Yamamoto C, Tanaka N (1965)

Inhibition of protein synthesis by Blastidicin S. I. Studies with cell-free systems from bacterial and mammalian cells
J Biochem (Tokyo) **57**: 667-677

Yang E, Zha J, Jockeö J, Boise L, Thompson CB, Korsmeyer SJ (1995)

Bad, a heterodimeric partner for Bcl-xL and Bcl-2 displaces bax and promotes cell death
Cell **80**: 285-291

Yang J, Liu X, Bhalla K, Kim CN, Ibrado AM, Cai J, Peng II, Jones DP, Wang X (1997)

Prevention of apoptosis by bcl-2: release of cytochrome c from mitochondria blocked
Science **275**: 1129–1132

Yano T, Teruya K, Shirahata S, Watanabe J, Osada K, Tachibani H, Ohashi H, Kim EH, Murakami H (1994)

Ras oncogene enhances the production of a recombinant protein regulated by the cytomegalovirus promoter in BHK21 cells
Cytotechnology **16**: 167-178

Yanokura M, Takase K, Yamamoto K, Teraoka H (2000)

Cell death and cell cycle arrest induced by incorporation of [3H] thymidine into human haemopoietic cell lines
Int J Radiat Biol **76**: 295-03

Yasuhara N, Eguchi Y, Tachibani T, Iamamoto N, Yoneda, Y Tsujimoto Y (1997)

Essential role of active nuclear transport in apoptosis
Genes Cells **2**: 55-64

Yokoyama H, Mukae N, Sakahira H, Okawa K, Iwamatsu A, Nagata S (2000)

A novel activation mechanism of caspase-activated DNase from *Drosophila melanogaster*
J Biol Chem **275**: 12978-12986

Yu J, Wang Z, Kinzler KW, Vogelstein B, Zhang L (2003)

PUMA mediates the apoptotic response to p53 in colorectal cancer cells
Proc Natl Acad Sci USA **100**: 1931-1936

Yuan J, Horvitz HR (1990)

The *Caenorhabditis elegans* genes *ced-3* and *ced-4* act cell autonomously to cause programmed cell death
Dev Biol **138**: 33-41

Yuan J, Horvitz HR (1992)

The *Caenorhabditis elegans* cell death gene *ced-4* encodes a novel protein and is expressed during the period of extensive programmed cell death
Development **116**: 309-320

Yuan J, Shaham S, Ledoux S, Ellis HM, Horvitz HR (1993)

The *C. elegans* cell death gene *ced-3* encodes a protein similar to mammalian interleukin-1 beta converting enzyme
Cell **75**: 641-652

Yuan J, Yankner BA (2000)

Apoptosis in the nervous system
Nature **407**: 802-809

Zamzami N, Susin A, Marchetti P, Hirsch T, Gomez-Monterrey I, Castedo M, Kroemer, G (1996)

Mitochondrial control of nuclear apoptosis
J Exp Med **183**: 1533–1544

Zha J, Harada H, Yang E, Jockel J, Korsmeyer, SJ (1996)

Serine phosphorylation of death agonist BAD in response to survival factor results in binding to 14-3-3 not Bcl-xL.
Cell **87**: 619-628

Zhang H, Huang Q, Ke N, Matsuyama S, Hammock B, Godzik A, Reed JC (2000)

Drosophila pro-apoptotic BCL-2/Bax homologue reveals evolutionary conservation of cell death mechanisms
J Biol Chem **275**: 27303-27306

Zhang J, Lee H, Agarwala A, Lou DW Xu M (2001)

DNA fragmentation factor 45 mutant mice exhibit resistance to kainic acid induced neuronal cell death
Biochem Biophys Res Comm **285**: 1143-1149

Zhang J, Lee H, Lou DW, Bovin GP, Xu M (2000b)

Lack of obvious 50 kilobase pair DNA fragments in DNA fragmentation factor 45-deficient thymocytes upon activation of apoptosis
Biochem Biophys Res Comm **274**: 225-229

Zhang J, Liu X, Scherer DC, van Kaer L, Wang X, Xu M (1998)

Resistance to DNA fragmentation and chromatin condensation in mice lacking the DNA fragmentation factor DFF45
Proc Natl Acad Sci USA **95**: 12480-12485

Zhang J, Wang X, Bove K, Xu M (1999)

DNA fragmentation factor 45-deficient cells are more resistant to apoptosis and exhibit different dying morphology than wild-type control cells
J Biol Chem **274**: 37450-37454

Zheng TS, Hunot S, Kuida K, Flavell RA (1999)

Caspase knockouts: Matter of life and death
Cell Death Differ **6**:1043-1053

Zou H, Henzel WJ, Liu X, Lutschg A, Wang X (1997)

Apaf-1, a human protein homologous to *C. elegans* CED-4, participates in cytochrome c-dependent activation of caspase-3
Cell **90**: 405-413

Zou H, Li Y, Liu X, Wang X (1999)

An apaf-1 cytochrome c multimeric complex is a functional apoptosome that activates procaspase-9
J Biol Chem **274**: 11549-11556

Danksagung

Ich möchte mich bei allen bedanken, die diese Arbeit ermöglicht haben und zu ihrem Gelingen beigetragen haben:

- Allen voran Herrn Prof. Dr. Doenecke und Herrn PD Dr. Albig für die Überlassung der Arbeit und die wissenschaftliche Betreuung
- Herrn Prof. Dr. Hardeland für seine sofortige Bereitschaft das Korreferat zu übernehmen
- Diana Otto für die gute Zusammenarbeit im Labor und tatkräftige Unterstützung
- Kristina Hänecke für die Einarbeitung und die Hilfe in der Zellkultur
- Christa Bode für fundierte technische Tipps in allen Laborbereichen
- Andreas Nolte vom Servicelabor für die zuverlässigen und schnellen Sequenzierarbeiten
- Natürlich danke ich auch allen weiteren Mitarbeitern in der Biochemie für die gute Zusammenarbeit und die schöne Zeit
- Den fleissigen Korrekturlesern dieser Arbeit – Nicoletta, Nadine und Maike – ein Dankeschön für die konstruktive Kritik in den verschiedenen Phasen der Entstehung dieser Arbeit
- Ein ganz besonderer Dank gebührt meinem Lebenspartner Sigi, meinen beiden Eltern und meiner Oma, die mich in guten und in schlechten Zeiten auch auf der „nichtwissenschaftlichen Basis“ im Laufe meines Studiums immer unterstützt und entlastet haben.

Lebenslauf

Name: Wiebke Goebel
Geburtsdatum: 10.05.1968
Geburtsort: Würselen
Staatsangehörigkeit: Deutsch

Ausbildung, Beruf und wissenschaftlicher Werdegang:

1974 - 1978 Grund- und Hauptschule Isernhagen N.B.
1978 - 1988 Gymnasium Großburgwedel, Abitur

1988 - 1990 Ausbildung zur staatlich geprüften Biologisch-technischen Assistentin.

11/1990 – 05/2000 Anstellung als BTA (teilweise in Teilzeit parallel zum Studium) in der Abteilung Elektronenmikroskopie und Zellbiologie der Medizinischen Hochschule Hannover.

10/1992 – 10/1999 Studiengang Biologie (Diplom) an der Universität Hannover. Anfertigung der Diplomarbeit im Physiologischen Institut der Tierärztlichen Hochschule Hannover unter Anleitung von Prof. Dr. G. Breves. Thema der Diplomarbeit: „Qualitativer Nachweis des Vitamin-D₃-Rezeptors im Gastrointestinaltrakt kleiner Wiederkäuer durch Westernblot-Analyse und RT-PCR“.

02/1999 - 05/2000 Anstellung als Wissenschaftliche Mitarbeiterin an der Tierärztlichen Hochschule Hannover, Physiologisches Institut. Mitarbeit an einem Projekt zur Charakterisierung transepithelialer Transportmechanismen von Calcium und Phosphat im Gastrointestinaltrakt kleiner Wiederkäuer.

ab 06/2000 Beginn der Arbeiten zur vorliegenden Dissertation mit dem Titel „Studies on the control and function of chromatin fragmentation during apoptosis“ im Institut für Biochemie und molekulare Zellbiologie der Georg-August-Universität Göttingen unter Anleitung von Prof. Dr. D. Doenecke.

